

The Role of Glutathione Transferases in Multiple Herbicide Resistance in Grass Weeds

David Jonathan Wortley

PhD thesis

Department of Biology

University of York

September 2013

In dedication to the most wonderful Gran a person could ever wish for

Utterly beloved

Always missed

This is for you

Abstract

Modern agriculture relies on chemical herbicides to control weedy species that compete with crops. In the UK, an estimated 80 % of cropland is infested with the weed species black-grass (*Alopecurus myosuroides*) that has evolved resistance to multiple herbicides with different modes-of-action. Studies in resistant black-grass identified a phi (F) class glutathione transferase, *AmGSTF1*, which was constitutively expressed. Heterologous expression of *AmGSTF1* in a transgenic host plant granted a multiple herbicide resistant (MHR) phenotype and it was found that the enzyme induced the activities of endogenous detoxification enzymes as well as catalytically detoxifying damaging hydroperoxides *in vitro*, which can form as a downstream consequence of herbicide treatment.

In the current work, *AmGSTF1* mutants have been derived and exploited to better understand the function of *AmGSTF1* in eliciting MHR. Using a catalytically-retarded mutant, it is shown that the enzyme elicited MHR without requiring catalysis. Instead, the mutant induced the activities of endogenous detoxification enzymes. Another mutant, lacking a cysteinyl residue (Cys120), has demonstrated that Cys120 plays a key role in the interaction of *AmGSTF1* with xenobiotics. In particular, Cys120 can be alkylated and inhibited by 4-chloro-7-nitro-benzoxadiazole (NBD-Cl), a compound that can reverse MHR when sprayed on black-grass plants. Enzyme inhibition and alkylation studies found that *AmGSTF1* could be alkylated by other chemicals but that this did not induce notable inhibition of the protein. The cysteinyl mutant also induced MHR in a transgenic host plant by inducing the activities of endogenous detoxification enzymes. The properties of *AmGSTF1* orthologues from annual rye-grass (*Lolium rigidum*) and maize (*Zea mays*) were also explored and found to display very similar functional properties as *AmGSTF1*. Transcriptome profiling demonstrated that *AmGSTF1* did not induce changes in host plant biochemistry by perturbing gene expression.

These studies have therefore demonstrated a central regulatory role for GSTF1 enzymes in co-ordinating MHR associated with manipulating host detoxification pathways and challenges the scientific dogma that glutathione transferases require catalytic activity to elicit herbicide resistance.

Table of Contents

Abstract.....	3
List of Figures.....	10
List of Tables	13
List of Equations.....	15
Acknowledgements.....	16
Declaration and copyright	17
Publications arising from this work	17
Chapter 1 Introduction	18
1.1 Overview of herbicide resistance	18
1.2 Target-site resistance	20
1.2.1 Adaptive mutations at the site-of-action	20
1.2.1.1 Substitution mutations	20
1.2.1.2 Deletion mutations.....	24
1.2.2 Target-site gene amplification.....	25
1.2.3 Summary of target-site resistance mechanisms	27
1.3 Non-target-site resistance (NTSR)	28
1.3.1 The xenome.....	28
1.3.2 Cytochrome P450 mixed-function oxidases and herbicide resistance.	30
1.3.3 Glutathione transferases and herbicide resistance.....	36
1.3.3.1 Introduction to the plant glutathione transferase enzyme family .	36
1.3.3.2 GST-mediated herbicide detoxification in crop species	37
1.3.3.3 GST-mediated herbicide detoxification in weed species.....	43
1.3.4 Glycosyl transferases, transporter proteins and herbicide resistance...	48

1.3.4.1	Glycosyl transferases	48
1.3.4.2	Transporter proteins.....	49
1.4	Herbicide resistant black-grass (<i>Alopecurus myosuroides</i>).....	50
1.5	Background and aims to the project	51

Chapter 2 Materials and Methods.....56

2.1	Materials	56
2.2	Instrumentation.....	56
2.3	Cloning techniques	56
2.3.1	Polymerase chain reaction (PCR)	56
2.3.2	Separation of DNA molecules using agarose gel electrophoresis	57
2.3.3	Excision and purification of separated DNA molecules	57
2.3.4	DNA restriction digests.....	57
2.3.5	DNA ligation reactions	58
2.3.6	Bacterial media.....	58
2.3.7	<i>E. coli</i> host transformation	58
2.3.8	Plasmid purification	58
2.3.9	DNA Sanger sequencing.....	59
2.4	<i>In vitro</i> studies with recombinant GST proteins.....	59
2.4.1	Generation of C120V and S12A point mutants	59
2.4.2	Recombinant protein expression in <i>E. coli</i>	60
2.4.3	Recombinant protein purification using <i>Strep-tactin</i> affinity chromatography.....	60
2.4.4	Quantification of purified recombinant protein concentrations	61
2.4.5	Sodium dodecyl sulfate polyacrylamide gel electrophoresis (SDS-PAGE).....	61

2.4.6	Determination of recombinant protein molecular weights using mass spectrometry.....	62
2.4.7	Reduction and desalting of purified recombinant protein.....	63
2.4.8	<i>In vitro</i> GSH-dependent enzyme assays	63
2.4.8.1	Assay using 1-chloro-2,4-dinitrobenzene (CDNB) as substrate...	63
2.4.8.2	Assay using cumene hydroperoxide (CuOOH) as substrate.....	63
2.4.8.3	Assay using linoleic acid hydroperoxide (LinOOH) as substrate.	64
2.4.8.4	Assay using 2-hydroxyethyl disulfide (HED) as substrate.....	65
2.4.8.5	Assay using crotonaldehyde as substrate	65
2.4.8.6	Assay using ethacrynic acid as substrate	66
2.4.8.7	Assay using 4-nitrophenyl acetate (NPA) as substrate	66
2.4.8.8	Assay using benzyl isothiocyanate (BITC) as substrate	66
2.5	Inhibition studies	67
2.5.1	IC ₅₀ determinations	67
2.5.2	Single time-point inhibition studies	67
2.5.3	Time-course inhibition studies.....	68
2.5.4	Studies of protein alkylation using mass spectrometry.....	68
2.6	GST expression in transgenic <i>Arabidopsis thaliana</i> plants.....	69
2.6.1	Cloning of GSTs into the pBIN-STRP3 vector.....	69
2.6.1.1	Cloning of <i>ZmGSTF1</i> into the pBIN-STRP3 vector	69
2.6.1.2	Cloning of <i>AmGSTF1</i> , C120V and S12A into the pBIN-STRP3 vector.....	69
2.6.2	Assembly of the pBIN-STRP3 vector designed to express the <i>Strep II</i> tag only.....	69
2.6.3	GV3101:MP90 agrobacterium transformations with GST-pBIN-STRP3 constructs	71
2.6.4	Infiltration of <i>Arabidopsis thaliana</i> with transformed Agrobacterium tumefaciens	71

2.6.5	Selection of homozygous lines.....	71
2.6.6	Western blotting of transgenic plant material	72
2.6.7	Spray trials	73
2.6.8	Biochemical characterisation of transgenic <i>Arabidopsis</i> plants.....	74
2.6.8.1	Soluble protein extractions	74
2.6.8.2	Enzyme assays	74
2.6.8.3	Flavonoid analysis	74
2.6.8.4	Protein pull-down experiments.....	75
Chapter 3	<i>In vitro</i> characterisation of <i>AmGSTF1</i> isoforms and further characterisation of transgenic <i>Arabidopsis</i> plants expressing <i>AmGSTF1</i>.....	77
3.1	Exploring the properties of <i>AmGSTF1</i> isoforms.....	77
3.1.1	Introduction	77
3.1.2	Expression of <i>AmGSTF1a</i> and <i>AmGSTF1c</i>	77
3.1.3	<i>In vitro</i> characterisation of <i>AmGSTF1a</i> and <i>AmGSTF1c</i>	79
3.2	Studies with <i>AmGSTF1</i> inhibitors.....	82
3.2.1	Introduction	82
3.2.2	IC_{50} studies	83
3.2.3	Studies with the NBD-Cl derivative 6-(7-nitro-1,2,3-benzoxadiazol-4-ylthio)hexanol (NBDHEX)	85
3.3	Analysis of the transcriptome of <i>AmGSTF1</i> -expressing <i>Arabidopsis</i> plants.....	87
3.3.1	Introduction	87
3.3.2	Transcriptome analysis of <i>AmGSTF1</i> -expressors	88
3.4	Discussion.....	89

Chapter 4 Probing *AmGSTF1* function using mutant isoforms...91

4.1	Introduction	91
4.2	<i>In vitro</i> characterisation of <i>AmGSTF1</i> mutant isoforms	92
4.2.1	Generation and purification of <i>AmGSTF1</i> mutant isoforms	92
4.2.2	Catalytic profiles of <i>AmGSTF1</i> mutant isoforms.....	94
4.2.3	Exploitation of the C120V mutant to study inhibition of <i>AmGSTF1</i> by alkylation.....	98
4.2.3.1	Inhibition studies with NBD-Cl.....	98
4.2.3.2	Inhibition studies with the nitrobenzoxadiazole-glutathione conjugate (NBD-SG).....	102
4.2.3.3	Inhibition studies with other known thiol alkylating agents.....	106
4.2.3.4	Inhibition studies with purine derivatives.....	111
4.3	Expression of <i>AmGSTF1</i> and mutant isoforms in transgenic <i>Arabidopsis thaliana</i> plants.....	114
4.3.1	Introduction	114
4.3.2	DNA construct generation.....	114
4.3.3	Transformation into <i>Arabidopsis thaliana</i> plants	117
4.3.4	Screening of transgenic plants for GST expression	120
4.3.5	Testing <i>AmGSTF1</i> -, C120V- and S12A-expressors for enhanced herbicide tolerance	122
4.3.6	Biochemical characterisation of <i>AmGSTF1</i> -, C120V and S12A-expressors.....	125
4.3.6.1	Enzyme activities of transgenic lines.....	125
4.3.6.2	Flavonoid profiles	127
4.3.7	Isolation of black-grass GSTs from transgenic <i>Arabidopsis</i> plants ...	128
4.4	Discussion and future work	130

Chapter 5 AmGSTF1 orthologues.....	134
5.1 Introduction	134
5.2 Identification of <i>AmGSTF1</i> orthologues	134
5.3 Expression and <i>in vitro</i> characterisation of <i>AmGSTF1</i> orthologues	136
5.3.1 Expression and purification of <i>AmGSTF1</i> orthologues	136
5.3.2 Catalytic profiles of <i>AmGSTF1</i> orthologues.....	137
5.3.3 Inhibition of <i>LrGSTF1</i>	139
5.4 Expression of <i>ZmGSTF1</i> in transgenic <i>Arabidopsis</i> plants.....	141
5.4.1 Generation of independent homozygous <i>ZmGSTF1</i> -expressing <i>Arabidopsis</i> lines.....	141
5.4.2 Screening of transgenic plants for GST expression	142
5.4.3 Testing <i>ZmGSTF1</i> -expressors for enhanced herbicide tolerance	143
5.4.4 Biochemical characterisation of <i>ZmGSTF1</i> -expressors.....	146
5.4.5 Isolation of <i>ZmGSTF1</i> from transgenic <i>Arabidopsis</i> plants	148
5.5 Discussion and future work	151
Chapter 6 Final Discussion.....	155
List of abbreviations and symbols	162
References.....	171

List of Figures

Figure 1: The 22 Herbicide Resistance Action Committee (HRAC) defined herbicide groups each with their respective target-site and an example herbicide of the group.....	19
Figure 2: Target-site mutation plasticity of ALS and ACCase enzymes.....	21
Figure 3: ACCase herbicides co-crystallised with yeast ACCase	24
Figure 4: EPSPS-interacting compounds	26
Figure 5: The plant xenome	28
Figure 6: Alternative routes of chlorotoluron metabolism in plants	31
Figure 7: Chlorsulfuron metabolism in wheat	33
Figure 8: CYP inhibitors used in herbicide metabolism studies	34
Figure 9: GST-catalysed detoxification of atrazine in plants	37
Figure 10: Detoxification of multiple herbicide classes by GST-catalysed glutathione conjugation in crop plants	38
Figure 11: GST subunit composition determines catalytic substrate specificities as demonstrated in maize.....	40
Figure 12: Scheme for <i>in vitro</i> glutathione peroxidase activity.....	41
Figure 13: Black-grass GST polypeptide sequences derived from the recombinant expression of an MHR black-grass cDNA library	46
Figure 14: Hydroperoxide accumulation in herbicide-sensitive and MHR biotypes of black-grass after herbicide treatment	47
Figure 15: Enhanced herbicide tolerance of transgenic <i>Arabidopsis</i> plants expressing <i>AmGSTF1</i>	52
Figure 16: Chemical structure of 4-chloro-7-nitro-benzoxadiazole (NBD-Cl)	53
Figure 17: Effect of 4-chloro-7-nitro-benzoxadiazole on herbicide resistance in black-grass when treated with the herbicides chlorotoluron, fenoxaprop-p-ethyl or clodinafop-propargyl.....	53
Figure 18: pET-STRP3 vector	78
Figure 19: Catalytic activities of <i>AmGSTF1a</i> and <i>AmGSTF1c</i>	80
Figure 20: Sequence alignment of <i>AmGSTF1a</i> and <i>AmGSTF1c</i>	82
Figure 21: Inhibitors of <i>AmGSTF1</i>	84

Figure 22: <i>AmGSTF1</i> inhibition studies with NBD-Cl and the NBD-Cl derivative 6-(7-nitro-1,2,3-benzoxadiazol-4-ylthio)hexanol (NBDHEX)	86
Figure 23: Amino acid sequence alignment of <i>AmGSTF1</i> and GSTP1.....	87
Figure 24: Analysis of sample RNA quality	88
Figure 25: Purity analysis of recombinant <i>AmGSTF1</i> and C120V.....	93
Figure 26: <i>In vitro</i> reaction schemes of known GST substrates used in this study to determine the catalytic profiles of <i>AmGSTF1</i> and associated mutant isoforms	95
Figure 27: Catalytic stability of <i>AmGSTF1</i> , C120V and S12A enzymes	98
Figure 28: Inhibition of <i>AmGSTF1</i> and C120V following treatment with 4-chloro-7-nitro-benzoxadiazole	99
Figure 29: Time-dependent inhibition of <i>AmGSTF1</i> by 4-chloro-7-nitro-benzoxadiazole	101
Figure 30: Inhibition of <i>AmGSTF1</i> and C120V following treatment with 4-chloro-7-nitro-benzoxadiazole (NBD-Cl) or a chemically-synthesized NBD-glutathione conjugate (NBD-SG).....	103
Figure 31: Time-dependent inhibition of <i>AmGSTF1</i> following treatment with 4-chloro-7-nitro-benzoxadiazole (NBD-Cl) or a chemically-synthesized NBD-glutathione (NBD-SG) conjugate.....	104
Figure 32: Specific activities of <i>AmGSTF1</i> and C120V following treatment with 4-chloro-7-nitro-benzoxadiazole, iodoacetamide or <i>N</i> -ethylmaleimide.....	107
Figure 33: Time-dependent activity profiles of <i>AmGSTF1</i> and C120V following treatment with 4-chloro-7-nitro-benzoxadiazole or iodoacetamide	108
Figure 34: Time-dependent activity profiles of <i>AmGSTF1</i> and C120V following treatment with 4-chloro-7-nitro-benzoxadiazole or <i>N</i> -ethylmaleimide	109
Figure 35: Specific activities of <i>AmGSTF1</i> and C120V following treatment with 4-chloro-7-nitro-benzoxadiazole or purine derivatives	112
Figure 36: Specific activities of <i>AmGSTF1</i> and C120V following treatment with 4-chloro-7-nitro-benzoxadiazole, 6-chloropurine or 3,3-deazonitro-6-chloropurine..	113
Figure 37: pBIN-STRP3 vector	115
Figure 38: Scheme for the generation of a modified pBIN-STRP3 vector allowing the expression of the <i>Strep</i> II tag only	116
Figure 39: Scheme for the generation of transgenic <i>Arabidopsis thaliana</i> plants containing a homozygous insert of the desired transgene.....	118
Figure 40: Phi class GST expression screens of homozygous insertion lines	121

Figure 41: Increased herbicide tolerance of transgenic Arabidopsis plants expressing <i>AmGSTF1</i> , C120V or S12A.....	123
Figure 42: Increased biomass of transgenic Arabidopsis plants expressing <i>AmGSTF1</i> , C120V or S12A relative to vector-only control plants following herbicide treatment.....	124
Figure 43: Flavonoid profiles of transgenic Arabidopsis plants expressing <i>AmGSTF1</i> , C120V, S12A or vector only.....	127
Figure 44: Isolation of <i>Strep</i> II tagged GSTs from transgenic Arabidopsis lines... 129	
Figure 45: Sequence alignment of <i>AmGSTF1</i> and the maize orthologue <i>ZmGSTF1</i>	134
Figure 46: Sequence alignment of <i>AmGSTF1</i> and the annual rye-grass orthologue <i>LrGSTF1</i>	135
Figure 47: Purity analysis of recombinant <i>AmGSTF1</i> and <i>LrGSTF1</i> 136	
Figure 48: Inhibitory profiles of <i>LrGSTF1</i> treated with compounds known to inhibit <i>AmGSTF1</i>	140
Figure 49: Phi class GST expression screens of <i>ZmGSTF1</i> homozygous insertion lines	143
Figure 50: Increased herbicide tolerance of transgenic Arabidopsis plants expressing <i>ZmGSTF1</i>	144
Figure 51: Increased biomass of transgenic Arabidopsis plants expressing <i>ZmGSTF1</i> relative to vector-only control plants following herbicide treatment.... 145	
Figure 52: Flavonoid profile of transgenic Arabidopsis plants expressing <i>ZmGSTF1</i> or vector only	148
Figure 53: Isolation of <i>Strep</i> II tagged GSTs from transgenic Arabidopsis lines... 150	
Figure 54: Early bolting phenotype of <i>ZmGSTF1</i> -expressors relative to other GST constructs and vector-only control plants	153
Figure 55: Multiple sequence alignment of <i>AmGSTF1</i> and orthologues.....	160

List of Tables

Table 1: Sequencing primers used in these studies	59
Table 2: Primers used to generate <i>AmGSTF1</i> point mutants	59
Table 3: Primers used to generate a pBIN-STRP3 vector designed to express the <i>Strep</i> II tag only.....	70
Table 4: High-performance liquid chromatography solvent gradient conditions	75
Table 5: Kinetic parameters for <i>AmGSTF1a</i> and <i>AmGSTF1c</i> with the substrate 1-chloro-2,4-dinitrobenzene (CDNB)	81
Table 6: Kinetic parameters for <i>AmGSTF1a</i> and <i>AmGSTF1c</i> with the substrate cumene hydroperoxide (CuOOH)	81
Table 7: Whole-protein mass measurements of purified recombinant <i>AmGSTF1</i> and C120V	93
Table 8: Substrate specificities of recombinant <i>AmGSTF1</i> , C120V and S12A enzymes.....	96
Table 9: Estimated k_{cat}/K_M values for <i>AmGSTF1</i> and C120V with 1-chloro-2,4-dinitrobenzene (CDNB) or cumene hydroperoxide (CuOOH) as substrates	97
Table 10: Analysis of <i>AmGSTF1</i> and C120V by mass spectrometry following treatment with 4-chloro-7-nitro-benzoxadiazole.....	102
Table 11: Analysis of <i>AmGSTF1</i> and C120V by mass spectrometry following treatment with 4-chloro-7-nitro-benzoxadiazole (NBD-Cl) or a chemically-synthesized NBD-glutathione (NBD-SG) conjugate	105
Table 12: Analysis of <i>AmGSTF1</i> and C120V by mass spectrometry following treatment with 4-chloro-7-nitro-benzoxadiazole or iodoacetamide	110
Table 13: Analysis of <i>AmGSTF1</i> and C120V by mass spectrometry following treatment with 4-chloro-7-nitro-benzoxadiazole or <i>N</i> -ethylmaleimide	111
Table 14: T ₁ transformant lines that segregated in a 3:1 alive:dead ratio following selection with glufosinate-ammonium	119
Table 15: <i>AmGSTF1</i> , C120V, S12A and vector-only homozygous single insertion lines selected for further study	119
Table 16: Enzyme activities of transgenic <i>Arabidopsis</i> plants expressing <i>AmGSTF1</i> , C120V, S12A or vector only.....	126

Table 17: Quantification of the major flavonoid accumulating in transgenic Arabidopsis plants expressing <i>AmGSTF1</i> , C120V, S12A or vector only	128
Table 18: Whole-protein mass measurement of purified recombinant <i>LrGSTF1</i> ..	137
Table 19: Substrate specificities of recombinant <i>AmGSTF1</i> and associated orthologues	139
Table 20: T ₁ transformant lines that segregated in a 3:1 alive:dead ratio following selection with glufosinate-ammonium	142
Table 21: <i>ZmGSTF1</i> homozygous single insertion lines selected for further study	142
Table 22: Enzyme activities of transgenic Arabidopsis plants expressing <i>ZmGSTF1</i> or vector only	147
Table 23: Quantification of the major flavonoid that accumulated in transgenic Arabidopsis plants expressing <i>ZmGSTF1</i> or vector only	148

List of Equations

Equation 1: Beer-Lambert law **78**

Equation 2: Approximation of enzyme catalytic efficiency (k_{cat} / K_M) at substrate concentrations well below the substrate K_M **96**

Acknowledgements

Hmmm...where to start?? I'd like to first start by thanking my supervisor Rob Edwards. Rob you have been an absolute pleasure to work for and you have taught me so much over these last four years. I will always be grateful. Thanks also to all the members of the RE group (old and new) over the last four years. I've really enjoyed working with you all - I know that during some of the harder parts of this PhD you've helped cheer me up and keep me going. In particular, a big thanks to Ian Cummins – thanks for showing me the ropes buddy (and going to heavy metal gigs with me!) Thanks also to Federico Sabbadin, cheers mi amigo for slogging down the MHR road with me. Good luck to the new bloods, Keir and Bekki, too – don't let the tea game die!!

Large thanks also to the University of York and Durham University for hosting my research and providing world-class research facilities. In particular, thank you to the Horticulture staff at York – always ready with a swift and cheery response! Thank you to the BBSRC and Syngenta for providing sponsorship. In particular, thank you Dave Hughes for being a great industrial supervisor and for organising my industrial placement at Jealott's Hill. I would also like to thank our collaborators in Durham for their chemical expertise and my Thesis Advisory Panel members, Neil Bruce and Simon McQueen-Mason, for their supportive and critical assessments of my work.

Last, but certainly not least, thank you to all my family and friends and to Poppy, the most amazing woman I've ever met. Without your love and support I wouldn't be where I am today. Thanks for putting up with my occasional mood swings and terrible taste in music!!! Who would have thought a lad from Rotherham would be submitting a PhD thesis, eh?!

Declaration and copyright

The work presented in this thesis is the sole effort of the author, except where explicitly stated. Reference to the work of others has been duly acknowledged. No portion of this work has been submitted for any other degree. Any reference to this work should be acknowledged and permission should be sought from the author prior to the publication of any quotation from this work.

Publications arising from this work

Ian Cummins^a, David J. Wortley^a, Federico Sabbadin, Zhesi He, Christopher R. Coxon, Hannah E. Straker, Jonathan D. Sellars, Kathryn Knight, Lesley Edwards, David Hughes, Shiv Shankhar Kaundun, Sarah-Jane Hutchings, Patrick G. Steel and Robert Edwards. (2013). Key role for a glutathione transferase in multiple-herbicide resistance in grass weeds. *Proceedings of the National Academy of Sciences of the United States of America* **110**: 5812-5817

^aAuthors contributed equally to this work.

David J. Wortley, Melissa Brazier-Hicks, Ian Cummins, Lesley Edwards and Robert Edwards. (2013). Probing the function of phi class glutathione transferases from weeds and maize for their roles in herbicide resistance. *In preparation*.

Chapter 1 – Introduction

1.1 Overview of herbicide resistance

Modern industrial arable farming relies on the use of herbicides that target and kill weedy plant species, which would otherwise directly compete with crops and damage crop yields. Herbicides act *in planta* by binding to a target site protein and disrupting metabolism to an extent that the plant can no longer survive (Powles and Yu, 2010). These compounds can be classified according to common chemical and structural motifs and also the site-of-action they specifically target in the plant. There are 301 herbicides in common use today which fall into one of 22 possible chemical classes and target one of 19 known sites-of-action (Heap, 2013) (Figure 1).

The intensive application of herbicides in modern farming has imposed a strong evolutionary pressure on weed species to select for individuals bearing mutations that promote weed survival upon herbicide exposure. Due to the strong lethality of herbicides on individuals bearing no adaptive mutations, herbicide resistant individuals rapidly dominate the seed bank leading to resistant weed populations (Jasieniuk *et al.*, 1996). Evolved resistance to herbicides in weed species has been observed now for over 40 years, since one of the first reports in 1970 of resistance to the triazine herbicide atrazine (Figure 1) in the weed species common groundsel (*Senecio vulgaris*) (Ryan, 1970). The continued use of herbicides in arable farming has now lead to a total of 397 independent documented cases of herbicide resistance globally with 217 weed species reported to contain at least one herbicide resistant population (Heap, 2013). Subsequently herbicide resistance is fast becoming one of the biggest threats to global agriculture, with an estimated cost in 1994 to the USA economy alone of US\$20 billion (Bridges, 1994), a figure which has increased with the continued rise in occurrences of herbicide resistant weed populations in the intervening 19 years. The threat is further compounded by a lack of novel modes-of-action and chemistries emerging from agrichemical research and development pipelines (Duke, 2012). Therefore it is of critical importance to understand the exact biochemical mechanisms that enable herbicide resistance in weed species so that rational strategies to overcome this phenomenon can be designed.

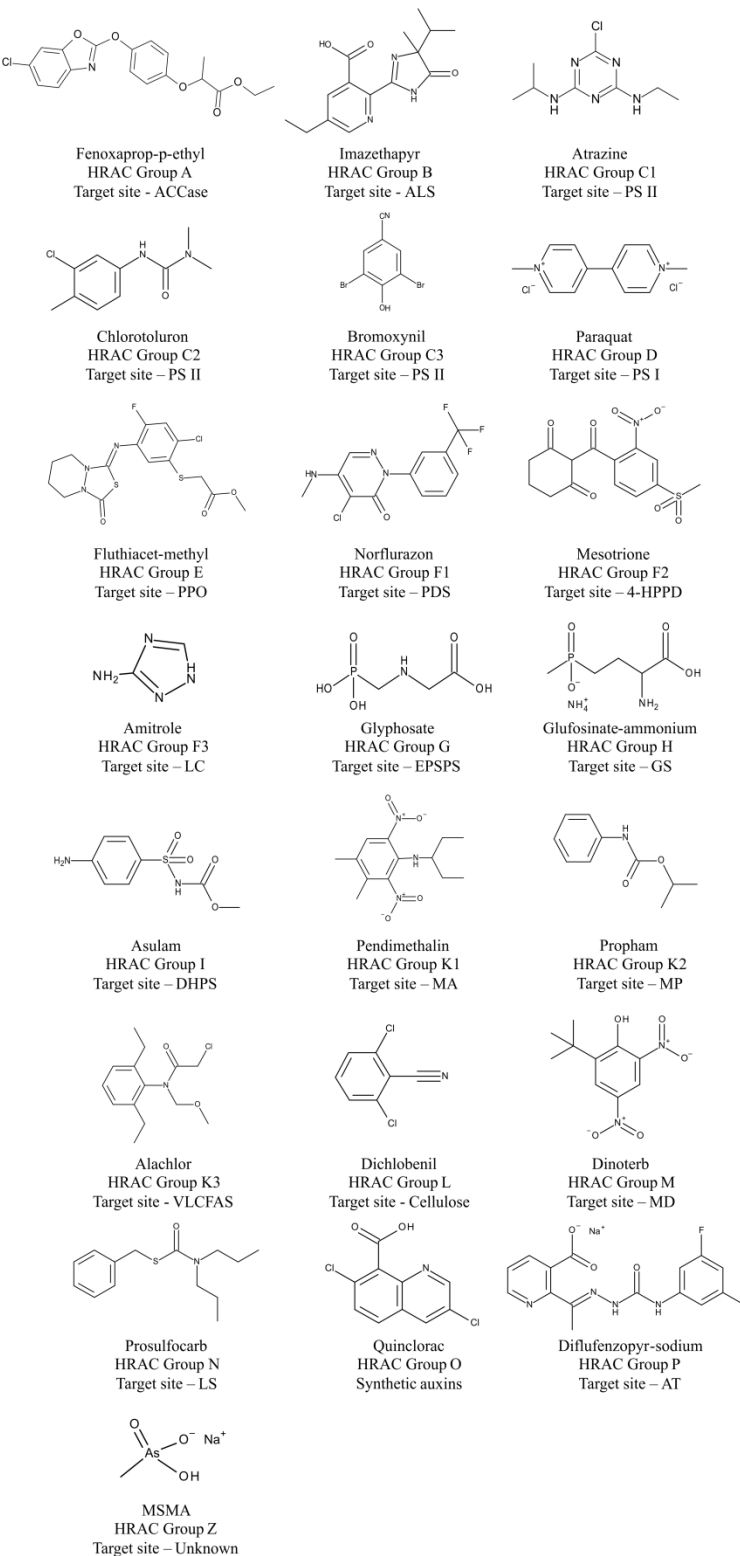


Figure 1: The 22 Herbicide Resistance Action Committee (HRAC) defined herbicide groups each with their respective target-site and an example herbicide of the group. Target-site abbreviations: ACCase, acetyl-coA carboxylase; ALS, acetolactate synthase; PS, photosystem; PPO, protoporphyrinogen oxidase; PDS, phytoene desaturase; 4-HPPD, 4-hydroxy-phenylpyruvate dioxygenase; LC, lycopene cyclase; EPSPS, 5-enolpyruvylshikimate-3-phosphate synthase; GS, glutamine synthetase; DHPS, dihydropteroate synthase; MA, microtubule assembly; MP, microtubule polymerisation; VLCFAS, very-long-chain fatty-acid synthesis; MD, membrane disruption; LS, lipid synthesis; AT, auxin transport.

It is already well established that there are multiple mechanisms that can elicit herbicide resistance in weeds and that each of these mechanisms fall into one of two broad classes; (i) target-site resistance, and (ii) non-target-site resistance (Powles and

Yu, 2010). Of these two classes, target-site resistance is far better understood especially for the most economically important weed species and chemical classes including, in some cases, a mechanistic understanding at the molecular level. On the other hand, very little is known about the mechanisms that enable non-target-site resistance in weeds. These two classes of herbicide resistance and the mechanisms contained in each class will now be explored in more detail in the following sections.

1.2 Target-site resistance

1.2.1 Adaptive mutations at the site-of-action

The most widely observed mechanism within the target-site resistance class is the evolution of adaptive mutations at a site-of-action. These mutations decrease the binding affinity between the site-of-action and the respective herbicides designed to target that site. Evolved resistance due to adaptive mutations has been extensively reviewed in the literature (Tranel and Wright, 2002; Delye, 2005; Duggleby *et al.*, 2008; Gressel, 2009; Powles and Yu, 2010) and so this section shall use select examples to highlight the mechanistic diversity across the spectrum of mutations observed in weed target-sites.

1.2.1.1 Substitution mutations

Acetyl-CoA carboxylase (ACCase) and acetolactate synthase (ALS; also known as acetohydroxy acid synthase, AHAS) are two widely exploited target-sites in weed species. The two enzymes are involved in *de novo* fatty acid synthesis and branched-chain amino acid synthesis respectively (Schloss, 1990; Incledon and Hall, 1997) and are targeted by 17 and 52 different herbicides respectively, extending across a total of 8 chemical classes (Heap, 2013). Numerous independent populations of multiple weed species have evolved resistance to ACCase and ALS-targeted herbicides due to amino acid substitutions in the primary sequence of the two enzymes including the damaging grass weed species black-grass (*Alopecurus myosuroides*) and annual rye-grass (*Lolium rigidum*) (Delye, 2005; Delye *et al.*, 2005; Zhang and Powles, 2006a; Zhang and Powles, 2006b; Delye and Boucansaud, 2008; Yu *et al.*, 2008; Tranel *et al.*, 2013). Both enzymes possess significant plasticity with regards to sites-of-mutation, with multiple positions in their primary

amino acid sequence able to evolve mutations that grant specific herbicide resistance profiles in the host weed plant (Delye, 2005; Tranell *et al.*, 2013) (Figure 2). For instance, according to the global database of ALS mutations, which records the first observation of novel ALS mutations across weed species, 21 discrete mutations of the ALS enzyme have been detected to date that confer some degree of resistance to ALS herbicides (Tranell *et al.*, 2013) (Figure 2 B).

A

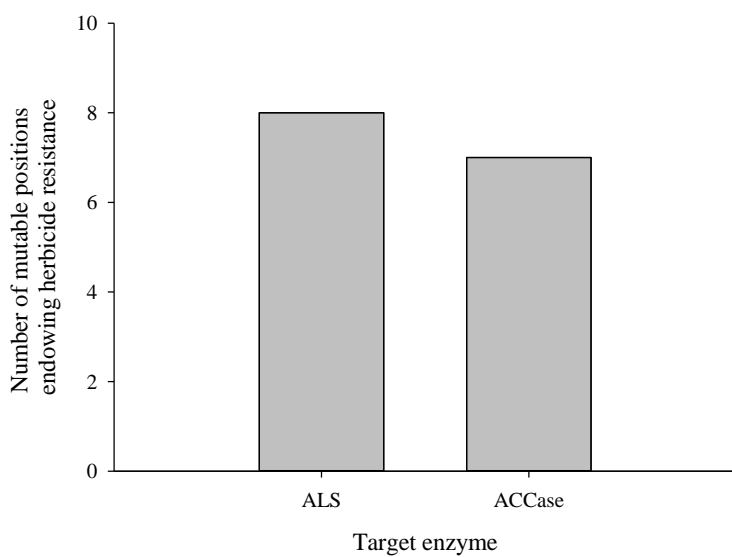
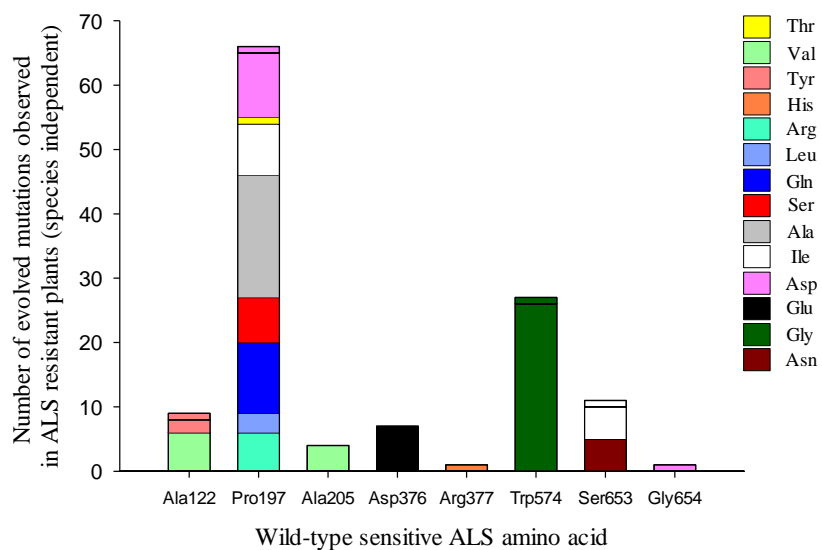


Figure 2: Target-site mutation plasticity of ALS and ACCase enzymes. (A) The total number of amino acid residues susceptible to mutation for ALS and ACCase enzymes that confer resistance to herbicides. **(B)** The frequency of mutation at each of the eight positions of ALS which confer ALS herbicide resistance. Coloured segments and the accompanying legend details the specific residue change whilst the size of each coloured segment reflects the occurrence of that mutation in independent weed species. ACCase data extracted from Jang *et al.* (2013) and Kaundun *et al.* (2013). ALS data extracted from Tranell *et al.* (2013).

B



Successful crystallographic studies of ALS derived from *Arabidopsis thaliana* (*At*), where it has been co-crystallised with various bound ALS-targeted herbicides, have provided strong evidence for the molecular mechanism of ALS inhibition *in planta*. ALS-binding herbicides occupy a site found on the surface of the catalytic subunit of ALS. The binding site covers access to a deep channel, at the bottom of which lies the catalytic centre of the enzyme meaning substrates are blocked from accessing the active site. Furthermore, co-crystallisation of *At*ALS with herbicides from the sulfonylurea and imidazolinone classes demonstrated that whilst herbicides of both classes bound ALS at the same general site, the modes of binding were different between classes. Sulfonylurea herbicides were found intruding further into the substrate channel and formed a much greater number of van der Waal's contacts and ionic interactions with residues of ALS. There was also found to be six ALS residues that bound to the sulfonylurea herbicides, but not the imidazolinone class, whilst two ALS residues were found to bind imidazolinones but not sulfonylureas (McCourt *et al.*, 2006).

The different modes of binding between herbicide classes and ALS provide a rational explanation for the specific resistance profiles that are seen for each recorded ALS mutation. For example, mutation of Trp574 can confer resistance to multiple ALS herbicide classes, including sulfonylureas and imidazolinones (Bernasconi *et al.*, 1995), because Trp574 plays a key role in securing ALS herbicides across the face of the substrate channel (McCourt *et al.*, 2006). Alternatively, other ALS residues only interact with one class of ALS herbicides and therefore mutation of these residues grants resistance to that class alone. For example, Ala122 interacts with imidazolinone herbicides via hydrophobic contacts and mutation of this residue to a Thr confers resistance to herbicides of the imidazolinone class but not to sulfonylureas (Bernasconi *et al.*, 1995). There are however exceptions to this generality with the mutation Ala122Tyr, recently observed in wild radish (*Raphanus raphanistrum*), granting resistance to all ALS herbicide classes tested including imidazolinone and sulfonylurea herbicides (Han *et al.*, 2012), presumably because the large indole substituent of Trp excludes a larger portion of the herbicide binding site than the Ala122Thr mutation.

Similar findings regarding target-site resistance have also been observed for ACCase, although the incidence of resistance to ACCase herbicides across weed species is much lower than that of ALS herbicides primarily because ACCase herbicides are selectively lethal to grass weed species. ACCase herbicides target the plastidic homomeric ACCase isoform found only in grass species (Konishi and Sasaki, 1994). A total of 12 discrete mutations of the ACCase enzyme at one of 7 possible amino acid residues have been detected to date that confer some degree of resistance to ACCase herbicides (Jang *et al.*, 2013; Kaundun *et al.*, 2013). As observed with ALS herbicide resistance, specific substitution mutations of the ACCase enzyme grant specific resistance profiles to the different ACCase herbicide classes (Powles and Yu, 2010). For instance, the point mutation Cys2088Arg, observed in annual rye-grass and Italian rye-grass (*Lolium multiflorum*), grants resistance to all ACCase herbicide classes tested (Yu *et al.*, 2007a; Kaundun *et al.*, 2012). In contrast, the point mutation Gly2096Ala, observed to date only in black-grass, grants resistance to ACCase herbicides of the aryloxyphenoxypropionate (AOPP) class and no others (Petit *et al.*, 2010). Current attempts to crystallise native plant ACCase enzymes bound to herbicides have been unsuccessful. However, the carboxyltransferase (CT) domain of ACCase from yeast has been crystallised bound to compounds of each of the three classes of commercial ACCase herbicides and provides some insight into ACCase-herbicide binding interactions *in planta* (Zhang *et al.*, 2004; Xiang *et al.*, 2009; Yu *et al.*, 2010). These structural studies found that AOPPs, cyclohexanediones and phenylpyrazolines (Figure 3), were bound close to the active site of the CT domain and therefore able to compete with the acetyl-CoA substrate for access to the active site.

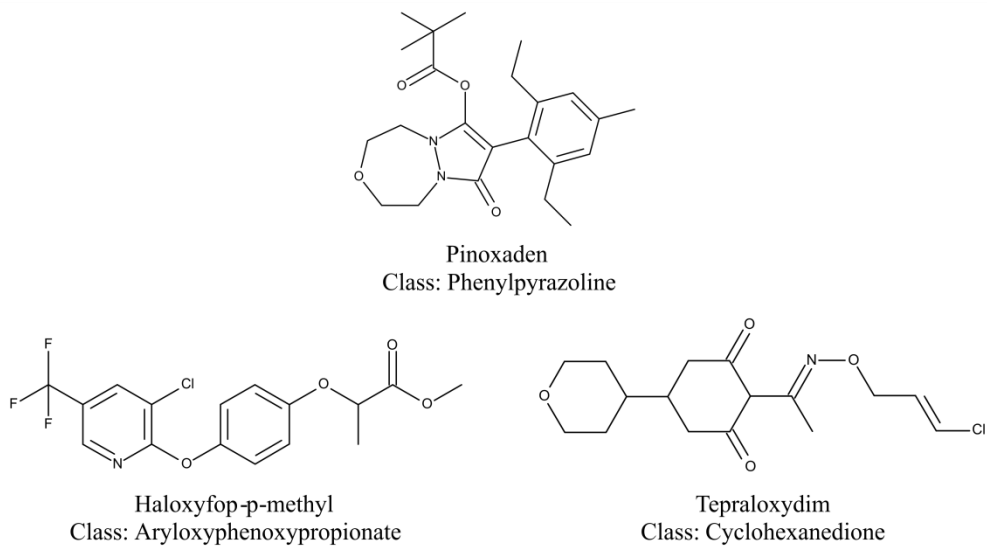


Figure 3: ACCase herbicides co-crystallised with yeast ACCase. The name of each herbicide is given along with the chemical class to which that herbicide belongs.

Pinoxaden and tepraloxydim (Figure 3) bound the CT domain in similar positions of the active site, whilst haloxyfop-p-methyl (Figure 3) bound the CT domain at a distinct site which induced large conformational changes in the protein. However, the crystallisation of sensitive and resistant grass ACCase enzymes in complex with herbicides is required to fully understand these interactions, particularly as the yeast ACCase has a primary amino acid sequence which more closely resembles resistant grass ACCase than it does sensitive ACCase. This can be evidenced by the observation that residue Leu1705 of the yeast ACCase CT domain, which is responsible for one of only two interactions shared across all three herbicide binding modes, is equivalent to the Ile1781 residue of plastidic grass ACCase (Yu *et al.*, 2010). For grass biotypes in which Ile1781 has been observed to be mutated to a Leu residue, this has rendered that biotype as resistant to ACCase herbicides (Petit *et al.*, 2010). This unexpected result exemplifies the need for a crystal structure of a sensitive grass ACCase bound to herbicides to be solved in complex.

1.2.1.2 Deletion mutations

Another, much rarer, mechanism of adaptive mutation at a target-site has been observed in waterhemp (*Amaranthus tuberculatus*) biotypes displaying resistance to protoporphyrinogen oxidase (PPO) inhibitors. PPO is involved in the biosynthesis of chlorophyll and heme in plants and disruption of its activity leads to the

accumulation of its substrate protoporphyrinogen IX, in the cytoplasm, where the substrate engages in light-dependent free radical chemistry and membrane disruption leading to cell death (Duke *et al.*, 1991). In resistant waterhemp biotypes, two genes encode PPO isoforms, of which one, *PPX2L*, was found to contain a 3-bp in-frame codon deletion causing the loss of Gly210 in the *PPX2L* polypeptide. Complementation studies using *E. coli* PPO mutant strains transformed with *PPX2L* and Δ G210 *PPX2L* confirmed that the Gly210 deletion granted resistance to PPO inhibitors (Patzoldt *et al.*, 2006). This resistance mechanism has since been observed in independent, geographically isolated PPO-resistant waterhemp biotypes (Thinglum *et al.*, 2011). Kinetic characterisation of recombinantly expressed *PPX2L* and Δ G210 *PPX2L* proteins revealed little change in the Michaelis constant of both enzymes for protoporphyrinogen IX, but did show a 10-fold reduction in catalytic turnover of the substrate in the resistant protein. Molecular dynamic simulations of both proteins (using PPO enzyme from tobacco as a model) revealed that deletion of Gly210 caused a significant enlargement of the active site of the enzyme. This served to increase the distance between key catalytic residues and hence the reduction in catalytic turnover meaning that both substrate and PPO herbicide could occupy the active site simultaneously. Furthermore, simulations suggested that a substitution mutation at PPO amino acid position 210 would result in strong steric clashes with adjacent residues and hence the selection for this rare deletion event (Dayan *et al.*, 2010).

1.2.2 Target-site gene amplification

A resistance mechanism quite distinct from target-site mutations is that of the expansion of the relative numbers of target-site gene copies per cell as first demonstrated in glyphosate-resistant Palmer amaranth (*Amaranthus palmeri*) (Gaines *et al.*, 2010). Glyphosate, the most widely used herbicide globally, belongs to the glycine class of herbicides and targets 5-enolpyruvylshikimate-3-phosphate synthase (EPSPS) in plants by behaving as a transition-state analogue of the EPSPS substrate phosphoenolpyruvate (Steinrucken and Amrhein, 1980; Duke and Powles, 2008; Shaner *et al.*, 2012) (Figure 4).

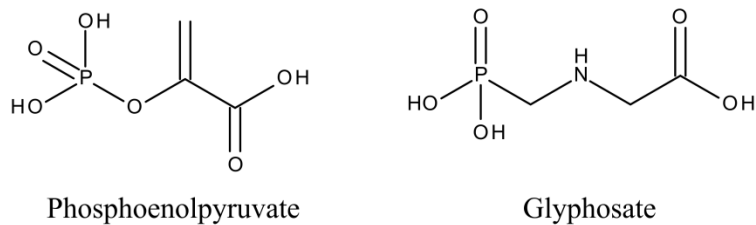


Figure 4: EPSPS-interacting compounds. Chemical structures are given of the EPSPS substrate molecule phosphoenolpyruvate along with the competitive inhibitor glyphosate, a transition-state analogue of phosphoenolpyruvate.

Inhibition of EPSPS activity disrupts the production of aromatic amino acids leading to plant death. All higher plants (prior to selection of resistance-endowing mutations under glyphosate exposure) contain a glyphosate-sensitive EPSPS enzyme; meaning glyphosate is non-selective regarding species lethality. As a highly effective herbicide, undergoing rapid distribution *in planta* and showing benign toxicological and environmental profiles, several crop species have been genetically engineered for glyphosate tolerance to allow selective use of the herbicide (Duke and Powles, 2008). The wide scale adoption of glyphosate-resistant crops and over-reliance on glyphosate as a sole method of weed control has imparted an enormous evolutionary pressure on weed species to select for mechanisms of glyphosate resistance (Shaner *et al.*, 2012). One of the resistance mechanisms observed, as mentioned above, is amplification of the EPSPS gene as discovered in a glyphosate-resistant biotype of Palmer amaranth. Resistant individuals contained, on average, 77-fold more EPSPS gene copies scattered throughout their genome, leading to significant fold-increases in EPSPS mRNA and protein production. EPSPS from resistant individuals was found to be as sensitive to glyphosate inhibition as EPSPS from sensitive counterparts. This demonstrated that the resistance phenotype occurs because the glyphosate field-rate capable of killing sensitive Palmer amaranth is not sufficient to saturate the enhanced number of EPSPS binding sites in the resistant biotype (Gaines *et al.*, 2010). This mechanism of resistance has also recently been reported in a glyphosate-resistant biotype of Italian rye-grass (Salas *et al.*, 2012) and it is therefore of critical importance that the molecular mechanisms responsible for EPSPS amplification are elucidated.

1.2.3 Summary of target-site resistance mechanisms

Intensive herbicide application has led to the evolution of multiple mechanisms of target-site resistance. The evidence presented suggests that an integration of multiple factors serves to define the observed mechanisms in different weed species including the binding mechanism to its target-site, the fitness cost of the respective mutation and the genetic plasticity of the host species. In the case of ALS and ACCase target-sites the herbicide binding site is close to, but not buried within, the enzyme active site. This has led to the evolution of a plethora of substitution mutations (Figure 2) that disrupt herbicide binding but retain enzymatic activity, in some cases with no observable fitness cost (Tranel and Wright, 2002; Menchari *et al.*, 2008). For ALS, the successful crystallisation of the enzyme complexed with herbicides provides mechanistic detail of the interaction (McCourt *et al.*, 2006). However, crystal structures of other target-sites in complex with herbicides are sorely lacking. Alongside substitution mutations at the target-site, intensive herbicide selection has led to the evolution of rarer evolutionary events including an in-frame codon deletion in the case of PPO resistance in waterhemp (Patzoldt *et al.*, 2006) and target-site gene amplification in the case of glyphosate resistance in Palmer amaranth and Italian rye-grass (Gaines *et al.*, 2010; Salas *et al.*, 2012). Codon deletion, as seen in PPO-resistant waterhemp biotypes, is a rare event and has not been observed for genes implicated in resistance to insecticides, anticancer drugs or antibiotics (Gressel, 2009). The ability of Nature to adapt to extreme conditions (herbicide application) should therefore not be underestimated.

1.3 Non-target-site resistance (NTSR)

The second major class of herbicide resistance mechanisms are those that involve the enhancement of herbicide detoxification and/or sequestration systems that limit the bioavailability of herbicides in the plant, such that they cannot bind to their site-of-action in sufficient dosage to disrupt metabolism (Yuan *et al.*, 2007; Cummins and Edwards, 2010). Collectively, the detoxification systems for the removal of foreign compounds (xenobiotics) in plants have been termed the ‘xenome’ (Edwards *et al.*, 2005a).

1.3.1 The xenome

The plant xenome is considered to behave as a four-phase process (Edwards *et al.*, 2005a; Yuan *et al.*, 2007) (Figure 5).

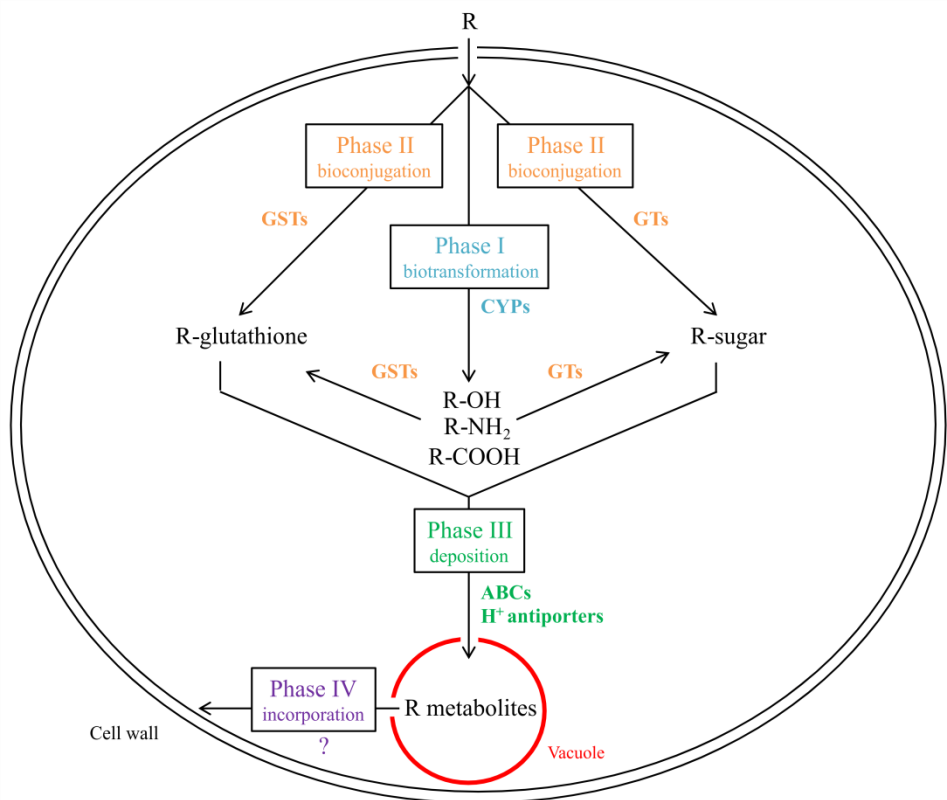


Figure 5: The plant xenome. A generalised scheme highlighting the four phases of xenobiotic detoxification that constitute the plant xenome. Abbreviations: R, xenobiotic; CYPs, cytochrome P450 mixed-function oxidases; GSTs, glutathione transferases; GTs, glycosyltransferases; ABCs, adenosine triphosphate binding cassette transporters; H⁺ antiporters, adenosine triphosphate-dependent transporters energetically coupled to a transmembrane H⁺ gradient.

Phase I of the xenome involves the biotransformation of xenobiotics typically via oxidative or dealkylation reactions catalysed by cytochrome P450 mixed-function oxidases (CYPs) (Van Eerd *et al.*, 2003). These activities serve to introduce, or reveal, a reactive functional group into the xenobiotic structure facilitating Phase II processing. As depicted (Figure 5), Phase I detoxification is a common route of metabolism for xenobiotic compounds but not wholly necessary to proceed to Phase II if the molecule already contains a suitably reactive centre. Phase II xenobiotic detoxification involves conjugation of the xenobiotic with the tri-peptide γ -Glu-Cys-Gly (glutathione; GSH) or with sugar moieties catalysed by glutathione transferases (GSTs) and glycosyltransferases (GTs) respectively. Conjugation with these biomolecules serves to increase the solubility of the xenobiotic, eliminate reactive centres (rendering the conjugate non-phytotoxic in most cases) and facilitate the entry of the xenobiotic-conjugate into Phase III metabolism (Bowles *et al.*, 2005; Cummins *et al.*, 2011). Phase III xenobiotic detoxification involves the transport of the xenobiotic-conjugate from the cytosol into the vacuole (Rea, 2007). Two transporter systems have been identified for the delivery of xenobiotic-conjugates into the plant vacuole. Transport of glutathionylated xenobiotics across the membrane relies on ATP-binding cassette transporters (ABCs) whilst the transport of glucosylated xenobiotics across the vacuolar membrane has been shown to utilise both ATP-dependent movement against an H⁺ gradient (H⁺ antiporters) and ABCs (Rea, 1999; Bartholomew *et al.*, 2002). Lastly, Phase IV detoxification in plants involves mineralisation or, more commonly, the incorporation of xenobiotic-derived metabolites into the plant cell wall. Whilst radioactive studies have confirmed these processes do occur, almost nothing is known about the biochemical mechanisms for these phenomena (Sandermann, 2004).

The xenome in plants is very large. For example, the relatively small genome of the well-studied model species *Arabidopsis* (*Arabidopsis thaliana*) contains 273 CYPs, 107 family 1 UDP-glucose GTs, 55 GSTs and 120 ABCs (Edwards *et al.*, 2011). By far the best studied are the CYP and GST families, although the large gene family sizes have made it difficult for researchers to understand the exact roles of individual genes in xenobiotic detoxification. Some of the first implications for the involvement of the xenome in herbicide metabolism came in the 1960-1970's. In 1966, Shimabukuro *et al.* reported that atrazine was metabolised in pea (*Pisum sativum*)

plants via oxidative dealkylation of the 4-ethylamino group to the respective free amine (Shimabukuro *et al.*, 1966). Whilst no enzyme was identified which catalysed this reaction, the action of CYPs could be inferred. The same group then went on to show that maize (*Zea mays*) cultivars with a relative tolerance to atrazine could detoxify the herbicide more rapidly than susceptible cultivars via the formation of a GST-catalysed glutathione conjugate (Frear and Swanson, 1970; Shimabukuro *et al.*, 1971). Following these observations in crop plants, it was little surprise then that similar mechanisms of xenome enhancement began to be observed in herbicide-resistant weed species (Anderson and Gronwald, 1991; Christopher *et al.*, 1991).

For example, a multiple herbicide resistant (MHR) biotype of black-grass, first identified in 1984 in Peldon, Essex, demonstrated resistance to herbicides from 4 chemical classes across three sites-of-action that was not due to TSR mechanisms (Moss, 1990; Hall *et al.*, 1997). Instead it was shown that herbicide metabolism, mediated by CYPs and GSTs, was enhanced in the resistant weeds and NTSR was, in the earlier literature, also referred to as enhanced metabolic resistance (Hyde *et al.*, 1996; Hall *et al.*, 1997). A very similar phenomenon of evolved herbicide resistance seemingly due to enhanced metabolism was demonstrated in MHR annual rye-grass biotypes (Christopher *et al.*, 1991; Preston *et al.*, 1996). These two examples demonstrate that enhancement of the xenome in herbicide-resistant weed biotypes can lead to resistance to multiple herbicide chemistries regardless of their site-of-action (multiple herbicide resistance, MHR), resulting in a loss of chemical control. Interestingly, evidence to date indicates that increased metabolism in resistant weed biotypes mimics the detoxification pathways of tolerant crop species (Christopher *et al.*, 1991; Hyde *et al.*, 1996; Ahmad-Hamdani *et al.*, 2013).

Evidence has now accumulated in the literature implicating all of the major xenome gene families (CYPs, GSTs, GTs, ABCs) in NTSR and these shall be discussed in turn in the following sections.

1.3.2 Cytochrome P450 mixed-function oxidases and herbicide resistance

Cytochrome P450 mixed-function oxidases (CYPs) are heme-containing proteins that utilise NADPH and molecular oxygen to catalyse the insertion of an oxygen

atom into a substrate molecule. Subsequent rearrangement of the oxygenated product can result in apparent oxidations, hydroxylations, dealkylations and reductions of the substrate (Werck-Reichhart *et al.*, 2000). In crop tissues, CYP-mediated degradation of herbicides has now been demonstrated for at least 25 different compounds across 8 different chemical classes (Siminszky, 2006). Furthermore, multiple routes of CYP-mediated degradation for a herbicide can exist within a plant. For instance, chlorotoluron, a member of the phenylurea class of herbicides and an inhibitor of photosystem II, can be metabolised via oxidation of a methyl substituent on the phenyl ring or, via successive *N*-dealkylation reactions (Figure 6). In both cases the ring-methyl oxidation product (**2**) and *di-N*-dealkylation product (**4**) are non-phytotoxic, however the *mono-N*-dealkylation product (**3**) is not (Ryan *et al.*, 1981).

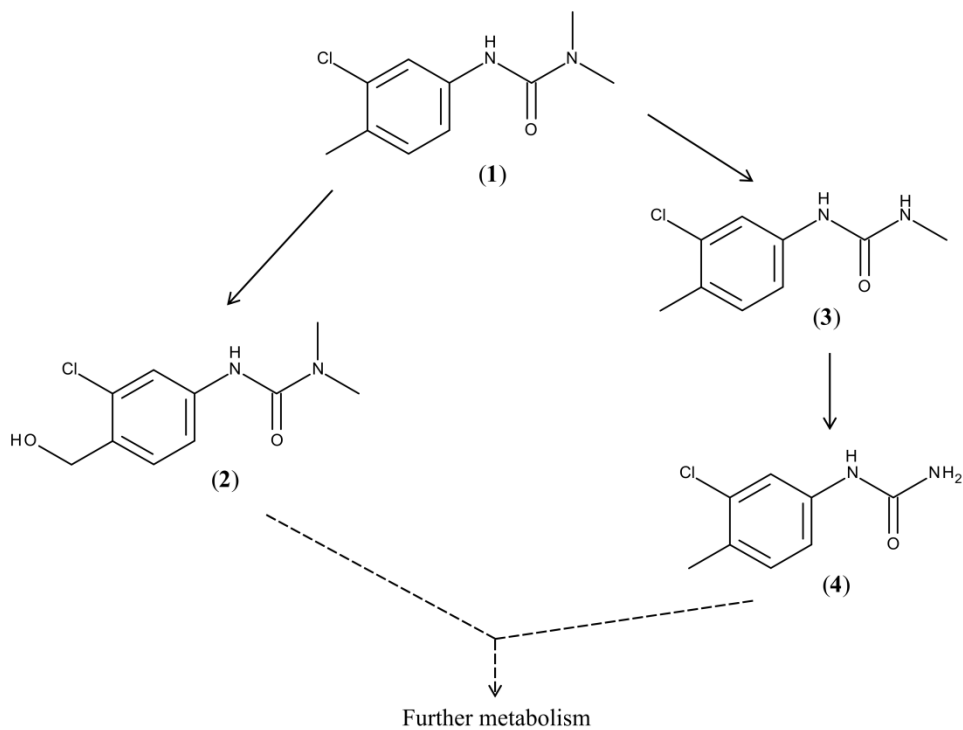


Figure 6: Alternative routes of chlorotoluron metabolism in plants. Chlorotoluron (**1**) can be primarily metabolised to the non-phytotoxic ring-methyl oxidation product (**2**) or it can undergo removal of the *N*-methyl groups to yield the phytotoxic *mono*- (**3**) and non-phytotoxic *di-N*-dealkylation (**4**) products (Ryan *et al.*, 1981).

Early studies using wheat (*Triticum aestivum*) and herbicide-sensitive black-grass exposed to chlorotoluron demonstrated that tolerance to chlorotoluron in the crop correlated well with the route and speed of chlorotoluron metabolism. Both species accumulated chlorotoluron metabolites (**2**)-(4), demonstrating two routes of herbicide metabolism were operational in both species. However, whilst wheat plants

preferentially and efficiently metabolised chlorotoluron to the non-phytotoxic ring-methyl oxidation product, herbicide-sensitive black-grass retained greater levels of chlorotoluron in the leaves and accumulated the phytotoxic *mono-N*-dealkylation product (Ryan *et al.*, 1981). Following the detection of MHR black-grass employing NTSR mechanisms (Moss, 1990), it was a logical step to explore the metabolism of chlorotoluron in the MHR biotype. Studies revealed that the MHR biotype had re-programmed xenome components to behave more like that of wheat and the MHR biotype now preferentially accumulated the non-phytotoxic ring-methyl oxidation product (Hyde *et al.*, 1996).

A similar scenario has been observed in MHR annual rye-grass resistant to chlorsulfuron, a member of the sulfonylurea class of herbicides which inhibit ALS. In chlorsulfuron-tolerant wheat, the herbicide was detoxified following hydroxylation of the phenyl ring and rapid conjugation of the newly-introduced hydroxyl group with glucose (Sweetser *et al.*, 1982) (Figure 7). Studies with annual rye-grass demonstrated that this pathway was minimally active in the sensitive biotype but enhanced in MHR weeds with the detoxified metabolite (**iii**) accumulating at significantly greater levels in the MHR biotype based on co-chromatography with chlorsulfuron-treated wheat extracts (Christopher *et al.*, 1991). Further studies with MHR annual rye-grass strengthened the conclusion of enhanced CYP-mediated chlorsulfuron metabolism by showing metabolism was greatly diminished after treatment with the CYP inhibitor malathion (Christopher *et al.*, 1994) (Figure 8).

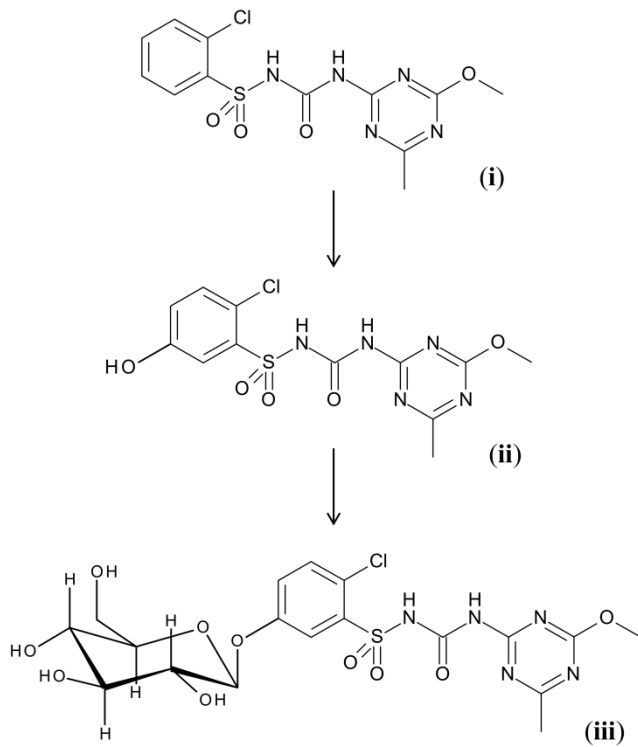


Figure 7: Chlorsulfuron metabolism in wheat. Chlorsulfuron (i) is metabolised in wheat to the hydroxylated derivative (ii) followed by rapid conversion to the glucosylated derivative (iii).

Significantly, these studies of CYP-mediated herbicide metabolism in MHR weed species provide strong evidence that components of the xenome of resistant weeds have been enhanced (by an unknown mechanism) in MHR biotypes rather than resistance being due to the expression of novel xenome detoxification genes.

Continued studies with MHR annual rye-grass have shown that activities of multiple herbicide-detoxifying CYPs can be enhanced in the same MHR biotype. For instance, in one MHR annual rye-grass biotype, plants were treated with various herbicide/CYP-inhibitor combinations and it was shown that; (i) piperonyl butoxide (Figure 8) significantly reduced resistance to chlorotoluron but not to chlorsulfuron, (ii) malathion (Figure 8) significantly reduced resistance to chlorsulfuron but not to chlorotoluron. In both cases, decreased resistance correlated with a significant increase in accumulation of the radiolabelled herbicide (Preston *et al.*, 1996). These observations are striking as they suggest that the mechanism of MHR in some biotypes is not due to a single mutation in the regulation of a specific CYP enzyme but rather due to enhancing multiple xenome enzymes.

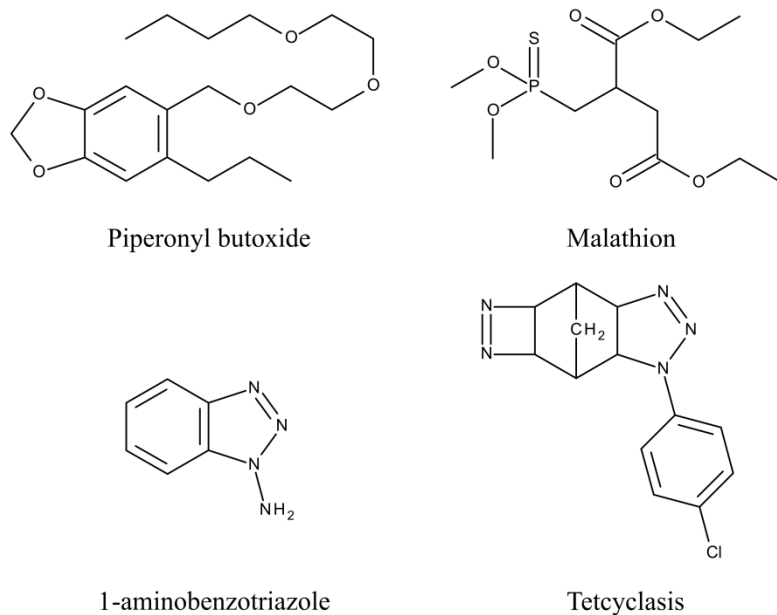


Figure 8: CYP inhibitors used in herbicide metabolism studies. The structures of four commonly used CYP inhibitors are given along with the common chemical name of each.

To date, the strategies of quantifying the rates and products of herbicide metabolism and the use of CYP inhibitors (Figure 8) have identified 10 weed species with populations demonstrating herbicide resistance due in part to CYP-mediated herbicide degradation (Hyde *et al.*, 1996; Preston *et al.*, 1996; Cocker *et al.*, 2001; Yun *et al.*, 2005; Yuan *et al.*, 2007; Ahmad-Hamdan *et al.*, 2013). However, CYP genes/proteins responsible for herbicide detoxification have yet to be isolated from resistant weed species. Multiple factors are likely to contribute to a lack of identification of weed CYPs such as the many homologous CYP genes per weed genome and the difficulty in purifying membrane-associated proteins. Of greatest impact, is the lack of genomic information for weed species. That may now be set to change though with the recent development of Next Generation Sequencing (NGS) technologies capable of rapidly sequencing complete genomes. NGS technologies have been successfully employed to sequence multiple complex crop genomes including barley and wheat (Brenchley *et al.*, 2012; Mayer *et al.*, 2012) and the first efforts have been made to use this technology with regards to weed species, although the strategy remains in its infancy (Peng *et al.*, 2010; Riggins *et al.*, 2010). An alternative strategy for cloning CYPs from annual rye-grass has been employed involving rapid amplification from cDNA ends polymerase chain reaction (RACE-PCR) of an annual rye-grass expressed sequence tag (EST) library resulting in the

successful cloning of 16 CYP genes. No functional characterisation of these CYPs was reported however and hence their roles in herbicide detoxification are unknown (Fischer *et al.*, 2001).

CYPs from non-weedy plant species have been isolated, cloned and expressed in transgenic host plants and have been shown to confer a herbicide-resistant phenotype. For instance CYP71A10 was isolated from soybean and shown *in vitro* to be able to metabolise chlorotoluron and related phenylurea herbicides by catalysing their *N*-demethylation and, in the case of chlorotoluron, to also catalyse the formation of the ring-methyl oxidation product (Figure 6). Expression of CYP71A10 in tobacco (*Nicotiana tabacum*) granted the transgenic host plants resistance to both chlorotoluron and linuron (chlorotoluron analogue) (Siminszky *et al.*, 1999). Similarly, CYP76B1 isolated from Jerusalem artichoke (*Helianthus tuberosus*) was shown to be able to catalyse the *N*-dealkylation of chlorotoluron to the non-phytotoxic *di-N*-dealkylation product (Figure 6). Expression of CYP76B1 in both Arabidopsis and tobacco granted a 10-fold increase in resistance to the herbicide (Didierjean *et al.*, 2002). Importantly these studies provide direct confirmation for the role of plant CYPs in conferring herbicide resistance *in planta* by enhancing herbicide metabolism. Perhaps the most powerful example of direct CYP-mediated herbicide resistance comes not from a plant source but from the expression of a human CYP (CYP2B6) in transgenic rice plants. CYP2B6 granted the transgenic host plant tolerance to 13 herbicides from 8 chemical classes with a combined total of 6 sites-of-action via CYP-mediated metabolism (Hirose *et al.*, 2005). This striking result is perhaps even more impressive considering that CYP2B6 has such a broad activity spectrum having little/no regular exposure to these chemicals *in vivo* and reveals the potential power of CYP-mediated herbicide detoxification. This should be of great concern considering the tremendous selection pressure weeds experience when exposed to herbicides.

1.3.3 Glutathione transferases and herbicide resistance

1.3.3.1 Introduction to the plant glutathione transferase enzyme family

Glutathione transferases (GSTs) are ubiquitous enzymes found in mammals, fungi, insects and plants. Originally discovered and so named for their ability to catalyse the detoxification of xenobiotics by conjugation with the tri-peptide γ -Glu-Cys-Gly (glutathione; GSH), they are now known to catalyse a variety of GSH-dependent reactions (Marrs, 1996; Hayes *et al.*, 2005). In plants, GSTs are a large family of enzymes with 55 and 79 *gst* genes identified in *Arabidopsis* and rice (*Oryza sp.*) respectively (Dixon and Edwards, 2010; Jain *et al.*, 2010). The large plant GST family can be sub-grouped into 7 classes with members of each class related by similarities in amino acid sequence, enzyme activity and immunodetection (Edwards *et al.*, 2000). Alongside catalytic conjugation of electrophilic substrates with GSH, studies with different members of the discrete GST classes have now shown that the plant GST family can catalyse a wide variety of GSH-dependent reactions including hydroperoxide reduction, thiol exchange, dehydroascorbate reduction and bond isomerisations. Some of these activities including GSH-conjugation and hydroperoxide reduction are catalysed by discrete GSTs across multiple classes whilst some activities are class-specific for example dehydroascorbate reduction (Dixon and Edwards, 2010).

Alongside the catalytic activities of plant GSTs these enzymes are also known to display ligand-binding functions. The first evidence for this came from the observation that plant GSTs play a direct role in anthocyanin deposition in the vacuole in both maize and petunia (*Petunia hybrida*) plants (Marrs *et al.*, 1995; Alfenito *et al.*, 1998). Since then direct evidence has accumulated for plant GSTs binding multiple plant secondary metabolites including anthocyanins, flavonoids, fatty acids, porphyrinogens and phytoalexins (Mueller *et al.*, 2000; Cummins *et al.*, 2003; Dixon *et al.*, 2008; Dixon and Edwards, 2009; Dixon *et al.*, 2011). Whilst still not fully understood, it appears that these interactions may help to stabilise and/or sequester these reactive molecules *in planta*.

Two plant GST classes, the phi (F; GSTF) and tau (U; GSTU), constitute a large proportion of *gst* genes (for example 42 of the 55 *Arabidopsis* GSTs) and are plant-specific. Studies of plant GSTs have shown that these two classes are widely responsible for herbicide detoxification *in planta* (Cummins *et al.*, 2011). The roles of plant GSTs in herbicide detoxification shall now be discussed.

1.3.3.2 GST-mediated herbicide detoxification in crop species

In plants, GST activity was first discovered in 1970 when studying maize plants able to detoxify the herbicide atrazine. A maize enzyme was purified and shown to detoxify the herbicide by nucleophilic displacement of the aryl chlorine atom with GSH, with further studies demonstrating that increases in this activity correlated well with atrazine tolerance in different maize cultivars (Frear and Swanson, 1970; Shimabukuro *et al.*, 1971) (Figure 9).

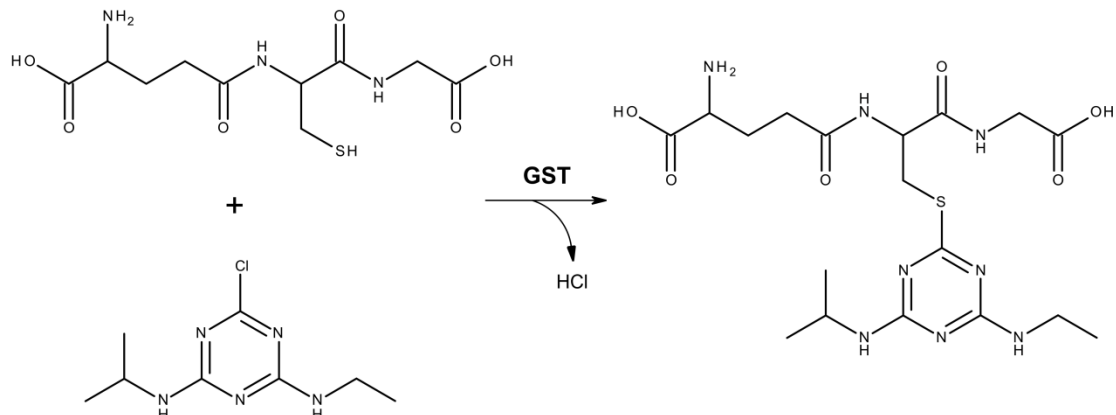


Figure 9: GST-catalysed detoxification of atrazine in plants. The photosystem II inhibitor atrazine can be detoxified in plants via conjugation with glutathione (top left) and displacement of the atrazine aryl chlorine. This was first demonstrated in atrazine-tolerant maize (Frear and Swanson, 1970).

Following from the first discovery of GST-mediated herbicide metabolism in 1970, extensive studies in crop plants have demonstrated that GSTs from the GSTF and GSTU classes can detoxify compounds from multiple herbicide classes with different sites-of-action by conjugation with GSH. The combined plethora of GSTF and GSTU isoenzymes can conjugate a variety of distinct herbicide structures with GSH, such that GSH-conjugation may simply displace a halogen atom as is the case with atrazine and alachlor in maize (Frear and Swanson, 1970; Mozer *et al.*, 1983; O'Connell *et al.*, 1988) or may result in cleavage of the herbicide into two distinct

moieties as is the case with fomesafen and fenoxaprop acid in soybean (*Glycine max*) and wheat respectively (Tal *et al.*, 1993; Andrews *et al.*, 1997) (Figure 10).

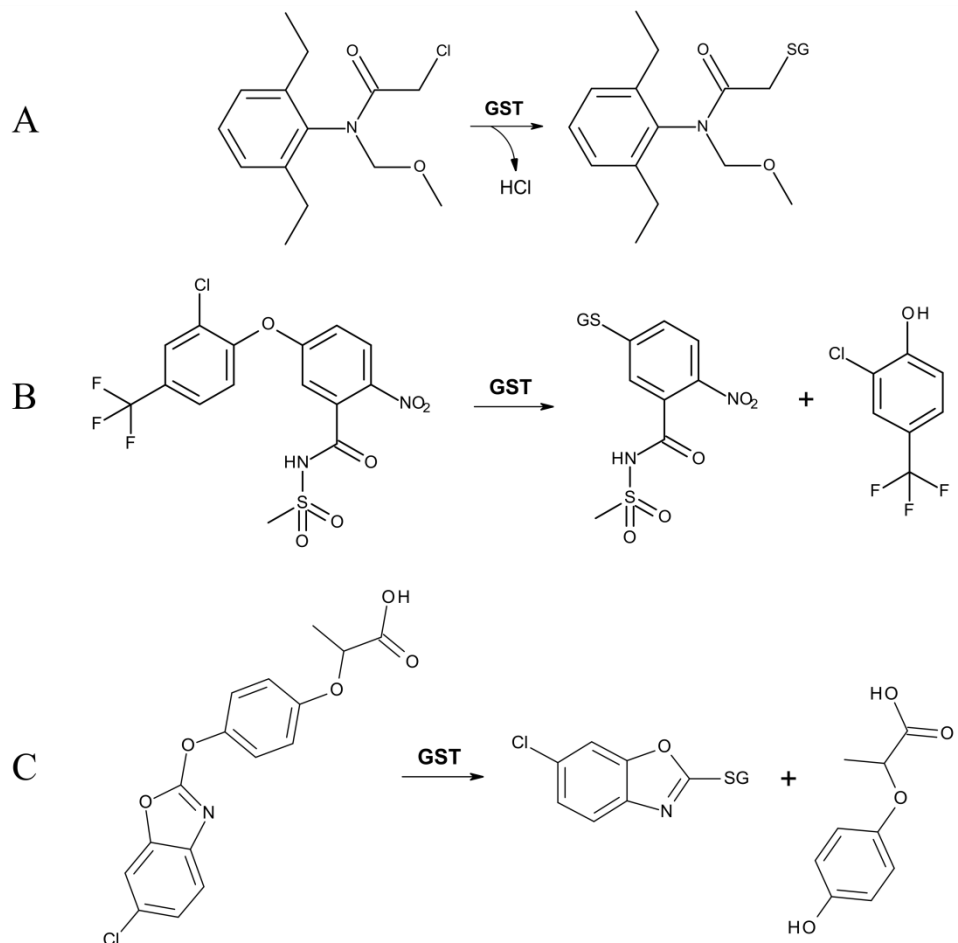


Figure 10: Detoxification of multiple herbicide classes by GST-catalysed glutathione conjugation in crop plants. (A) Alachlor detoxification (chloroacetanilide class) in maize, (B) fomesafen detoxification (diphenylether class) in soybean and (C) fenoxaprop detoxification (aryloxyphenoxypropionate class) in wheat (Mozer *et al.*, 1983; O'Connell *et al.*, 1988; Tal *et al.*, 1993; Andrews *et al.*, 1997). Alachlor, fomesafen and fenoxaprop inhibit fatty acid synthesis, protoporphyrinogen oxidase and acetyl-coA carboxylase respectively *in planta*.

In all cases, these studies used plant species with different herbicidal tolerances to demonstrate that increased tolerance correlated with increased conjugation of the herbicide with GSH. A study by Hatton *et al.* demonstrated that in maize and the herbicide-sensitive weed species giant foxtail (*Setaria faberi*) this was consistent with maize expressing 20-fold greater levels of herbicide-detoxifying GSTs compared to the weed (Hatton *et al.*, 1999). Some of these enzymes can also use the closely-related thiols hydroxymethylglutathione (γ -Glu-Cys-Ser; hmGSH) and homoglutathione (γ -Glu-Cys-Ala; homoGSH), present in wheat and predominant in

soybean respectively, in place of GSH in these detoxification reactions (Skipsey *et al.*, 1997; Cummins *et al.*, 2009).

The study by Mozer *et al.* to isolate the GSTs responsible for alachlor detoxification in maize found two distinct active fractions during enzyme purification, with each enzyme composed of two GST subunits (Mozer *et al.*, 1983). This demonstrated that GSTFs and GSTUs assemble as dimers as is known to be the case for the vast majority of mammalian GSTs (Armstrong, 1997). Furthermore, one fraction appeared to contain a homodimer composed of two 29 kDa subunits whilst the other fraction contained a heterodimer composed of 29 kDa and 27 kDa subunits (Mozer *et al.*, 1983). Therefore GSTs responsible for herbicide detoxification could assemble and operate as both homo- and heterodimers.

Continued studies in maize identified further herbicide-detoxifying GST homo- and heterodimers. It was found that only subunits within the same GST class can form dimers (Dixon *et al.*, 1999) and that subunit composition plays a key role in determining catalytic activity of the dimer towards different xenobiotic substrates including herbicides (Irzyk and Fuerst, 1993; Dixon *et al.*, 1997; Dixon *et al.*, 1998; Sommer and Boger, 1999) (Figure 11).

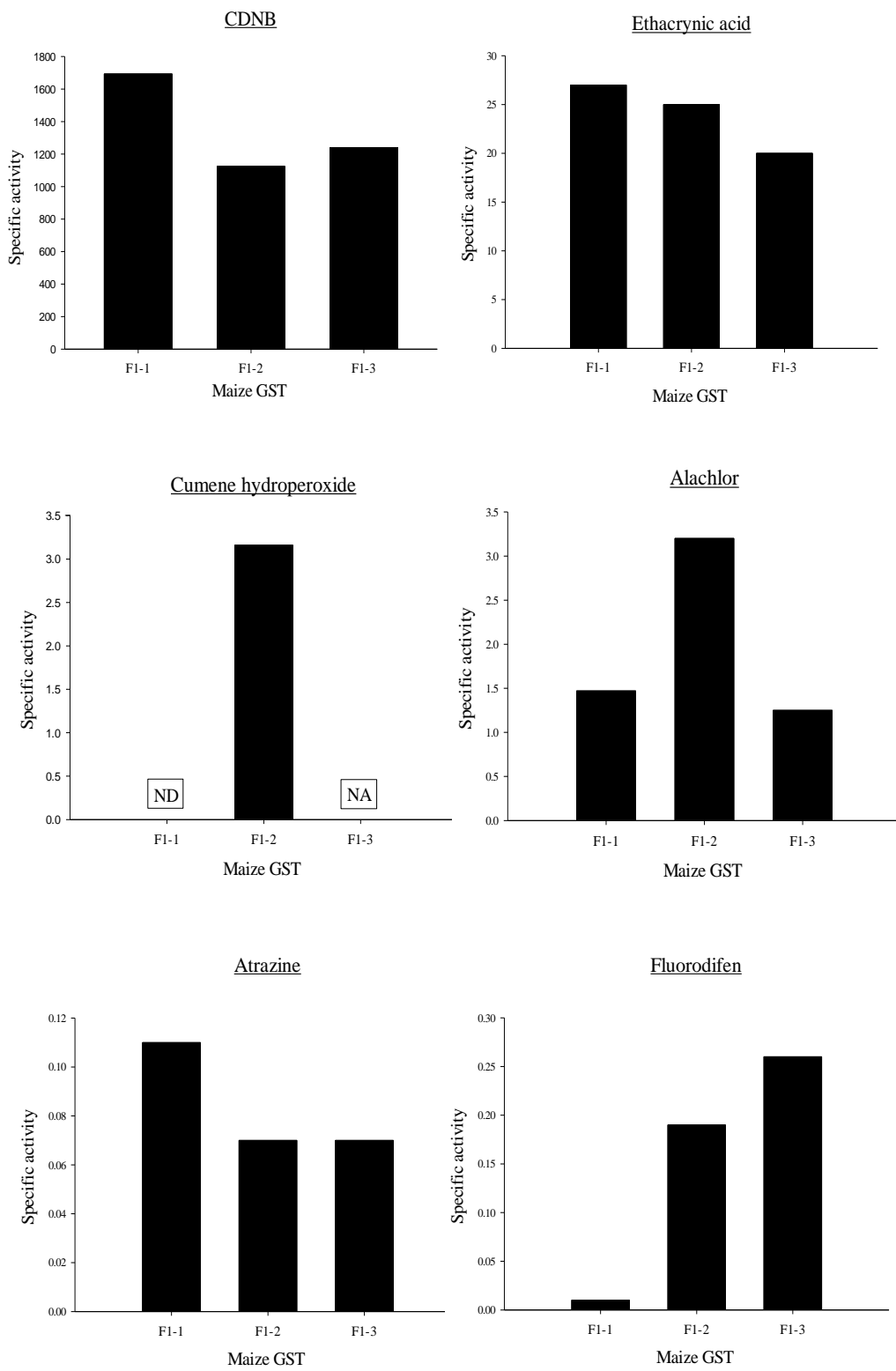


Figure 11: GST subunit composition determines catalytic substrate specificities as demonstrated in maize.
 Purified ZmGSTF1-1 homodimer, ZmGSTF1-2 heterodimer and ZmGSTF1-3 heterodimer were tested for activity with a range of substrates: the xenobiotics 1-chloro-2,4-dinitrobenzene (CDNB) and ethacrynic acid, cumene hydroperoxide and the herbicides alachlor (chloroactenilide class), atrazine (triazine class) and fluorodifen (diphenylether class). Specific activities are expressed as nkats mg^{-1} protein. ND – not detected. NA – not assayed. Data re-formatted from Dixon *et al.* (1997).

The activity of maize heterodimer *ZmGSTF1-2* to use GSH to detoxify a non-natural hydroperoxide (cumene hydroperoxide) (glutathione peroxidase activity; GPOX) (Figure 11) was a particularly interesting discovery as at that time it was known that some herbicides primary mode of action was the generation of reactive oxygen species causing extensive damage to cellular membranes by peroxidation of membrane lipids (Kunert *et al.*, 1985). Furthermore, detoxification of cumene hydroperoxide using GSH *in vitro* is mechanistically distinct from GSH-conjugation and does not conjugate the hydroperoxide with GSH but instead reduces the hydroperoxide to the alcohol species and generates an unstable glutathione-sulfenic acid derivative which rapidly forms oxidised glutathione (Flohe and Gunzler, 1984) (Figure 12).

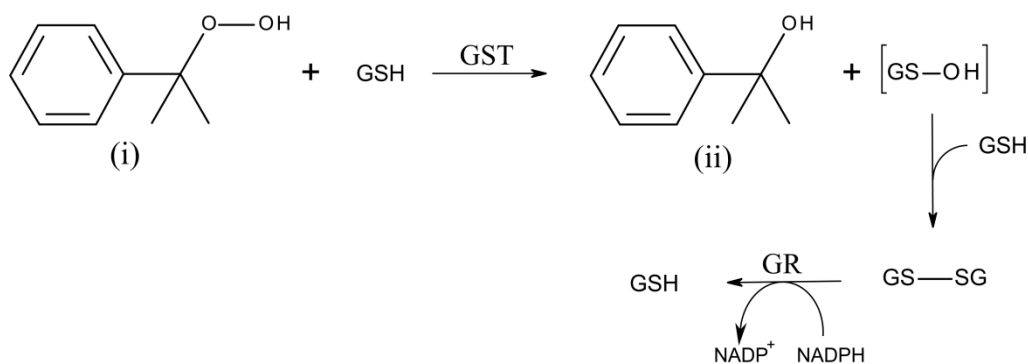


Figure 12: Scheme for *in vitro* glutathione peroxidase activity. Cumene hydroperoxide (i) is reduced to the alcohol-derivative (ii) by GST-catalysed abstraction of the terminal hydroperoxide hydroxyl group using GSH. This forms an unstable glutathione-sulfenic acid derivative (GS-OH) which reacts rapidly with another molecule of GSH to form oxidised glutathione (GSSG). This is coupled to a glutathione reductase (GR) system which uses nicotinamide adenine dinucleotide phosphate (NADPH) as a co-factor to reduce GSSG to two molecules of GSH (Flohe and Gunzler, 1984).

In support of a possible role for *ZmGSTF1-2* in detoxifying lipid hydroperoxides, studies with recombinant *ZmGSTF1-2* found that the GPOX activity of the heterodimer toward long-chain fatty acid hydroperoxides *in vitro* was 2.5-fold greater than with the non-natural substrate (Sommer and Boger, 1999). Therefore there was now evidence that, as a family, plant GSTs could not only use GSH as a co-substrate to conjugate with herbicides but that they could also use GSH as a co-factor to reduce toxic hydroperoxides formed as a consequence of herbicidal activity. Whilst maize has been used here as an example, very similar findings of GST-mediated herbicide metabolism by multiple GST homo- and heterodimers each with distinct catalytic profiles with some also possessing GPOX activity have been

demonstrated in other major crops such as wheat and soybean (Andrews *et al.*, 1997; Cummins *et al.*, 1997a; Cummins *et al.*, 2003; Andrews *et al.*, 2005).

To date, the structures of 10 plant GST homodimers have been reported 7 of which are of known herbicide-detoxifying GSTs from crops (Neufeld *et al.*, 1997a; Neufeld *et al.*, 1997b; Prade *et al.*, 1998; Thom *et al.*, 2002; Dixon *et al.*, 2003; Axarli *et al.*, 2009a; Axarli *et al.*, 2009b). All of these structures are of GSTF or GSTU homodimers and show that whilst divergent in amino acid sequence, the tertiary structures and overall topology of the GSTs are well conserved. All contain a conserved GSH binding site with a variable hydrophobic binding domain for xenobiotics thereby providing some rationale for the divergent and somewhat broad substrate specificities of the different subunits. Successful crystallisation of GST subunits in complex with GSH shows that the GSH-thiol is positioned close to a conserved serine residue in the active site of both GSTFs and GSTUs. This allows the hydroxyl group of the serine to co-ordinate to the sulphydryl hydrogen of GSH and increase the nucleophilicity of the thiol (Neufeld *et al.*, 1997a). This was confirmed with mutagenesis studies of ZmGSTF1 that could demonstrate that the catalytic serine residue is responsible for lowering the apparent pK_a of the GSH sulphydryl group such that the thiolate anion is the predominant species at physiological pH (Labrou *et al.*, 2001).

Not all crop plant GST subunits are constitutively expressed. In fact most subunits are only expressed after induction by specific chemical and/or environmental triggers (McGonigle *et al.*, 2000; Wagner *et al.*, 2002). The trigger that is perhaps best studied for GST induction is that of chemical treatment of plants with compounds called herbicide safeners (also referred to as herbicide antidotes in the early literature). Safeners are a curious and agronomically important family of compounds which, when applied to crop plants, enhance the herbicide tolerance of the crop. Many studies have demonstrated that they do this by enhancing the activity of all the major phases (I-IV) of the crop xenome and hence accelerate herbicide detoxification but that the weed xenome remains unaffected (Hatzios and Burgos, 2004), although this relatively simple concept has recently been challenged by demonstrating safening in weeds (Cummins *et al.*, 2009). Whilst a detailed review of safener chemistry and mode-of-action extends beyond this work it is worth noting

that many of the plant GST subunits associated with herbicide detoxification are expressed following safener application for instance the maize *ZmGSTF2* subunit (Mozer *et al.*, 1983; Dixon *et al.*, 1997; Cummins *et al.*, 1997a; Andrews *et al.*, 2005). It is not known how safeners induce GSTs or other xenome enzymes. Importantly though, safeners help demonstrate that plants possess not only constitutively-expressed herbicide-metabolising GSTs but also inducible genes coding for further detoxifying GST subunits.

The expression of crop GSTFs and GSTUs in transgenic host plants have provided further proof of the ability for these enzymes to elicit a herbicide-resistant phenotype. *ZmGSTF1* has been expressed in tobacco and granted the host plants resistance to alachlor via conjugation of the herbicide with GSH (Figure 10 A) (Karavangeli *et al.*, 2005). The *ZmGSTF2* subunit has been expressed in tobacco and wheat and granted the host plants resistance to alachlor via conjugation of the herbicide with GSH (Figure 10 A) with the wheat plants also demonstrating resistance to the unrelated thiocarbamate class of herbicides (Milligan *et al.*, 2001). Of the GSTUs, two subunits from soybean (*GmGSTU4* and *GmGSTU21*) have been independently expressed in tobacco and shown to confer increased herbicide resistance in the transgenic host plants. *GmGSTU4* expression in tobacco increased the resistance of the host plant to both alachlor and fluorodifen (Benekos *et al.*, 2010) both of which are known to be detoxified via conjugation with GSH by the enzyme (Axarli *et al.*, 2009b). The transgenic plants were also more resistant to oxyfluorfen, a peroxidising herbicide which is not detoxified by GSH-conjugation, with resistance suggested to be due to the known GPOX activity of *GmGSTU4* (Axarli *et al.*, 2009b; Benekos *et al.*, 2010). In a slightly different study *GmGSTU21*, known to preferentially detoxify herbicides using homoGSH rather than GSH, was co-expressed with a homoGSH synthetase enzyme in tobacco plants and shown to detoxify fomesafen via homoGSH-conjugation (using an analogous reaction mechanism as that presented in Figure 10 B using GSH) (Skipsey *et al.*, 2005).

1.3.3.3 GST-mediated herbicide detoxification in weed species

In comparison to the relatively well-studied GSTs responsible for herbicide-detoxification in crops, GSTs that perform similar roles in weed species are poorly

understood. One of the first observations of herbicide resistance in weeds due to enhanced GST-mediated herbicide detoxification was reported by Gronwald *et al.* in an atrazine-resistant biotype of the weed species velvetleaf (*Abutilon theophrasti*). The resistant biotype had no differences in herbicide uptake, nor in target-site sensitivity compared with a sensitive biotype, but rapidly accumulated the atrazine-GSH conjugate previously described in maize (Gronwald *et al.*, 1989) (Figure 9). It was quickly shown that the resistant biotype contained increased levels of GST activity toward atrazine (Anderson and Gronwald, 1991). Whilst it was suggested that this may be due to over-expression of atrazine-detoxifying GSTs, later studies suggested that it was more likely to be a mutant GST with enhanced catalytic activity toward atrazine (Plaisance and Gronwald, 1999). This has yet to be confirmed by GST isolation and sequencing. Soon after the reports of increased GST-mediated herbicide detoxification via GSH-conjugation in velvetleaf, this mechanism was also observed in foxtail (*Setaria spp.*) biotypes resistant to atrazine (Gimenez-Espinosa *et al.*, 1996) and in multiple MHR biotypes of black-grass resistant to fenoxaprop-p-ethyl (Hall *et al.*, 1997; Cummins *et al.*, 1997b). This mechanism has also more recently been reported in biotypes of late watergrass (*Echinocloa phyllopogon*) and sow thistle (*Sonchus oleraceus*) which are resistant to fenoxaprop-p-ethyl and simazine (atrazine analogue) respectively (Fraga and Tasende, 2003; Bakkali *et al.*, 2007).

Black-grass is perhaps the best-studied weed species with respect to GST-mediated herbicide detoxification and the only weed species for which the molecular basis of enhanced GST-mediated herbicide detoxification has been investigated. In black-grass, two biotypes, ‘Peldon’ and ‘Lincs E1’, were already known to be resistant to herbicides from multiple chemical classes (Moss, 1990), due in part to the up-regulation of herbicide-detoxifying CYP activities (Hyde *et al.*, 1996). These populations also demonstrated increased rates of fenoxaprop-p-ethyl detoxification to unidentified polar metabolites compared with a herbicide-sensitive biotype. Enhanced detoxification appeared independent of CYP action, as CYP inhibitors had no effect on detoxification (Hall *et al.*, 1997). In a concurrent study Cummins *et al.* used protein extracts to demonstrate that the same two MHR black-grass biotypes expressed GSTs capable of detoxifying fenoxaprop-p-ethyl via its conjugation with GSH (Figure 10 C) but this activity could not be detected in the herbicide-sensitive

biotype. Activity towards fenoxaprop-p-ethyl was similar in both MHR biotypes and correlated with the expression of two novel GSTs in the MHR biotypes recognised by an antibody raised to a herbicide-detoxifying GSTU enzyme from wheat. However, whilst the rates of fenoxaprop-p-ethyl detoxification were similar in both MHR biotypes, ‘Lincs E1’ plants were 10-fold more resistant to fenoxaprop-p-ethyl in whole-plant spray trials than ‘Peldon’ plants indicating additional mechanisms of herbicide tolerance were invoked in at least the Lincs E1 biotype (Cummins *et al.*, 1997b). Continued studies with these black-grass biotypes, using antibodies raised to the herbicide-detoxifying maize *ZmGSTF1-2* enzyme, led Cummins *et al.* to discover further GSTs, this time belonging to the phi class, which were constitutively expressed in protein extracts of both the MHR biotypes but absent in both a herbicide-sensitive biotype and an ACCase target-site resistant biotype (Cummins *et al.*, 1999). Rather than attempt to purify the GST isoforms from black-grass protein extracts, RNA was extracted from MHR biotype ‘Peldon’, reverse-transcribed to the complementary cDNA and a cDNA library constructed which when expressed in bacteria allowed the colonies to be screened for plant GSTU and GSTF enzyme isoforms using antibody detection. Using this strategy Cummins *et al.* identified three clones encoding polypeptides that were recognised by the anti-GSTU-serum and four clones encoding polypeptides that were recognised by the anti-GSTF-serum (Figure 13). Within each class the polypeptides were highly similar in amino acid sequence but not identical. Recombinant expression and purification of the proteins demonstrated that they co-migrated with the immunodetected bands present in MHR protein extracts and hence what may at first be interpreted as the expression of one novel GST isoform in protein extracts may actually be a composition of highly similar polypeptides. Recombinant enzymes were assayed for activity towards a range of substrates including general xenobiotics, herbicides and hydroperoxides. GSTs within each class had very similar activity profiles. *AmGSTU* enzymes had appreciable activity towards the herbicides fluorodifen and fenoxaprop-p-ethyl and no activity towards hydroperoxides. Conversely *AmGSTF* enzymes had little activity towards the herbicide substrates, but were highly active towards hydroperoxide substrates, being 4-fold more active towards a long-chain fatty acid hydroperoxide substrate compared with cumene hydroperoxide (Cummins *et al.*, 1999).

A

<i>AmGSTU1a</i>	MAGGNDLKL LGTWPSPYAIRVKLALAHKGLSYEYAEEDLANKSELLSSNPVHRKIPVLI	60
<i>AmGSTU1b</i>	MAGGDDLKL LGTWPSPYAIRVKLALAHKGLSYEYAEEDLANKSELLSSNPVHRKIPVLI	60
<i>AmGSTU1c</i>	MAGGDDLKL LGTWPSPYAIRVKLALAHKGLSYEYAEEDLANTSELLSSNPVHKKIPALI	60
	*****:*****:*****:*****:*****:*****:*****:*****:*****:*****:*****:	*****:*****:*****:*****:*****:*****:*****:*****:*****:*****:*****:
<i>AmGSTU1a</i>	HNGPVCESNIILEYIDEAFAGRSILPADPYERAMARFWAAYVDDKLLAAWATMVFKGKT	120
<i>AmGSTU1b</i>	HNGPVCESNIILEYIDEAFAGPSILPADPYERAMARFWAAYVDDKLLAAWATMVFKGKT	120
<i>AmGSTU1c</i>	HNGVAVCESNIIVEYIDEAFAGPSILPADPYERAIRFWAAYVDDKLFGAWATMLFSGKT	120
	*****:*****:*****:*****:*****:*****:*****:*****:*****:*****:*****:	*****:*****:*****:*****:*****:*****:*****:*****:*****:*****:*****:
<i>AmGSTU1a</i>	EEEKLEGKKALFAALETLEGALAKCSDGKDFFGGDTVGLVDMVLGSHLSFLKATEAMAGE	180
<i>AmGSTU1b</i>	EEEKLEGKKALFAALETLEGALAKCSDGKDFFGGDTVGLVDMVLGSHLSFLKATEAMAGE	180
<i>AmGSTU1c</i>	EEEKLEGKNALFAALETLEGALAECS DGKDFFGGHTVGLVDMALGSHLSWLKATEVMAGE	180
	*****:*****:*****:*****:*****:*****:*****:*****:*****:*****:*****:	*****:*****:*****:*****:*****:*****:*****:*****:*****:*****:*****:
<i>AmGSTU1a</i>	EILRSRTQLLAAMMARFSELDAAKAALPDVDRVVEFKMRQARLAAAAAAASNN	235
<i>AmGSTU1b</i>	EILRSRTQLLAAMMARFSELDAAKAALPDVDRVVEFAKMRQARLAAAAAAASNN	235
<i>AmGSTU1c</i>	EILRSRTQLLAAMMARFSELYAAKAALPDVDR---MAKMRQERLAAAAAA---	229
	*****:*****:*****:*****:*****:*****:*****:*****:*****:*****:*****:	*****:*****:*****:*****:*****:*****:*****:*****:*****:*****:*****:

B

<i>AmGSTF1a</i>	MAPVKVFGPAMSTNVARVILCLEEVGAEEYEVVNIDMKGQEHKSPPEHLARNPFGQIPAFQD	60
<i>AmGSTF1b</i>	MAPVKVFGPAMSTNVARVILCLEEVGAEEYEVVNIDMKSQEHKSPPEHLARNPFGQIPAFQD	60
<i>AmGSTF1c</i>	MAPVKVFGPAMSTNVARTLCLEEVGAEEYEVVNIDFNTMEHKSPPEHLARNPFGQIPAFQD	60
<i>AmGSTF1d</i>	MAPVKVFGPAMSTNVARTLFLEEVGAEEYEVVNIDFNTMEHKSPPEHLARNPFGQIPAFQD	60
	*****:*****:*****:*****:*****:*****:*****:*****:*****:*****:*****:	*****:*****:*****:*****:*****:*****:*****:*****:*****:*****:*****:
<i>AmGSTF1a</i>	GDLLLWESRAISKYVLRKYKKDEVDLLREGNLEEAAMVDVWTEVEAHTYNPALSPIVYQC	120
<i>AmGSTF1b</i>	GHLLLWESRAISKYVLRKYKKDEVDLLREGNLEEAAMVDVWTEVEAHTYNPALSPIVYQC	120
<i>AmGSTF1c</i>	GDLLLWESRAISKYVLRKYKTDEVDLLRESNLEEAAMVDVWTEDAHTYNPALSPIVYQC	120
<i>AmGSTF1d</i>	GDLLLWESRAISKYVLRKYKTDGVDLLREGNLEEAAMVDVWTEVEAHTYNPALSPIVYQC	120
	*****:*****:*****:*****:*****:*****:*****:*****:*****:*****:*****:	*****:*****:*****:*****:*****:*****:*****:*****:*****:*****:*****:
<i>AmGSTF1a</i>	LIGPMMRGVPTDEKVVAESLEKLKKVLEVYEARLSKHSYLAGDFVSFADLNHFPTFYFM	180
<i>AmGSTF1b</i>	LIGPMMRGVPTDEKVVAESLEKLKKVLEVYEARLSKHSYLAGDFVSFADLNHFPTFYFM	180
<i>AmGSTF1c</i>	LFNPMMRGLPTDEKVVAESLEKLKKVLEVYEARLSKHSYLAGDFVSFADLNHFPTFYFM	180
<i>AmGSTF1d</i>	LINPMMRGIPTDEKVVAESLEKLKKVLEVYEARLSKHSYLAGDFASFADLNHFPTFYFM	180
	*****:*****:*****:*****:*****:*****:*****:*****:*****:*****:*****:	*****:*****:*****:*****:*****:*****:*****:*****:*****:*****:*****:
<i>AmGSTF1a</i>	ATPHAALFDSPHVKAWWDRLMARPAVKIAATMVPKA	219
<i>AmGSTF1b</i>	ATPHAALFDSPHVKAWWDRLMARPAVKIAATMVPKA	219
<i>AmGSTF1c</i>	ATPHAALFDSPHVKAWWDRLMARPAVKIAATMVPKA	219
<i>AmGSTF1d</i>	ATPHAALFDSPHVKAWWERLMARPAVKIAATMVPKA	219
	*****:*****:*****:*****:*****:*****:*****:*****:*****:*****:*****:	*****:*****:*****:*****:*****:*****:*****:*****:*****:*****:*****:

Figure 13: Black-grass GST polypeptide sequences derived from the recombinant expression of an MHR black-grass cDNA library. (A) Polypeptide sequences of three clones (a-c) recognised by antibodies raised to a herbicide-detoxifying GSTU homodimer from wheat. (B) Polypeptide sequences of four clones (a-d) recognised by antibodies raised to a herbicide-detoxifying GSTF heterodimer from maize. *Am* – *Alopecurus myosuroides*. Sequences derived from Cummins *et al.* (1999). Sequence names have been updated from Cummins *et al.* (1999) to reflect the revised GST nomenclature proposed by Edwards *et al.* (2000).

In combination with these experiments, Cummins *et al.* demonstrated that herbicide-sensitive black-grass treated with a range of herbicides accumulated hydroperoxides irrespective of the herbicide mode-of-action whilst MHR black-grass maintained hydroperoxide content at a basal level (Figure 14). These results lead Cummins *et al.* to conjecture that a downstream consequence of herbicide mode-of-action, irrespective of the target-site, may be damaging peroxidation of cellular membranes which MHR plants had evolved to tolerate by the constitutive expression of GPOX-active *AmGSTF1* enzymes (Cummins *et al.*, 1999).

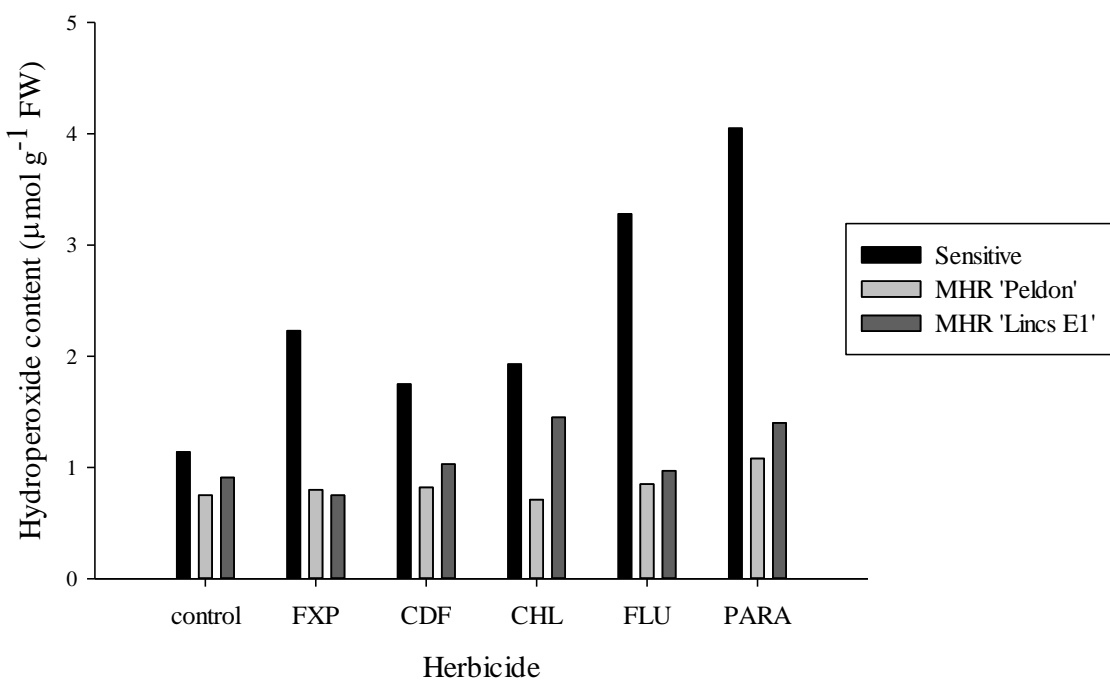


Figure 14: Hydroperoxide accumulation in herbicide-sensitive and MHR biotypes of black-grass after herbicide treatment. Cut shoots of all biotypes were treated for 24 hours with either: fenoxaprop-p-ethyl, FXP, ACCase inhibitor; clodinafop-propargyl, CDF, ACCase inhibitor; chlorotoluron, CHL, photosystem I inhibitor; fluorodifen, FLU, PPO inhibitor; paraquat, PARA, photosystem II inhibitor or formulation-only (control). Shoots were then analysed for hydroperoxide content and expressed as standardised $\mu\text{mol g}^{-1}$ fresh weight (FW) tissue. Data re-formatted from Cummins *et al.* (1999).

Exposure of herbicide-sensitive plants to biotic and abiotic stresses induced the expression of *AmGSTF1* proteins, indicating that *AmGSTF1* could be transiently expressed under stress conditions and hence that MHR plants appeared to be constitutively expressing the proteins by an unknown mechanism. Analysis of genomic DNA did not indicate that the gene had been amplified. However, analysis of total RNA extracted from un-treated herbicide-sensitive and MHR plants easily detected *AmGSTF1* transcripts in MHR plants that were absent in the sensitive plants (Cummins *et al.*, 1999).

In summary, GST-mediated herbicide resistance in black-grass appears to be due to the evolution of mechanism/s that allows the constitutive expression of stress-inducible GSTs from both GSTU and GSTF classes. Expression of these enzymes appears to grant multiple mechanisms of protection on the MHR plants with GSTU enzymes directly able to detoxify a subset of herbicide chemistries with GSH whilst

GSTF enzymes can detoxify toxic hydroperoxide compounds which may form as a downstream consequence of herbicide treatment (Cummins *et al.*, 1997b; Cummins *et al.*, 1999).

To date similar studies to identify GSTs responsible for herbicide detoxification in other weed species have not been reported. A recent study in Italian rye-grass (*Lolium multiflorum*) reported GST activity towards herbicides in crude protein extracts but this was not investigated in relation to biotypes with different herbicide sensitivities (Del Buono and Ioli, 2011).

1.3.4 Glycosyltransferases, transporter proteins and herbicide resistance

In comparison to studies of the roles for CYPs and GSTs in mediating herbicide resistance, far less is known regarding the roles for glycosyltransferases or transporter proteins.

1.3.4.1 Glycosyltransferases

Glycosyltransferases (GTs) are a large family of enzymes in plants responsible for the conjugation of acceptor molecules, including flavonoids, hormones and xenobiotics, with an activated UDP-sugar moiety (Bowles *et al.*, 2005). In crops, glycosylation plays a clear role in the metabolism of multiple herbicides including chlorsulfuron and diclofop-methyl (Shimabukuro *et al.*, 1979; Sweetser *et al.*, 1982). In both of these cases, the parent herbicide is first hydroxylated by CYP enzymes followed by glycosylation of the newly-introduced hydroxyl group. It is also possible for herbicides to be detoxified by glycosylation of free amine groups as reported for amiben and picloram (Swanson *et al.*, 1966; Frear *et al.*, 1989).

In weeds, the extent to which enhanced glycosylation is required to elicit herbicide resistance is not clear. For instance, in the cases of chlorsulfuron and diclofop-methyl, evidence has suggested that CYP-mediated hydroxylation of the parent herbicide, prior to glycosylation, is the key step contributing to herbicide resistance (Christopher *et al.*, 1991; Ahmad-Hamdan *et al.*, 2013). However, in black-grass GT activity is increased in MHR biotypes that are also known to have elevated CYP

and GST activities (Brazier *et al.*, 2002). Induced GT activities in other herbicide resistant weed species is yet to be reported.

1.3.4.2 Transporter proteins

Two membrane-bound transporter protein systems have been reported for the transport of herbicide conjugates into the vacuole for further degradation. In barley, hydroxyprimisulfuron-glucoside has been shown to be transported into isolated vacuoles by ATP-binding cassette (ABC) transporter proteins (Klein *et al.*, 1996). Whilst in red beet (*Beta vulgaris*), chlorsulfuron-glucoside is transported into the vacuole by ATP-dependent proton antiporter proteins (Bartholomew *et al.*, 2002). It is not yet clear if the two systems for the clearance of herbicide-glucoside conjugates are species- or herbicide-dependent, nor if they co-exist and co-ordinate in the same plant. To date, glutathionylated herbicides have been shown to be transported into the vacuole by ABC transporter proteins (Martinoia *et al.*, 1993; Bartholomew *et al.*, 2002; Rea, 2007). The isolation and *in vitro* characterisation of two *Arabidopsis* ABC transporter proteins, *AtMRP1* and *AtMRP2*, capable of transporting glutathionylated herbicides has found that these proteins closely resemble multi-drug resistance transporter proteins in mammals (Lu *et al.*, 1997; Lu *et al.*, 1998). Furthermore, over-expression of the ABC transporter, *AtPgp1*, in *Arabidopsis* plants enhanced the plants resistance to multiple herbicides with different modes-of-action. This included herbicides that are not known to be detoxified by glycosylation or glutathionylation in plants and may instead be as a result of a more generalised efflux mechanism with the parent compound (Windsor *et al.*, 2003).

In weeds, the equivalent studies to isolate and characterise transporter proteins involved in herbicide metabolism have not been reported. However, an emerging mechanism of evolved resistance is that of altered translocation and/or sequestration in the plant. Significantly, reduced translocation of glyphosate, the world's most commercially-exploited herbicide, has now been observed in multiple resistant *Lolium* and *Conyza* biotypes (Powles and Yu, 2010).

1.4 Herbicide resistant black-grass (*Alopecurus myosuroides*)

Alongside annual rye-grass, black-grass is the most well-studied weed species to date with regards to herbicide resistance. Black-grass is an obligate out-crossing species and herbicide resistant populations are particularly prevalent in the UK and Northern Europe (Moss *et al.*, 2007). For instance, in the UK an estimated 80 % of arable farmland suffers from herbicide-resistant black-grass infestation (Moss *et al.*, 2011). Black-grass has proven remarkably adaptable to exposure to herbicides and multiple geographically-discrete populations have evolved TSR and NTSR resistance mechanisms. For instance, as a species, black-grass is known to have evolved a total of 2 and 12 point mutations in ACCase and ALS enzymes respectively (Jang *et al.*, 2013; Tranel *et al.*, 2013), with newly-evolved point mutations still being identified (Kaundun *et al.*, 2013). Furthermore, single black-grass populations are known to have evolved point mutations in both ACCase and ALS enzymes concurrently (Bailly *et al.*, 2012). Black-grass also readily evolves NTSR mechanisms that can render the plants resistant to multiple herbicides with different modes-of-action (Moss, 1990; Delye *et al.*, 2011). These mechanisms include enhanced herbicide metabolism mediated by CYPs and GSTs as well as the expression of GSTs that function as GPOXs and up-regulated GT activities (Hyde *et al.*, 1996; Hall *et al.*, 1997; Cummins *et al.*, 1997b; Cummins *et al.*, 1999; Brazier *et al.*, 2002). Alarmingly, NTSR in black-grass can lead to resistance to herbicides that the plants have never previously been exposed to, for instance resistance to the recently commercialised herbicide pinoxaden (Delye *et al.*, 2011). Therefore, elucidating the molecular mechanisms that underpin NTSR in black-grass is essential to develop rational strategies to combat herbicide resistance in this species.

1.5 Background and aims to the project

The project described in this thesis builds from the discovery by Cummins *et al.* of the novel expression of four highly homologous phi-class GST (GSTF) isoforms in multiple herbicide resistant biotypes of the weed species black-grass (Cummins *et al.*, 1999) (see also Chapter 1 section 1.3.3.3). Whilst some plant GSTs are known to detoxify herbicides by conjugating these phytotoxic compounds with glutathione and/or glutathione homologues, characterisation of one of these isoforms (*AmGSTF1c*) found that *AmGSTF1* has very limited ability to catalyse these reactions. Instead *AmGSTF1* functions *in vitro* as a glutathione peroxidase (GPOX) enzyme and can detoxify organic and long-chain fatty acid hydroperoxides to the less toxic alcohol species. This correlates with the ability of MHR biotypes to maintain cellular hydroperoxide concentrations at a basal level following treatments with herbicides of different modes-of-action. This is unlike herbicide sensitive biotypes of black-grass which accumulate significant levels of damaging hydroperoxides following the same treatments. Therefore it was proposed that the constitutive expression of *AmGSTF1* isoforms in MHR black-grass may be linked to enhanced herbicide tolerance by protecting the plant from oxidative injury caused by herbicide treatment (Cummins *et al.*, 1999).

To better understand the role of *AmGSTF1* in MHR, *AmGSTF1c* has been constitutively expressed in a transgenic host plant (*Arabidopsis thaliana*) with the resulting transgenic plants tested for changes in herbicide tolerance. Multiple independent *AmGSTF1*-expressing lines displayed enhanced herbicide tolerance to herbicides with multiple modes-of-action including chlorotoluron, a herbicide which cannot be detoxified by GSTs (Figure 15) (Dr. I. Cummins and Prof. R. Edwards, unpublished work at the start of this project). Analysis of the biochemical phenotype of the *AmGSTF1*-expressors found increases in GST, GPOX, thiol transferase and glycosyltransferase activities as well as increases in endogenous GST-mediated detoxification of alachlor and atrazine as these are not substrates for *AmGSTF1* (Cummins *et al.*, 1999). *AmGSTF1*-expressors also accumulated greater levels of flavonoids and anthocyanins, plant secondary metabolites associated with antioxidant defence systems (Dr. I. Cummins and Prof. R. Edwards, unpublished work at the start of this project).

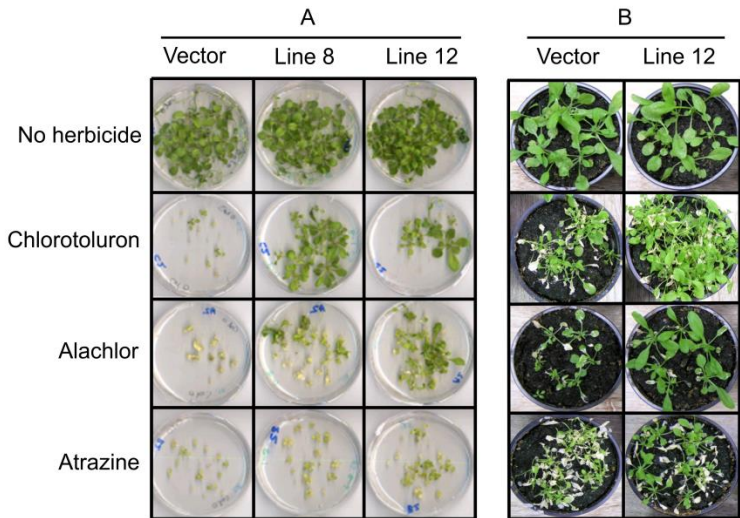


Figure 15: Enhanced herbicide tolerance of transgenic *Arabidopsis* plants expressing *AmGSTF1*. (A) Plants were germinated on agar containing 2 µM herbicides (chloroturon, alachlor or atrazine) or an equivalent volume of acetone (no herbicide). (B) Plants were sprayed with chloroturon (30 g ai hectare⁻¹), alachlor (1200 g ai hectare⁻¹), atrazine (30 g ai hectare⁻¹) or formulation-only. Plants were assessed 9 days after treatment. Vector – transgenic *Arabidopsis* plants expressing the transformation vector only. Line 8 – a mid-level *AmGSTF1*-expressing line as judged by Western blotting. Line 12 - a high-level *AmGSTF1*-expressing line as judged by Western blotting. ai – active ingredient. Data shown with the permission of Dr. I. Cummins and Prof. R. Edwards.

Hence this startling and unexpected set of results demonstrated that not only could *AmGSTF1* enhance herbicide tolerance in a transgenic host plant to herbicides with different modes-of-action but that *AmGSTF1* also co-ordinated the up-regulation of a subset of endogenous detoxification enzymes and the accumulation of protective secondary metabolites.

Of strong significance, these results mirrored the biochemical changes that had already been observed in MHR black-grass plants relative to wild-type sensitive plants (Cummins *et al.*, 2009). Therefore these results would strongly suggest that *AmGSTF1* plays a key role in eliciting MHR in both a transgenic host plant and in black-grass.

In parallel with these studies a chemical library was screened for compounds capable of inhibiting *AmGSTF1c* and of reversing the MHR black-grass phenotype. Compounds (100 µM) were each incubated with recombinant *AmGSTF1c* *in vitro* before assaying for enzyme activity alongside which each compound was sprayed onto MHR black-grass prior to an application of herbicide. The preliminary *in vitro* studies identified 4-chloro-7-nitro-benzoxadiazole (NBD-Cl; Figure 16) as an

AmGSTF1 inhibitor with concurrent spray trials demonstrating that the compound was capable of restoring herbicide efficacy in black-grass (Figure 17).

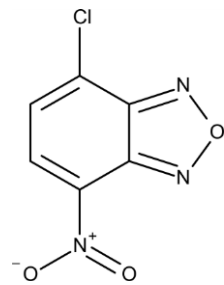


Figure 16: Chemical structure of 4-chloro-7-nitro-benzoxadiazole (NBD-Cl).

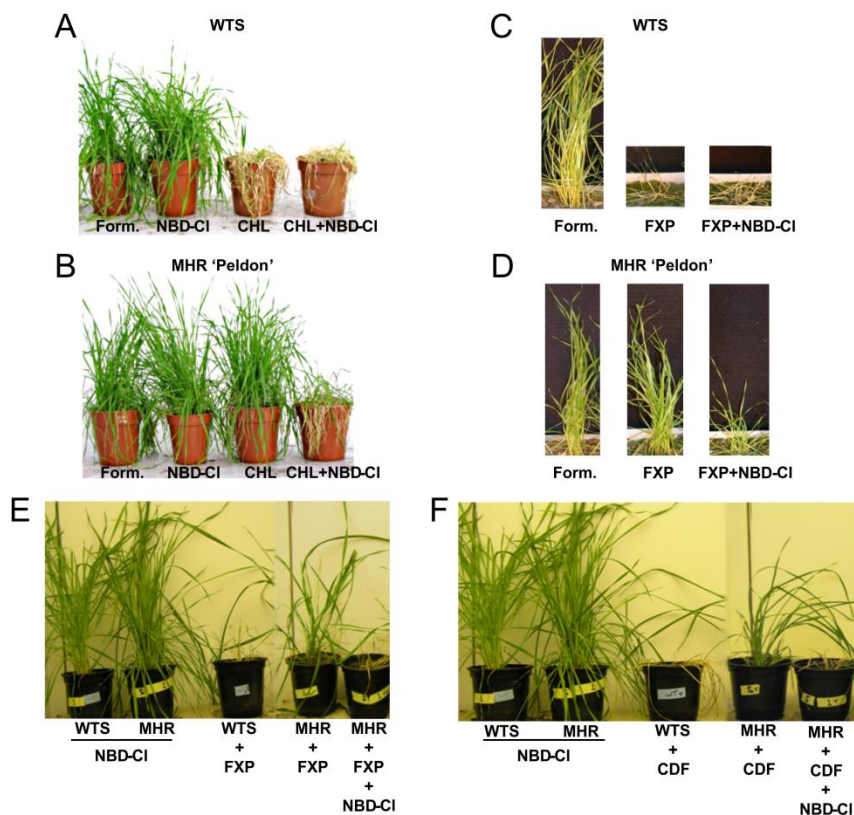


Figure 17: Effect of 4-chloro-7-nitro-benzoxadiazole on herbicide resistance in black-grass when treated with the herbicides chlorotoluron, fenoxaprop-p-ethyl or clodinafop-propargyl. (A and B) For studies with chlorotoluron, (A) wild-type sensitive (WTS) and (B) multiple herbicide resistant (MHR) Peldon black-grass plants were treated at 12 d with either formulation or 4-chloro-7-nitro-benzoxadiazole (NBD-Cl; 270 g ai hectare⁻¹), before an application of either formulation only (Form) or chlorotoluron (CHL; 500 g ai hectare⁻¹). (C and D) For studies with fenoxaprop-p-ethyl formulated as Cheetah Super, (C) WTS or (D) MHR Peldon plants were pre-treated with NBD-Cl (80 g ai hectare⁻¹), before spraying with formulation control (Form) or fenoxaprop-p-ethyl (XP; 85 g ai hectare⁻¹). (E and F) For studies with the independent MHR Spain black-grass biotype, WTS and MHR Spain black-grass plants were pre-treated with NBD-Cl (270 g ai hectare⁻¹) or formulation only followed by a treatment with (E) FXP (165 g ai hectare⁻¹) or formulation only or (F) clodinafop-propargyl (CDF; 250 mL hectare⁻¹), as the commercial formulation Topik, or formulation only. In all cases plants were evaluated for phytotoxic injury 21 d postherbicide application. ai – active ingredient. Data shown with the permission of Dr. I. Cummins and Prof. R. Edwards.

Analysis of NBD-Cl treated *AmGSTF1* by mass spectrometry revealed that the enzyme had been alkylated by the compound on a specific cysteine residue (Cys120) via nucleophilic displacement of the NBD-Cl chloride ion (Dr. I. Cummins and Prof. R. Edwards, unpublished work at the start of this project).

Aims of this project

The prior and unpublished work on *AmGSTF1* raised many interesting questions about the mechanism of action of the enzyme and its role in MHR. Ultimately this project aimed to elucidate the mechanism by which *AmGSTF1* elicited an MHR phenotype in a transgenic host plant. To do this, the following articles were explored:

- i. The properties of the multiple *AmGSTF1* isoforms first discovered by Cummins *et al.* (Cummins *et al.*, 1999).
- ii. The mechanism by which *AmGSTF1* up-regulated endogenous antioxidant enzyme activities and caused flavonoid accumulation in transgenic *Arabidopsis* plants.
- iii. The relative contributions of catalytic activity and Cys120 for an MHR phenotype.
- iv. The interaction between *AmGSTF1* and NBD-Cl.
- v. The properties of *AmGSTF1* orthologues in crops and weeds.

This project used a combination of *in vitro* biochemical studies and transgenesis studies to answer the questions proposed.

The properties of *AmGSTF1* isoforms were explored *in vitro* and the inhibition of *AmGSTF1* by NBD-Cl more fully characterised. The transcriptomes of transgenic *Arabidopsis* plants expressing *AmGSTF1* (generated by Dr. I. Cummins) were analysed for perturbations related to the observed changes in endogenous antioxidant enzyme activities and flavonoid accumulation (**Chapter 3**).

A catalytically-retarded *AmGSTF1* mutant and a mutant lacking Cys120 were generated and used to explore the necessity of GPOX activity and Cys 120 for an MHR phenotype by expressing these enzymes in transgenic *Arabidopsis* plants and

challenging these plants with herbicides. Transgenic plants were also tested for the changes in endogenous antioxidant enzyme activities and flavonoid accumulation seen with *AmGSTF1*-expressors. Furthermore the Cys120 mutant was used *in vitro* to probe the mechanism of inhibition of *AmGSTF1* by NBD-Cl (**Chapter 4**).

An *AmGSTF1* orthologue from maize has been characterised *in vitro* and expressed in transgenic *Arabidopsis* plants and tested in an analogous manner to the *AmGSTF1* mutants. An orthologue from the damaging weed species annual rye-grass has also been isolated and characterised *in vitro* alongside *AmGSTF1* (**Chapter 5**).

The conclusions from these studies and new understanding for the role of *AmGSTF1* and orthologues in MHR as a product of this work is then discussed (**Chapter 6**).

Chapter 2 Materials and Methods

2.1 Materials

Unless stated otherwise, all chemicals were of analytical grade and purchased from Sigma-Aldrich. All molecular biology reagents and enzymes were purchased from New England Biolabs, Promega or Thermo Scientific. Oligonucleotide primers were synthesized and purchased from Eurofins MWG Operon. All buffers were formulated in ultrapure water ($18.2\text{ M}\Omega\text{ cm}^{-1}$) followed by filtration and de-gassing. All reagents were used as solids or formulated in ultrapure water. All growth media was autoclaved prior to use.

2.2 Instrumentation

Polymerase chain reactions were performed using a Mastercycler® gradient thermal cycler (Eppendorf, Germany). Protein purification and desalting was performed using an ÄKTA-FPLC system (GE Healthcare, UK). Spectrophometric assays were measured using a Shimadzu UV-1800 UV spectrophotometer (Shimadzu Corporation, Japan). High-performance liquid chromatography was performed using a Thermo SpectraSystem equipped with ChromQuest 4.2 software (Thermo Fisher Scientific, USA). Mass spectrometry was performed using a HCT Ultra EDT II mass spectrometer equipped with Compass DataAnalysis software (Bruker Daltonics, USA).

2.3 Cloning techniques

2.3.1 Polymerase chain reaction (PCR)

For PCR, a reaction mix containing 1x *Pfu* DNA polymerase buffer (supplied by the manufacturer), 5 µL template DNA, 300 nM forward primer, 300 nM reverse primer, 1.25 U *Pfu* DNA polymerase and 200 µM dNTPs was prepared, in a total volume of 50 µL. Typically, samples were denatured at 95 °C for 2 min and then exposed to 30 heating cycles composed of: 1 min 95 °C, 30 s 55 °C, 1 min 72 °C. This was followed by a final extension step at 72 °C for 2 min.

2.3.2 Separation of DNA molecules using agarose gel electrophoresis

Agarose-TAE gels were prepared by first dissolving 0.8 % (w/v) agarose in TAE buffer (40 mM Tris-acetate, 1 mM EDTA, pH 8.0). The solution was then cooled to room temperature, followed by the addition of 0.00004 % (v/v) ethidium bromide. The solution was poured into a pre-assembled cast and allowed to set. Once the gel was set, the comb was carefully removed to reveal the wells and the tank filled with TAE buffer. Each DNA sample was mixed thoroughly with an appropriate volume of 6 x loading buffer (10 mM Tris-HCl, 50 mM EDTA, 15 % (w/v) Ficoll 400, 0.03 % (w/v) bromophenol blue, 0.03 % (w/v) xylene cyanol FF, 0.4 % (w/v) Orange G, pH 7.5). Samples were run alongside 5 µL DNA 1 kb ladder to allow estimation of the nucleotide length of unknown DNA fragments. Once all samples were loaded into the gel, 1 µL ethidium bromide was added to the running buffer at the cathode end of the tank. Samples were run at 125 V for 20 min. DNA molecules were visualised using UV light.

2.3.3 Excision and purification of separated DNA molecules

The excised gel piece, containing the desired DNA molecules, was first heated at 50 °C in 0.5 mL binding buffer (6 M sodium perchlorate, 50 mM Tris, 10 mM EDTA, pH 8.0). To the resulting solution, 10 µL silica fines were added and slowly mixed for 10 min. The silica fines were then clarified by centrifugation (18000 g, 2 min) and the supernatant was discarded. The silica fines were re-suspended in 150 µL wash buffer (400 mM NaCl, 20 mM Tris-HCl, 2 mM EDTA, 50 % (v/v) ethanol (EtOH), pH 7.5) and clarified again by centrifugation (18000 g, 2 min). The wash step was repeated. The supernatant was then discarded and the silica fines re-suspended in 20 µL H₂O, followed by heating at 37 °C for 2 min. The silica fines were clarified by centrifugation (18000 g, 2 min) and the sample stored at -20 °C.

2.3.4 DNA restriction digests

Typically, a reaction mix was prepared containing 8 µL DNA sample, 5 U restriction enzyme, 1 x restriction buffer (recommended by the manufacturer), in a total volume

of 10 µL. Samples were incubated for 60 min at a temperature recommended by the manufacturer for the specific restriction enzyme being used.

2.3.5 DNA ligation reactions

A reaction mix containing 40 U T4 DNA ligase, 1 x T4 DNA ligase buffer (supplied by the manufacturer), 1 µL linearised vector DNA and 7 µL insert DNA was prepared and incubated at 20 °C for 30 min.

2.3.6 Bacterial media

Luria-Bertani (LB) broth was prepared as the following formulation; 1 % (w/v) peptone, 1 % (w/v) NaCl, 0.5 % (w/v) yeast extract, pH 7. LB-agar was prepared as above with the addition of 1.5 % (w/v) agar.

2.3.7 *E. coli* host transformation

Unless stated otherwise, 2 µL plasmid DNA was gently mixed with 50 µL of the desired bacterial host strain cells on ice. The sample was left to sit on ice for a further 30 min. Cells were then heated at 42 °C for 30 s followed by rapid cooling on ice for 2 min. Following heat treatment, 1 mL LB, warmed to 42 °C, was added and the sample shaken at 200 rpm for 60 min at 37 °C. After shaking, 200 µL of transformed cells were incubated at 37 °C overnight on LB-agar containing 100 µg mL⁻¹ kanamycin and 35 µg mL⁻¹ chloramphenicol (prepared as a 35 mg mL⁻¹ stock solution in EtOH). For downstream applications requiring plasmid purification, plasmid DNA was transformed into XL-10 Gold Ultracompetent cells (Agilent Technologies, USA). For recombinant protein expression, plasmid DNA was transformed into *E. coli* strain Tuner(DE3) cells that also contained the pRARE plasmid derived from *E. coli* strain Rosetta, subsequently termed Tunetta cells (Dixon *et al.*, 2009).

2.3.8 Plasmid purification

A single, transformed bacterial colony was selected and cells were grown overnight in 10 mL LB, containing the appropriate antibiotics, with shaking at 200 rpm and

heating at 37 °C. The overnight culture was clarified by centrifugation (4000 g, 10 min) and plasmid DNA purified using the Wizard® Plus SV Minipreps DNA Purification System (Promega, UK) following the manufacturer's instructions.

2.3.9 DNA Sanger sequencing

Plasmid DNA was sequenced using a 3130 Genetic Analyser at the Technology Facility, University of York, UK. Sequencing primers are given (Table 1).

Table 1: Sequencing primers used in these studies. The names and sequences of primers used for plasmid sequencing are given. for – forward primer using the antisense DNA strand as template. rev – reverse primer using the sense DNA strand as template.

Plasmid	Primer	Primer sequence (5'→3')
pET-STRP3	T7_for	taatacgactcaatctatagg
	T7_rev	tatgcgttgttattgctcagagg
pBIN-STRP3	Tap_for	aagcattctacttctattgcagc
	Tap_rev	tggcggtttgtatgtcatttcg

2.4 In vitro studies with recombinant GST proteins

2.4.1 Generation of C120V and S12A point mutants

Using *AmGSTF1* sub-cloned in the pET-24a vector (Cummins *et al.*, 1999) as a template, the plasmid was amplified using primer sets containing either the S12A or C120V codon mutation respectively (Table 2).

Table 2: Primers used to generate *AmGSTF1* point mutants. Forward - primer using the antisense DNA strand as template. Reverse - primer using the sense DNA strand as template.

Point mutation	Primer	Primer sequence (5'→3')
S12A	Forward	ggcccgccatggcaaccaacgttgacg
	Reverse	cgtcaacgttggccatggccggcc
C120V	Forward	ccgatgttatcaggtctgttaacccg
	Reverse	cgggttaaacagaacacctgatacacgtcg

Following PCR, samples were incubated with 5 U *Dpn*I restriction enzyme for 60 min at 37 °C to remove methylated template DNA. Plasmids were then transformed into XL-10 Gold Ultracompetent *E. coli* cells followed by plasmid purification and

sequencing. For protein expression, *AmGSTF1* point mutant sequences were cut from the pET-24a plasmid using *NdeI/SalI* DNA restriction enzymes, purified and ligated into *NdeI/SalI*-digested pET-STRP3 plasmid. Ligated plasmids were first transformed into XL-10 Gold Ultracompetent cells before purification and sequencing of the construct. Following confirmation that the sequences of the constructs were correct, the constructs were transformed into Tunetta cells.

2.4.2 Recombinant protein expression in *E. coli*

For protein expression, GSTs sub-cloned into the pET-STRP3 vector (Dixon *et. al.*, 2008) were transformed into *E. coli* strain Tunetta cells (Dixon *et al.*, 2009). For each construct, one colony was selected and grown overnight, in 10 mL LB media containing 100 $\mu\text{g mL}^{-1}$ kanamycin and 35 $\mu\text{g mL}^{-1}$ chloramphenicol (prepared as a 35 mg mL^{-1} stock solution in EtOH), with shaking at 200 rpm at 37 °C. The overnight culture was then added to 0.5 L LB media containing 100 $\mu\text{g mL}^{-1}$ kanamycin and 35 $\mu\text{g mL}^{-1}$ chloramphenicol, with shaking at 200 rpm at 37 °C. The culture was maintained under these conditions until it reached an optical density of 0.6 at an absorbance wavelength of 600 nm (determined against an LB blank). The culture was cooled to 20 °C and recombinant protein expression was induced by adding 0.1 mM isopropyl-D-thiogalactopyranoside (IPTG) to the growing culture. The culture was left for a further 16-20 hrs with shaking at 200 rpm at a temperature of 20 °C. Cells were then collected via centrifugation (7500 rpm, 15 min, 4 °C) of the overnight cell culture and the bacterial cell pellet stored at -20 °C until required.

2.4.3 Recombinant protein purification using Strep-tactin affinity chromatography

The frozen bacterial cell pellet was thawed to room temperature and re-suspended in 30 mL HEPES buffer (20 mM HEPES free acid, 150 mM NaCl, 1 mM EDTA, pH 7.6). Cells were lysed via sonication (70 % amplitude, 4 min total sonication time, 3 s sonication, 7 s cooling) on ice. Following sonication, 2 mM dithiothreitol (DTT), 2 $\mu\text{g mL}^{-1}$ avidin and DNase I were added to the lysate, which was then clarified by centrifugation (10000 g, 15 min). The supernatant was further clarified using a 0.45 μm Millex-HA syringe filter unit (Merck Millipore, USA). *Strep* II tagged proteins

were purified using a 5 mL *Strep*-Tactin Superflow High Capacity column (Stratech Scientific Ltd, Suffolk, UK). The column was firstly pre-equilibrated with HEPES buffer and then loaded with cell lysate at a flow rate of 1 mL min⁻¹. Once all unbound protein had been removed from the column (as judged by A₂₈₀ measurement), recombinant protein was eluted with 2.5 mM desthiobiotin (DTB; formulated in HEPES buffer). Eluted protein fractions were combined and mixed with 10 % (v/v) glycerol before being split into 0.5 mL aliquots, flash-frozen and stored at -80 °C. The column was regenerated by washing with 5 column volumes of 1 mM 2-(4-hydroxyphenylazo)benzoic acid (HABA; formulated in HEPES buffer) followed by washing with regeneration buffer (100mM Tris, 150 mM NaCl, 1mM EDTA, pH 10.5). Finally, the column was re-equilibrated in HEPES buffer prior to storage at 4 °C.

2.4.4 Quantification of purified recombinant protein concentrations

The concentration of purified recombinant *Strep* II tagged proteins was determined by UV-vis spectrophotometry using a Nanodrop ND1000 spectrophotometer (Thermo Scientific, USA). The absorbance at 280 nm of 2 µL protein sample was determined and related to the protein concentration using the estimated extinction coefficient of the recombinant protein (ProtParam, ExPASy web program, Swiss Institute of Bioinformatics).

2.4.5 Sodium dodecyl sulfate polyacrylamide gel electrophoresis (SDS-PAGE)

SDS-PAGE experiments were performed using a discontinuous gel system (Laemmli, 1970), with Mini-Protean Tetra cell apparatus (Bio-Rad, USA). The resolving gel was composed of 2.5 ml resolving buffer (1.5 M Tris-HCl, 0.4 % (v/v) tetramethylethylenediamine (TEMED), 0.4 % (w/v) SDS, pH 9), 4.27 ml H₂O and 3.12 ml 40 % acrylamide/bis-acrylamide. The gel solution was de-gassed and acrylamide polymerisation was induced by the addition of 0.1 ml 10 % (w/v) ammonium persulfate. The solution was immediately transferred into a pre-assembled gel apparatus and allowed to solidify. The stacking gel was composed of 4.5 ml stacking buffer (0.14 M Tris-HCl, 0.11 % (v/v) TEMED, 0.11 % (w/v) SDS, pH 6.8) and 0.5 ml 40 % acrylamide/bis-acrylamide. The gel solution was de-gassed

and 0.1 ml 10 % (w/v) ammonium persulfate was added. The solution was immediately applied to the top of the resolving gel, the well-comb was added and the gel allowed to solidify. The tank apparatus was then assembled, and filled with running buffer (25 mM Tris, 192 mM glycine, 0.1 % (w/v) SDS, pH 8.3), according to the manufacturer's instructions. Protein samples were mixed with an appropriate volume of 4 x SDS loading buffer (83.3 mM Tris-HCl, 16.7 % (v/v) glycerol, 2.67 % (w/v) SDS, 6.67 % (v/v) β-mercaptoethanol, 0.003 % (w/v) bromophenol blue, pH 6.8), boiled at 95 °C for 5 min, and the supernatant clarified by centrifugation (13000 g, 2 min). Samples were run alongside 10 µL pre-stained broad-range protein markers to allow the estimation of the molecular weights of unknown proteins. Once all samples were loaded, gels were run at 100 V as proteins moved through the stacking gel and 200 V thereafter, until the marker dye-front eluted from the gel. To visualise proteins, gels were washed twice with H₂O and then stained using the commercially available InstantBlue dye reagent (Expedeon Inc., USA), according to the manufacturer's instructions.

2.4.6 Determination of recombinant protein molecular weights using mass spectrometry

Protein samples were concentrated by size exclusion chromatography using 2 mL Vivaspin columns (GE Healthcare, UK), according to the manufacturer's instructions. The recovered protein was then mixed with an equal volume of 2 % (v/v) formic acid in acetonitrile. Samples were injected into the ionisation chamber at a flow rate of 3 µL min⁻¹ and mass ions generated, using electrospray ionisation, with a dry gas flow rate of 5 L min⁻¹ at 300 °C, and nebuliser gas pressure of 10 psi. Mass spectra were acquired in positive ion mode, with a source voltage of 4000 V and skimmer voltage of 40 V, over the mass range 400 – 2500 m / z. Multiply-charged mass ions were deconvoluted using Compass DataAnalysis software (Bruker Daltonics, USA). Before use, the mass spectrometer was calibrated using a myoglobin reference standard; theoretical mass = 16951 Da, observed mass = 16951 Da. In some cases, stated in the main text, mass spectrometry was performed by the Technology Facility, University of York, UK.

2.4.7 Reduction and desalting of purified recombinant protein

Prior to studies with recombinant enzymes, a 0.5 mL aliquot of each recombinant purified protein was removed from storage at -80 °C, thawed, and incubated with 5 mM DTT on ice for 15 min. After which, each protein was desalted in HEPES buffer using a HiTrap Desalting 5 mL column (GE Healthcare, UK), according to the manufacturer's instructions.

2.4.8 *In vitro* GSH-dependent enzyme assays

2.4.8.1 Assay using 1-chloro-2,4-dinitrobenzene (CDNB) as substrate

CDNB assays were based on the method described by Habig *et al.* (1974). Assay buffer (0.1 M potassium phosphate, pH 6.5) was warmed to 30 °C and contained 5 mM GSH, 375 nM recombinant enzyme and 1 mM CDNB (prepared as a 40 mM stock solution in EtOH), in a total assay volume of 1 mL. The solution was thoroughly mixed, and the increase in absorbance at 340 nm was measured for 30 s at 30 °C by UV-vis spectrophotometry. The chemical rate of reaction was measured by replacing recombinant enzyme with an appropriate volume of HEPES buffer. GST-catalysed reactions were duly corrected for non-enzymatic contributions. Corrected enzymatic rates were expressed as nmol of the glutathionylated product formed per second per mg of recombinant protein, using the molar extinction coefficient of the product ($\epsilon = 9.6 \text{ mM}^{-1} \text{ cm}^{-1}$). Assays were performed in technical triplicate. In the case of ZmGSTF1, 7.5 nM recombinant enzyme was used to obtain linear kinetics.

2.4.8.2 Assay using cumene hydroperoxide (CuOOH) as substrate

Assays using CuOOH were based on the method described by Flohe and Gunzler (1984). Assay buffer (0.25 M potassium phosphate, 2.5 mM EDTA, pH 7.0) was warmed to 37 °C and contained 0.6 U glutathione reductase, 250 µM reduced nicotinamide adenine dinucleotide phosphate (NADPH; prepared as a 2.5 mM stock in 0.1 % (w/v) NaHCO₃) and 1 mM GSH. The solution was incubated at 37 °C for 3 min. Following this incubation period, 375 nM recombinant enzyme and 1.2 mM

CuOOH were added to the assay, with thorough mixing, in a total assay volume of 1 mL. The decline in absorbance at 340 nm was measured for 2 min at 37 °C by UV-vis spectrophotometry. The chemical rate of reaction was measured by replacing recombinant enzyme with an appropriate volume of HEPES buffer. GST-catalysed reactions were duly corrected for non-enzymatic contributions. Corrected enzymatic rates were expressed as nmol of NADP⁺ formed per second per mg of recombinant protein, using the molar extinction coefficient of NADPH ($\epsilon = 6.22 \text{ mM}^{-1} \text{ cm}^{-1}$). Assays were performed in technical triplicate.

2.4.8.3 Assay using linoleic acid hydroperoxide (LinOOH) as substrate

LinOOH (13-hydroperoxy-(E)-9-(Z)-11-octadecadienoic acid) was synthesized based on a previously described protocol (Edwards and Dixon, 2005). 25 mL Tris buffer (50 mM Tris-HCl, pH 9) was warmed to 30 °C, with shaking at 200 rpm. After 15 min, 43.5 µmol linoleic acid was added to the solution. Soybean lipoxidase was re-suspended in 2 mL Tris buffer to a final concentration of 125536 U ml⁻¹ and added to the linoleic acid solution in 0.25 mL aliquots over a period of 10 min, with shaking at 200 rpm. The reaction was shaken for a further 10 min at 200 rpm before adding 6.5 mL EtOH. The reaction was then cooled to 4 °C and acidified to pH 3 using glacial acetic acid. The supernatant was clarified by centrifugation (17000 g, 30 min, 4 °C) and maintained at 4 °C. LinOOH was purified using 3 mL Strata-X solid phase extraction DSC-18 cartridges (Sigma Aldrich). Cartridges were first washed with 12 mL EtOH, followed by 12 mL H₂O. After cartridge preparation, 3 mL clarified supernatant was applied to each cartridge and each cartridge washed with 12 mL 20 % (v/v) EtOH, followed by 24 mL H₂O, and finally 6 mL hexane. LinOOH was recovered with 6 mL methanol (MeOH). Recovered methanolic fractions were combined, and concentrated to an oily, white residue under reduced pressure, before re-suspending with 0.5 mL MeOH. LinOOH was quantified by UV-vis spectrophotometry, at a wavelength of 235 nm, using the molar extinction coefficient $\epsilon = 23000 \text{ M}^{-1} \text{ cm}^{-1}$. Assays with LinOOH as substrate were performed as described for CuOOH, with the following modifications; LinOOH was used at a final substrate concentration of 38 µM, with 34.6 nM recombinant enzyme.

2.4.8.4 Assay using 2-hydroxyethyl disulfide (HED) as substrate

Assays using HED were based on the method described by Dixon *et al.* (2002). Assay buffer (0.1 M potassium phosphate, 2 mM EDTA, pH 7.8) was warmed to 30 °C and contained 0.6 U glutathione reductase, 250 µM NADPH (prepared as a 2.5 mM stock in 0.1 % (w/v) NaHCO₃), 1 mM GSH and 0.7 mM HED. The solution was incubated at 30 °C for 3 min. Following this incubation period, 3.75 µM recombinant enzyme was added to the assay, with thorough mixing, in a total assay volume of 1 mL. The decline in absorbance at 340 nm was measured for 3 min at 30 °C by UV-vis spectrophotometry. The chemical rate of reaction was measured by replacing recombinant enzyme with an appropriate volume of HEPES buffer. GST-catalysed reactions were duly corrected for non-enzymatic contributions. Corrected enzymatic rates were expressed as nmol of NADP⁺ formed per second per mg of recombinant protein, using the molar extinction coefficient of NADPH ($\epsilon = 6.22 \text{ mM}^{-1} \text{ cm}^{-1}$). Assays were performed in technical triplicate.

2.4.8.5 Assay using crotonaldehyde as substrate

Assays using crotonaldehyde were based on the method described by Berhane *et al.* (1994). In a quartz cuvette, assay buffer (0.1 M potassium phosphate, pH 6.5) was warmed to 37 °C and contained 1 mM GSH, 938 nM recombinant enzyme and 0.1 mM crotonaldehyde (prepared as a 10 mM stock solution in EtOH), in a total assay volume of 1 mL. The solution was thoroughly mixed and incubated at 37 °C for 2 min. The increase in absorbance at 230 nm was measured for 2 min at 37 °C by UV-vis spectrophotometry. The chemical rate of reaction was measured by replacing recombinant enzyme with an appropriate volume of HEPES buffer. GST-catalysed reactions were duly corrected for non-enzymatic contributions. Corrected enzymatic rates were expressed as nmol of the glutathionylated product formed per second per mg of recombinant protein, using the molar extinction coefficient of crotonaldehyde ($\epsilon = 10.7 \text{ mM}^{-1} \text{ cm}^{-1}$). Assays were performed in technical triplicate.

2.4.8.6 Assay using ethacrynic acid as substrate

Assays using ethacrynic acid were based on the method described by Habig *et al.* (1974). In a quartz cuvette, assay buffer (0.1 M potassium phosphate, pH 6.5) was warmed to 30 °C and contained 5 mM GSH, 938 nM recombinant enzyme and 0.2 mM ethacrynic acid (prepared as an 8 mM stock solution in EtOH), in a total assay volume of 1 mL. The solution was thoroughly mixed and the increase in absorbance at 270 nm was measured for 30 s at 30 °C by UV-vis spectrophotometry. The chemical rate of reaction was measured by replacing recombinant enzyme with an appropriate volume of HEPES buffer. GST-catalysed reactions were duly corrected for non-enzymatic contributions. Corrected enzymatic rates were expressed as nmol of the glutathionylated product formed per second per mg of recombinant protein, using the molar extinction coefficient of the product ($\epsilon = 5 \text{ mM}^{-1} \text{ cm}^{-1}$). Assays were performed in technical triplicate.

2.4.8.7 Assay using 4-nitrophenyl acetate (NPA) as substrate

Assays using NPA were based on the method described by Keen and Jakoby (1978). Assay buffer (0.1 M potassium phosphate, pH 7) containing 0.2 mM NPA (prepared as a 100 mM stock solution in MeOH), was warmed to 30 °C. To this, was added 938 nM recombinant enzyme and 1 mM GSH, in a total assay volume of 1 mL. The increase in absorbance at 400 nm was measured for 1 min at 30 °C by UV-vis spectrophotometry. The chemical rate of reaction was measured by replacing recombinant enzyme with an appropriate volume of HEPES buffer. GST-catalysed reactions were duly corrected for non-enzymatic contributions. Corrected enzymatic rates were expressed as nmol of the 4-nitrophenol product formed per second per mg of recombinant protein, using the molar extinction coefficient of the product ($\epsilon = 17 \text{ mM}^{-1} \text{ cm}^{-1}$). Assays were performed in technical triplicate.

2.4.8.8 Assay using benzyl isothiocyanate (BITC) as substrate

Assays using BITC were based on the method described by Kolm *et al.* (1995). In a quartz cuvette, assay buffer (0.1 M potassium phosphate, pH 6.5) was warmed to 30 °C and contained 1 mM GSH, 938 nM recombinant enzyme and 0.16 mM BITC

(prepared as a 16 mM stock solution in acetonitrile), in a total assay volume of 1 mL. The solution was thoroughly mixed and the increase in absorbance at 274 nm was measured for 30 s at 30 °C by UV-vis spectrophotometry. The chemical rate of reaction was measured by replacing recombinant enzyme with an appropriate volume of HEPES buffer. GST-catalysed reactions were duly corrected for non-enzymatic contributions. Corrected enzymatic rates were expressed as nmol of the glutathionylated product formed per second per mg of recombinant protein, using the molar extinction coefficient of the product ($\epsilon = 9.25 \text{ mM}^{-1} \text{ cm}^{-1}$). Assays were performed in technical triplicate.

2.5 Inhibition studies

2.5.1 IC₅₀ determinations

IC₅₀ measurements were determined with the following inhibitors; 4-chloro-7-nitrobenzoxadiazole (NBD-Cl), ethacrynic acid, cyanuric chloride and bromoenol lactone (kindly donated by Dr. J. D. Sellars, Department of Chemistry, Durham University, UK). For studies with each inhibitor, recombinant GSTs were assayed for activity toward CDNB as substrate as described (see section 2.4.8.1), in the presence of 1 nM – 100 µM inhibitor (prepared as 100 x stock solutions in an appropriate organic solvent), with 344 nM recombinant enzyme. For each inhibitor concentration, the non-enzymatic rate of reaction was determined by replacing recombinant enzyme with an equivalent volume of HEPES buffer. Uninhibited enzyme reaction rates were determined by replacing inhibitor with an equivalent volume of organic solvent. For all assays, organic solvent concentration did not exceed 3.5 % (v/v). Assays were performed in technical triplicate. NBD-Cl was solubilised in dimethyl sulfoxide (DMSO), ethacrynic acid and bromoenol lactone were solubilised in EtOH and cyanuric chloride was solubilised in acetone. IC₅₀ values were calculated using non-linear regression with Prism 3.0 software (Graphpad Software Inc., USA).

2.5.2 Single time-point inhibition studies

For inhibition studies at a single time-point, unless stated otherwise in the main text, 37.5 µM recombinant enzyme was first incubated with 100 µM inhibitor (prepared

as a 10 mM stock solution in DMSO), at 20 °C for 10 min. Following this incubation period, enzymes were assayed for activity toward CDNB as described (see section 2.4.8.1), replacing 375 nM enzyme with 10 µL enzyme-inhibitor pre-incubated solution. Uninhibited enzyme reaction rates were determined by replacing inhibitor with an equivalent volume of DMSO. The non-enzymatic rate of reaction was determined by replacing recombinant enzyme with an equivalent volume of HEPES buffer. For all assays, organic solvent concentration did not exceed 3.5 % (v/v). Assays were performed in technical triplicate. For studies with iodoacetamide, all incubations were carried out in the dark. The NBD-glutathione conjugate was kindly donated by Dr. J. D. Sellars (Department of Chemistry, Durham University, UK). Purine derivatives were kindly donated by Dr. C. Coxon (Department of Chemistry, Durham University, UK).

2.5.3 Time-course inhibition studies

For time-course inhibition studies, 37.5 µM recombinant enzyme was first incubated with 100 µM inhibitor (prepared as a 10 mM stock solution in DMSO), at 20 °C for 0 - 60 min. At discrete time-points, aliquots were assayed for activity as described (see section 2.5.2). Uninhibited enzyme reaction rates were determined by replacing inhibitor with an equivalent volume of DMSO.

2.5.4 Studies of protein alkylation using mass spectrometry

For protein alkylation studies, 37.5 µM recombinant enzyme was first incubated with 100 µM inhibitor (prepared as a 10 mM stock solution in DMSO), at 20 °C for 60 min. To serve as negative controls, 37.5 µM recombinant enzyme was incubated with an equivalent volume of DMSO, at 20 °C for 60 min. Following incubation, each sample was concentrated and desalted with 6 mL H₂O, using 2 mL Vivaspin columns (GE Healthcare, UK), according to the manufacturer's instructions. Concentrated protein was recovered, raised to a total volume of 50 µL with H₂O and mixed with an equal volume of 2 % (v/v) formic acid in acetonitrile. Samples were then analysed by mass spectrometry as described (see section 2.4.6). For studies with iodoacetamide, all incubations were carried out in the dark.

2.6 GST expression in transgenic *Arabidopsis thaliana* plants

2.6.1 Cloning of GSTs into the pBIN-STRP3 vector

2.6.1.1 Cloning of *ZmGSTF1* into the pBIN-STRP3 vector

The *ZmGSTF1*-pET-STRP3 plasmid (kindly donated by Dr. D. P. Dixon, GlaxoSmithKline, Stevenage, UK), was purified and digested with *Nco*I and *Bst*XI DNA restriction enzymes. Digestion products were separated by agarose gel electrophoresis, followed by purification of *ZmGSTF1* DNA. *ZmGSTF1* was ligated into *Nco*I/*Bst*XI-digested pBIN-STRP3 plasmid (kindly donated by Dr. M. Brazier-Hicks, Department of Biology, University of York, UK), and transformed into XL-10 Gold Ultracompetent cells using LB growth media supplemented with 100 µg mL⁻¹ spectinomycin. The *ZmGSTF1*-pBIN-STRP3 construct was purified and the sequence confirmed as correct.

2.6.1.2 Cloning of *AmGSTF1*, C120V and S12A into the pBIN-STRP3 vector

AmGSTF1-pET-STRP3, C120V-pET-STRP3 and S12A-pET-STRP3 plasmids were purified and digested with *Pac*I and *Bst*XI DNA restriction enzymes. Digestion products were separated by agarose gel electrophoresis, followed by purification of *AmGSTF1*, C120V and S12A DNA. *AmGSTF1*, C120V and S12A were each ligated into *Pac*I/*Bst*XI-digested pBIN-STRP3 plasmid, and transformed into XL-10 Gold Ultracompetent cells using LB growth media supplemented with 100 µg mL⁻¹ spectinomycin. The assembled pBIN-STRP3 constructs were purified and the sequences confirmed as correct.

2.6.2 Assembly of the pBIN-STRP3 vector designed to express the *Strep* II tag only

Using S12A-pBIN-STRP3 plasmid DNA as a template, two PCR reactions were carried out with primer sets (Table 3) that amplified upstream and downstream of the GST transgene sequence respectively.

Table 3: Primers used to generate a pBIN-STRP3 vector designed to express the *Strep II tag* only. Tap_for, pBIN_cusfor - primers using the antisense DNA strand as template. pBIN_cusrev3, Tap_rev - primers using the sense DNA strand as template.

Position of amplification relative to the transgene	Primer	Primer sequence (5'→3')
Upstream	Tap_for pBIN_cusrev3	aagcattctacttctattgcagg cgccttcactctagatcagccttctcgaaactgcgg
Downstream	pBIN_cusfor Tap_rev	tgatcttagagtgaaggcgccaccgatatggccagtggtgc tggcgttttgtatgtcatttcg

PCR reactions were performed using temperature gradient cycling based on a previously described method (Szewczyk *et al.*, 2006). Specifically, samples were denatured at 95 °C for 2 min and then exposed to 30 heating cycles composed of: 20 s 95 °C, 1 s 70°C, cooling to 55 °C at a rate of 0.3 °C s⁻¹, 30 s 55 °C, heating to 72 °C at a rate of 0.3 °C s⁻¹, 20 s 72 °C. This was followed by a final extension step at 72 °C for 2 min. PCR products were separated using 2 % (w/v) agarose gel electrophoresis and purified. The purified Upstream and Downstream PCR products were then annealed and amplified using Tap_for and Tap_rev primers (Table 3). Reaction solutions contained 1x *Pfu* DNA polymerase buffer (supplied by the manufacturer), 1 uL Upstream PCR product, 1 uL Downstream PCR product, 400nM Tap_for primer, 400 nM Tap_rev primer, 1.25 U *Pfu* DNA polymerase and 200 μM dNTPs, in a total volume of 50 μL. PCR reactions were performed using temperature gradient cycling as just described. PCR products were separated using 2 % (w/v) agarose gel electrophoresis and the Annealed PCR product was purified. The Annealed PCR product was digested with *Nco*I and *Bst*XI DNA restriction enzymes, purified and ligated into *Nco*I/*Bst*XI-digested pBIN-STRP3 plasmid. The ligated plasmid was transformed into XL-10 Gold Ultracompetent cells, using LB growth media supplemented with 100 μg mL⁻¹ spectinomycin, purified and the sequence confirmed as correct.

2.6.3 GV3101:MP90 agrobacterium transformations with GST-pBIN-STRP3 constructs

For each pBIN-STRP3 construct, 50 µL electrocompetent *Agrobacterium tumefaciens* strain GV3101:MP90 cells (kindly donated by Dr. M. Brazier-Hicks, Department of Biology, University of York, UK) were gently mixed with 1 µL pBIN-STRP3 construct DNA, on ice. The sample was transferred to a chilled electroporation cuvette and pulsed (2.4 kV, 25 µF, 200 Ω, 5.2 ms) using a Gene Pulser® II electroporator (Bio-Rad Laboratories Inc., USA). Immediately after pulsing, 0.5 mL LB was added to the cuvette and cells were incubated at 28 °C for 4 hr. Following this recovery period, 100 µL transformed cells were incubated on LB-agar supplemented with 100 µg mL⁻¹ spectinomycin, 26 µg mL⁻¹ gentomycin and 50 µg mL⁻¹ rifampicin (prepared as a 50 mg mL⁻¹ stock solution in DMSO), at 28 °C for 48 hrs.

2.6.4 Infiltration of *Arabidopsis thaliana* with transformed Agrobacterium tumefaciens

Arabidopsis thaliana plants were transformed according to the protocol of Clough and Bent (1998). For each transformed agrobacterial culture, transformed colonies were grown in 100 mL LB, supplemented with 100 µg mL⁻¹ spectinomycin, 26 µg mL⁻¹ gentomycin and 50 µg mL⁻¹ rifampicin (prepared as a 50 mg mL⁻¹ stock solution in DMSO), for 16 hr at 28 °C with shaking at 180 rpm. The culture was then clarified by centrifugation (3900 g, 10 min), and the supernatant was discarded. Cells were re-suspended in 100 mL 5 % (w/v) sucrose supplemented with 50 µL SILWET L-77 (Momentive, USA). Five flowering *Arabidopsis thaliana* plants were then thoroughly dipped in the agrobacterial suspension, covered, and maintained in the dark for 24 hr. After this time, plants were uncovered and maintained under glasshouse conditions, and allowed to self-fertilize.

2.6.5 Selection of homozygous lines

For each set of plants transformed with a pBIN-STRP3 construct, the seeds of inoculated plants (T₀ generation) were combined, sown and, at the 2-leaf stage,

treated with 150 g L⁻¹ Kaspar (13.52 % (w / w) glufosinate-ammonium; Sanofi, France). Plants were treated a total of 3 times over a period of 14 days. 24 surviving individuals were separated, allowed to self-fertilise, and the seed (T₁ generation) of each individual was collected. Approximately 50 seeds of each T₁ line were sown, the numbers of seedlings of each T₁ line were counted and then treated with Kaspar as described with T₀ seedlings. Following Kaspar treatment, the numbers of seedlings of each T₁ line were re-counted and statistically analysed for a 3:1 alive:dead ratio using χ^2 statistical testing methods. The null hypothesis was that the observed alive:dead ratio would not deviate from the expected 3:1 ratio, predicted using the number of seedlings alive before Kaspar treatment. For those lines that tested strongly positive for a 3:1 alive:dead ratio, 24 individuals were selected, separated, allowed to self-fertilise, and the seed (T₂ generation) of each individual was collected. Seeds of 8 arbitrarily-selected T₂ lines were sown and treated with Kaspar as described with T₀ seedlings. Those T₂ lines, for which all individuals survived Kaspar treatment, were used for further experimentation.

2.6.6 Western blotting of transgenic plant material

For each transgenic line, approximately 30 mg leaf tissue was ground to a fine powder in liquid nitrogen and combined with 2 volumes 1 x SDS loading buffer. The sample was then heated at 95 °C for 5 min, and the supernatant clarified by centrifugation (13000 g, 10 min). Proteins were separated by SDS-PAGE as described (see section 2.4.5), using 15 µL sample, alongside 1 µg recombinant *AmGSTF1*. Once electrophoresis was complete, the resolving gel was immersed in H₂O and proteins were transferred to a polyvinylidene difluoride (PVDF) membrane using an iBlot® Gel Transfer Device (Life Technologies, USA) according to the manufacturer's instructions. Once the transfer was complete, the membrane was immersed in TBS buffer (10 mM Tris, 150 mM NaCl, pH 7.4) before incubating in Blocking buffer, (10 mM Tris, 150 mM NaCl, 3 % (w/v) skimmed milk powder, pH 7.4), for 60 min. The membrane was then incubated with Blocking buffer supplemented with 0.1 % (v/v) antiserum raised against the *ZmGSTF1-2* heterodimer (Cummins *et al.*, 1999), with gentle agitation at 4 °C. After 16 hr, the membrane was washed twice with TBST buffer (10 mM Tris, 150 mM NaCl, 0.1 % (v/v) Triton X-100, pH 7.4) for 10 min, followed by washing with TBS buffer for 10 min. After

washing, the membrane was incubated with Blocking buffer supplemented with 0.025 % (v/v) anti-rabbit IgG (whole molecule)-alkaline phosphatase antibody. After 1 hr, the membrane was washed twice with TBST buffer for 10 min, followed by washing with TBS buffer for 10 min. The membrane was then rinsed in Staining buffer (100 mM Tris, pH 9.5) before incubating in Staining buffer supplemented with 0.5 mM 5-bromo-4-chloro-3-indolyl phosphate (prepared as a 153 mM stock solution in 70 % (v/v) dimethyl formamide) and 0.4 mM nitro blue tetrazolium chloride (prepared as a 122 mM stock solution in 70 % (v/v) dimethyl formamide). Once proteins could be visibly detected, the membrane was immersed in 500 mL H₂O and dried in air.

2.6.7 Spray trials

Thirty seeds of each selected homozygous T₂ line were sown on Levington F2 seed and modular compost in 6.5 cm x 6 cm x 6 cm pots. Once sown, all pots were chilled at 4 °C for 5 days before being maintained in environmental growth chambers (20 °C, illumination rate 100 µE m⁻² s⁻¹, 16 hr photoperiod). After a further 14 days, plants were sprayed with herbicide formulations. Herbicides were first dissolved in acetone and then diluted 100-fold with 0.1 % (v/v) Biopower (Bayer CropScience, Germany). Chlorotoluron was formulated to deliver 60 g active ingredient (ai) ha⁻¹. Alachlor was formulated to deliver 1200 g ai ha⁻¹. Plants were contained within a 0.2 m² area and sprayed with a hand-sprayer calibrated to deliver 1500 L ha⁻¹. As a negative control, plants were sprayed with 0.1 % (v/v) Biopower containing 1 % acetone. After spraying, plants were maintained in environmental growth chambers and visually assessed at 7 days. For quantification of biomass, the spray trial was performed in biological duplicate and aerial tissue in each pot was harvested after counting the number of individuals. For each pot, aerial tissue mass was divided by the total number of individuals (alive and dead). For each spray treatment, the mass per plant of each GST-expressing transgenic line was expressed as a percentage change relative to the mass per plant of the vector 22-24 transgenic line.

2.6.8 Biochemical characterisation of transgenic *Arabidopsis* plants

2.6.8.1 Soluble protein extractions

For each transgenic line, approximately 450 mg leaf tissue was ground to a fine powder in liquid nitrogen and extracted with 3 volumes of Extraction buffer (50 mM Tris-HCl, 2 mM EDTA, 1 mM DTT, 5 % (w/v) PVPP, 1 % (v/v) protease inhibitor cocktail, pH 7.4), on ice for 1 hr. The supernatant was then clarified by centrifugation (13000 g, 7.5 min, 4 °C), insoluble matter was discarded and ammonium sulfate was slowly added to 80 % saturation (0.561 g mL⁻¹). The sample was spun on a rotating wheel at 4 °C for 45 min before clarifying by centrifugation (10000 g, 15 min, 4 °C). The supernatant was discarded and the protein pellet stored at -20 °C until required.

2.6.8.2 Enzyme assays

Protein pellets were removed from storage at -20 °C and re-solubilised in 1 mL protein buffer (20 mM Tris, pH 7.4). Samples were reduced with 5 mM DTT, on ice for 15 min, before desalting in protein buffer, using 5 mL Zeba Spin 7K MWCO desalting columns (Thermo Scientific, USA), according to the manufacturer's instructions. The protein concentration of each sample was quantified using the BCA Protein Assay Kit (Thermo Scientific, USA), according to the manufacturer's instructions. Samples were assayed for GSH-dependent activity toward CDNB, CuOOH, HED and crotonaldehyde as substrates as previously described (see section 2.4.8), using 50 µL protein sample, or an equivalent volume of protein buffer as a negative control.

2.6.8.3 Flavonoid analysis

For each transgenic line, approximately 400 mg leaf tissue was ground to a fine powder in liquid nitrogen and extracted with 3 volumes of Flavonoid extraction solution (MeOH, 3 % (v/v) acetic acid, 400 µM kaempferol), on ice for 15 min. Samples were clarified by centrifugation (10000 g, 5 min), the supernatant was decanted and retained (Extract 1), and the pellet was re-extracted with 3 volumes of

Flavonoid extraction solution (Extract 2). The methanolic extracts were separated by high-performance liquid chromatography and visualised at 280 nm by UV-vis spectrophotometry, based on a previously published method (Cummins *et al.*, 2006). 50 µL extract was injected onto a Synergi Polar-RP column (250 mm x 4 mm internal diameter, 4 µm particle size, 80 Å pore size. Phenomenex, UK) equilibrated with a mobile phase comprised of 90 % (v/v) aqueous solution (A; H₂O, 0.1 % (v/v) formic acid) and 10 % (v/v) organic solution (B; acetonitrile, 0.1 % (v/v) formic acid), at a flow rate of 1 mL min⁻¹. Compounds were eluted using a 3-stage gradient (Table 4), with a total run time of 35 min.

Table 4: High-performance liquid chromatography solvent gradient conditions. A - H₂O + 0.1 % (v/v) formic acid. B – acetonitrile + 0.1 % (v/v) formic acid.

Time (min)	A (% volume)	B (% volume)
0	10	90
2	10	90
7	20	80
27	60	40
30	90	10
32.5	10	90

The absorbance peak area units of all extracts were then normalised and quantified using the peak area of the 20 nmol kaempferol internal standards. Quantified metabolite masses of Extract 1 and Extract 2, of each transgenic line, were combined to yield the total mass per metabolite. Extracts were separated and analysed in technical triplicate.

2.6.8.4 Protein pull-down experiments

The isolation of *Strep* II tagged proteins from transgenic plants was based on a previously described method (Witte *et al.*, 2004). For each transgenic line, approximately 1 g leaf tissue was ground to a fine powder in liquid nitrogen and extracted with 3 volumes of Extraction buffer (50 mM Tris-HCl, 2 mM EDTA, 1 mM DTT, 1 % (v/v) protease inhibitor cocktail, 150 mM NaCl, pH 7.4), on ice for 1 hr. The supernatant was then clarified by centrifugation (4000 rpm, 10 min, 4 °C), insoluble matter was discarded and avidin was added to a final concentration of 100

μ g / mL. A custom column, filled with 1 mL *Strep*-Tactin Superflow High Capacity resin, was assembled and washed with 5 mL Extraction buffer. Total soluble protein samples were applied to the column, centrifuged (1000 rpm, 2 min, 4 °C) and the flow-through discarded. The column was washed with 5 x 2 mL Extraction buffer, in each case the column was centrifuged (1000 rpm, 2 min, 4 °C) and the flow-through discarded. *Strep* II tagged proteins were eluted with 1 mL 2.5 mM desthiobiotin, by centrifugation (1000 rpm, 2 min, 4 °C). The eluted sample was concentrated using a 2 mL Vivaspin column (GE Healthcare, UK), according to the manufacturer's instructions, and made to a total volume of 45 μ L with extraction buffer. 15 uL 4 x SDS loading buffer was added and the sample was analysed by Western blotting as described (see section 2.6.6). Alternatively, following SDS-PAGE, proteins were detected using silver staining based on a published method (Heukeshoven and Dernick, 1985). Gels were incubated twice with fixing solution (40 % (v/v) EtOH, 10 % (v/v) acetic acid) for 10 min, followed by a 30 min incubation with sensitisation solution (30 % (v/v) EtOH, 10 % (v/v) acetic acid, 0.2 % (v/v) sodium thiosulfate (prepared as a 5 % (v/v) stock solution), 0.83 M sodium acetate). Following sensitisation, gels were washed three times with H₂O for 5 min, before incubating with 15 mM silver nitrate solution for 10 min, followed by two further wash steps with H₂O for 1 min. Gels were then incubated with development solution (236 mM sodium carbonate, 0.04 % (v/v) formaldehyde (37 % (v/v) stock solution)). Once proteins could be visibly detected, the staining reaction was stopped by immersing gels in 50 mM EDTA solution.

Chapter 3 - *In vitro* characterisation of *AmGSTF1* isoforms and further characterisation of transgenic *Arabidopsis* plants expressing *AmGSTF1*

3.1 Exploring the properties of *AmGSTF1* isoforms

3.1.1 Introduction

In prior studies, screening of soluble protein extracts of wild-type sensitive (WTS) and multiple herbicide resistant (MHR) black-grass by Western blotting with an antiserum raised against the maize *ZmGSTF1-2* heterodimer identified the presence of a novel immunoreactive GSTF protein band in MHR plants. Expression and screening of a cDNA library prepared from MHR black-grass subsequently identified four closely related GSTF isoforms (approximately 95 % amino acid sequence identity), which following expression of the respective recombinant proteins, yielded polypeptides that co-migrated during gel electrophoresis with the GSTF band in MHR plant extracts. These four isoforms (termed GSTF1a-d), could be further classified into two subsets based on amino acid sequence similarity. *AmGSTF1a* and *AmGSTF1b* showed 99 % similarity to each other and *AmGSTF1c* and *AmGSTF1d* showed 99 % similarity to each other. These two clades were in turn 95 % similar to one another (Cummins *et al.*, 1999).

As the sequence similarity is very high across all four isoforms the presumption was made that the multiple *AmGSTF1* isoforms would perform similar roles *in vitro* and *in planta*. Isoform *AmGSTF1c* was then selected for expression in transgenic *Arabidopsis* plants (Dr. I. Cummins and Prof. R. Edwards, unpublished work at the start of this project).

3.1.2 Expression of *AmGSTF1a* and *AmGSTF1c*

As the amino acid identity of isoforms within each paired subset is close to 100 %, one isoform of each subset, *AmGSTF1a* and *AmGSTF1c*, were expressed and characterised *in vitro*.

For ease of purification GSTs were cloned into the pET-STRP3 vector (Figure 18) which rendered the polypeptide fused with an N-terminal *Strep* II tag (Dixon *et al.*, 2009). This modification allows for swift and selective isolation of the translated protein from a heterogeneous mixture using *Strep*-tactin resin which selectively binds the *Strep* II tag with very high affinity. Furthermore, the tag has been shown to be biologically inert and not to interfere with protein folding (Schmidt and Skerra, 2007).

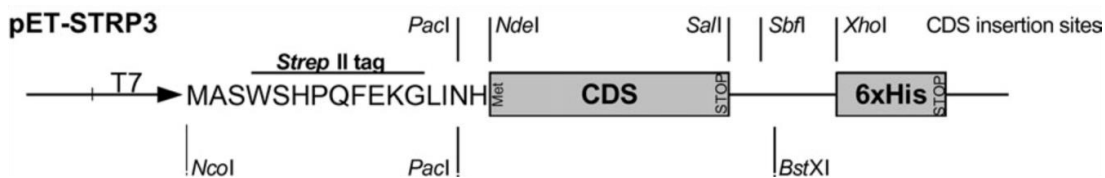


Figure 18: pET-STRP3 vector. The cloned DNA sequence (CDS) of choice is inserted such that it becomes fused to a *Strep* II tag of which the translated amino acid sequence is shown. Expression of the construct is driven by the inducible T7 promoter. The relative positions of DNA restriction sites required for manipulation of the vector are shown (*Nco*I, *Pac*I, *Nde*I, *Sal*I, *Sbf*I, *Bst*XI and *Xba*I). Copied with permission (Dixon *et al.*, 2009).

GSTs in the pET-STRP3 vector (kindly donated by Dr. I. Cummins, School of Biological and Biomedical Sciences, Durham University, UK) were transformed and expressed in *E. coli* Tuner(DE3) cells containing the pRARE plasmid which allowed enrichment of rare tRNAs to facilitate translation of plant proteins in a bacterial host. Protein production was induced using isopropyl β-D-1-thiogalactopyranoside (IPTG) and the *Strep* II-fusion protein purified, following cellular membrane disruption, using *Strep*-tactin resin as described in previous studies (Dixon *et al.*, 2009). The purity of recombinant GSTs was confirmed using mass spectrometry, which determined the presence of a single protein in each purified sample. The protein concentration of each sample was estimated by measuring the absorbance of the sample at 280 nm and calculating according to the Beer-Lambert law (Equation 1) using the predicted extinction coefficient of each protein (ProtParam, ExPASy web program, Swiss Institute of Bioinformatics).

$$A = \epsilon \cdot c \cdot l$$

Equation 1: Beer-Lambert law. This function describes the relationship between the light absorbance of a sample and the concentration of the sample. A – absorbance of the sample. ε – molar extinction coefficient of the sample. c – concentration of the sample. l – path length of light.

3.1.3 *In vitro* characterisation of *AmGSTF1a* and *AmGSTF1c*

Purified recombinant GSTs were assayed for two different catalytic activities; (i) conjugation of the halogenated aromatic compound, 1-chloro-2,4-dinitrobenzene (CDNB) with reduced glutathione (GSH) as a co-substrate (Figure 19A) and (ii) reduction of an organic hydroperoxide, cumene hydroperoxide (CuOOH), to the alcohol species using GSH as a co-factor (Figure 19B). For assays with CDNB, the glutathionylated conjugate contains a strongly absorbing chromophore allowing direct detection of conjugate formation (Habig *et al.*, 1974). In the case of CuOOH, the substrate and the reduced product contain no suitable chromophore. Instead, the GST-catalysed reaction is coupled to a glutathione reductase (GR) system that reverts oxidised glutathione (GSSG) formed as a consequence of the GST-catalysed reaction, back to GSH. In doing so, GR oxidises reduced nicotinamide adenine dinucleotide phosphate (NADPH) to NADP which contains a chromophore that can be suitably detected (Flohe and Gunzler, 1984). The reduction of one molecule of CuOOH causes the stoichiometric oxidation of one molecule of NADPH and so whilst the catalytic rate of NADP formation is measured experimentally it is directly proportional to the catalytic rate of CuOOH reduction.

Calculating the specific activities of the two GST isoforms with each substrate, as the rate of product formation per unit time per milligram of protein, demonstrated that *AmGSTF1a* is more active towards both substrates relative to *AmGSTF1c*. With CDNB as a substrate, *AmGSTF1a* has 2.9-fold higher specific activity compared with *AmGSTF1c*. Whilst with CuOOH as a substrate, *AmGSTF1a* has 1.5-fold higher specific activity compared with *AmGSTF1c* (Figure 19C).

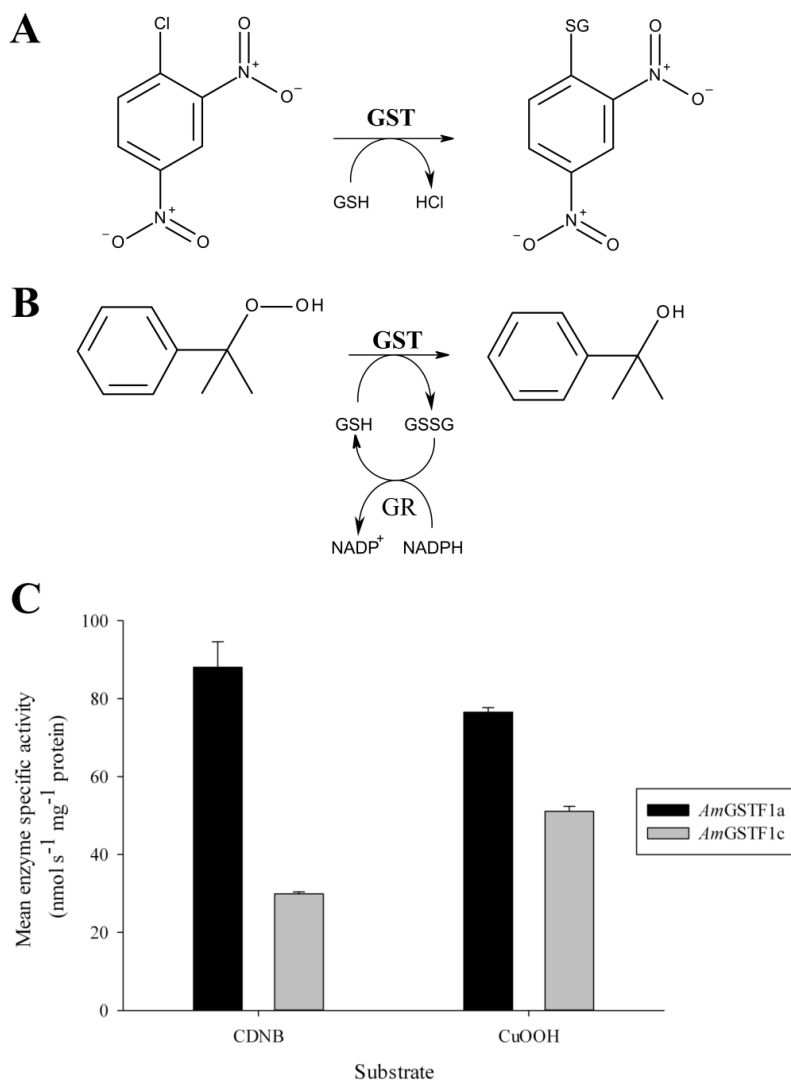


Figure 19: Catalytic activities of *AmGSTF1a* and *AmGSTF1c*. Enzymes were tested for the ability to (A) conjugate the electrophile 1-chloro-2,4-dinitrobenzene (CDNB) with reduced glutathione (GSH) and (B) reduce cumene hydroperoxide (CuOOH) to the alcohol species using GSH. Activity toward CuOOH was detected using a glutathione reductase (GR) system which reduces oxidised glutathione (GSSG) whilst oxidising nicotinamide adenine dinucleotide phosphate (NADPH). (C) Enzymes were assayed for activity with each substrate and mean specific activities were calculated. Measurements were performed in technical triplicate. Mean specific activities are shown \pm SD, $n = 3$.

Classical enzyme kinetics studies were then employed to better understand the functional basis for the differences in specific activities between the two *AmGSTF1* isoforms. Enzymes were assayed for activity towards CDNB and CuOOH using multiple substrate concentrations. The data was used to determine the maximum velocity (V_{max}) and the Michealis constant (K_M) of each enzyme with each substrate.

Whilst activity toward CDNB as a substrate was readily detected with both enzymes, kinetic studies demonstrated it was a relatively poor substrate for both GSTs. *AmGSTF1a* was calculated to have a $V_{max} = 317 \pm 40$ nmol s⁻¹ mg⁻¹ protein with a

high K_M value indicative of a weakly bound enzyme-substrate complex. CDNB proved to be an even poorer substrate for *AmGSTF1c* as rate velocity increased linearly with increasing substrate concentrations meaning V_{max} and K_M could not be determined (Table 5).

Table 5: Kinetic parameters for *AmGSTF1a* and *AmGSTF1c* with the substrate 1-chloro-2,4-dinitrobenzene (CDNB). Enzymes were assayed for activity toward CDNB over the concentration range 0-5 mM. Measurements were performed in technical triplicate. Values are shown \pm SD, n = 3. V_{max} and K_M values were calculated by hyperbolic regression (HYPER-32, The University of Liverpool). N/A – not applicable. a – specific activities calculated at a CDNB concentration of 1.25 mM.

Enzyme	Kinetic parameters		
	V_{max} (CDNB) (nmol s ⁻¹ mg ⁻¹ protein)	K_M (CDNB) (mM)	Specific activity ^a (nmol s ⁻¹ mg ⁻¹ protein)
<i>AmGSTF1a</i>	317 \pm 40	3.03 \pm 0.7	88.0 \pm 7
<i>AmGSTF1c</i>	N/A	> 5	29.9 \pm 1

CuOOH also proved to be a relatively poor substrate for both GSTs, displaying low maximal velocities and high K_M values (Table 6).

Table 6: Kinetic parameters for *AmGSTF1a* and *AmGSTF1c* with the substrate cumene hydroperoxide (CuOOH). Enzymes were assayed for activity toward CuOOH over the concentration range 0-3 mM. Measurements were performed in technical triplicate. Values are shown \pm SD, n = 3. V_{max} and K_M values were calculated by hyperbolic regression (HYPER-32, The University of Liverpool). a – specific activities calculated at a CuOOH concentration of 1.2 mM.

Enzyme	Kinetic parameters		
	V_{max} (CuOOH) (nmol s ⁻¹ mg ⁻¹ protein)	K_M (CuOOH) (mM)	Specific activity ^a (nmol s ⁻¹ mg ⁻¹ protein)
<i>AmGSTF1a</i>	128 \pm 11	0.745 \pm 0.2	76.5 \pm 1
<i>AmGSTF1c</i>	135 \pm 30	1.63 \pm 0.8	51.1 \pm 1

With both CDNB and CuOOH as substrates, *AmGSTF1a* displayed lower K_M values relative to *AmGSTF1c* indicative of a more tightly bound enzyme-substrate complex. Alignment of the amino acid sequences of the two GST isoforms revealed 11 point mutations between the two enzymes. Two of these mutations are predicted to be of residues that form direct contacts with hydrophobic substrates based on the *ZmGSTF1* structure (63 % amino acid sequence identity with the *AmGSTF1* isoforms) (Figure 20).

Figure 20: Sequence alignment of AmGSTF1a and AmGSTF1c. Sequences were aligned using Clustal Omega (1.1.0) (EBI web servers). AmGSTF1a accession: Q9ZS18, AmGSTF1c accession: Q9ZS17. Bold residues indicate active-site residues based on the ZmGSTF1 crystal structure (accession: 1axd). Boxed residues indicate non-identical active-site residues. * denote identical amino acid residues whilst : and . denote amino acid residues with similar chemical properties.

Fundamentally, while the two isoforms displayed small differences in catalytic kinetics, both were active in GSH-conjugation and as GPOXs and did not display major differences in activity. These results therefore validate the presumption that the *AmGSTF1* isoforms would display similar properties *in vitro* and strengthen the presumption that *AmGSTF1* isoforms likely perform very similar roles to each other *in planta*.

In order to be consistent with prior studies of *AmGSTF1*, particularly the transgenesis studies expressing *AmGSTF1c* in Arabidopsis (Dr. I. Cummins and Prof. R. Edwards, unpublished work at the start of this project), *AmGSTF1c* was chosen as the isoform for which all further studies would be performed with. For ease of reference all further citations of *AmGSTF1* in this thesis refer to the *AmGSTF1c* isoform.

3.2 Studies with *AmGSTF1* inhibitors

3.2.1 Introduction

With transgenesis studies demonstrating that *AmGSTF1* elicits an MHR phenotype in a transgenic host plant, a chemical library was screened for compounds that could inhibit *AmGSTF1* *in vitro* and hence be developed as potential herbicide synergists. These studies identified four compounds that, following incubation with the enzyme, significantly inhibited *AmGSTF1* activity toward CDNB; namely 4-chloro-7-nitro-

benzoxadiazole (NBD-Cl), ethacrynic acid, cyanuric chloride and bromoenol lactone (Figure 21A). Inhibition studies were performed by incubating *AmGSTF1* with each compound (100 µM) for 10 min and then assaying for activity toward CDNB (Dr. I. Cummins and Prof. R. Edwards, unpublished work at the start of this project).

Of the four compounds, NBD-Cl, ethacrynic acid and bromoenol lactone are known GST inhibitors. Ethacrynic acid and NBD-Cl are known GST substrates (Awasthi *et al.*, 1993; Caccuri *et al.*, 1996). Specifically, all three compounds are known to inhibit a mammalian-specific pi-class GST (GSTP1) that plays a key role in eliciting multi-drug resistance in human cancers (Ploemen *et al.*, 1994; Zheng *et al.*, 1996; Ricci *et al.*, 2003). All three compounds inhibit GSTP1 by binding to a reactive cysteine residue (Cys47) near the enzyme's active site. The glutathione conjugate of ethacrynic acid is also known to inhibit the enzyme (Awasthi *et al.*, 1993).

To better characterise the inhibitory properties of these compounds with respect to *AmGSTF1*, the enzyme was treated with increasing concentrations of each inhibitor, and the concentration of each compound that caused a 50 % decrease in enzyme specific activity (IC_{50}) was determined.

3.2.2 IC_{50} studies

Recombinant *Strep* II tagged *AmGSTF1* was purified as described (see section 3.1.2) and assayed for activity toward CDNB in the presence and absence of each inhibitor. Inhibitors were used over the concentration range of 0.001 – 100 µM, in the presence of saturating GSH (5 mM). Unlike the initial screen, there was no prior incubation of each inhibitor with *AmGSTF1* before assaying for activity toward CDNB to avoid the possible alkylation of Cys120. This was done to more accurately reflect the consequences of each compound entering a plant cell following spray treatment, in which the major cellular thiol is GSH (1-2 mM cellular concentration) (Noctor *et al.*, 2011). Ethacrynic acid proved the most effective inhibitor of *AmGSTF1* ($IC_{50} = 0.822 \mu M$) closely followed by NBD-Cl ($IC_{50} = 6.91 \mu M$) under these conditions. Cyanuric chloride and bromoenol lactone proved poor inhibitors for *AmGSTF1* under these conditions (Figure 21B).

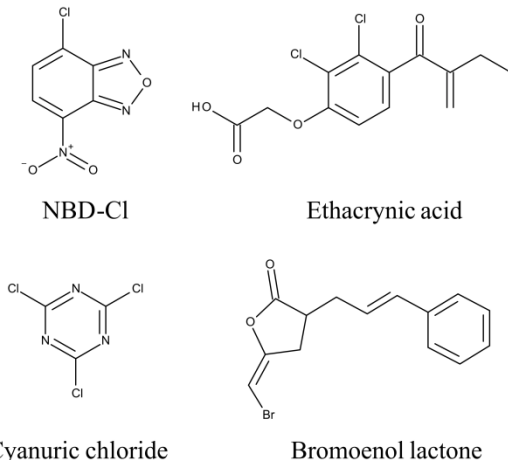
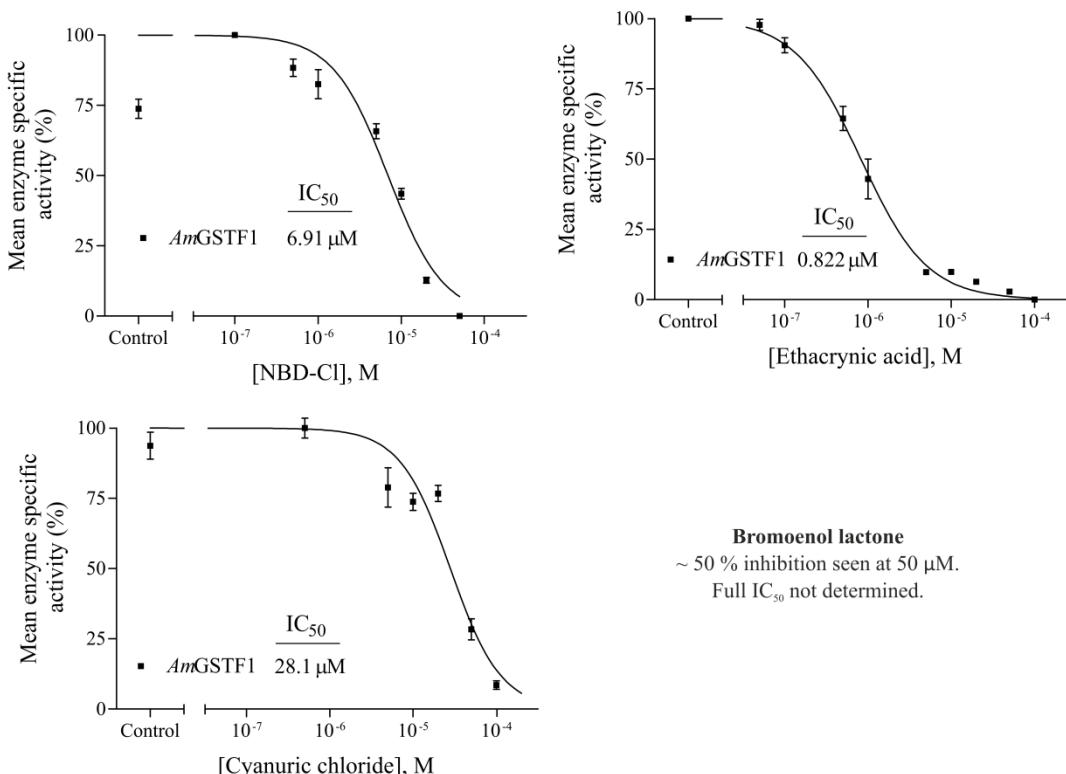
A**B**

Figure 21: Inhibitors of AmGSTF1. (A) Compounds used in IC₅₀ studies. (B) IC₅₀ curves determined with AmGSTF1 and each of the four compounds tested. In each case, AmGSTF1 was tested for activity toward CDNB (1 mM). Measurements were performed in technical triplicate. Mean specific activities are shown ± SD, n = 3. IC₅₀ curves were calculated using non-linear regression (Prism 3.0, Graphpad Software).

Samples were not analysed for alkylation following activity assays, so it is not clear if the inhibition was caused by enzyme alkylation or by competitive inhibition at the active-site by either the inhibitor, or by the respective GSH conjugate, or as a combination of these mechanisms. Studies with bromoenol lactone have strongly suggested that its mode-of-action of GSTP1 inhibition is via alkylation of Cys47 (Wu *et al.*, 2004) and there are no reports it is a GST substrate. Since no prior

incubation of *AmGSTF1* with bromoenol lactone was carried out in these IC₅₀ studies, this may explain its lack of inhibitory potency in these studies.

Comparison with MHR black-grass plants treated with each compound, followed with an application of the herbicide chloroturon, found that only NBD-Cl could enhance herbicide sensitivity in MHR plants (Dr. I. Cummins, Dr. J. Sellars, Prof. P. G. Steel and Prof. R. Edwards, unpublished work at the start of this project). In addition, cyanuric chloride, bromoenol lactone and ethacrynic acid all caused overt phytotoxic damage to black-grass. These results suggested that NBD-Cl was a viable lead compound for the development of *AmGSTF1* inhibitors that can reverse the MHR phenotype.

3.2.3 Studies with the NBD-Cl derivative 6-(7-nitro-1,2,3-benzoxadiazol-4-ylthio)hexanol (NBDHEX)

Having determined that NBD-Cl was a good inhibitor of *AmGSTF1* and a viable lead compound as a herbicide synergist, the scientific literature was explored for NBD-Cl derivatives with inhibitory properties toward GSTs. This analysis revealed that the NBD-Cl derivative 6-(7-nitro-1,2,3-benzoxadiazol-4-ylthio)hexanol (NBDHEX) (Figure 22A) had been developed as a strong competitive inhibitor of GSTP1. NBDHEX cannot alkylate cysteine residues. Instead, the mode-of-action of NBDHEX involves the formation of the respective glutathione conjugate in the GSTP1 active-site which remained tightly bound to the enzyme (Ricci *et al.*, 2005). Furthermore, treatment of multi-drug resistant cancer cells, associated with the overexpression of GSTP1, with NBDHEX reverted cells to a drug-sensitive phenotype (Turella *et al.*, 2005).

NBDHEX was tested for inhibition of *AmGSTF1* alongside NBD-Cl as a positive control. In both cases, *AmGSTF1* was incubated with each compound (100 µM) before diluting 1:100 (v/v) and assaying for enzyme activity toward CNDNB. With NBD-Cl, enzyme activity was reduced by 40 % whilst no inhibition was seen with NBDHEX (Figure 22B). Whilst alkylation of *AmGSTF1* was not established here, under similar experimental conditions *AmGSTF1* has been shown to be alkylated by NBD-Cl on the Cys120 residue (Dr. I. Cummins and Prof. R. Edwards, unpublished

work at the start of this project). Hence, alkylation of *AmGSTF1* appears to be the principal mechanism of action for inhibition by NBD-Cl. Though these results suggest that alkylation of the protein does not completely inhibit the enzyme activity of the protein, it does suggest that alkylation of *AmGSTF1* is a key mechanism in disrupting the enzyme's function in MHR.

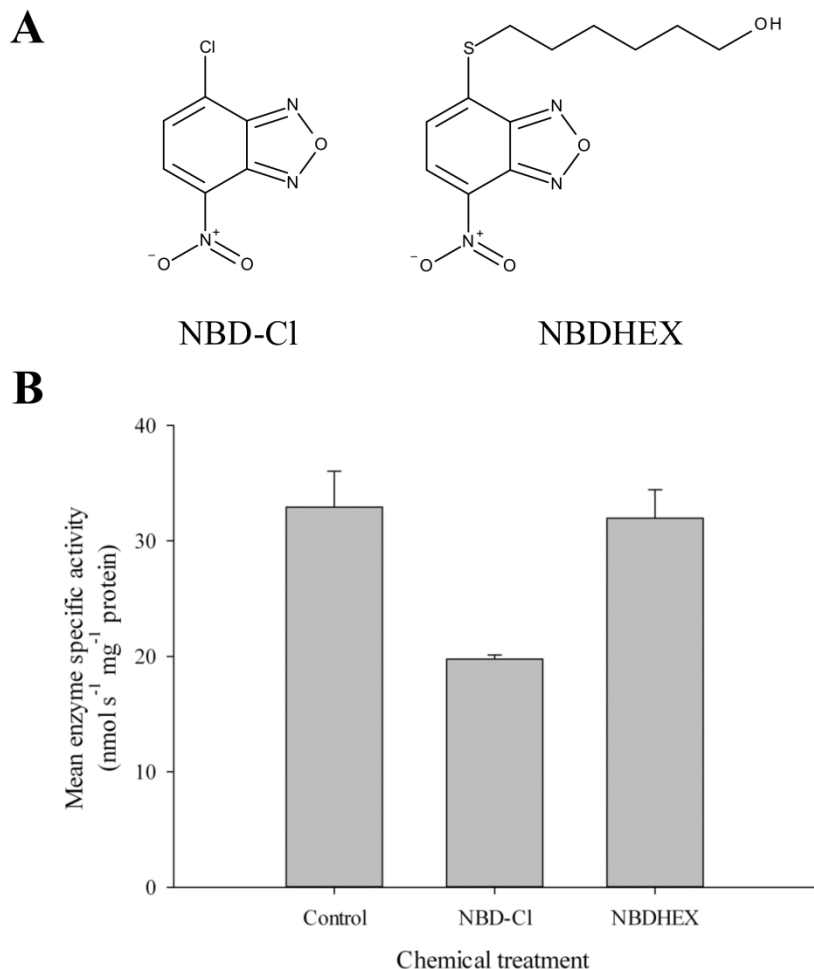


Figure 22: *AmGSTF1* inhibition studies with NBD-Cl and the NBD-Cl derivative 6-(7-nitro-1,2,3-benzoxadiazol-4-ylthio)hexanol (NBDHEX). (A) Chemical structures of NBD-Cl and NBDHEX. (B) Enzymes were incubated with 100 µM NBD-Cl, 100 µM NBDHEX or solvent control (DMSO) for 10 min before diluting 1:100 (v/v) and assaying for enzyme activity towards 1-chloro-2,4-dinitrobenzene. Measurements were performed in technical triplicate. Mean specific activities are shown ± SD, n = 3.

GSTP1 has been successfully crystallised in complex with NBDHEX with eight amino acid residues required to stabilise inhibitor binding at the active-site (Federici *et al.*, 2009). Alignment of the amino acid sequences of *AmGSTF1* and GSTP1 shows that of these eight GSTP1 residues, only one (Tyr109), responsible for pi-stacking interactions with the benzoxadiazole ring (Federici *et al.*, 2009), is conserved in the *AmGSTF1* sequence (Figure 23). These differences in active-site

chemistry provide a rationale for the low binding affinity of NBDHEX for *AmGSTF1*.

<i>AmGSTF1</i>	MAPVKVFGPAMSTNVARVTLCLEEVGAEYEVNIDFNTMEHKSPFHARNPFGQIPAFQD	60
GSTP1	MPPYTVV YFPVRGR CAALRMLLADQGQSWEVVT VETWQ --EGSLKASCLYGQLPKFQD	58
	* * . * : . * : * : * .. : . : * : . . * : ** : * ***	
<i>AmGSTF1</i>	GDLLLWESRAISKYVLRKYKTDEVDLLRESNLEEAAMVDVWTEVDAHTYNPALSPIVYQC	120
GSTP1	GDLTLYQSNTILRHLGRTLGLYG-----KDQQEAALVDMVNDGVEDL-RCKY ISLI Y --	109
	*** * : * : * : * .. * . : . : *** : * : . . : * :	
<i>AmGSTF1</i>	LFPNPMMRGLPTDEKVVAESLEKLKKLEVYEARLSKHSYLAGDFVSFADLNHFPTFYFM	180
GSTP1	--TNYEAGKDDYVKALP---GQLKPFETLLSQNQGGKTFIVGDQISFADYNLLDLLLH-	163
	. * * : . : * * . : . . : . : * : * : * : * : . .	
<i>AmGSTF1</i>	ATPHAALFDSDYPHVKAACWDRIMARPAVKKIAATMVPK-----	219
GSTP1	EVLAPGCLDAFPILLSAYVGRLSARPKLKAFLASPEYVNLPINGNGKQ	210
	. . : * : * : . * : * * * : * : * : .	

Figure 23: Amino acid sequence alignment of *AmGSTF1* and **GSTP1.** Sequences were aligned using Clustal Omega (1.1.0) (EBI web servers). *AmGSTF1* accession: Q9ZS17, **GSTP1** accession: P09211. Bold residues indicate **GSTP1** active-site residues that directly interact with NBDHEX based on the crystal structure (Federici *et al.*, 2009). * denote identical amino acid residues whilst : and . denote amino acid residues with similar chemical properties.

3.3 Analysis of the transcriptome of *AmGSTF1*-expressing *Arabidopsis* plants

3.3.1 Introduction

Expression of *AmGSTF1* in transgenic *Arabidopsis* plants elicited an MHR phenotype (Figure 15) and unexpectedly caused an up-regulation in the activities of endogenous GSTs, thiol transferases and glycosyltransferases. *AmGSTF1* expression also caused the hyper-accumulation of flavonoid and anthocyanin secondary metabolites (Dr. I. Cummins and Prof. R. Edwards, unpublished work at the start of this project).

One possible mechanism for *AmGSTF1* eliciting these changes would be perturbation of the expression of the respective genes. Multiple GSTs in mammals, including **GSTP1**, are known to perturb gene expression by regulating the function of cellular kinases via protein-protein interactions (Adler *et al.*, 1999; Cho *et al.*, 2001). However, such a regulatory mechanism has not been described for GSTs in plants.

To determine whether *AmGSTF1* perturbed gene expression in transgenic *Arabidopsis* plants, total RNA was extracted and quantified from both *AmGSTF1*-

expressors and non-transgenic Arabidopsis plants and the mRNA transcriptomes compared.

3.3.2 Transcriptome analysis of *AmGSTF1*-expressors

RNA was extracted from leaves of *AmGSTF1*-expressing plants and non-transgenic Arabidopsis plants and used for quantification of gene expression with Arabidopsis GeneChip microarray technology. Screening of sample RNA quality confirmed that all samples were of good quality with no detectable RNA degradation (Figure 24).

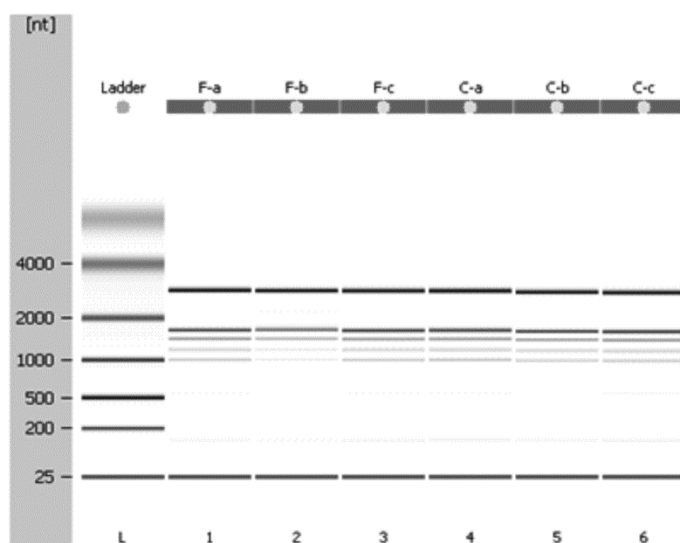


Figure 24: Analysis of sample RNA quality. RNA samples were analysed for quality and potential RNA degradation using gel electrophoresis (performed by the Technology Facility, University of York, York, UK). The discrete band pattern indicates no observable RNA degradation. Fa-c represent three biological replicate samples of *AmGSTF1*-expressor RNA. Ca-c represent three biological replicate samples of non-transgenic Arabidopsis RNA. nt – nucleotide base-pair length.

Samples were processed to yield the complementary biotin-labelled RNA molecules before quantification of gene expression (performed by the Technology Facility, University of York, York, UK). Bioinformatic analysis of the resulting gene expression data revealed few significant changes between the *AmGSTF1*-expressors and non-transgenic control plants with no changes detected in endogenous detoxification or flavonoid metabolism genes (Dr. Z. He, University of York, York, UK). The few statistically significant changes in gene expression that were detected in the *AmGSTF1*-expressors transcriptome were not confirmed in multiple independent *AmGSTF1*-expressing lines using quantitative PCR (Dr. F. Sabbadin,

University of York, York, UK). These few small changes in gene expression were most likely a result of small variations of the experimental conditions.

Significantly, these results demonstrate that *AmGSTF1* must be exerting the observed changes in *AmGSTF1*-expressing plants via a post-transcriptional mechanism. One possibility is that *AmGSTF1* directly interacts with flavonoids, anthocyanins and endogenous detoxification enzymes. Some plant GSTs are known to bind flavonoids and anthocyanins and shuttle these metabolites to cellular compartments (Marrs *et al.*, 1995; Alfenito *et al.*, 1998; Gomez *et al.*, 2011; Kitamura *et al.*, 2012). In support of this, preliminary studies with immobilised *AmGSTF1* have indicated that the enzyme selectively retains flavonoid-like compounds following exposure to plant methanolic extracts (Dr. F. Sabbadin, University of York, York, UK). There is a precedent for GSTs directly regulating detoxification enzyme activity, as mammalian GSTP1 is known to directly interact and regulate the activity of a glutathione peroxidase enzyme (Zhou *et al.*, 2013), but there are no reports of plant GSTs fulfilling a similar role.

3.4 Discussion

The results presented in this chapter sought to answer the questions raised regarding the properties of *AmGSTF1* isoforms, inhibition of *AmGSTF1* by potential herbicide synergists and the mechanism by which *AmGSTF1* elicits changes in endogenous detoxification enzyme activities and flavonoid metabolism in a transgenic host plant. With regards to multiple *AmGSTF1* isoforms, these results show that the multiple enzymes have very similar catalytic properties supporting the conjecture that they play very similar roles *in planta*. Due to their high sequence and catalytic similarities one isoform, *AmGSTF1c*, was chosen as a model for further studies.

As prior studies have demonstrated that *AmGSTF1* plays a key role in MHR (Dr. I. Cummins and Prof. R. Edwards, unpublished work at the start of this project), *AmGSTF1* was chosen as a target for inhibition in attempts to reverse the resistance phenotype. *In vitro* studies with potential *AmGSTF1* inhibitors identified NBD-Cl as a strong *AmGSTF1* inhibitor ($IC_{50} = 6.91 \mu\text{M}$), for which the principal mode-of-action for inhibition appears to be alkylation of the enzyme on the Cys120 residue.

Finally, gene expression studies of MHR *AmGSTF1*-expressing Arabidopsis plants have found no significant changes in expression. Hence, the biochemical changes reported in the *AmGSTF1*-expressors (Dr. I. Cummins and Prof. R. Edwards, unpublished work at the start of this project) must be induced post-transcriptionally.

Importantly, by characterising an inhibitor of *AmGSTF1* that is also known to reverse the MHR black-grass phenotype and identifying that *AmGSTF1* post-transcriptionally activates endogenous enzymes and flavonoid accumulation in an MHR transgenic host, these results suggest that *AmGSTF1* may elicit an MHR phenotype in transgenic Arabidopsis plants by both catalytic and non-catalytic mechanisms. These results have also corroborated the identification of a key amino acid residue, Cys120, for the interaction of *AmGSTF1* with the inhibitor NBD-Cl. It was now of interest to study the roles of catalysis and Cys120 in eliciting an MHR phenotype.

Chapter 4 – Probing *AmGSTF1* function using mutant isoforms

4.1 Introduction

Studies have shown that *AmGSTF1* elicited MHR in a transgenic host plant and that this correlated with increased activities of endogenous detoxification enzymes and hyperaccumulation of protective flavonoids and anthocyanins (Dr. I. Cummins and Prof. R. Edwards, unpublished work at the start of this project). These changes mirrored those induced in MHR black-grass plants relative to wild-type sensitive (WTS) plants (Cummins *et al.*, 2009). *AmGSTF1* is also known to function *in vitro* as a GPOX enzyme and can detoxify toxic organic and long-chain fatty acid hydroperoxides. This activity correlated with the ability of MHR black-grass plants, which constitutively express *AmGSTF1*, to maintain hydroperoxide concentrations at a basal level following herbicide treatment (Cummins *et al.*, 1999). Therefore, *AmGSTF1* may elicit MHR using both catalytic and non-catalytic mechanisms. Regarding catalysis, Cys120 has been shown to play a key role in the interaction between *AmGSTF1* and the inhibitor NBD-Cl by forming a covalent bond with the nitrobenzoxadiazole moiety. NBD-Cl also reverted MHR black-grass to a WTS phenotype when sprayed onto MHR plants (Dr. I. Cummins and Prof. R. Edwards, unpublished work at the start of this project) indicating that *AmGSTF1* catalytic activity appears to be important for the phenotype.

The increases in endogenous detoxification enzyme activities and the interaction between Cys120 and NBD-Cl bear a surprising resemblance to that seen with the evolutionarily distinct mammalian-specific GSTP1, an enzyme that plays a key role in eliciting multi-drug resistance in human cancers. This GST can directly regulate the activity of a glutathione peroxidase enzyme via protein-protein interactions (Zhou *et al.*, 2013) and is inhibited by NBD-Cl due to alkylation of a reactive cysteine residue (Cys47) (Ricci *et al.*, 2003). Furthermore, Cys47 of GSTP1 is required for the reversible interaction of this enzyme with flavonoids (van Zanden *et al.*, 2003). This suggested that Cys120 of *AmGSTF1* could play a similar role in the interaction of *AmGSTF1* with flavonoids.

In order to investigate the relative contributions of GPOX activity and Cys120 in promoting the MHR phenotype, a catalytically retarded mutant and a mutant lacking Cys120 were generated, characterised *in vitro* and expressed in transgenic Arabidopsis plants. The transgenic plants were then screened for changes in herbicide tolerance, endogenous detoxification enzyme activities and flavonoid accumulation.

4.2 *In vitro* characterisation of *AmGSTF1* mutant isoforms

4.2.1 Generation and purification of *AmGSTF1* mutant isoforms

Phi-class GSTs are known to use a serine residue within the active-site as the principal residue for catalysis (Cummins *et al.*, 2011). The hydroxyl side-chain of the serine residue promotes deprotonation of bound GSH to the thiolate anion by abstracting the sulphhydryl proton via hydrogen bonding (Labrou *et al.*, 2001). Sequence alignment of *AmGSTF1* with the well-studied maize orthologue *ZmGSTF1* (63 % amino acid identity) identified Ser12 as the catalytic serine residue in *AmGSTF1*. Using site-directed mutagenesis, a mutant isoform where Ser12 had been mutated to alanine, was generated (termed S12A). The alkyl side-chain of alanine is non-nucleophilic and so cannot promote the deprotonation of GSH. It is also sterically small and so should not perturb the overall structural architecture of *AmGSTF1*.

Using the same strategy, a further mutant was generated in which Cys120 was mutated to a valine residue (C120V). The non-nucleophilic side-chain of valine should abolish any alkylation of the protein at this position.

To generate both point mutants, the coding sequence of *AmGSTF1* in the pET-24a vector was used to design two sets of primers containing the appropriate codon changes to produce the C120V and S12A mutants respectively. Following PCR of the plasmid using these primer sets and digestion of template DNA, amplified products were purified using agarose gel electrophoresis and transformed into competent *E. coli* cells. Plasmid DNA was purified and the mutant coding sequences confirmed by DNA sequencing. To allow easy and rapid purification of both

mutants, C120V and S12A coding sequences were sub-cloned into the pET-STRP3 vector to generate the respective *N*-terminal *Strep* II tag fusions and re-sequenced to confirm the correct constructs. Recombinant *Strep* II tagged mutants, alongside recombinant *Strep* II tagged *AmGSTF1*, were then expressed in *E. coli* and purified as described (see section 3.1.2). The purity of recombinant proteins was tested using sodium dodecyl sulfate polyacrylamide gel electrophoresis (SDS-PAGE). No contaminating bands were detected, even when loading with 5 µg purified recombinant protein (Figure 25).

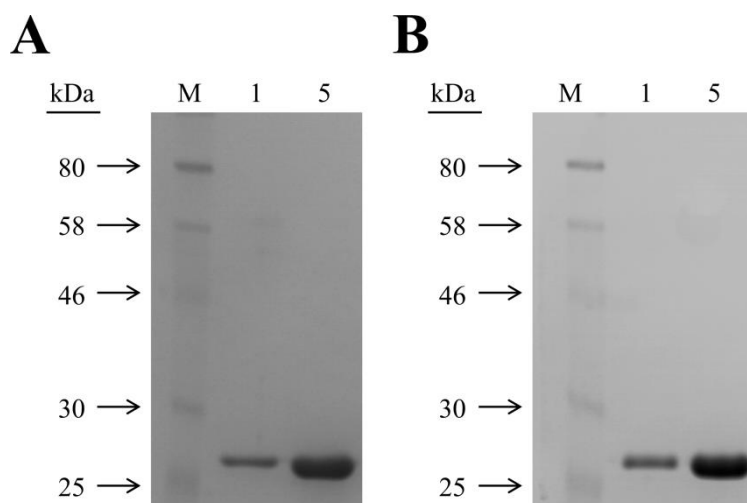


Figure 25: Purity analysis of recombinant *AmGSTF1* and C120V. Purified (A) *AmGSTF1* and (B) C120V enzymes were analysed using sodium dodecyl sulfate polyacrylamide gel electrophoresis (SDS-PAGE). 1 µg (1) and 5 µg (5) enzyme were loaded per gel. M – protein markers. Molecular weights (kDa) of protein markers are shown.

As a further check for purity, enzymes were analysed by mass spectrometry and found to contain only the desired protein (Table 7). Data for the C120V mutant is shown as an example with analogous results obtained with the S12A mutant.

Table 7: Whole-protein mass measurements of purified recombinant *AmGSTF1* and C120V. Purified recombinant *Strep* II tagged enzymes were analysed using electrospray ionisation mass spectrometry (ESI-MS) in positive ion mode (Technology Facility, University of York, UK). The theoretical masses assume complete loss of the *N*-terminal methionine residue as is known to occur for *Arabidopsis Strep* II tagged GSTs. The observed masses with an increase of 42 Da above the theoretical mass of each enzyme is due to *N*-acetylation of the revealed *N*-terminal alanine residue as is known to occur with *Arabidopsis Strep* II tagged GSTs (Dixon *et al.*, 2009).

Enzyme	Theoretical mass (Da)	Observed masses (Da)
<i>AmGSTF1</i>	26665	26664, 26706
C120V	26661	26661, 26703

4.2.2 Catalytic profiles of *AmGSTF1* mutant isoforms

Following purification, recombinant *AmGSTF1*, C120V and S12A were screened with a range of potential substrates (Figure 26). These substrates included; **(A)** 1-chloro-2,4-dinitrobenzene (CDNB), **(B)** cumene hydroperoxide (CuOOH), **(C)** 2-hydroxyethyl disulfide (HED), **(D)** 4-nitrophenyl acetate (NPA), **(E)** ethacrynic acid, **(F)** crotonaldehyde and **(G)** benzyl isothiocyanate (BITC). The use of these substrates allowed *AmGSTF1* and the mutant isoforms to be tested for four different catalytic activities. CDNB, ethacrynic acid, crotonaldehyde and BITC were used to test for activity as a GSH-conjugation enzyme using GSH as a co-substrate (Habig *et al.*, 1974; Berhane *et al.*, 1994; Kolm *et al.*, 1995). CuOOH tested for activity as a GPOX enzyme using GSH as a co-factor (Flohe and Gunzler, 1984). HED was used as a substrate so far shown to be specific for lambda-class plant GSTs which tests for thiol transferase activity in which GSH is used as a co-factor to reduce the disulfide substrate to the respective free thiol components (Dixon *et al.*, 2002). NPA was used to test for ester thiolytic activity using GSH as a co-substrate (Keen and Jakoby, 1978).

Previous studies with *AmGSTF1* had screened the enzyme with CDNB, CuOOH, ethacrynic acid, crotonaldehyde and BITC and found it to be active towards 4 of these 5 substrates with no activity detected toward crotonaldehyde (Cummins *et al.*, 1999). Hence, these substrates were useful to determine catalytic differences between *AmGSTF1* and the mutant isoforms. HED and NPA have not been previously tested as substrates for *AmGSTF1*.

Equimolar concentrations of *AmGSTF1*, C120V or S12A were assayed for activity towards each substrate in the presence of excess GSH. In all cases, activity toward each substrate was detected using UV-vis spectrophotometry. In the case of CDNB, ethacrynic acid, crotonaldehyde, NPA and BITC, product formation could be directly measured due to the occurrence of an appropriate chromophore in the product molecule. For studies with CuOOH and HED, a lack of a convenient chromophore in either the substrate or product molecule meant that the GST-catalysed reaction was indirectly monitored by coupling to a glutathione reductase redox system (as described in section 3.1.3).

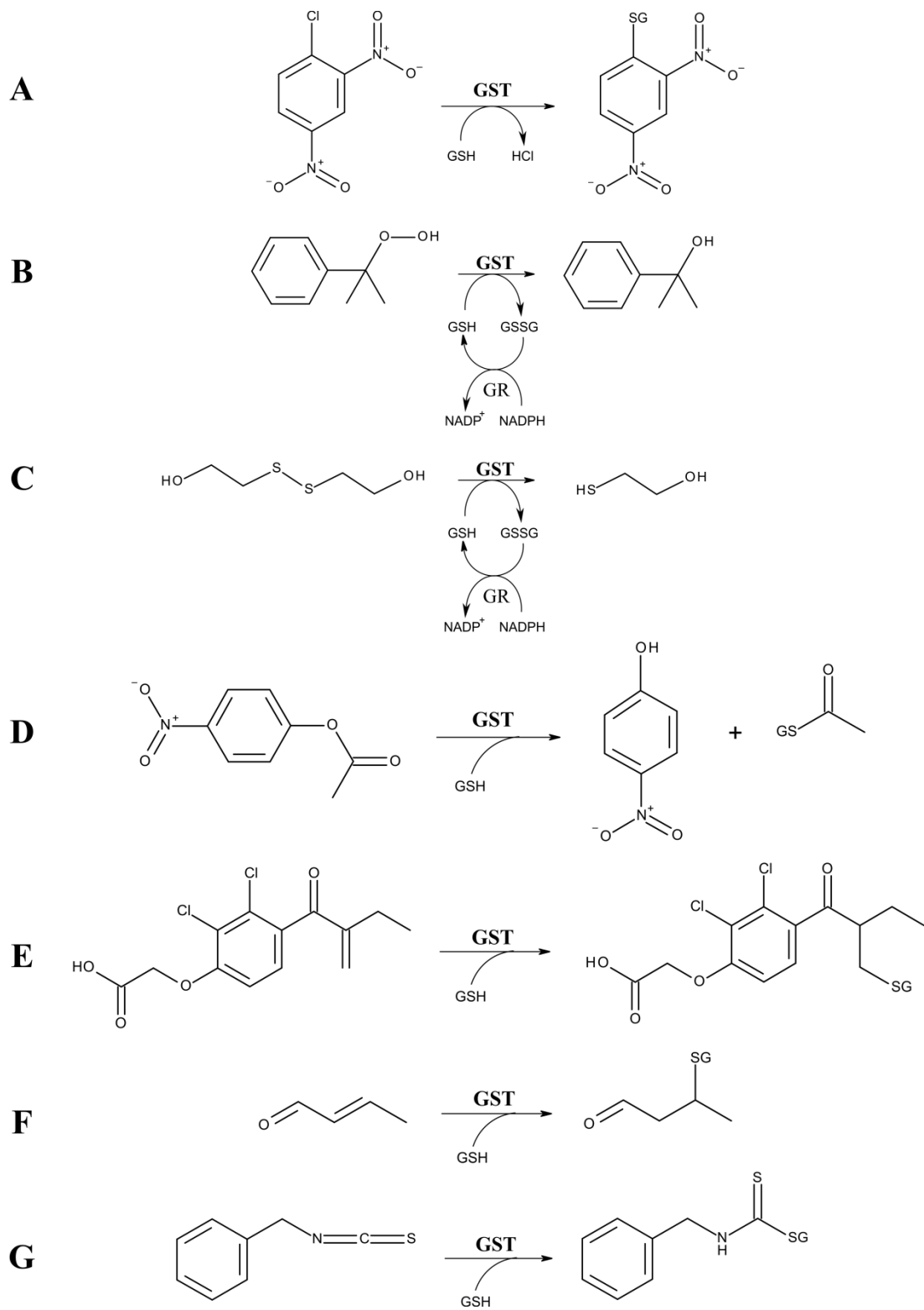


Figure 26: *In vitro* reaction schemes of known GST substrates used in this study to determine the catalytic profiles of AmGSTF1 and associated mutant isoforms. GSTs in this study were tested with the following substrates; (A) 1-chloro-2,4-dinitrobenzene, (B) cumene hydroperoxide, (C) 2-hydroxyethyl disulfide, (D) 4-nitrophenyl acetate, (E) ethacrynic acid, (F) crotonaldehyde and (G) benzyl isothiocyanate. Substrates are shown to the left of the respective reaction scheme arrow with reaction products shown to the right. For A, D-G, product formation is measured directly. For B and C, the coupled oxidation of reduced nicotinamide adenine dinucleotide phosphate (NADPH) is measured. In all cases, measurements are recorded using UV-vis spectrophotometry. Additional abbreviations: GSH – reduced glutathione, GSSG – oxidised glutathione, GR – glutathione reductase, NADP⁺ - oxidised nicotinamide adenine dinucleotide phosphate.

AmGSTF1, S12A and C120V were all active towards the same subset of substrates, with no activity detected towards the lambda GST-specific substrate HED, or toward crotonaldehyde (Table 8).

Table 8: Substrate specificities of recombinant *AmGSTF1*, C120V and S12A enzymes. CDNB: 1-chloro-2,4-dinitrobenzene. ND: not detected. Measurements were performed in technical triplicate. Mean specific activities are shown \pm SD, n = 3.

Substrate	Mean specific activity (nmol s ⁻¹ mg ⁻¹ protein)		
	<i>AmGSTF1</i>	C120V	S12A
CDNB	25.4 \pm 0.8	27.8 \pm 1.6	5.5 \pm 0.5
Cumene hydroperoxide	19.6 \pm 1.4	24.1 \pm 0.8	5.1 \pm 0.1
2-hydroxyethyl disulfide	ND	ND	ND
4-nitrophenyl acetate	1.06 \pm 0.07	1.10 \pm 0.03	0.80 \pm 0.02
Ethacrynic acid	16.4 \pm 0.8	15.7 \pm 0.3	3.0 \pm 0.5
Crotonaldehyde	ND	ND	ND
Benzyl isothiocyanate	34.2 \pm 0.7	34.8 \pm 1.0	13.0 \pm 0.8

As expected, S12A had severely retarded activity toward all substrates, including a 74 % reduction in GPOX activity relative to *AmGSTF1*. Somewhat unexpectedly, C120V displayed a small but significant increase in specific activity relative to *AmGSTF1* toward both CDNB and CuOOH as substrates. This observation was explored further by calculating the catalytic efficiency (k_{cat} / K_M) of both *AmGSTF1* and C120V with each substrate. Previous attempts to determine V_{max} and K_M kinetic constants for *AmGSTF1* with CDNB and CuOOH as substrates had proven largely unsuccessful, due to a lack of active-site saturation within the range of substrate solubility (see section 3.1.3). However, catalytic efficiency (k_{cat} / K_M) can be calculated by assaying the enzyme at a substrate concentration well below the substrate K_M as reported in studies with mammalian GSTs (Berhane *et al.*, 1994) (Equation 2).

$$(k_{cat} / K_M) = V / [E][S]$$

Equation 2: Approximation of enzyme catalytic efficiency (k_{cat} / K_M) at substrate concentrations well below the substrate K_M . V – rate of product formation. [E] – enzyme concentration. [S] – substrate concentration.

Previous studies with *AmGSTF1* indicated that the K_M for CDNB and CuOOH were > 5 mM and 1.6 ± 0.8 mM respectively (Table 5 and Table 6). Therefore *AmGSTF1* and C120V were assayed with substrates at a concentration of 0.1 mM in the presence of excess GSH. With both substrates, C120V displayed a significant increase in catalytic efficiency relative to *AmGSTF1* with a 57 % increase in efficiency toward CDNB turnover and a 63 % increase in efficiency toward CuOOH turnover (Table 9).

Table 9: Estimated k_{cat}/K_M values for *AmGSTF1* and C120V with 1-chloro-2,4-dinitrobenzene (CDNB) or cumene hydroperoxide (CuOOH) as substrates. Kinetic parameters were estimated using substrate concentrations (100 μ M) well below the respective substrate K_M whilst maintaining the co-substrate (glutathione) at a saturating concentration (1-5 mM). Measurements were performed in technical triplicate. k_{cat}/K_M values are shown \pm SEM, $n = 3$.

Enzyme	k_{cat}/K_M ($M^{-1} s^{-1}$)	
	CDNB	CuOOH
<i>AmGSTF1</i>	466 ± 34	439 ± 36
C120V	730 ± 43	715 ± 34

With no available crystallographic data, it was not clear why the C120V mutant showed increased catalytic efficiency with these two substrates. Studies with GSTP1 mutants have found that Cys47 plays a role in controlling catalytic activity by transmitting conformational changes across the GST dimer and decreasing structural flexibility (Ricci *et al.*, 1995; Ricci *et al.*, 2003) although equivalent studies with *AmGSTF1* were not pursued. Importantly, with respect to understanding the role of GPOX activity for an MHR phenotype, the S12A and C120V mutants behave with significantly lower and higher GPOX activities respectively relative to *AmGSTF1*.

All three purified enzymes were shown to be catalytically stable during storage at 4 °C (Figure 27).

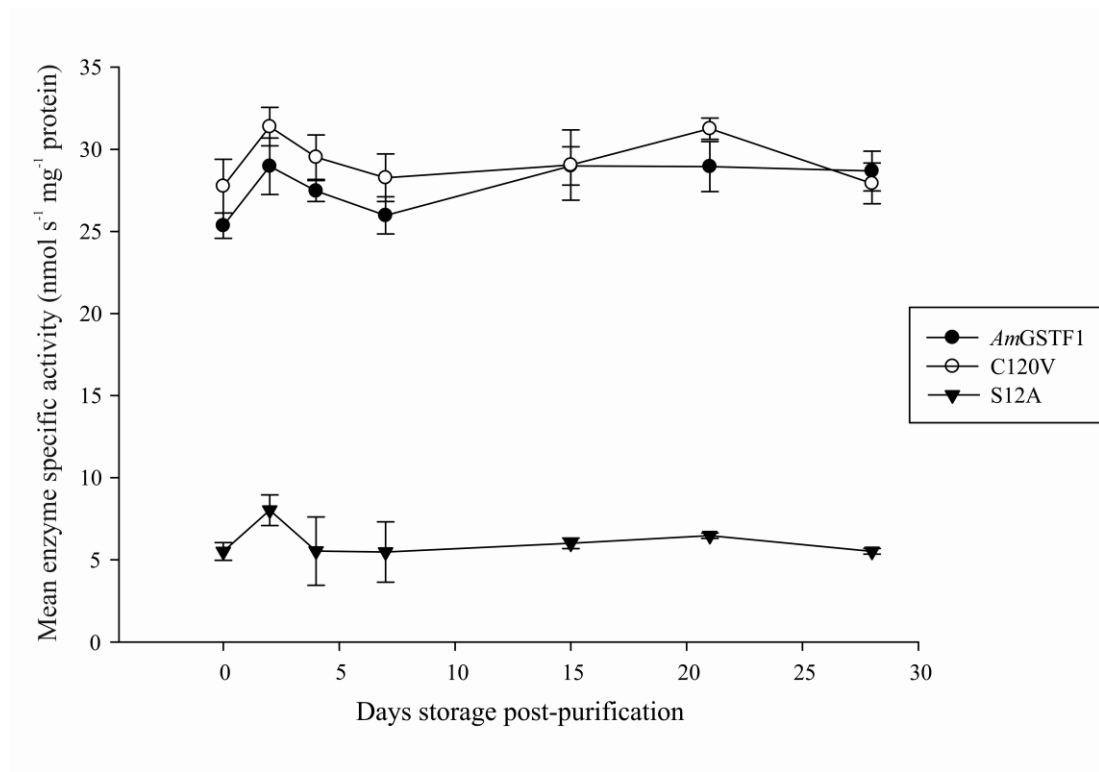


Figure 27: Catalytic stability of *AmGSTF1*, *C120V* and *S12A* enzymes. Recombinant enzymes were purified and assayed over a 28 day period for activity towards 1-chloro-2,4-dinitrobenzene (CDNB) and otherwise maintained at 4 °C. Measurements were performed in technical triplicate. Mean specific activities are shown ± SD, n = 3.

4.2.3 Exploitation of the **C120V** mutant to study inhibition of *AmGSTF1* by alkylation

4.2.3.1 Inhibition studies with NBD-Cl

The data suggested that inhibition of *AmGSTF1* by NBD-Cl was largely a consequence of covalent binding of the nitrobenzoxadiazole moiety to Cys120. Therefore, the C120V mutant was explored for its interaction with NBD-Cl. It was hypothesized that if alkylation of Cys120 was the sole mode of *AmGSTF1* inhibition, then no modification or inhibition of C120V would be observed.

In a first experiment, equimolar concentrations of purified recombinant *AmGSTF1* and C120V were incubated with two different concentrations of NBD-Cl (100 µM or 1 mM), with an equivalent volume of dimethyl sulfoxide (DMSO), the solvent used to solubilise NBD-Cl, serving as a negative control. Enzymes were incubated with

each respective treatment for 10 min before diluting 1:100 (v/v) and assaying for activity toward CDNB.

The C120V mutant proved far more resistant to inhibition by NBD-Cl relative to *AmGSTF1*. Following exposure to 100 μ M NBD-Cl, the C120V mutant experienced an 8 % loss in mean specific activity whilst *AmGSTF1* mean specific activity fell by 47 %. Exposure to a very high NBD-Cl concentration (1 mM) abolished *AmGSTF1* activity (>99 % loss). However, a significant proportion of C120V activity remained (28 % activity remaining) (Figure 28B).

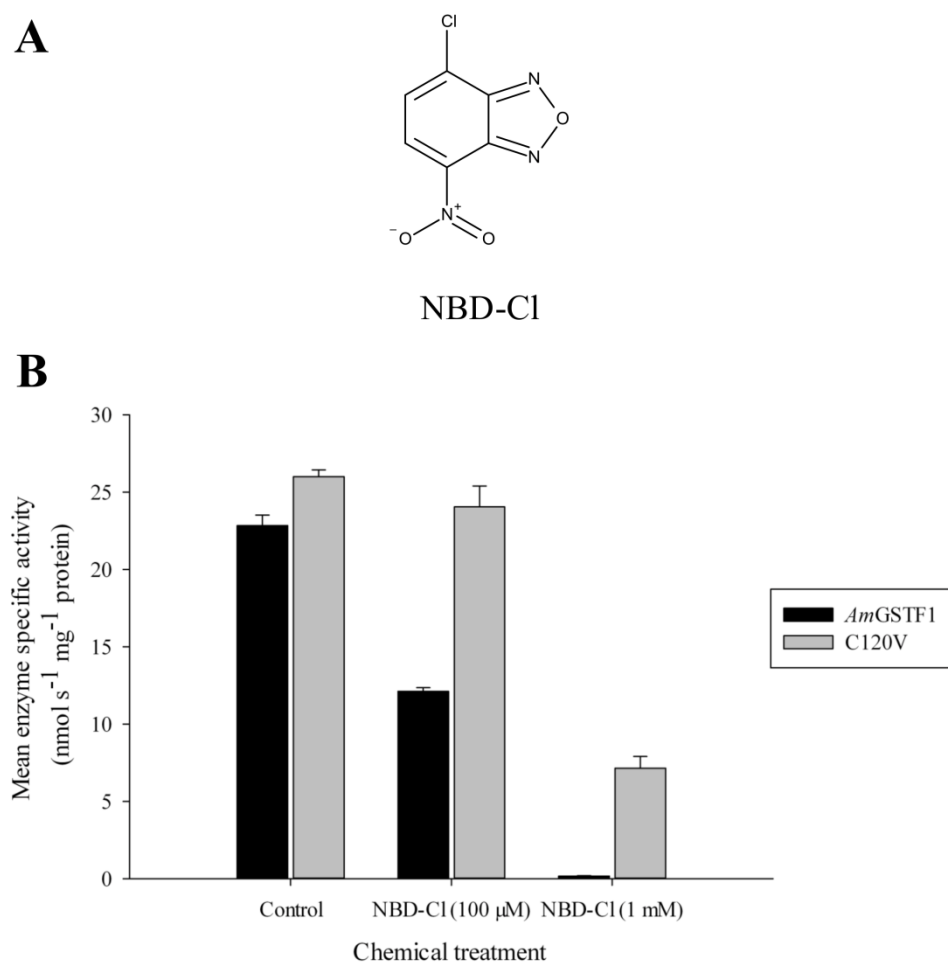


Figure 28: Inhibition of *AmGSTF1* and C120V following treatment with 4-chloro-7-nitro-benzoxadiazole. (A) Chemical structure of 4-chloro-7-nitro-benzoxadiazole (NBD-Cl). (B) Enzymes were incubated with NBD-Cl or solvent control (DMSO) for 10 min before diluting 1:100 (v/v) and assaying for enzyme activity towards 1-chloro-2,4-dinitrobenzene. The NBD-Cl concentration, to which the enzymes were exposed prior to assaying for activity, is shown in brackets on the x-axis. Measurements were performed in technical triplicate. Mean specific activities are shown \pm SD, n = 3.

This first experiment highlighted two important observations regarding the interaction between NBD-Cl and *AmGSTF1*. Firstly, prevention of alkylation of *AmGSTF1* greatly reduced inhibition of the enzyme by NBD-Cl. Hence, alkylation appears to be the primary mode of inhibition of *AmGSTF1* as suggested with studies using the non-alkylating NBD-Cl derivative NBD HEX. Secondly, the C120V mutant is still inhibited by NBD-Cl, albeit to a much lesser degree than *AmGSTF1*. Mass spectrometry would be required to absolutely determine that C120V is not alkylated by NBD-Cl but based on this assumption it would appear that the protein may also be weakly inhibited by competition at the active site with NBD-Cl or the NBD-glutathione conjugate (NBD-SG).

Prior to mass spectrometry studies, a time-course treatment was employed to further understand the alkylation event. It would be expected that non-competitive inhibition of *AmGSTF1* would be time-dependent. Equimolar concentrations of *AmGSTF1* and C120V were incubated for 0 - 60 min with either a fixed concentration of NBD-Cl (100 µM) or an equivalent volume of DMSO as a negative control and assayed for activity towards CDNB at fixed time-points.

C120V displayed no significant time-dependent inhibition when exposed to NBD-Cl. Instead, C120V was weakly inhibited by NBD-Cl in a time-independent manner possibly due to competitive inhibition at the active-site by NBD-Cl or the NBD-glutathione (NBD-SG) conjugate formed non-enzymatically under the assay conditions (molar excess of GSH). *AmGSTF1* however displayed apparent bi-phasic inhibition behaviour when treated with NBD-Cl with rapid inhibition over the period 0-5 min followed by a slower rate of inhibition over the period 5-60 min (Figure 29).

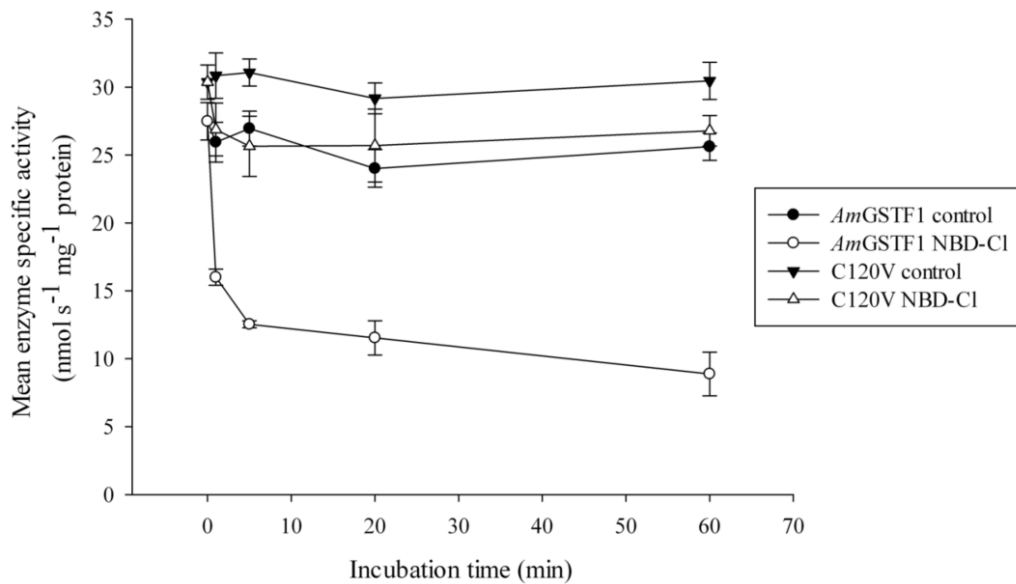


Figure 29: Time-dependent inhibition of *AmGSTF1* by 4-chloro-7-nitro-benzoxadiazole. Enzymes were incubated with 100 μ M 4-chloro-7-nitro-benzoxadiazole (NBD-Cl) or an equivalent volume of DMSO (control) over a period of 0 - 60 min. Aliquots were diluted 1:100 (v/v) before assaying for activity towards 1-chloro-2,4-dinitrobenzene at discrete time-points. Measurements were performed in technical triplicate. Mean specific activities are shown \pm SD, n = 3.

Interestingly, this bi-phasic behaviour is very similar to that seen with NBD-Cl-treated *HsGSTP1* which was proposed to be due to non-equivalent Cys47 residues on each monomer of the GSTP1 dimer (Ricci *et al.*, 2003). Molecular dynamic simulations of the interaction between GSTP1 and NBD-Cl suggested that the bi-phasic behaviour was due to intersubunit communication across the GST dimer, with alkylation of one monomer Cys47 transmitting a conformational signal to allow the second monomer Cys47 to become more recalcitrant to alkylation and so preserve activity (Ricci *et al.*, 2003). Whilst molecular dynamic simulations fell outside the scope of our biochemical studies Figure 29 would suggest that a similar phenomenon of communication exists for *AmGSTF1*.

These studies however still did not determine alkylation of the proteins. To resolve this, *AmGSTF1* and C120V were first treated with NBD-Cl or DMSO in an identical manner to that described for the time-course. After 60 min exposure to each compound, treated enzymes were desalted using size-exclusion chromatography and whole protein molecular weights were determined using mass spectrometry. A single alkylation of *AmGSTF1* would cause an increase in mass of 163 Da if the chloride ion of NBD-Cl was displaced. The observed mass ions of NBD-Cl treated *AmGSTF1* were 163 Da greater than the mass ions detected following DMSO treatment proving

that *AmGSTF1* had been completely alkylated by NBD-Cl after a 60 min treatment. No alkylation of C120V was detected following NBD-Cl treatment confirming that Cys120 is the sole site of *AmGSTF1* modification by NBD-Cl (Table 10).

Table 10: Analysis of *AmGSTF1* and C120V by mass spectrometry following treatment with 4-chloro-7-nitro-benzoxadiazole. Enzymes were incubated with 100 µM 4-chloro-7-nitro-benzoxadiazole (NBD-Cl) or an equivalent volume of DMSO for 60 min before desalting and whole-protein molecular weight determination using electrospray ionisation mass spectrometry. Theoretical masses for *AmGSTF1* are shown assuming alkylation of the protein by NBD-Cl. Theoretical masses assume complete loss of the *N*-terminal methionine residue as is known to occur for *Arabidopsis Strep II* tagged GSTs (Dixon *et al.*, 2009).

Enzyme	Chemical treatment	Theoretical mass (Da)	Observed masses (Da)
<i>AmGSTF1</i>	DMSO	26665	26663
	NBD-Cl	26828	26826
C120V	DMSO	26661	26661
	NBD-Cl	26661	26658

Hence, the weak inhibition of C120V was most likely due to competitive inhibition at the active-site of the enzyme by NBD-Cl or the NBD-Cl glutathione conjugate (NBD-SG). This hypothesis has been tested using a chemically synthesized NBD-SG.

4.2.3.2 Inhibition studies with the nitrobenzoxadiazole-glutathione conjugate (NBD-SG)

To try and establish the cause of weak C120V inhibition by NBD-Cl, equimolar concentrations of *AmGSTF1* and C120V enzymes were treated with NBD-SG (kindly donated by Dr. J. D. Sellars, Department of Chemistry, Durham University, UK; Figure 30A), alongside NBD-Cl and DMSO treatments as positive and negative controls respectively. Both NBD-Cl and NBD-SG were used at a fixed concentration (100 µM) and all treatments consisted of a 10 min incubation period. Following treatments, enzymes were diluted 1:100 (v/v) and assayed for activity toward CDNB in the presence of excess GSH.

C120V experienced similar levels of inhibition with both NBD-Cl and NBD-SG (Figure 30B). Hence, the inhibition of C120V by NBD-Cl appears to be due to non-enzymatic formation of the NBD-SG conjugate under the assay conditions.

AmGSTF1 was inhibited significantly by both NBD-Cl and NBD-SG with a 47 % and 35 % reduction of enzyme activity respectively (Figure 30B).

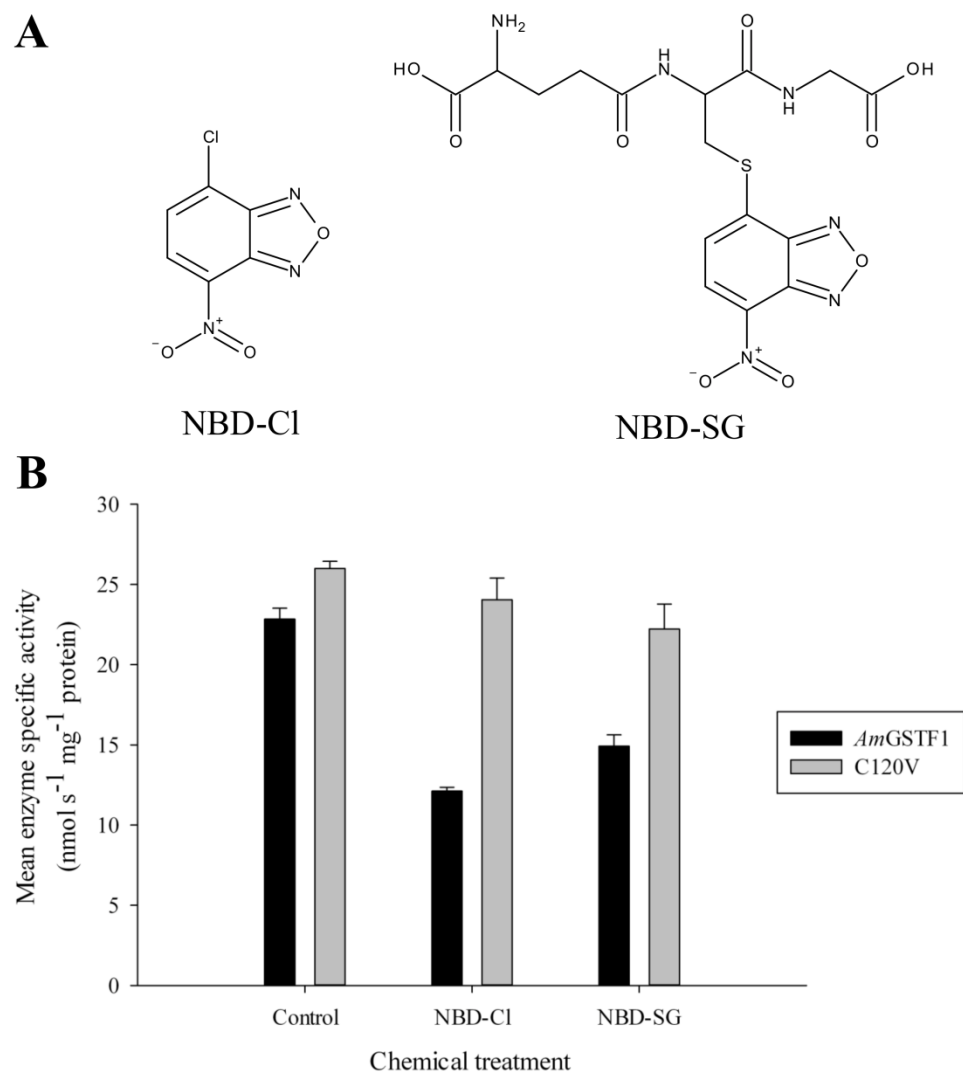


Figure 30: Inhibition of *AmGSTF1* and C120V following treatment with 4-chloro-7-nitro-benzoxadiazole (NBD-Cl) or a chemically-synthesized NBD-glutathione conjugate (NBD-SG). (A) Chemical structures of NBD-Cl and NBD-SG. (B) Enzymes were incubated with 100 μ M NBD-Cl, 100 μ M NBD-SG or solvent control (DMSO) for 10 min before diluting 1:100 (v/v) and assaying for enzyme activity towards 1-chloro-2,4-dinitrobenzene. Measurements were performed in technical triplicate. Mean specific activities are shown \pm SD, n = 3.

It was possible that the greater level of inhibition seen following NBD-Cl treatment of *AmGSTF1* relative to NBD-SG treatment was due to a more rapid alkylation of *AmGSTF1* by the more potent electrophile. To determine relative rates of inhibition, equimolar concentrations of *AmGSTF1* and C120V were incubated for 0 - 60 min with either a fixed concentration (100 μ M) of NBD-Cl, NBD-SG or an equivalent

volume of DMSO as a negative control and assayed for activity towards CDNB at fixed time-points.

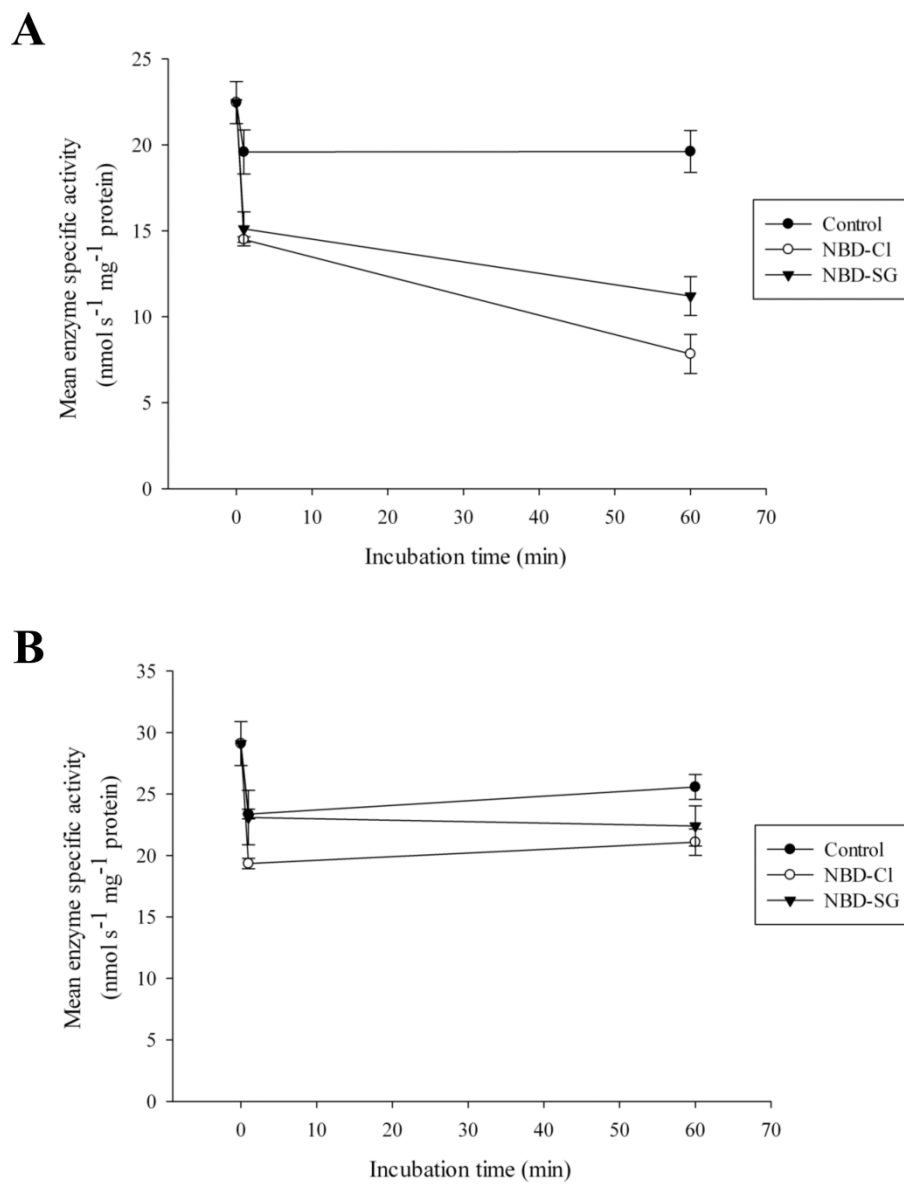


Figure 31: Time-dependent inhibition of AmGSTF1 following treatment with 4-chloro-7-nitrobenzoxadiazole (NBD-Cl) or a chemically-synthesized NBD-glutathione (NBD-SG) conjugate. (A) AmGSTF1 and (B) C120V were each incubated with 100 μ M NBD-Cl, 100 μ M NBD-SG or solvent control (DMSO) over a period of 60 min. At discrete time-points aliquots were diluted 1:100 (v/v) and assayed for activity towards 1-chloro-2,4-dinitrobenzene. Measurements were performed in technical triplicate. Mean specific activities are shown \pm SD, n = 3.

Whilst C120V was only weakly inhibited by both NBD-Cl and NBD-SG independent of incubation time (Figure 31B), AmGSTF1 displayed time-dependent inhibition of activity following treatment with both NBD-Cl and NBD-SG with a

faster rate of inhibition detected when exposed to NBD-Cl relative to NBD-SG (Figure 31A).

To determine if the faster rate of inhibition correlated with an increased rate of alkylation, equimolar concentrations of each enzyme were once again treated with NBD-Cl, NBD-SG or DMSO under the same conditions as for the time-course study. After 60 min, treated enzymes were desalted using size-exclusion chromatography and whole protein molecular weights were determined using mass spectrometry. Mass analysis found that *AmGSTF1* was fully labelled by NBD-Cl as only NBD-modified mass ions could be detected. However, analysis of *AmGSTF1* treated with NBD-SG detected both NBD-labelled and unlabelled protein mass ions indicating a slower rate of alkylation. No alkylation of C120V was detected with any treatment (Table 11). For all treatments with both *AmGSTF1* and C120V, a proportion of mass ions were detected that were 346 Da lower than the theoretical mass (Table 11). Mathematically this loss could be accounted for by loss of the *N*-terminal MASW sequence of the *Strep* II tag although this modification has not been previously reported. Importantly though, NBD-modified *AmGSTF1* mass ions were all 163 Da larger than the respective DMSO-treated counterparts.

Table 11: Analysis of *AmGSTF1* and C120V by mass spectrometry following treatment with 4-chloro-7-nitro-benzoxadiazole (NBD-Cl) or a chemically-synthesized NBD-glutathione (NBD-SG) conjugate. Enzymes were incubated with 100 µM NBD-Cl, 100 µM NBD-SG or an equivalent volume of DMSO for 60 min before desalting and whole-protein molecular weight determination using electrospray ionisation mass spectrometry. Theoretical masses for *AmGSTF1* are shown assuming alkylation of the protein by both NBD-Cl and NBD-SG. Theoretical masses assume complete loss of the *N*-terminal methionine residue as is known to occur for *Arabidopsis Strep* II tagged GSTs (Dixon *et al.*, 2009). The observed mass ions with a decrease of 346 Da relative to the respective theoretical mass mathematically correlate with the loss of the *N*-terminal MASW sequence of the *Strep* II tag.

Enzyme	Chemical treatment	Theoretical mass (Da)	Observed masses (Da)
<i>AmGSTF1</i>	DMSO	26665	26320, 26665
	NBD-Cl	26828	26482, 26828
	NBD-SG	26828	26321, 26482, 26663, 26828
C120V	DMSO	26661	26316, 26658
	NBD-Cl	26661	26316, 26659
	NBD-SG	26661	26317, 26659

Therefore, these results demonstrate that NBD-Cl has two modes-of-action with respect to *AmGSTF1*. NBD-Cl can alkylate *AmGSTF1* on Cys120 or can also weakly compete at the active site if it forms the NBD-SG conjugate. However, NBD-SG can also alkylate the protein albeit at a slower chemical rate than NBD-Cl. Studies with C120V show that alkylation is the principal and favoured mode of inhibition of *AmGSTF1* as C120V is only weakly inhibited by both NBD-Cl and NBD-SG to similar degrees. Significantly, if *AmGSTF1* alkylation by the NBD moiety is responsible for the observed reversal of the MHR black-grass phenotype (Dr. I. Cummins and Prof. R. Edwards, unpublished work at the start of this project) then the demonstrated alkylation of *AmGSTF1* by NBD-SG *in vitro* suggests this may also happen *in planta*. So, even if NBD-Cl is quenched to the NBD-SG derivative in the plant cell due to the high cellular concentrations of GSH, *AmGSTF1* may still be alkylated and its function inhibited. This is also dependent of course on the relative rates of glutathione-conjugate metabolism and vacuolar deposition and would require detailed metabolism studies but is an interesting hypothesis.

4.2.3.3 Inhibition studies with other known thiol alkylating agents

Having characterised the alkylation and inhibition of *AmGSTF1* by NBD-Cl and NBD-SG, it was then of interest to determine if Cys120 could be modified by other known thiol alkylating agents and how this would affect catalytic activity of the enzyme. Therefore, analogous experiments to those conducted with NBD-Cl and NBD-SG were carried out with the well-studied thiol alkylating agents iodoacetamide and *N*-ethylmaleimide (NEM) (Figure 32A).

Equimolar concentrations of *AmGSTF1* and C120V enzymes were incubated with iodoacetamide or NEM, alongside treatments with NBD-Cl or DMSO as positive and negative controls respectively. Iodoacetamide, NEM and NBD-Cl were all used at a fixed concentration (100 µM) with all treatments consisting of a 10 min incubation period. Unlike the previously described inhibition studies these treatments were all performed in the dark to prevent the decomposition of iodoacetamide to molecular iodine and unwanted side-reactions. Following treatments, enzymes were diluted 1:100 (v/v) and assayed for activity toward CDNB in the presence of a molar excess of GSH.

Iodoacetamide and NEM proved weak inhibitors of both *AmGSTF1* and C120V. In the case of *AmGSTF1*, iodoacetamide and NEM caused a 12 % and 10 % decrease in mean *AmGSTF1* specific activity respectively as compared to a 53 % reduction following treatment with NBD-Cl (Figure 32B).

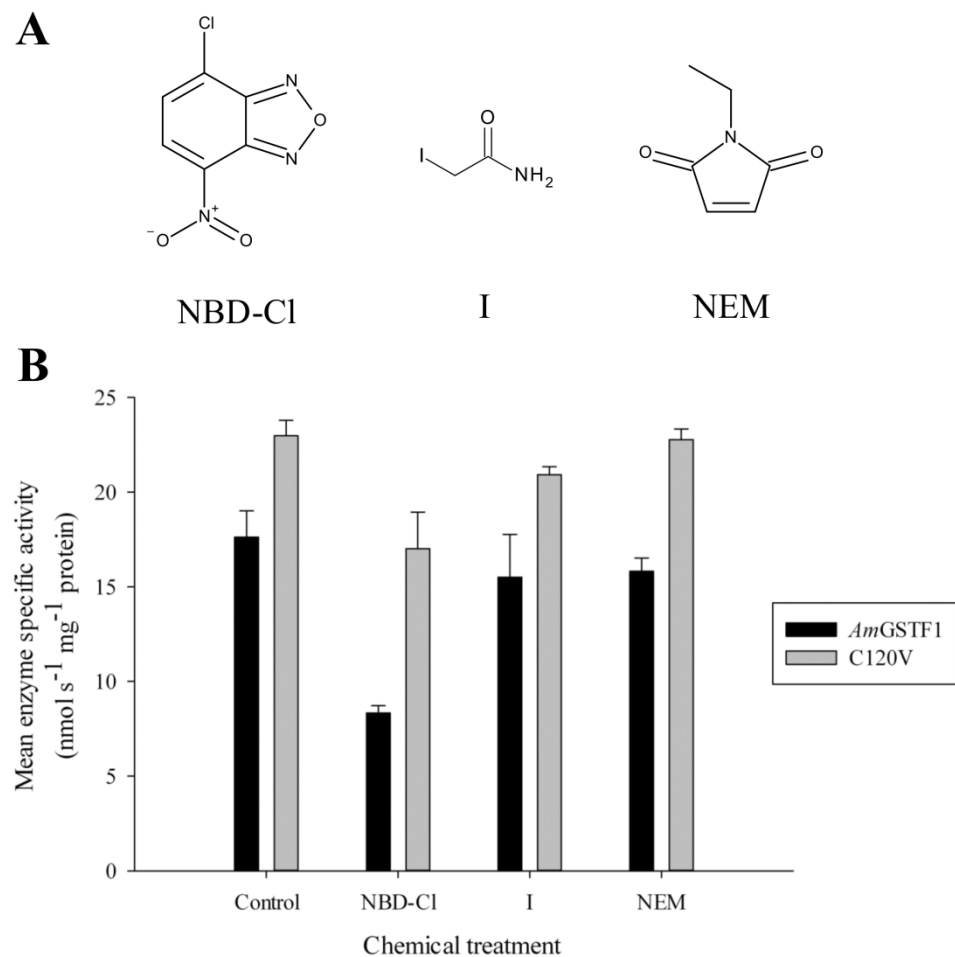


Figure 32: Specific activities of *AmGSTF1* and C120V following treatment with 4-chloro-7-nitrobenzoxadiazole, iodoacetamide or N-ethylmaleimide. (A) Chemical structures of 4-chloro-7-nitrobenzoxadiazole (NBD-Cl), iodoacetamide (I) or N-ethylmaleimide (NEM). (B) Enzymes were incubated with 100 μ M NBD-Cl, 100 μ M I, 100 μ M NEM or solvent control (DMSO) for 10 min in the dark before diluting 1:100 (v/v) and assaying for enzyme activity towards 1-chloro-2,4-dinitrobenzene. Measurements were performed in technical triplicate. Mean specific activities are shown \pm SD, n = 3.

As these compounds are expected to behave as non-competitive alkylating agents, the weak inhibition of *AmGSTF1* by iodoacetamide and NEM relative to NBD-Cl may be a consequence of relative chemical reactivity toward Cys120. To determine this, equimolar concentrations of *AmGSTF1* and C120V were each incubated for 0 - 60 min in the dark with either a fixed concentration (100 μ M) of NBD-Cl,

iodoacetamide, NEM or an equivalent volume of DMSO as a negative control and assayed for activity towards CDNB at fixed time-points.

Following these treatments, no significant levels of inhibition of *AmGSTF1* or C120V were detected with either iodoacetamide (Figure 33) or NEM (Figure 34), even after 60 min incubation. On the contrary, *AmGSTF1* displayed the bi-phasic inhibition behaviour when incubated with NBD-Cl that was observed previously (see section 4.2.3.1).

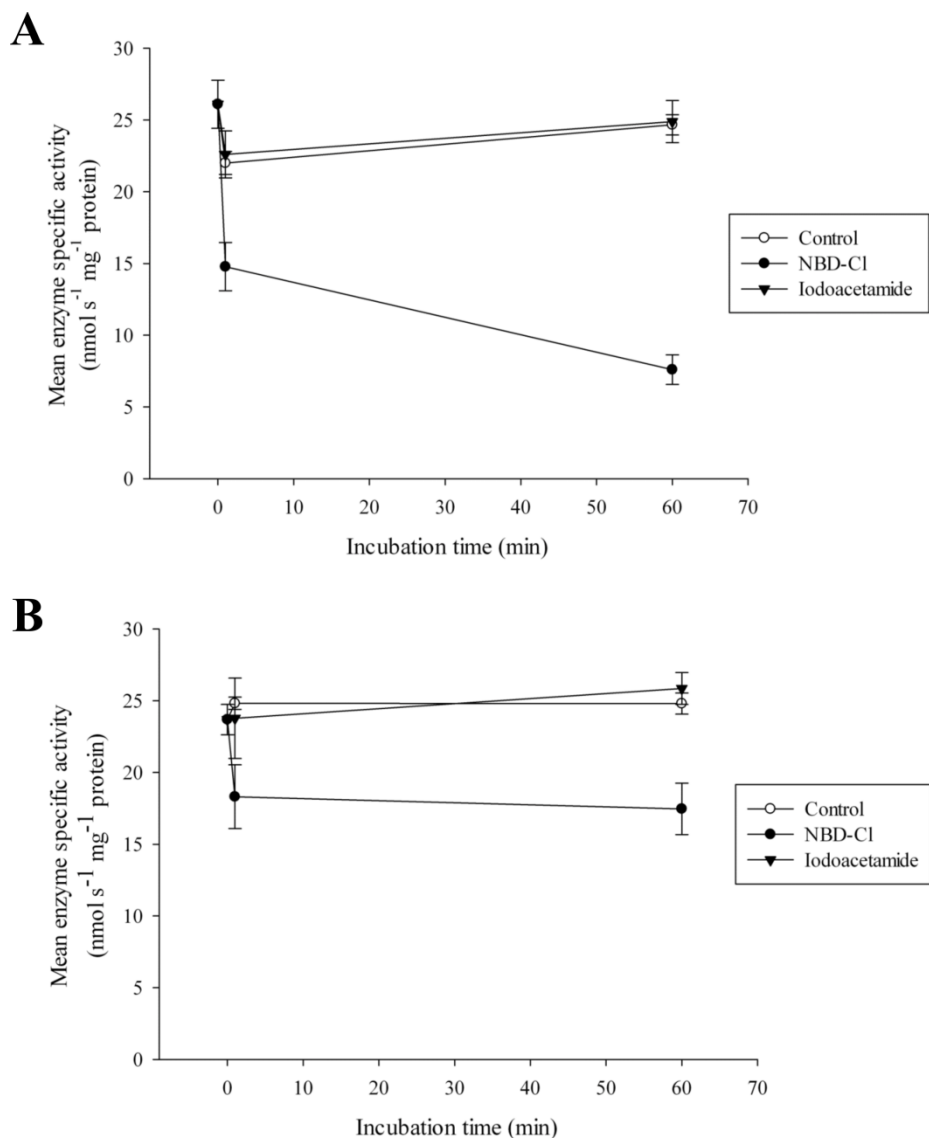


Figure 33: Time-dependent activity profiles of *AmGSTF1* and C120V following treatment with 4-chloro-7-nitro-benzoxadiazole or iodoacetamide. (A) *AmGSTF1* and (B) C120V were each incubated with 100 µM 4-chloro-7-nitro-benzoxadiazole (NBD-Cl), 100 µM iodoacetamide or solvent control (DMSO) in the dark over a period of 60 min. At discrete time-points aliquots were diluted 1:100 (v/v) and assayed for activity towards 1-chloro-2,4-dinitrobenzene. Measurements were performed in technical triplicate. Mean specific activities are shown ± SD, n = 3.

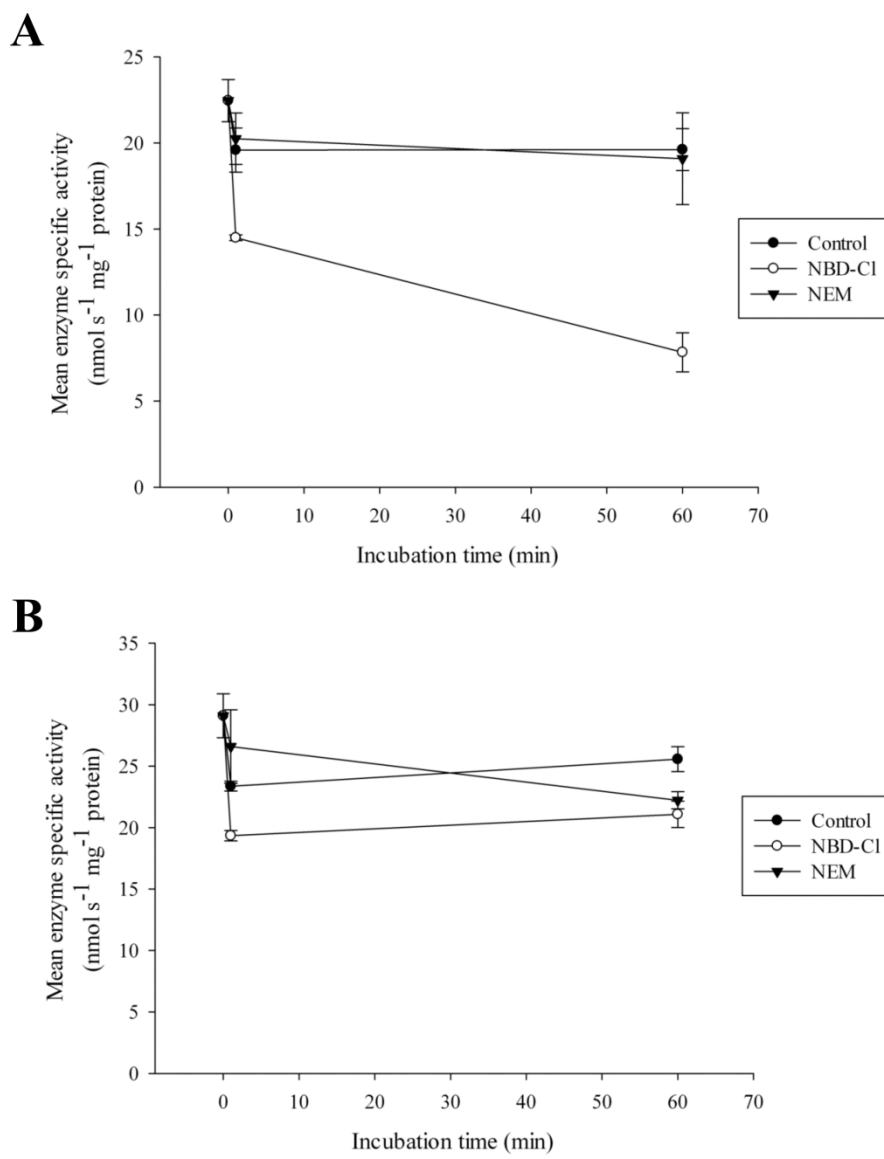


Figure 34: Time-dependent activity profiles of *AmGSTF1* and C120V following treatment with 4-chloro-7-nitro-benzoxadiazole or *N*-ethylmaleimide. (A) *AmGSTF1* and (B) C120V were each incubated with 100 µM 4-chloro-7-nitro-benzoxadiazole (NBD-Cl), 100 µM *N*-ethylmaleimide (NEM) or solvent control (DMSO) in the dark over a period of 60 min. At discrete time-points aliquots were diluted 1:100 (v/v) and assayed for activity towards 1-chloro-2,4-dinitrobenzene. Measurements were performed in technical triplicate. Mean specific activities are shown ± SD, n = 3.

To determine if the lack of *AmGSTF1* inhibition when treated with iodoacetamide or NEM correlated with a lack of alkylation, treated enzymes were analysed by mass spectrometry. Equimolar concentrations of each enzyme were once again treated with NBD-Cl, iodoacetamide, NEM or DMSO under the same conditions as for the time-course studies. After 60 min, treated enzymes were desalted using size-exclusion chromatography and whole protein molecular weights were determined using mass spectrometry. If iodoacetamide had successfully labelled *AmGSTF1* a mass increase of 57 Da would be expected due to nucleophilic displacement of the

iodide functional group. However, no such mass ions were detected for *AmGSTF1* or C120V when treated with iodoacetamide demonstrating that iodoacetamide cannot react with Cys120 (Table 12) with this being the likely reason for the minimal levels of inhibition.

Table 12: Analysis of *AmGSTF1* and C120V by mass spectrometry following treatment with 4-chloro-7-nitro-benzoxadiazole or iodoacetamide. Enzymes were incubated with 100 µM 4-chloro-7-nitro-benzoxadiazole (NBD-Cl), 100 µM iodoacetamide, or an equivalent volume of DMSO in the dark for 60 min before desalting and whole-protein molecular weight determination using electrospray ionisation mass spectrometry. Theoretical masses for *AmGSTF1* are shown assuming alkylation of the protein by both NBD-Cl and iodoacetamide. Theoretical masses assume complete loss of the *N*-terminal methionine residue as is known to occur for *Arabidopsis Strep II* tagged GSTs (Dixon *et al.*, 2009).

Enzyme	Chemical treatment	Theoretical mass (Da)	Observed masses (Da)
<i>AmGSTF1</i>	DMSO	26665	26663
	NBD-Cl	26828	26826
	Iodoacetamide	26722	26663
C120V	DMSO	26661	26661
	NBD-Cl	26661	26658
	Iodoacetamide	26661	26659

If NEM successfully labelled *AmGSTF1* an increase in whole protein mass of 125 Da would be expected following nucleophilic addition to one of the two equivalent α,β -unsaturated carbonyl centres in the NEM molecule. Surprisingly, unlike iodoacetamide treatment, the observed mass ions of NEM-treated *AmGSTF1* were 125 Da larger than the corresponding mass ions observed with DMSO-treated *AmGSTF1* indicating that *AmGSTF1* had been fully labelled by NEM. No labelled mass ions were detected with C120V with any treatment indicating that NEM-modification of *AmGSTF1* occurred on Cys120 (Table 13). For all treatments with both *AmGSTF1* and C120V, a proportion of mass ions were detected that were 346 Da lower than the theoretical mass as seen previously with NBD-SG experiments (Table 11) possibly due to loss of the *N*-terminal MASW sequence of the *Strep II* tag. Importantly though, NEM-treated *AmGSTF1* mass ions were all 125 Da larger than the respective DMSO-treated counterparts.

Table 13: Analysis of *AmGSTF1* and C120V by mass spectrometry following treatment with 4-chloro-7-nitro-benzoxadiazole or *N*-ethylmaleimide. Enzymes were incubated with 100 µM 4-chloro-7-nitro-benzoxadiazole (NBD-Cl), 100 µM *N*-ethylmaleimide (NEM), or an equivalent volume of DMSO in the dark for 60 min before desalting and whole-protein molecular weight determination using electrospray ionisation mass spectrometry. Theoretical masses for *AmGSTF1* are shown assuming alkylation of the protein by both NBD-Cl and NEM. Theoretical masses assume complete loss of the *N*-terminal methionine residue as is known to occur for *Arabidopsis Strep II* tagged GSTs (Dixon *et al.*, 2009). The observed mass ions with a decrease of 346 Da relative to the respective theoretical mass mathematically correlate with the loss of the *N*-terminal MASW sequence of the *Strep II* tag.

Enzyme	Chemical treatment	Theoretical mass (Da)	Observed masses (Da)
<i>AmGSTF1</i>	DMSO	26665	26320, 26665
	NBD-Cl	26828	26482, 26828
	NEM	26790	26444, 26790
C120V	DMSO	26661	26316, 26658
	NBD-Cl	26661	26316, 26659
	NEM	26661	26316, 26659

These results would therefore suggest that solely alkylating Cys120 is not sufficient for *AmGSTF1* inhibition and instead implies a further level of interaction between *AmGSTF1* and NBD-Cl that promotes enzyme inhibition. This is opposed to studies performed with GSTP1 which is consistently inhibited following alkylation by a host of compounds including NBD-Cl and NEM (Tamai *et al.*, 1990; Ricci *et al.*, 2003). Crystallographic studies are required to understand the interaction of *AmGSTF1* with NBD-Cl and NEM respectively.

4.2.3.4 Inhibition studies with purine derivatives

Alongside the work discussed so far, collaborators on this project had also identified a set of purine-based compounds which appeared to show efficacy for reversing chlorotoluron resistance of MHR black-grass in spray trials (Dr. C. Coxon, H. E. Straker and Prof. P. G. Steel, unpublished work). Having established the importance of *AmGSTF1* for an MHR phenotype and its intriguing interaction with NBD-Cl, *AmGSTF1* was screened with the purine derivatives for inhibition of the enzyme.

After obtaining the purine derivatives, they were screened in an analogous manner to that described for previous inhibition studies, alongside NBD-Cl as a positive control. The first experiment screened 6-chloropurine (6-CP), 6-mercaptopurine (6-

MP) and 6-bromopurine (6-BP) (Figure 35A) for inhibition of *AmGSTF1* activity. These compounds are relatively reactive electrophiles and may inhibit *AmGSTF1* by alkylating Cys120. Therefore, compounds were also screened for inhibition of the C120V mutant. No significant levels of *AmGSTF1* or C120V inhibition were detected with any of the purine derivatives (Figure 35B). The lack of inhibition correlated with a lack of protein modification determined using mass spectrometry (Dr. C. Coxon and Prof. P. G. Steel, unpublished work).

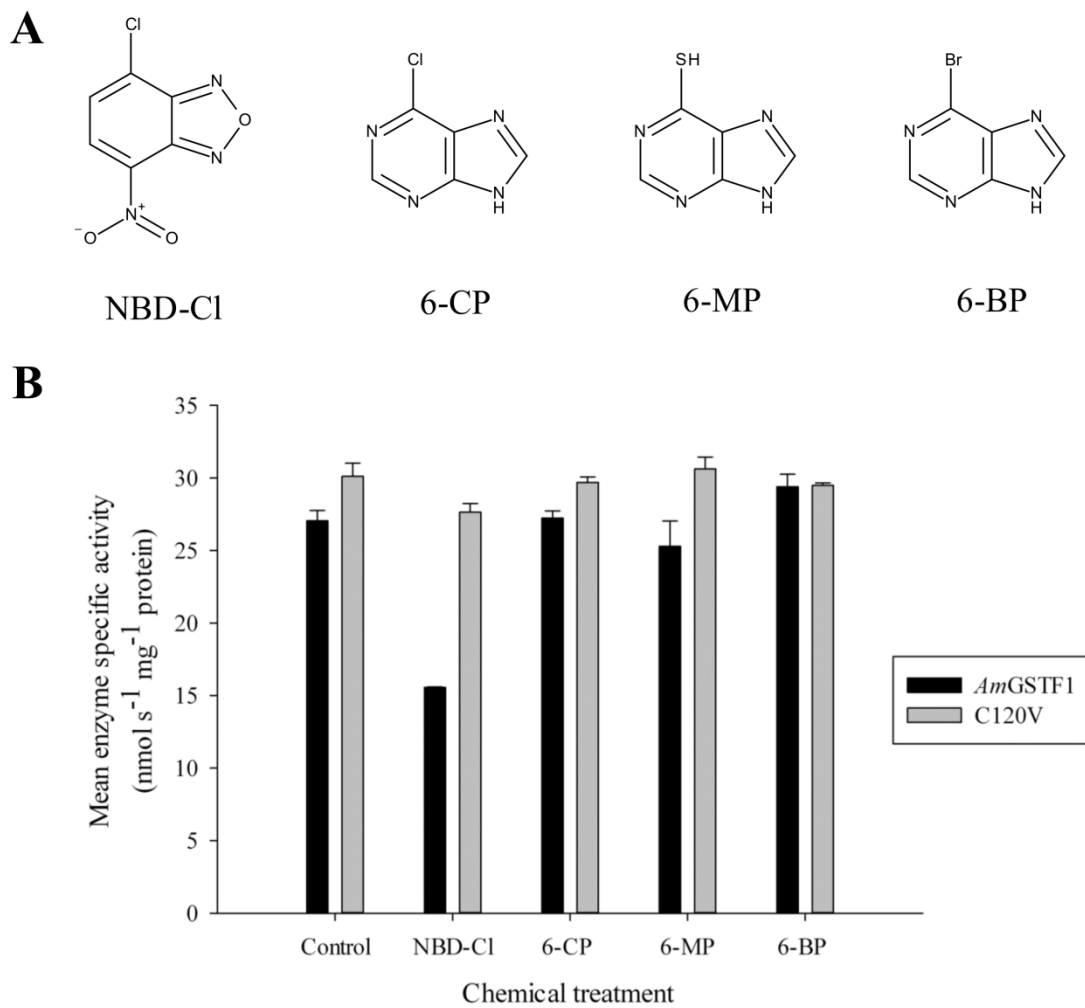


Figure 35: Specific activities of *AmGSTF1* and C120V following treatment with 4-chloro-7-nitrobenzoxadiazole or purine derivatives. (A) Chemical structures of 4-chloro-7-nitro-benzoxadiazole (NBD-Cl), 6-chloropurine (6-CP), 6-mercaptopurine (6-MP) and 6-bromopurine (6-BP). (B) Enzymes were incubated with 100 µM NBD-Cl, 100 µM of each purine derivative or solvent control (DMSO) for 10 min in the dark before diluting 1:100 (v/v) and assaying for enzyme activity towards 1-chloro-2,4-dinitrobenzene. Measurements were performed in technical triplicate. Mean specific activities are shown ± SD, n = 3.

It was possible that the lack of the nitro group *para*- to the leaving group of the purine derivatives meant that the compounds were not sufficiently electrophilic to

react with Cys120. Therefore, a 3,3-deazonitro-6-chloropurine (NDA-6-CP) derivative (Figure 36A) was synthesized and tested for inhibition of *AmGSTF1* and C120V in an analogous manner to that described for previous inhibition studies. Again, no significant inhibition of *AmGSTF1* or C120V was detected (Figure 36B).

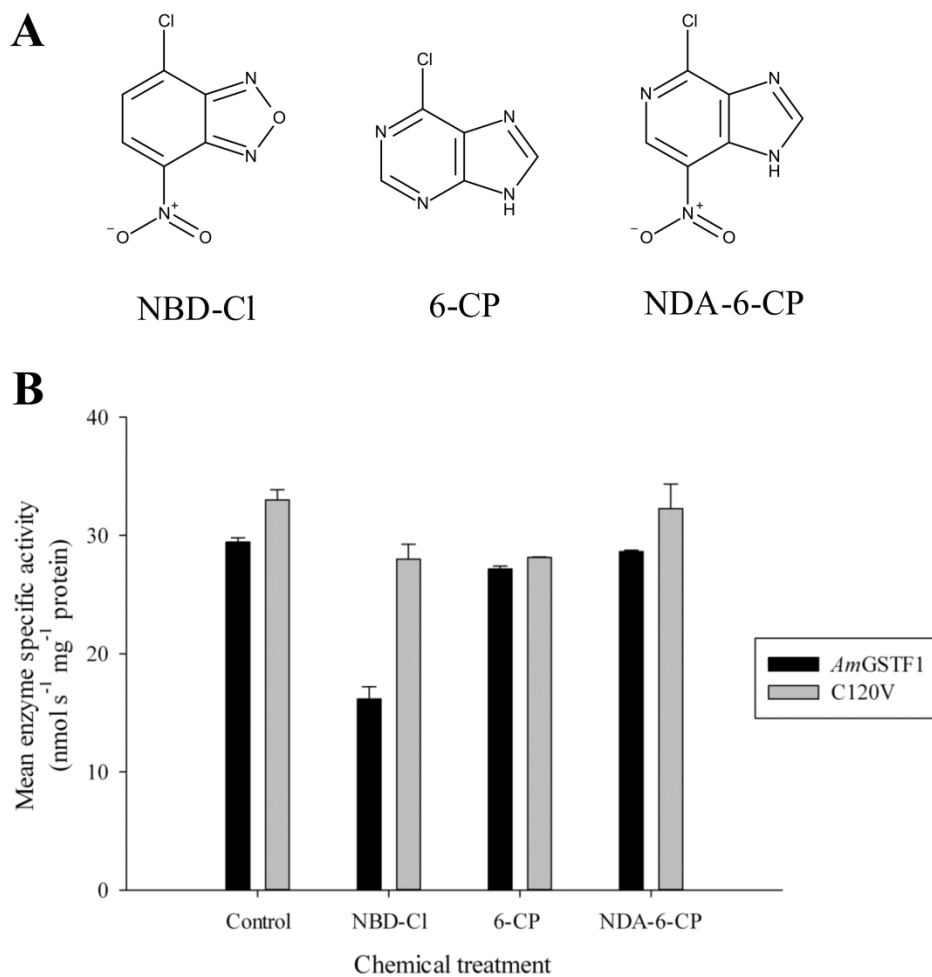


Figure 36: Specific activities of *AmGSTF1* and C120V following treatment with 4-chloro-7-nitrobenzoxadiazole, 6-chloropurine or 3,3-deazonitro-6-chloropurine. (A) Chemical structures of 4-chloro-7-nitrobenzoxadiazole (NBD-Cl), 6-chloropurine (6-CP), and 3,3-deazonitro-6-chloropurine (NDA-6-CP). (B) Enzymes were incubated with 100 μ M NBD-Cl, 100 μ M of each purine derivative or solvent control (DMSO) for 10 min in the dark before diluting 1:100 (v/v) and assaying for enzyme activity towards 1-chloro-2,4-dinitrobenzene. Measurements were performed in technical triplicate. Mean specific activities are shown \pm SD, n = 3.

It is not yet clear if the purine-based compounds can restore herbicide sensitivity to MHR black-grass treated with chlorotoluron alone or to herbicides with other modes-of-action also. With regards to chlorotoluron resistance in MHR black-grass, up-regulated CYP activity has been shown to be responsible for resistance (Hall *et al.*, 1995) and hence the purine-based derivatives tested here may be targeting the

CYPs required for chlorotoluron degradation *in planta*. An extensive set of further studies are required to understand the function of the purine-based compounds for restoring a WTS phenotype in black-grass. These studies fell outside the scope of this project but the results presented here can confirm their mode-of-action is not via a direct interaction with *AmGSTF1*.

4.3 Expression of *AmGSTF1* and mutant isoforms in transgenic *Arabidopsis thaliana* plants

4.3.1 Introduction

In vitro studies demonstrated that the *AmGSTF1* mutants had significantly perturbed catalytic activities. S12A was significantly retarded with all substrates tested including a large reduction in GPOX activity. Conversely, C120V had a significant increase in GPOX activity. Studies with C120V also suggested that Cys120 may play a role in transmitting conformational signals across the GST dimer and that the residue was the principal determinant for the interaction of *AmGSTF1* with reactive electrophiles. In order to understand how the altered properties of the mutants may affect MHR, *AmGSTF1*, C120V and S12A were each independently and stably expressed in transgenic *Arabidopsis thaliana* host plants. Independent homozygous lines were then screened for changes in herbicide tolerance, endogenous detoxification enzyme activities and flavonoid accumulation.

4.3.2 DNA construct generation

In order to successfully transform *Arabidopsis* to allow stable expression of the GSTs, the DNA open reading frame of each GST needed to be sub-cloned into a suitable expression vector. Therefore, GSTs were sub-cloned from the pET-STRP3 vector into the pBIN-STRP3 vector (Figure 37), a plant binary vector designed for stable plant transformation. This vector retains the *Strep II* tag fused to the *N*-terminus of each GST sequence and allows constitutive expression of the *Strep II* tagged GST from the Cauliflower Mosaic Virus 35S promoter. The vector also contains the *Bar* gene, the product of which grants resistance to glufosinate-ammonium and allows for selection of transformants (Dixon *et al.*, 2008; Dixon *et al.*, 2009).

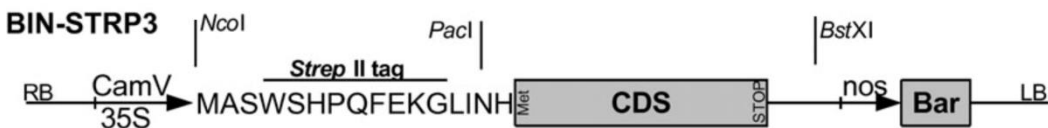


Figure 37: pBIN-STRP3 vector. The cloned DNA sequence (CDS) of choice is inserted such that it becomes fused to a *Strep II tag* of which the translated amino acid sequence is shown. Expression of the construct is driven by the constitutive Cauliflower Mosaic Virus 35S promoter (CamV 35S). Expression of the *Bar* gene using the nopaline synthase promoter grants resistance to glufosinate-ammonium and allows selection for transformants carrying the vector. The relative positions of DNA restriction sites required for manipulation of the vector are shown (*NcoI*, *PacI* and *BstXI*). RB – right border, LB – left border. Copied with permission from (Dixon *et al.*, 2009).

In order to transform *Arabidopsis* plants, the vector was first transformed into a modified strain of *Agrobacterium tumefaciens*. This is because this *Agrobacterium* species is capable of stably integrating a portion of its DNA into a susceptible plant host genome. The pBIN-STRP3 vector contains DNA recognition sequences upstream and downstream (RB and LB respectively, Figure 37) of the DNA region to be transferred (T-DNA). These sites are used by vir proteins, maintained on a helper plasmid within the *Agrobacterium* species, to excise the T-DNA region and integrate it into the plant host genome (Gelvin, 2003). Flowering *Arabidopsis* plants were then transformed with the *Agrobacterium* strain containing the assembled pBIN-STRP3 constructs.

To sub-clone *AmGSTF1*, C120V and S12A into the pBIN-STRP3 vector, GSTs in the pET-STRP3 were digested with the restriction enzymes *PacI* and *BstXI* and ligated into *PacI/BstXI*-digested pBIN-STRP3. Constructs were transformed into *E. coli* XL-10 gold ultracompetent cells followed by plasmid purification. Constructs were confirmed as correct using DNA sequencing.

To serve as a negative control for downstream experiments with successfully transformed *Arabidopsis* plants, independent lines of *Arabidopsis* plants needed to be generated that expressed the pBIN-STRP3 vector alone with no GST insert. It was decided that the most appropriate set of control plants would be those that constitutively expressed only the *Strep II tag*. This construct did not already exist and so was generated using an overhang PCR method (Figure 38).

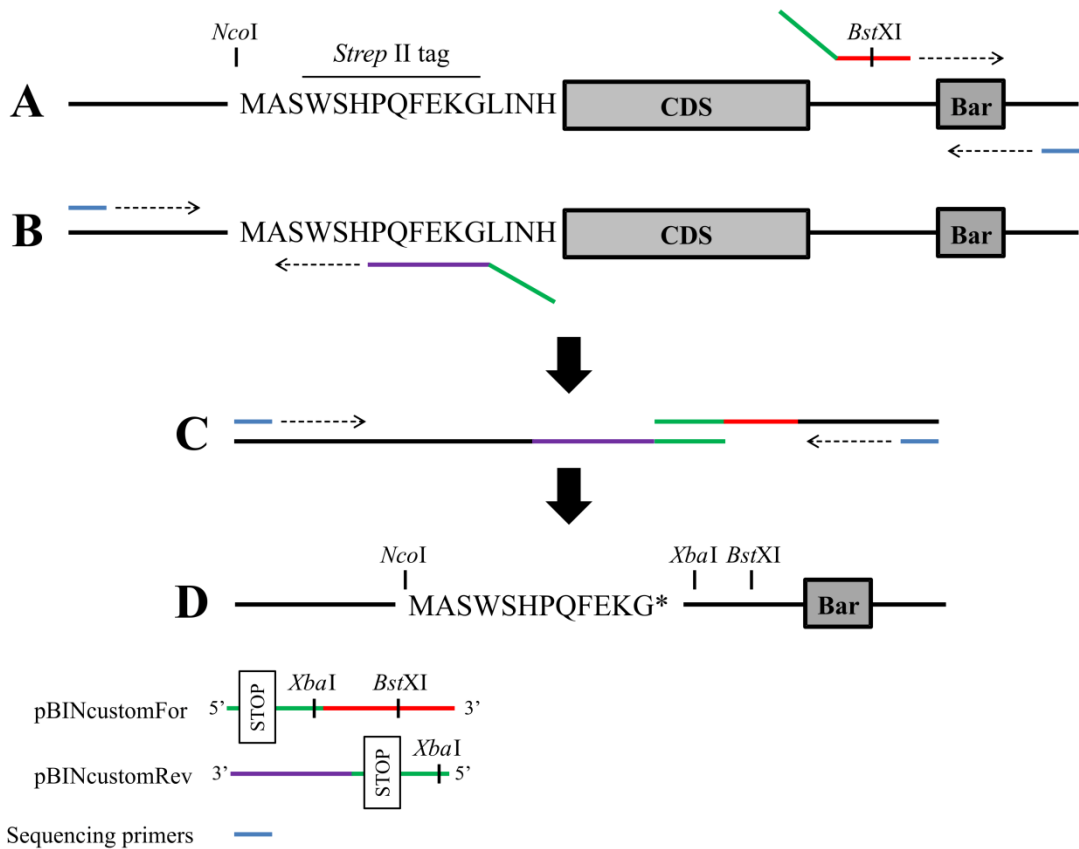


Figure 38: Scheme for the generation of a modified pBIN-STRP3 vector allowing the expression of the Strep II tag only. The pBIN-STRP3 vector was amplified using two distinct primer sets. These primer sets allowed amplicons to be generated (**A**) downstream and (**B**) upstream of the cloned DNA sequence (CDS) with the upstream primers designed to amplify from the *Strep II tag*. Each primer set also used a primer with a novel overhang that did not anneal to the vector and included a translational stop codon and a unique diagnostic restriction site (*XbaI*). (**C**) Purification of the amplicons, annealing of the complementary overhangs and another round of PCR generated the desired vector sequence (**D**) which allowed expression of the *Strep II tag* only. The relative positions of DNA restriction sites required for manipulation of the vector are shown (*NcoI* and *BstXI*). The promoter sequences denoted in Figure 37 are still present but are not shown here to more easily define the sites of primer binding.

Primers were designed to amplify upstream and downstream of the GST insert. The upstream primer set amplified from the respective codon of the C-terminus of the *Strep II tag* and contained a novel antisense primer 5' stop codon (Figure 38B). The downstream primer set contained a novel sense primer 5' overhang that was complementary in sequence to the overhang of the upstream antisense primer (Figure 38A). Purification and annealing of the amplified sequences via the complementary overhangs followed by a further round of PCR generated the desired DNA sequence, to allow constitutive expression of the *Strep II tag* only (Figure 38C and D). This was then cloned into the full pBIN-STRP3 vector using complementary restriction sites.

An arbitrary GST-pBIN-STRP3 construct (S12A-pBIN-STRP3) was used as a template for amplification with the primer sets described in Figure 38A and B. Following PCR, the resulting amplicons were purified using agarose gel electrophoresis. The purified amplicons were annealed using the introduced complementary overhangs and the full-length DNA sequence generated by PCR with vector-specific sequencing primers. The amplified full-length DNA sequence was purified using gel electrophoresis and digested with *Nco*I and *Bst*XI restriction enzymes. The digested fragment was then ligated into *Nco*I/*Bst*XI digested pBIN-STRP3 vector and transformed into ultra-competent *E. coli* XL-10 gold cells followed by plasmid purification. The construct was confirmed as correct using DNA sequencing and is hereby referred to as the vector.

4.3.3 Transformation into *Arabidopsis thaliana* plants

As described, in order to transform the assembled pBIN-STRP3 constructs into *Arabidopsis* plants they first needed to be transformed into *Agrobacterium tumefaciens*. Using electroporation, all constructs were transformed into *Agrobacterium tumefaciens* strain GV3101 containing the MP90 helper plasmid that harboured the *vir* genes required for T-DNA excision and integration (Koncz and Schell, 1986). Successful transformants were selected with the appropriate antibiotics. *Arabidopsis* plants were then transformed as described (Clough and Bent, 1998) by inoculating flowering plants with *Agrobacterium* cultures transformed with the respective GST-pBIN-STRP3 vectors. Homozygous stably-integrated transgenic lines were generated as depicted in Figure 39.

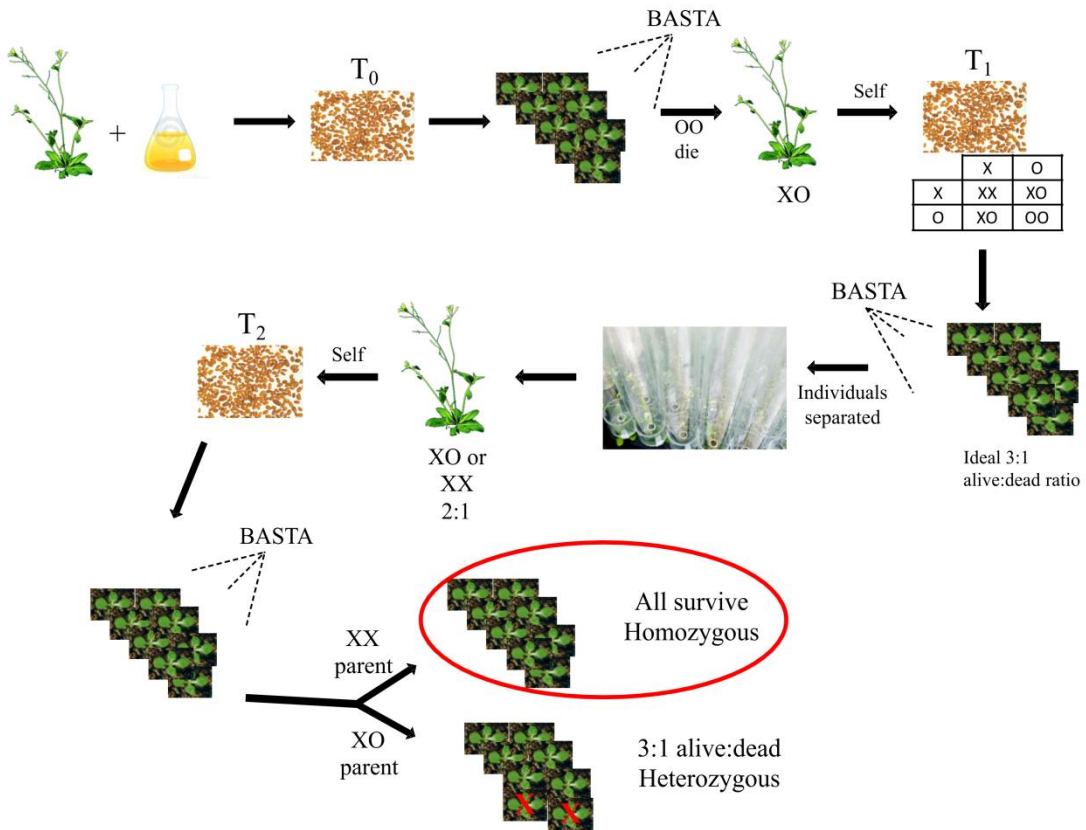


Figure 39: Scheme for the generation of transgenic *Arabidopsis thaliana* plants containing a homozygous insert of the desired transgene. Flowering *Arabidopsis* plants are inoculated with *Agrobacterium tumefaciens* transformed with a pBIN-STRP3 construct containing the desired transgene. Inoculated plants are grown to seed (*T₀*) and the seed collected. *T₀* seed is sown and seedlings are treated with the commercial herbicide BASTA (active ingredient – glufosinate-ammonium). Transformed plants containing a single vector insert (denoted XO) express the *Bar* gene, coding for a protein that degrades glufosinate-ammonium, and survive. Untransformed plants (denoted OO) cannot express the *Bar* gene and die. Surviving plants are allowed to self-fertilise (Self) and the seed (*T₁*) of each is collected. Genetic recombination during self-fertilisation generates homozygous (XX), heterozygous (XO) and reverted wild-type (OO) progeny. *T₁* seed is sown and treated with BASTA with single insert lines displaying a 3:1 alive:dead ratio due to the three possible progeny genotypes generated during genetic recombination. Surviving individuals are now either heterozygous (XO) or homozygous (XX) for the transgene with a relative ratio of 2:1 heterozygous:homozygous. Individuals are separated and allowed to self-fertilise (*T₂* seed) followed by another round of BASTA selection. Genetic recombination during self-fertilisation, in the process of generating *T₂* seed, means that only the progeny of homozygous *T₁* lines will all be resistant to BASTA selection. Heterozygous *T₁* lines will generate a proportion of revertant wild-type (OO) individuals as described. Therefore *T₂* lines for which all seedlings survive BASTA selection are homozygous single insertion lines and can be used for further study.

Three *T₁* lines of each GST construct and two *T₁* lines expressing the vector construct were identified that were statistically strongly significant ($p \geq 0.5$) representing a 3:1 alive:dead ratio (Table 14) after treatment with glufosinate-ammonium, indicating an expressed single-insertion event.

Table 14: T₁ transformant lines that segregated in a 3:1 alive:dead ratio following selection with glufosinate-ammonium. Seed of each T₁ line was sown on soil and maintained in glasshouses for 14 days before spraying with glufosinate-ammonium. The numbers of seedlings were counted before and after spraying. A χ^2 statistical test was used to prove these lines granted the desired 3:1 ratio for a stably-integrated single insert.

Construct	T ₁ line	Expected		Observed		χ^2 p-value
		Alive	Dead	Alive	Dead	
AmGSTF1	5	30.75	10.25	29	12	0.528
	8	30.75	10.25	30	11	0.787
	13	40.5	13.5	41	13	0.875
C120V	7	28.5	9.5	28	10	0.851
	11	24.75	8.25	25	8	0.920
	16	30	10	29	11	0.715
S12A	2	51	17	51	17	1.000
	4	30	10	31	9	0.715
	12	39.75	13.25	40	13	0.937
Vector	21	31.5	10.5	31	11	0.859
	22	36	12	36	12	1.000

24 individuals of each of these 11 T₁ lines were separated and allowed to self-fertilise. The resulting seed (T₂) of each individual was then collected. 8 T₂ lines from each of the 11 selected T₁ lines were sown and seedlings selected again with glufosinate-ammonium. This identified a homozygous T₂ line from each T₁ line and hence three independent homozygous lines for each pBIN-STRP3 construct (Table 15).

Table 15: AmGSTF1, C120V, S12A and vector-only homozygous single insertion lines selected for further study.

Construct	Homozygous T ₂ line
AmGSTF1	5-19
	8-8
	13-24
C120V	7-20
	11-3
	16-17
S12A	2-19
	4-2
	12-17
Vector	21-24
	22-24

4.3.4 Screening of transgenic plants for GST expression

The selected homozygous T₂ lines were screened for GST protein expression using an antiserum raised against the ZmGSTF1-2 heterodimer known to recognise AmGSTF1 and the mutant isoforms (see section 4.2.1). The antiserum recognised endogenous phi-class GSTs in all samples including the vector plants. It also recognised a novel GSTF band in 8 of the 9 black-grass GST-expressor lines that co-migrated with recombinant AmGSTF1 corresponding to the respective black-grass GST proteins (Figure 40).

Variable construct expression was detected between the independent lines, as is expected for transgenic lines generated using *Agrobacterium tumefaciens*. This is because the site of construct integration into the plant host genome by the agrobacterium is non-specific and hence the construct can be inserted into highly transcribed or lowly transcribed genomic regions (Gelvin, 2003). No AmGSTF1 protein was detected in the AmGSTF1 8-8 line, although the selection trials had identified it as a homozygous insertion line. It is most likely that this was due to levels of AmGSTF1 expression below the detection limit of the antiserum. This was not pursued however and the line was not used for further study.

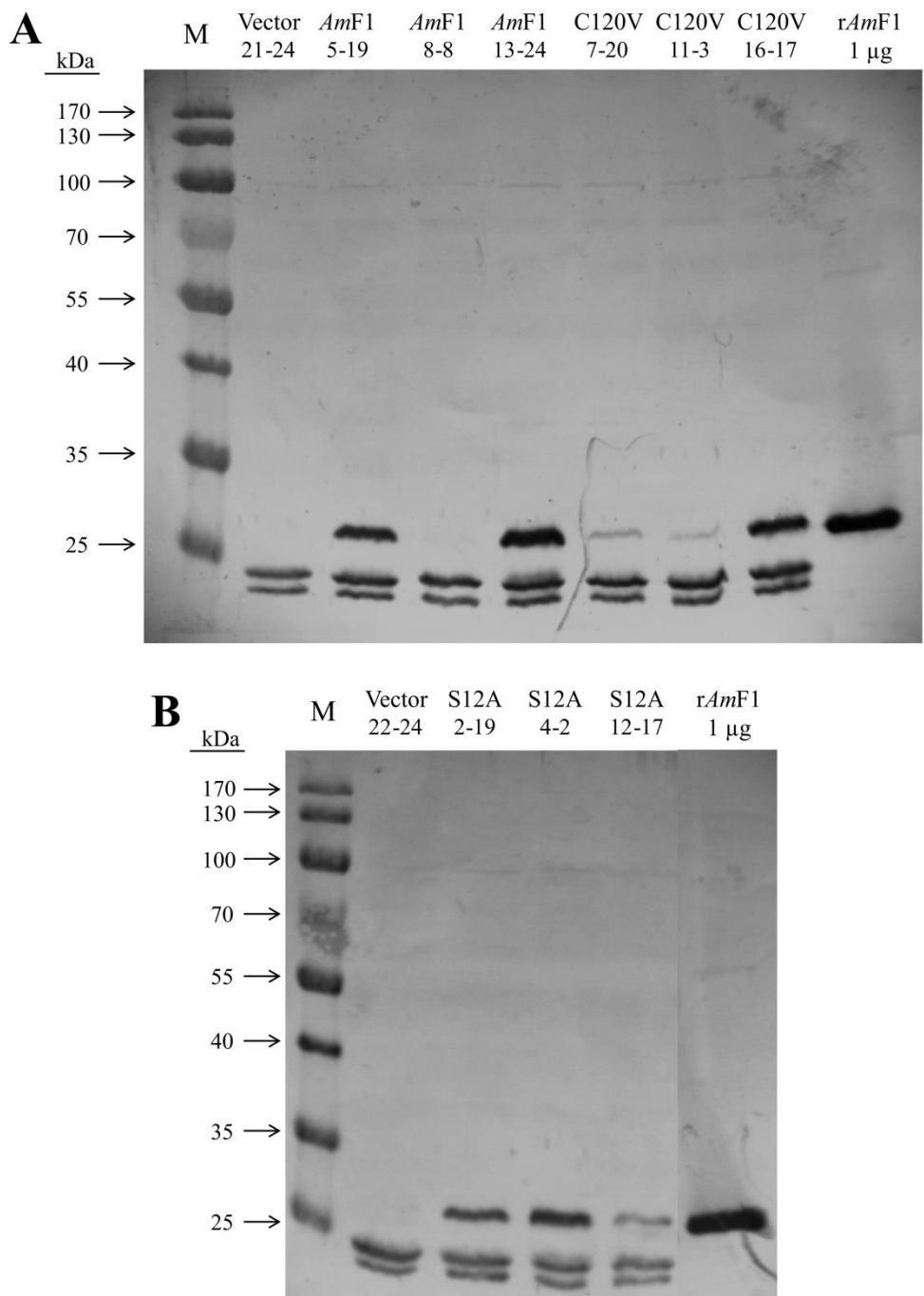


Figure 40: Phi class GST expression screens of homozygous insertion lines. Transgenic Arabidopsis lines designed to express *AmGSTF1*, C120V or S12A, for which all T₂ progeny survived glufosinate-ammonium selection, were screened for construct expression by Western blotting using an antiserum raised against the ZmGSTF1-2 heterodimer. Two vector-only lines designed to express the *Strep II* tag, for which all T₂ progeny survived glufosinate-ammonium selection, were also screened. Recombinant *AmGSTF1* (rAmF1) was run alongside samples as a positive control. M – protein markers. The molecular weights (kDa) of protein markers are shown. Numbers below vector and enzyme names (e.g. AmF1 5-19) denote unique identification numbers of each independent line.

4.3.5 Testing AmGSTF1-, C120V- and S12A-expressors for enhanced herbicide tolerance

As T-DNA insertion into the plant host genome mediated by *Agrobacterium tumefaciens* is non-specific for location, the observed changes in a single homozygous line cannot be confidently assumed to be as a result of transgene expression. Therefore, two homozygous lines of each *AmGST* construct were tested for changes in herbicide tolerance with chlorotoluron, a herbicide that cannot be detoxified directly by GSTs. The two selected lines were those with the highest relative expression of the transgene except for S12A constructs for which lines 2-19 and 12-17 were used. This was due to very poor germination of the S12A 4-2 seed. Seeds of the selected lines (30 per pot) were sown on soil and grown for 14 days in environmental growth chambers (20 °C, 100 µE m⁻² s⁻¹, 16 hr photoperiod). Seedlings of the GST-expressors and the vector control plants were then sprayed with chlorotoluron (60 g active ingredient per hectare) formulated with 0.1 % (v/v) Biopower, 1 % (v/v) acetone or with formulation alone. Plants were then maintained in growth chambers for a further 7 days before imaging.

AmGSTF1-, C120V- and S12A-expressors along with vector control plants all behaved in a similar manner following treatment with formulation alone. However, *AmGSTF1-*, C120V- and S12A-expressors all accumulated significantly more biomass following treatment with chlorotoluron relative to vector control plants by visual assessment (Figure 41).

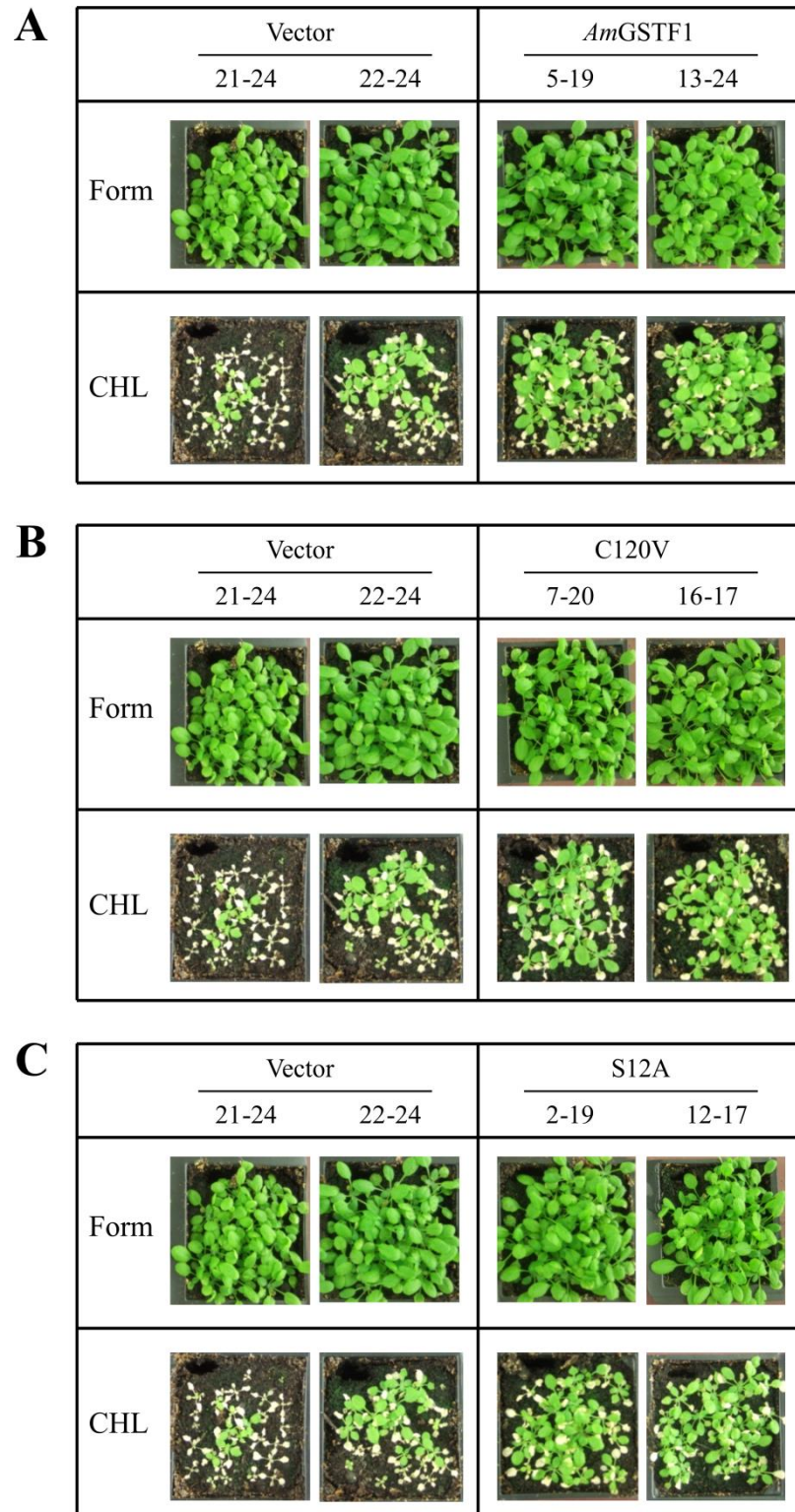


Figure 41: Increased herbicide tolerance of transgenic *Arabidopsis* plants expressing *AmGSTF1*, *C120V* or *S12A*. Seeds of two independent lines expressing (A) *AmGSTF1*, (B) *C120V* or (C) *S12A* were sown on soil (30 per pot) and maintained in environmental growth chambers for 14 days followed by an application of chlorotoluron (CHL; 60 g ai hectare⁻¹, 0.1 % biopower, 1 % acetone) or an equivalent volume of formulation only (Form; 0.1 % biopower, 1 % acetone). Plants were maintained in environmental growth chambers for a further 7 days and then photographed. Numbers below vector and enzyme names (e.g. *AmGSTF1* 5-19) denote unique identification numbers of each independent line.

In order to quantify magnitudes of resistance, the spray trial was repeated using the highest expressing line of each GST construct and the vector 22-24 line which appeared the more tolerant of the two vector lines. Relative biomass of the respective lines was then calculated following chlorotoluron and formulation-only treatments. Plants were also challenged with the herbicide alachlor, a herbicide that can be detoxified by GSTs but is not a substrate for *AmGSTF1* (Cummins *et al.*, 1999), to determine if the GST-expressors were resistant to multiple herbicides with differing modes-of-action. To calculate the relative changes in biomass between GST-expressors and vector control plants, treated pots were first counted for the number of individuals in each pot and then aerial tissue of each pot was harvested and weighed. For each pot, the mass per plant was calculated to normalise for small differences in germination and the differences in mass per plant were calculated between GST-expressors and vector control plants expressed as a percentage increase of the vector.

AmGSTF1-, C120V- and S12A-expressors all accumulated more biomass relative to vector only plants when exposed to formulation alone. However, this increase in biomass was significantly greater when plants were exposed to herbicides (Figure 42).

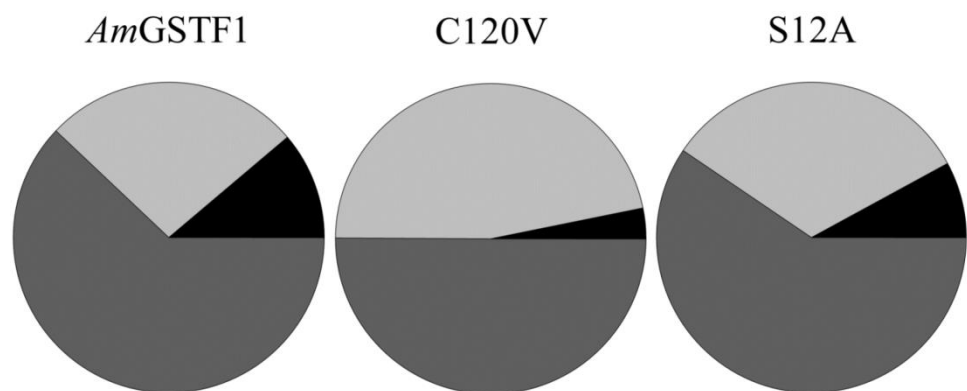


Figure 42: Increased biomass of transgenic *Arabidopsis* plants expressing *AmGSTF1*, C120V or S12A relative to vector-only control plants following herbicide treatment. Plants of the following transgenic lines: *AmGSTF1* 5-19, C120V 16-17, S12A 2-19 and vector 22-24, (20 seeds per pot) were grown in environmental growth chambers in duplicate for 14 days followed by an application of chlorotoluron (60 g ai hectare⁻¹, 0.1 % biopower, 1 % acetone), alachlor (1200 g ai hectare⁻¹, 0.1 % biopower, 1 % acetone) or an equivalent volume of formulation only (Form; 0.1 % biopower, 1 % acetone) and then maintained in growth chambers for a further 10 days. At this time aerial tissue of all lines was harvested and weighed. For each replicate, the percentage increase in fresh weight per plant of the *AmGSTF1*-, C120V- and S12A-expressors was calculated relative to the vector-only control plants and the mean percentage increase in fresh weight per plant for the GST-expressors relative to vector-only control plants is shown for the three chemical treatments; formulation only (black), chlorotoluron (light grey) and alachlor (dark grey).

These results clearly show that *AmGSTF1*, S12A and C120V all elicit MHR in transgenic Arabidopsis plants. Hence, catalytic activity and Cys120 are not essential for *AmGSTF1* to elicit an MHR phenotype.

4.3.6 Biochemical characterisation of *AmGSTF1*-, C120V and S12A-expressors

It was then of interest to determine if the *AmGSTF1*-, C120V and S12A-expressors had similar increases in endogenous detoxifying enzyme activities and flavonoid accumulation as seen with previous *AmGSTF1*-expressors (Dr. I. Cummins and Prof. R. Edwards, unpublished work at the start of this project) and in MHR black-grass plants (Cummins *et al.*, 2009).

4.3.6.1 Enzyme activities of transgenic lines

For enzyme activity measurements, soluble protein extracts of the highest expressing line of each construct (*AmGSTF1* 5-19, C120V 16-17, S12A 2-19) and vector only (vector 22-24) plants were prepared by homogenising frozen tissue in aqueous buffer, discarding the solid cellular debris and precipitating protein using ammonium sulfate. Protein pellets were re-solubilised in aqueous buffer and reduced with dithiothreitol (DTT). DTT and other small molecular weight contaminants were removed using size-exclusion chromatography. The protein concentration of each sample was then estimated using commercially available dye reagents. Samples were then assayed for specific activity towards four different substrates; namely CDNB, cumene hydroperoxide (CuOOH), 2-hydroxyethyl disulfide (HED) and crotonaldehyde.

With CDNB as a substrate, a significant increase in activity was detected in *AmGSTF1*- and C120V-expressors but not in S12A-expressors relative to vector control plants. However, with crotonaldehyde, another substrate for GSH-conjugation by GSTs, a significant increase in activity was detected in all GST-expressors relative to vector control plants with no activity toward crotonaldehyde able to be detected in vector plants under these assay conditions (Table 16). These results indicate that activity towards CDNB is a direct result of catalysis by the

transgene proteins with no activity detected in S12A-expressors due to the S12A mutant being severely catalytically retarded. However conjugation of crotonaldehyde with GSH cannot be as a result of the expression of the black-grass GSTs as neither *AmGSTF1*, nor the mutant enzymes, can use this compound as a substrate (Table 8). Therefore increased activity toward crotonaldehyde in *AmGSTF1*-, C120V- and S12A-expressors must be as a result of changes in the expression and/or activities of endogenous GSTs which have little activity toward CDNB.

With CuOOH, a substrate for glutathione peroxidases (GPOXs), specific activity toward the substrate was increased approximately 2-fold in the *AmGSTF1*-, C120V- and S12A-expressing lines relative to vector control plants (Table 16). As the S12A mutant is severely catalytically retarded toward CuOOH, the similar fold increases in GPOX activity in the *AmGSTF1*-, C120V- and S12A-expressors indicates that the increase is most likely due to changes in the expression and/or activities of endogenous GPOX enzymes.

Similarly, with HED, a substrate for thiol transferases, a significant increase in activity was detected in the *AmGSTF1*-, C120V- and S12A-expressing lines relative to vector control plants (Table 16). HED cannot be used as a substrate by *AmGSTF1* or the mutant isoforms (Table 8) and hence the increases in activity must be due to changes in the expression and/or activities of endogenous thiol transferase enzymes.

Table 16: Enzyme activities of transgenic *Arabidopsis* plants expressing *AmGSTF1*, C120V, S12A or vector only. Soluble protein extracts of the following transgenic lines: *AmGSTF1* 5-19, C120V 16-17, S12A 2-19 and vector 22-24, were tested for activity towards 1-chloro-2,4-dinitrobenzene (CDNB; GST substrate), cumene hydroperoxide (GPOX substrate), 2-hydroxyethyl disulfide (thiol transferase substrate) and crotonaldehyde (GST substrate). All measurements were performed in technical triplicate and are shown \pm SEM, n = 3. ND: not detected.

Substrate	Transgenic line			
	Vector	<i>AmGSTF1</i>	C120V	S12A
CDNB	220 \pm 50	320 \pm 10	320 \pm 10	240 \pm 20
Cumene hydroperoxide	19.3 \pm 5	46.8 \pm 4	47.5 \pm 7	38.2 \pm 2
2-hydroxyethyl disulfide	175 \pm 6	208 \pm 5	202 \pm 5	239 \pm 6
Crotonaldehyde	ND	20 \pm 5	23 \pm 6	25 \pm 2

4.3.6.2 Flavonoid profiles

For flavonoid analysis, frozen tissue from the transgenic lines was homogenised in acidified methanol containing the flavonol kaempferol as an internal standard with the solid cellular debris being discarded. Samples were then separated into component compounds using high-performance liquid chromatography (HPLC) based on a published method (Cummins *et al.*, 2006) using a chromatographic matrix designed to better retain and hence separate aromatic compounds. Eluting compounds were measured for absorbance at 287 nm. To allow for reliable quantification, samples were run in technical triplicate. Flavonoid profiles of all extracts were then normalised and quantified relative to that of vector 22-24 using the peak areas of the respective internal kaempferol standards.

The samples from all transgenic lines displayed very similar profiles to one another with no novel peaks detected between lines. The only major difference observed was that *AmGSTF1*-, C120V- and S12A- expressors had a 26 – 40 % increase in the accumulation of the major flavonoid compound detected with a retention time of 15.8 min (Figure 43 and Table 17).

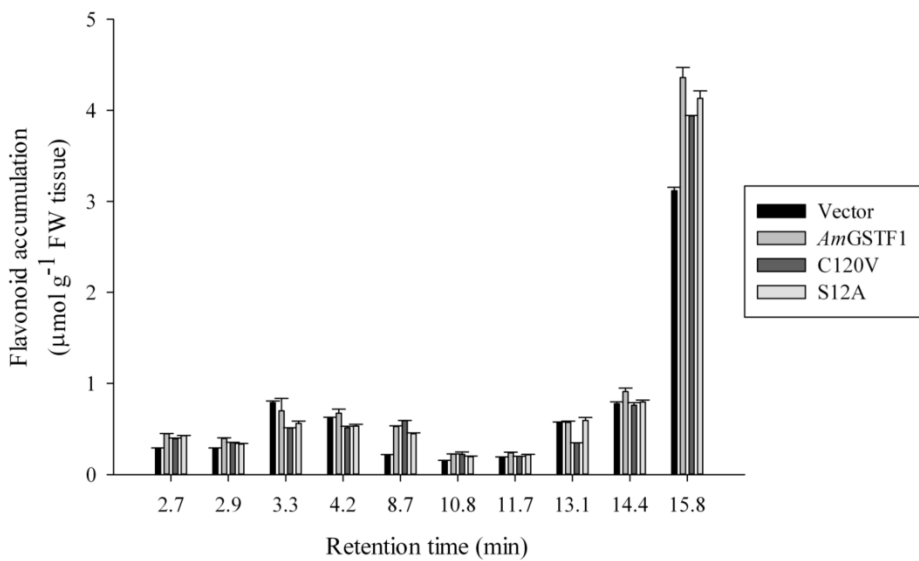


Figure 43: Flavonoid profiles of transgenic *Arabidopsis* plants expressing *AmGSTF1*, C120V, S12A or vector only. Acidified methanolic extracts of the following transgenic lines: *AmGSTF1* 5-19, C120V 16-17, S12A 2-19 and vector 22-24, were separated using high performance liquid chromatography and visualised at 287 nm. Profiles were normalised to an internal kaempferol standard with the standard used to quantify flavonoid concentrations. Quantified peaks are shown as a function of chromatographic retention time (min). All measurements were performed in technical triplicate and are shown \pm SEM, n = 3. FW – fresh weight.

Table 17: Quantification of the major flavonoid accumulating in transgenic Arabidopsis plants expressing AmGSTF1, C120V, S12A or vector only. Flavonoid accumulation was calculated relative to an internal kaempferol standard. The quantified metabolite is shown \pm SEM, n = 3. RT – chromatographic retention time. FW- fresh weight.

Metabolite	RT (min)	Transgenic line Metabolite accumulation ($\mu\text{mol g}^{-1}$ FW tissue)			
		Vector	AmGSTF1	C120V	S12A
Major flavonoid	15.8	3.12 \pm 0.04	4.36 \pm 0.11	3.94 \pm 0.004	4.13 \pm 0.08

4.3.7 Isolation of black-grass GSTs from transgenic Arabidopsis plants

DNA microarrays demonstrated that *AmGSTF1* expression in *Arabidopsis* did not elicit increases in endogenous detoxification enzymes activities and flavonoid accumulation by perturbing expression of the respective genes (see section 3.3). Therefore, *AmGSTF1* must elicit these changes post-transcriptionally. One possible mechanism is a physical interaction with regulatory proteins or small molecules. Using the *Strep* II tag, *AmGSTF1*, C120V and S12A were isolated from the respective transgenic host plants and probed for binding proteins using SDS-PAGE analysis and silver staining.

Soluble protein extracts of the highest expressing line of each construct (*AmGSTF1* 5-19, C120V 16-17, S12A 2-19) and vector only (vector 22-24) plants were prepared by homogenising approximately 1 g frozen tissue in aqueous buffer and discarding the solid cellular debris. Samples were then passed over *Strep*-tactin resin and the resin washed extensively with buffer. Retained proteins were eluted using desthiobiotin to competitively displace *Strep*-tagged components from the resin. Eluted samples were then concentrated using size-exclusion chromatography and protein components separated using SDS-PAGE. Detection of proteins by silver staining, identified small amounts of the black-grass GSTs from the respective transgenic lines. Two additional proteins were also detected. However, these were also present in the vector sample and appear to be non-specific contaminants (Figure 44A). The *Strep* II tagged proteins were isolated in very low yields, as demonstrated using an antiserum raised to the maize *ZmGSTF1-2* heterodimer, that barely detected extracted polypeptides (Figure 44B).

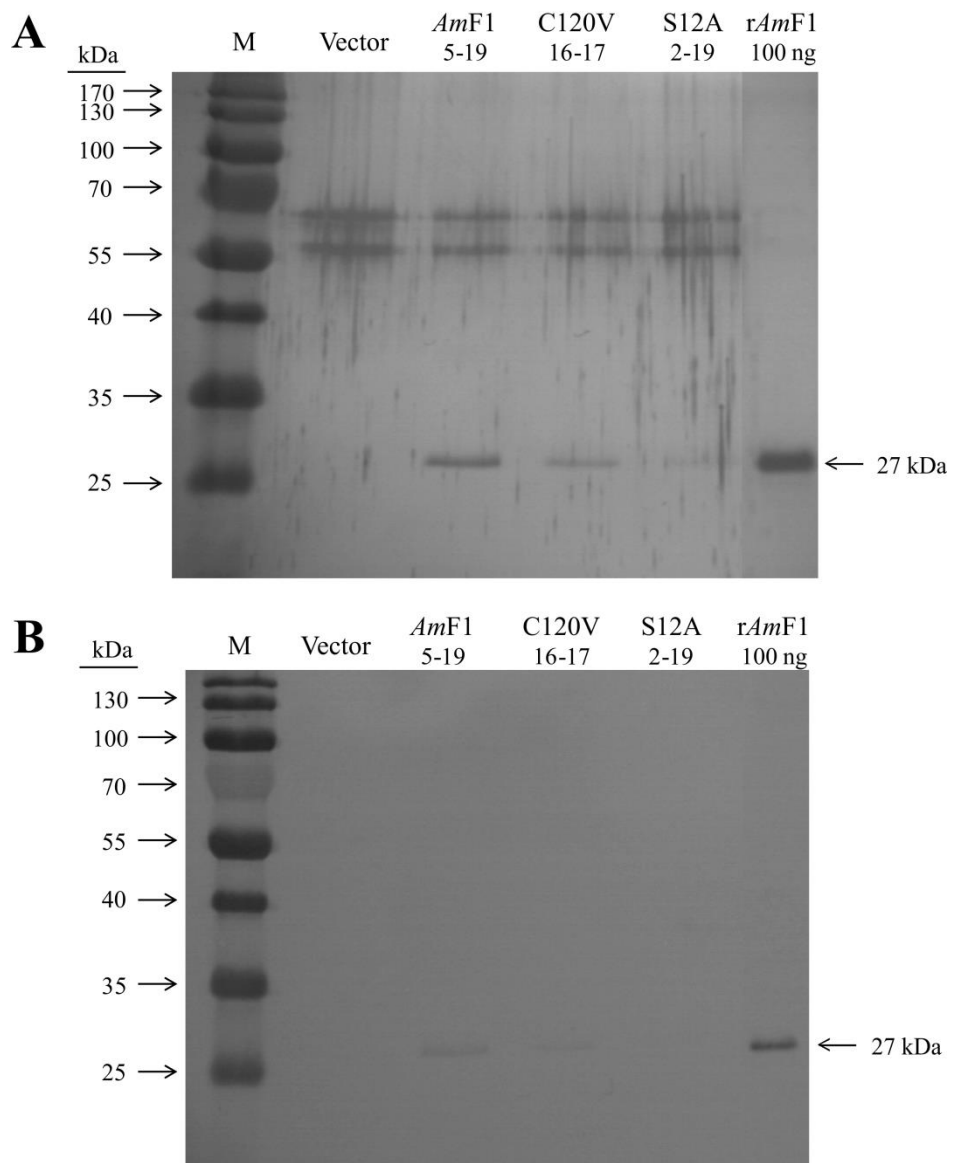


Figure 44: Isolation of Strep II tagged GSTs from transgenic Arabidopsis lines. Strep II tagged GSTs were isolated from soluble protein extracts of the following transgenic lines: *AmGSTF1* 5-19, C120V 16-17, S12A 2-19 and vector 22-24, using Strep-tactin affinity chromatography. Proteins were detected by (A) staining with silver nitrate or (B) Western blotting with an antiserum raised against the maize *ZmGSTF1-2* heterodimer. Black-grass GSTs are indicated (black arrow). Recombinant *AmGSTF1* (r*AmF1*) was stained as a positive control. M – protein markers. Molecular weights (kDa) of protein markers are shown.

4.4 Discussion and future work

AmGSTF1 was known to elicit MHR in a transgenic host plant and to induce increases in detoxification enzyme activities and flavonoid accumulation (Dr. I. Cummins and Prof. R. Edwards, unpublished work at the start of this project). *AmGSTF1* was also known to function as a GPOX enzyme *in vitro* and be able to detoxify organic and long-chain fatty acid hydroperoxides (Cummins *et al.*, 1999). It was not clear whether GPOX function was required for an MHR phenotype in a transgenic host plant, or if the phenotype was due to the increases in endogenous detoxification enzymes and flavonoids. To determine this, an S12A mutant of *AmGSTF1* was generated which was largely catalytically inactive, displaying a dramatic reduction (74 %) in activity as a GPOX enzyme (Table 8). Expression of the mutant enzyme in *Arabidopsis* plants, alongside transgenic plants expressing *AmGSTF1* as a positive control or the transformation vector only as a negative control, demonstrated that S12A-expressors displayed an MHR phenotype toward herbicides with multiple modes-of-action (Figure 41 and Figure 42). Increased tolerance was similar to that of *AmGSTF1*-expressors and demonstrated that catalytic activity is not essential for *AmGSTF1* to elicit MHR. Instead, both *AmGSTF1*-expressors and S12A-expressors induced the activities of endogenous detoxification enzymes including endogenous GPOX enzymes (Table 16). S12A-expressors also caused the accumulation of the major flavonoid that could be detected similar to *AmGSTF1*-expressors (Figure 43 and Table 17), indicating that flavonoid accumulation was also independent of catalytic activity.

A second C120V mutant was generated to probe the role of Cys120 which had been shown to be covalently labelled by the inhibitor NBD-Cl, a compound which reversed MHR in black-grass. Activity studies with *AmGSTF1* and C120V found that the C120V mutant had a higher catalytic efficiency with both CDNB and CuOOH as substrates (Table 9) and hence Cys120 may play some role in regulating catalysis. Time-course experiments with NBD-Cl found that Cys120 was the principal residue for inhibition, as C120V was only weakly inhibited by the compound relative to *AmGSTF1* (Figure 29) and could not be modified by NBD-Cl (Table 10). These same experiments found that *AmGSTF1* displayed a bi-phasic inhibition behaviour with NBD-Cl (Figure 29) which is very similar to that seen

when NBD-Cl binds to the reactive cysteine of human GSTP1 associated with multi-drug resistance in cancer cells. In the case of GSTP1, this behaviour is due to conformational signalling between the monomers of the GSTP1 dimer following the alkylation of the reactive cysteine of one monomer by NBD-Cl. Results with *AmGSTF1* suggest a similar phenomenon may exist with Cys120 and provide a secondary level of evidence for its involvement in regulating catalysis. Studies with other alkylating agents found that Cys120 could be labelled by compounds other than NBD-Cl but this interaction did not lead to inhibition of *AmGSTF1* (Figure 32 and Table 13). Therefore, alkylation alone of Cys120 does not inhibit *AmGSTF1* directly but instead indicates a further level of interaction between *AmGSTF1* and NBD-Cl that disrupts protein function. Crystallographic studies of *AmGSTF1* in complex with NBD-Cl would be of great benefit to understand the molecular interaction but successfully diffracting crystals have remained elusive (Dr. E. Pohl, Department of Chemistry, Durham University, UK, unpublished data).

The *in vitro* studies with the C120V mutant suggested that Cys120 may be critical for eliciting MHR, as alkylation of Cys120 is the predominating mechanism of interaction between *AmGSTF1* and NBD-Cl, a compound that can reverse the MHR phenotype. However, transgenesis studies with C120V found that the mutant induced MHR in a transgenic host plant with similar levels of enhanced tolerance to that of *AmGSTF1*-expressors (Figure 41 and Figure 42). C120V also induced the same increases in activities of endogenous detoxification enzymes and flavonoid accumulation (Table 16, Figure 43 and Table 17). It can therefore be concluded that while Cys120 is not essential for an MHR phenotype, it does regulate MHR reversal by NBD-Cl. NEM can also alkylate Cys120 but this does not cause inhibition of the enzyme (Table 13 and Figure 32). Whilst catalytic activity has now been shown to be non-essential for an MHR phenotype, this is suggestive of a further level of interaction between *AmGSTF1* and NBD-Cl, most likely a conformational change of the protein following alkylation. As an enzyme's structure is critical for its function, it is reasonable to suggest that a conformational change of *AmGSTF1* may disrupt the ability of *AmGSTF1* to elicit MHR. As a crystal structure of *AmGSTF1* in complex with NBD-Cl is unavailable, the structure of NBD-modified *AmGSTF1* could be explored using techniques such as circular dichroism in an attempt to detect conformational changes. If further studies were to demonstrate that NBD-Cl

appeared to reverse MHR by altering the conformation of *AmGSTF1* then the results with the C120V mutant are worrisome. Simply, the mutant shows that a single point mutation would eliminate interaction of the enzyme with NBD-Cl whilst preserving an MHR phenotype.

The mutant studies show that catalytic activity and Cys120 are not required for the induction of endogenous detoxification enzymes or for flavonoid accumulation (Table 16, Table 17 and Figure 43). It is now known that *AmGSTF1* is not eliciting these changes via perturbing gene expression (see section 3.3), suggesting that *AmGSTF1* must elicit these changes via a post-transcriptional mechanism. It is still not clear how this occurs. One possible mechanism could be physical interactions with regulatory proteins or small molecules. The transformation of *Arabidopsis* plants with *Strep* II tagged GSTs was designed to facilitate the isolation of transgenic GSTs and to detect possible binding-partners. Isolation of the transgenic GST proteins from the heterologous host did not identify protein binding-partners. However, the possibility of isolating a protein binding partner should not yet be dismissed. The preliminary experiments reported here isolated very weak concentrations of the *Strep* II tagged proteins (Figure 44) making it unlikely that a partner would be present at a sufficient concentration to be detected. These experiments should be repeated using a much greater mass of tissue and a much greater volume of *Strep*-tactin resin. Alternatively, a yeast two-hybrid approach could be used to identify proteins that physically interact with *AmGSTF1*. By using *AmGSTF1* as the ‘bait’ protein, a library of *Arabidopsis* ‘prey’ proteins could be generated from the respective cDNA library and screened for interactions with *AmGSTF1*.

With regards to the increase of endogenous enzyme activities, it is unknown whether this is due to increased protein expression, possibly via stabilisation of the respective gene transcripts, by a structural modification of the expressed proteins, or by reducing protein turnover. To determine this, it would be useful to separate the components of total protein samples from each transgenic line using two-dimensional gel electrophoresis and compare vector samples with GST-expressors. This approach may also potentially reveal alterations of proteins not detected using the selective detection methods of the current studies. For instance, is enhanced

chlorotoluron resistance, detected in the *AmGSTF1*-expressors, a result of an increase in expression of detoxifying CYPs that were not identified using the selective activity screens employed in the current studies? An alternative approach to answer this question would be to measure the relative rates of chlorotoluron metabolism in the transgenic lines. Prior work to the studies in this thesis did identify that GST-catalysed detoxification of alachlor and atrazine was enhanced in *AmGSTF1*-expressors (Dr. I. Cummins and Prof. R. Edwards, unpublished work at the start of this project). This must be due to endogenous GSTs as *AmGSTF1* cannot use either alachlor or atrazine as substrates (Cummins *et al.*, 1999). However, the effects on chlorotoluron metabolism were not determined (Dr. I. Cummins and Prof. R. Edwards, unpublished work at the start of this project).

Finally, *AmGSTF1*-, C120V- and S12A-expressors accumulated a significantly greater proportion (25 – 40 %) of the major flavonoid present in all samples (Table 17). Whilst *AmGSTF1*-expressors in previous studies also accumulated flavonoids, plants in these prior studies accumulated much greater levels of two flavonoid derivatives and two anthocyanin derivatives (Dr. I. Cummins and Prof. R. Edwards, unpublished work at the start of this project). No anthocyanins were detected in acidified methanol samples used in the present studies. With no detectable changes in the expression of flavonoid biosynthesis genes, it is most likely that *AmGSTF1* binds to and stabilises an intermediary metabolite. Intrinsically, this would depend on that intermediary metabolite being first synthesized by the plant. Flavonoid metabolism is a well-studied branch of plant secondary metabolism and known to be regulated by a variety of input signals, including a particular sensitivity to light intensity (Hernandez and Van Breusegem, 2010). Changes in growth conditions between different experiments will likely have an impact on the biosynthesis of secondary metabolites and may be why different flavonoids are accumulated between different experiments. It is therefore unclear as to the role of flavonoids in the MHR phenotype. Do they contribute to enhanced tolerance, or are they an artefact of *AmGSTF1* expression?

Chapter 5 – AmGSTF1 orthologues

5.1 Introduction

AmGSTF1 was able to induce MHR in a transgenic host plant with it being shown that this was not due to its catalytic properties. Instead, the protein exerts a regulatory role leading to an increase in the activities of endogenous detoxification enzymes and the accumulation of flavonoids. More specifically, *AmGSTF1* caused changes in host plant biochemistry that closely mirrored those seen in MHR-black-grass plants (Cummins *et al.*, 2009). Hence, *AmGSTF1* appears to be a central component of the MHR phenotype. It was therefore of interest to explore the properties of *AmGSTF1* orthologues from other plant species.

5.2 Identification of *AmGSTF1* orthologues

Firstly, an orthologue from maize, *ZmGSTF1* (63 % amino acid sequence identity; Figure 45), was chosen for study.

<i>AmGSTF1</i>	MAPVKVFGPAMSTINVARVTLCLEEVGAEYEVVNIDFNTMEHKSPFHARNPFGQIPAFQD	60
<i>ZmGSTF1</i>	MAPMKLYGAVMSWNLRCTALEEAGSDYEIVPINFATAEHKSPEHLVRNPFQVPAQLQD	60
	*****:***:*** . *::* : .***.*:***:***:***:*** * *****:*****:***:***	
<i>AmGSTF1</i>	GDLLLWESRAISKYVLRKYKTDEVDLLRESNLEEAAMVDVWTEVDAHTYNPALSPIVYQC	120
<i>ZmGSTF1</i>	GDLYLFESRAICKYAARKNKP---ELLREGNLEEAAMVDVWIEVEANQYTAALNPIIFQV	117
	*** *:*****.*** . ** *. :*****.*****:***** ***:***: *...***.***:***	
<i>AmGSTF1</i>	I[FNPMMRGLPTDEKVVAESLEKKVLEVYEARLSKHSYLAGDFVSFADLNHFPTFYFM	180
<i>ZmGSTF1</i>	I[LSEMLLEG-TTDQKVVDENLEKKVLEVYEARLTCKYLAGDFSLADLNHVSVTLCLF	176
	*:***: * .*:*** * .*****:*****:*** .*****:***:*****.. *: :	
<i>AmGSTF1</i>	ATPHAAFLFDSDYPHVKAWWDRLMARPAVKKIAATMVPKA	219
<i>ZmGSTF1</i>	ATPYASVLDAYPHVKAWWSGLMERPSVQKVAALMKPSA-	214
	::***:*****. ** ***:***:*** * *	

Figure 45: Sequence alignment of *AmGSTF1* and the maize orthologue *ZmGSTF1*. *AmGSTF1* was aligned with *ZmGSTF1* using Clustal Omega (1.1.0) (EBI web servers). *AmGSTF1* accession: Q9ZS17, *ZmGSTF1* accession: NP_001105412. Boxed residues indicate active-site residues based on the *ZmGSTF1* crystal structure (accession: 1axd). * denote identical amino acid residues whilst : and . denote amino acid residues with similar chemical properties.

This enzyme has been relatively well-studied, having first been identified in maize 30 years ago due to its ability to detoxify the herbicide alachlor, by catalysing the formation of the glutathione conjugate (Mozer *et al.*, 1983). It has since been shown to catalyse the detoxification of the related herbicide metolachlor, as well as the unrelated herbicide atrazine, by GSH-conjugation (Dixon *et al.*, 1997). *ZmGSTF1* possesses very little GPOX activity (Sommer and Boger, 1999) and has a valine

residue at the equivalent position to Cys120 in the *AmGSTF1* primary amino acid sequence (Figure 45). *AmGSTF1* cannot detoxify alachlor, metolachlor or atrazine using GSH (Cummins *et al.*, 1999) and is a highly active GPOX enzyme. Hence, whilst being relatively similar in amino acid sequence identity to *AmGSTF1*, *ZmGSTF1* appears to be functionally orthogonal. As such, *ZmGSTF1* represents an interesting target for comparative study with *AmGSTF1*. Therefore, *Strep* II tagged *ZmGSTF1* has been characterised *in vitro* and expressed in transgenic *Arabidopsis* plants. The transformed plants were screened for changes in herbicide tolerance, endogenous detoxification enzyme activities and flavonoid accumulation in an analogous manner to that described for *Arabidopsis* plants expressing *AmGSTF1* and the mutant isoforms (see Chapter 4).

During these studies, a further *AmGSTF1* orthologue with high amino acid identity (91 %; Figure 46) was identified in annual rye-grass and termed *LrGSTF1* (Dr. F. Sabbadin and Prof. R. Edwards, unpublished work at the start of this project).

<i>AmGSTF1</i>	MAPVKVFGPAMSTINVARVTLCLLEEVGAEYEVNIDFNTMEHKSPFHARNPFGQIPAFQD	60
<i>LrGSTF1</i>	MAPVKVFGPAMSTINVARVLFLEEVGADYEVVDMDFKVMEHKSPFHARNPFGQIPAFQD	60
	***** : * : * : * : . *****	
<i>AmGSTF1</i>	GDLLLWESRAISKYVLKYKTDEVDLLRESNLLEAAMVDVWTEVDAHTYNPALSPIVYQC	120
<i>LrGSTF1</i>	GDLLLFESENRAISKYVLKYKTGEVDLLREGNLKEAAMVDVWTEVDAHTYNPALSPIVYQC	120
	* : ***** . * : *****	
<i>AmGSTF1</i>	LFNPMMRGLPTDEKVVAESLEKLKKVLEVYEARLSKHSYLAGDFVSFADLNHFPTFYFM	180
<i>LrGSTF1</i>	LFNPMMRGIPTDEKVVAESLEKLKKVLEVYEARLSQHEYLAGDFVSFADLNHFPTFYFM	180
	* : *****	
<i>AmGSTF1</i>	ATPHAALFDSDYPHVKAWWDRLMARPAVKKIAATMVPPKA	219
<i>LrGSTF1</i>	ATPHAALFGSYPHVKAWWERIMARPAIKKISATMVPPKA	219
	* : * : * : *	

Figure 46: Sequence alignment of *AmGSTF1* and the annual rye-grass orthologue *LrGSTF1*. *AmGSTF1* was aligned with *LrGSTF1* using Clustal Omega (1.1.0) (EBI web servers). *AmGSTF1* accession: Q9ZS17, *LrGSTF1* accession: M5BPX4. Boxed residues indicate active-site residues based on the *ZmGSTF1* crystal structure (accession: 1axd). * denote identical amino acid residues whilst : and . denote amino acid residues with similar chemical properties.

In an analogous manner to *AmGSTF1*, *LrGSTF1* was constitutively up-regulated in MHR annual rye-grass relative to WTS plants (Dr. F. Sabbadin and Prof. R. Edwards, unpublished work at the start of this project). Due to the discovery of *LrGSTF1* mid-way through this project, there was not sufficient time to express this enzyme in transgenic *Arabidopsis* plants and assess the phenotype. The enzyme has however been expressed and characterised *in vitro* alongside *AmGSTF1* for comparison.

5.3 Expression and *in vitro* characterisation of *AmGSTF1* orthologues

5.3.1 Expression and purification of *AmGSTF1* orthologues

Both *ZmGSTF1* and *LrGSTF1* were available already sub-cloned into the pET-STRP3 vector to render the open reading frames of each enzyme fused with an *N*-terminal *Strep* II tag (*ZmGSTF1* in pET-STRP3 vector kindly donated by Dr. D. P. Dixon, GlaxoSmithKline, Stevenage, UK; *LrGSTF1* in pET-STRP3 vector kindly donated by Dr. F. Sabbadin, Department of Biology, University of York, UK). Both *Strep* II tagged enzymes, alongside *AmGSTF1*, were expressed in *E. coli* and purified using *Strep*-tactin affinity chromatography as described (see section 3.1.2). Recombinant *ZmGSTF1* had been previously characterised and found to elute as a single pure protein by SDS-PAGE analysis and mass spectrometry (Dr. D. P. Dixon, GlaxoSmithKline, Stevenage, UK) however this remained to be determined with recombinant *LrGSTF1*. Following the purification of recombinant *Strep* II tagged *LrGSTF1*, eluted protein was analysed using SDS-PAGE with a single band detected, even when loading with 5 µg purified recombinant protein (Figure 47).

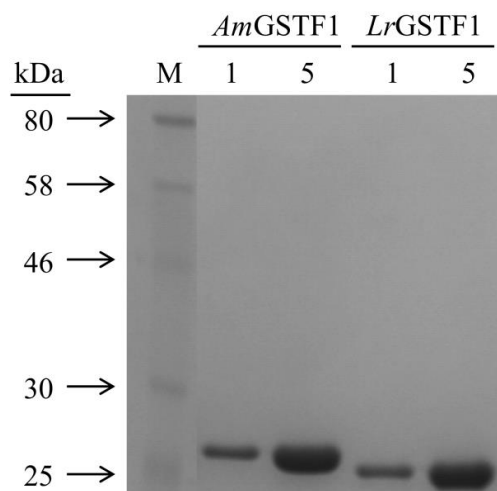


Figure 47: Purity analysis of recombinant *AmGSTF1* and *LrGSTF1*. Purified *AmGSTF1* and *LrGSTF1* enzymes were analysed using sodium dodecyl sulfate polyacrylamide gel electrophoresis (SDS-PAGE). 1 µg (1) and 5 µg (5) enzyme were loaded per gel. M – protein markers. Molecular weights (kDa) of protein markers are shown.

LrGSTF1 behaved as if smaller in molecular weight than *AmGSTF1* even though it was predicted to be larger by 824 Da. The reason for this large increase in predicted

molecular weight, even though the amino acid sequences of *LrGSTF1* and *AmGSTF1* are 91 % identical, was primarily due to the insertion of a 6 amino acid sequence, MKQWYK, between the *Strep* II tag and the *N*-terminal methionine of the protein as an artefact of the cloning method used to isolate *LrGSTF1*. The phenomenon of GSTs behaving anomalously during SDS-PAGE analysis has been reported previously (Hayes and Mantle, 1986; Mannervik and Danielson, 1988), but in order to confirm that *LrGSTF1* had been correctly purified the sample was analysed by mass spectrometry. Mass spectrometry confirmed that the sample had an identical observed mass to that of the predicted protein (Table 18) demonstrating that *LrGSTF1* had been correctly purified.

Table 18: Whole-protein mass measurement of purified recombinant *LrGSTF1*. Purified recombinant *Strep* II tagged *LrGSTF1* was analysed using electrospray ionisation mass spectrometry (ESI-MS) in positive ion mode (Technology Facility, University of York, UK). The theoretical mass assumes complete loss of the *N*-terminal methionine residue as is known to occur for *Arabidopsis* *Strep* II tagged GSTs. (Dixon *et al.*, 2009).

Enzyme	Theoretical mass (Da)	Observed mass (Da)
<i>LrGSTF1</i>	27489	27489

5.3.2 Catalytic profiles of *AmGSTF1* orthologues

Following purification, *ZmGSTF1* and *LrGSTF1*, alongside recombinant *AmGSTF1*, were tested for activity towards the same set of substrates used with *AmGSTF1* and the mutant isoforms (see section 4.2.2). These substrates were; 1-chloro-2,4-dinitrobenzene (CDNB), cumene hydroperoxide (CuOOH), 2-hydroxyethyl disulfide (HED), 4-nitrophenyl acetate, ethacrynic acid, crotonaldehyde and benzyl isothiocyanate (BITC). CDNB, ethacrynic acid, crotonaldehyde and BITC undergo GSH-conjugation, while CuOOH is a substrate that tests for GPOX activity. HED is a substrate that tests for GSH-dependent thiol transferase activity and NPA is a substrate that tests for ester thiolysis activity. *AmGSTF1* and *LrGSTF1* were also tested against linoleic acid hydroperoxide, a long-chain (18-carbon) fatty acid hydroperoxide, as a substrate.

Equimolar concentrations of *ZmGSTF1*, *LrGSTF1* or *AmGSTF1* were assayed for activity toward each substrate in the presence of excess GSH. The exception to this

was when *ZmGSTF1* was assayed for activity toward CDNB for which *ZmGSTF1* required diluting 50-fold to obtain linear kinetics. In all cases, activity toward each substrate was determined using UV-vis spectrophotometry. Activity towards linoleic acid hydroperoxide was detected in an analogous manner to that of CuOOH using a glutathione reductase redox system.

The catalytic profile of *ZmGSTF1* in these studies was in accordance with that previously reported for recombinant His-tagged *ZmGSTF1* (Sommer and Boger, 1999), confirming that the enzyme is catalytically orthogonal to *AmGSTF1*. *ZmGSTF1* was highly active toward CDNB (138-fold greater than *AmGSTF1*), showing lower activity toward ethacrynic acid and displaying little detectable GPOX activity (Table 19). Very low levels of activity toward crotonaldehyde have been reported previously for *ZmGSTF1* (Sommer and Boger, 1999), but no activity could be detected in these studies. There are no previous reports of BITC, NPA and HED having been tested as substrates for *ZmGSTF1*. No activity could be detected with HED as a substrate, whilst low levels of thiolysis activity toward NPA could be detected with *ZmGSTF1* that were identical to *AmGSTF1* in magnitude. *ZmGSTF1* showed strong activity toward BITC as a substrate being 2.4-fold greater than *AmGSTF1* (Table 19).

The catalytic profile of *LrGSTF1* appeared to be very similar to that of *AmGSTF1*. Both enzymes displayed very similar levels of activity towards CDNB, NPA, ethacrynic acid and BITC. No activity could be detected with either enzyme towards HED or crotonaldehyde. The one significant difference between *LrGSTF1* and *AmGSTF1* was found when enzymes were assayed for activity toward hydroperoxide substrates. *LrGSTF1* was 2.4-fold and 2.8-fold more active toward the organic and fatty acid hydroperoxides respectively relative to *AmGSTF1* (Table 19).

Table 19: Substrate specificities of recombinant *AmGSTF1* and associated orthologues. CDNB: 1-chloro-2,4-dinitrobenzene. ND: not detected. NA: not assayed. Measurements were performed in technical triplicate. Mean specific activities are shown \pm SD, n = 3.

Substrate	Mean specific activity (nmol s ⁻¹ mg ⁻¹ protein)		
	<i>AmGSTF1</i>	<i>LrGSTF1</i>	<i>ZmGSTF1</i>
CDNB	25.4 \pm 0.8	31.7 \pm 1.3	3462.9 \pm 145
Cumene hydroperoxide	19.6 \pm 1.4	47.0 \pm 1.9	3.2 \pm 0.3
Linoleic acid hydroperoxide	98.6 \pm 15.9	272.6 \pm 22.5	NA
2-hydroxyethyl disulfide	ND	ND	ND
4-nitrophenyl acetate	1.06 \pm 0.07	2.66 \pm 0.09	1.07 \pm 0.01
Ethacrynic acid	16.4 \pm 0.8	11.5 \pm 0.1	17.1 \pm 0.5
Crotonaldehyde	ND	ND	ND
Benzyl isothiocyanate	34.2 \pm 0.7	44.2 \pm 3.1	81.8 \pm 0.8

Hence, *LrGSTF1* appears to be highly similar to *AmGSTF1* in both amino acid sequence and catalytic function. This suggested that *LrGSTF1* may display similar inhibitory profiles when treated with inhibitors as seen with *AmGSTF1*.

5.3.3 Inhibition of *LrGSTF1*

To study *LrGSTF1* inhibition, IC₅₀ concentrations were determined with four compounds tested previously for inhibition of *AmGSTF1* (see section 3.2.2). These compounds were; NBD-Cl, ethacrynic acid, cyanuric chloride and bromoenol lactone (Figure 48A). Recombinant *LrGSTF1* was assayed for activity toward CDNB in the presence and absence of each inhibitor. Inhibitors were used over the concentration range 0.001 – 100 μ M in the presence of excess GSH. There was no prior incubation of each inhibitor with *LrGSTF1* before assaying for activity toward CDNB. The molar concentration of *LrGSTF1* used was equal to the concentration of *AmGSTF1* used in analogous studies.

LrGSTF1 displayed near-identical inhibitory profiles with each compound as was seen with *AmGSTF1* (Figure 48B). Ethacrynic acid proved the most potent inhibitor of *LrGSTF1* (IC₅₀ = 1.03 μ M), closely followed by NBD-Cl (IC₅₀ = 6.58 μ M). Cyanuric chloride and bromoenol lactone proved weak inhibitors of *LrGSTF1* under these assay conditions (Figure 48B).

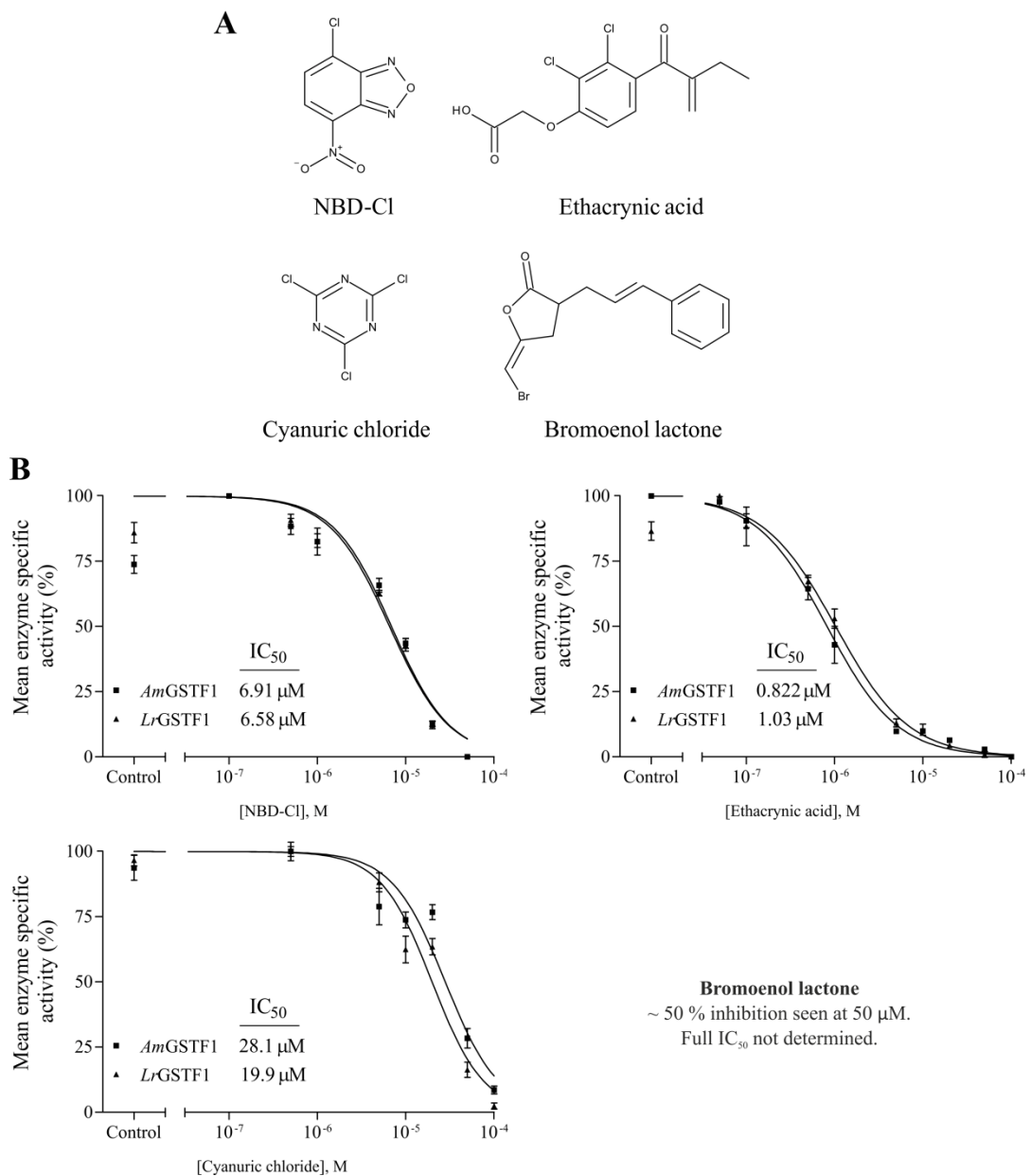


Figure 48: Inhibitory profiles of *LrGSTF1* treated with compounds known to inhibit *AmGSTF1*. (A) Structures of compounds tested as potential inhibitors of *LrGSTF1*. (B) *LrGSTF1* (344 nM) was assayed for activity towards 1-chloro-2,4-dinitrobenzene in the presence of discrete concentrations of each inhibitor (0–100 μM). Measurements were performed in technical triplicate. Mean specific activities are shown ± SD, n = 3. Equivalent *AmGSTF1* profiles are shown for aid of comparison. *AmGSTF1* (344 nM) was treated in exactly the same manner as *LrGSTF1*.

Hence, *LrGSTF1* appears to be highly similar to *AmGSTF1* in amino acid sequence, catalytic function and interactions with xenobiotics. Whilst definitive proof of *LrGSTF1* being able to induce MHR is required, the *in vitro* data strongly suggests that the proteins would play similar roles *in planta*. If this proved to be the case then up-regulation of GSTF1s would have independently evolved in multiple weed

species to enable an MHR phenotype and would represent a tremendous breakthrough in understanding the molecular mechanism/s of MHR.

5.4 Expression of *ZmGSTF1* in transgenic *Arabidopsis* plants

With regards to *ZmGSTF1*, this enzyme appears to be catalytically orthogonal to both *AmGSTF1* and *LrGSTF1*. However, as studies with *AmGSTF1* mutants have shown that catalysis is not essential for *AmGSTF1* to elicit an MHR phenotype in transgenic *Arabidopsis* plants, it was of interest to determine the phenotype of *Arabidopsis* plants expressing *ZmGSTF1*.

5.4.1 Generation of independent homozygous *ZmGSTF1*-expressing *Arabidopsis* lines

Transgenic *Arabidopsis* plants expressing *ZmGSTF1* were generated and analysed in an analogous manner to that described for *AmGSTF1* and the mutant isoforms (see section 4.3). Firstly, *ZmGSTF1* was sub-cloned from the pET-STRP3 vector into the pBIN-STRP3 vector. *ZmGSTF1* in the pET-STRP3 vector was digested with *NcoI/BstXI* DNA restriction enzymes and ligated into *NcoI/BstXI* digested pBIN-STRP3 vector. The ligated vector was transformed into competent *E. coli* cells followed by purification of the *ZmGSTF1*-pBIN-STRP3 plasmid. The construct sequence was confirmed as correct by DNA sequencing. The construct was then transformed into *Agrobacterium tumefaciens* strain GV3101 containing the MP90 helper plasmid that harboured the *vir* genes required for T-DNA excision and integration (Koncz and Schell, 1986). Successful transformants were selected with the appropriate antibiotics. *Arabidopsis* plants were then transformed as described (Clough and Bent, 1998) by inoculating flowering plants with *Agrobacterium* cultures transformed with the *ZmGSTF1*-pBIN-STRP3 vector. Homozygous independent transgenic lines were generated using successive rounds of selection with glufosinate-ammonium as described in Figure 39. Three T₁ lines expressing the *ZmGSTF1* construct were identified showing a statistically strong correlation ($p \geq 0.5$) to the expected 3:1 alive:dead ratio (Table 20) following selection with glufosinate-ammonium, indicating an expressed single-insertion event.

Table 20: T₁ transformant lines that segregated in a 3:1 alive:dead ratio following selection with glufosinate-ammonium. Seed of each T₁ line was sown on soil and maintained in glasshouses for 14 days before spraying with glufosinate-ammonium. The number of seedlings was counted before and after spraying. A χ^2 statistical test was used to prove these lines granted the desired 3:1 ratio for a stably-integrated single insert.

Construct	T ₁ line	Expected		Observed		χ^2 p-value
		Alive	Dead	Alive	Dead	
ZmGSTF1	10	34.5	11.5	36	10	0.610
	13	29.25	9.75	28	11	0.644
	20	39.75	13.25	38	15	0.579

Twenty four individuals of each of these 3 T₁ lines were separated and allowed to self-fertilise with the resulting seed (T₂) of each individual collected. Eight T₂ lines from each of the 3 selected T₁ lines were sown and seedlings selected again with glufosinate-ammonium. This identified a homozygous T₂ line from each T₁ line (all T₂ progeny survived selection with glufosinate-ammonium) and hence three independent homozygous lines for the ZmGSTF1-pBIN-STRP3 construct (Table 21).

Table 21: ZmGSTF1 homozygous single insertion lines selected for further study.

Construct	Homozygous T ₂ line
ZmGSTF1	10-17
	13-3
	20-22

5.4.2 Screening of transgenic plants for GST expression

The selected homozygous T₂ lines (Table 21) were screened for GST protein expression using an antiserum raised against the maize ZmGSTF1-2 heterodimer. The antiserum recognised endogenous phi class GSTs in all samples, including the vector plants. It also recognised a novel GSTF band in the 3 homozygous T₂ ZmGSTF1-expressor lines corresponding to expression of the ZmGSTF1 polypeptide. ZmGSTF1 appeared to be strongly expressed in lines 10-17 and 20-22 and expressed at much weaker levels in line 13-3 (Figure 49).

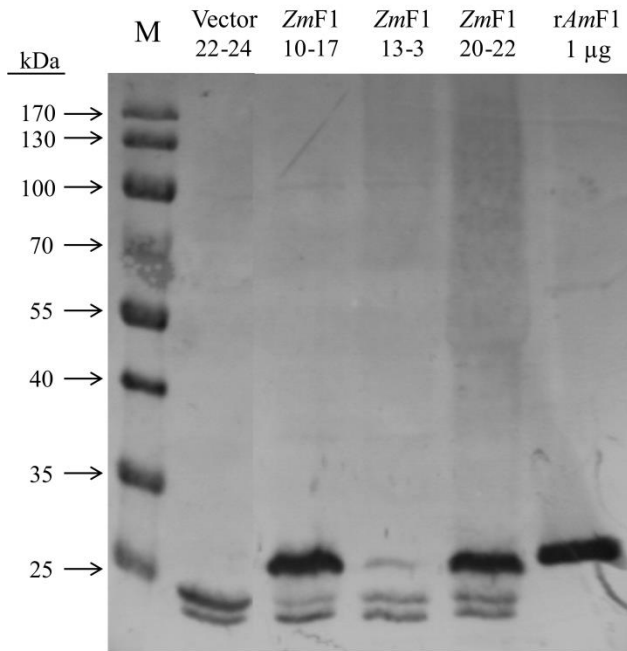


Figure 49: Phi class GST expression screens of *ZmGSTF1* homozygous insertion lines. Transgenic Arabidopsis lines designed to express *ZmGSTF1*, for which all T₂ progeny survived glufosinate-ammonium selection, were screened for construct expression by Western blotting using an antiserum raised against the *ZmGSTF1*-2 heterodimer. The vector 22-24 line designed to express the *Strep* II tag, for which all T₂ progeny survived glufosinate-ammonium selection, served as a negative control. Recombinant *AmGSTF1* (rAmF1) was run alongside samples as a positive control for antiserum detection. M – protein markers. The molecular weights (kDa) of protein markers are shown. Numbers below vector and enzyme names (e.g. *ZmF1* 10-17) denote unique identification numbers of each independent T₂ line.

5.4.3 Testing *ZmGSTF1*-expressors for enhanced herbicide tolerance

In order to determine a stable phenotype, two homozygous T₂ *ZmGSTF1*-expressor lines (10-17 and 13-3) were tested for changes in herbicide tolerance with chlorotoluron, a herbicide that cannot be detoxified directly by GSTs. Line 20-22 had very poor germination and was not studied further. Seeds of the two selected lines (30 per pot) were sown on soil and grown for 14 days in environmental growth chambers (20 °C, 100 µE m⁻² s⁻¹, 16 hr photoperiod). Seedlings of the *ZmGSTF1*-expressors and the vector control plants were then sprayed with chlorotoluron (60 g active ingredient per hectare) formulated with 0.1 % (v/v) Biopower, 1 % (v/v) acetone or with formulation alone. Following spray treatments, plants were maintained in growth chambers for a further 7 days before imaging.

ZmGSTF1-expressors appeared to behave differently to vector control plants following both formulation-only and chlorotoluron treatments. With both treatments,

ZmGSTF1-expressors accumulated more biomass with this accumulation appearing significantly greater after chlorotoluron treatment by visual assessment (Figure 50).

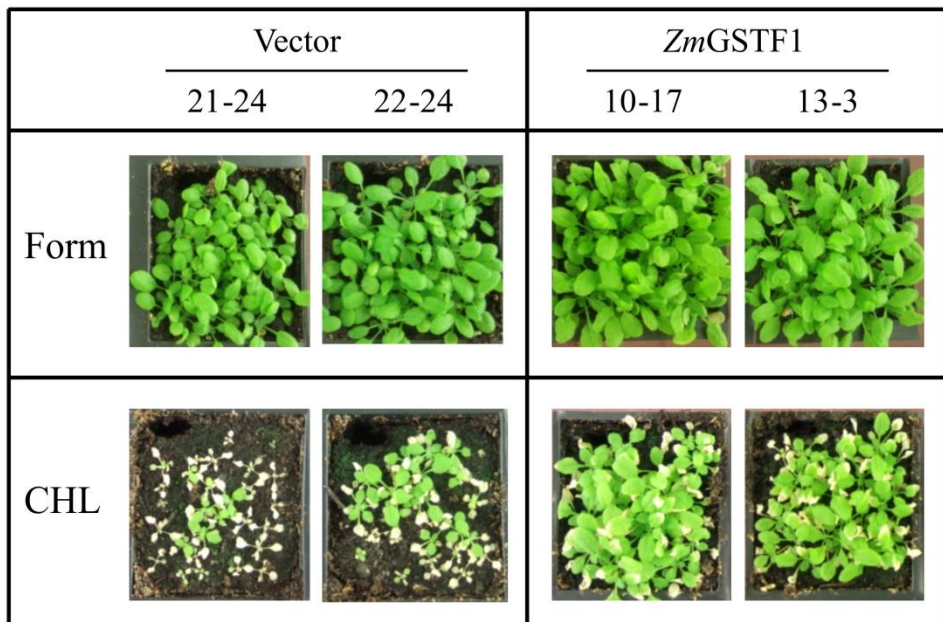


Figure 50: Increased herbicide tolerance of transgenic *Arabidopsis* plants expressing *ZmGSTF1*. Seeds of two independent lines of each construct were sown on soil (30 per pot) and maintained in environmental growth chambers for 14 days followed by an application of chlorotoluron (CHL; 60 g ai hectare⁻¹, 0.1 % biopower, 1 % acetone) or an equivalent volume of formulation only (Form; 0.1 % biopower, 1 % acetone). Plants were maintained in environmental growth chambers for a further 7 days and then photographed. Numbers below vector and enzyme names (e.g. *ZmGSTF1* 10-17) denote unique identification numbers of each independent line.

As the biomass of *ZmGSTF1*-expressors increased following both chlorotoluron and formulation-only treatments, it was ambiguous as to whether the biomass accumulation following chlorotoluron treatment was as a direct result of increased tolerance or an artefact of perturbations in plant growth caused by *ZmGSTF1* expression. To clarify this, the spray trial was repeated using the highest *ZmGSTF1* expressing line (10-17) and the vector 22-24 line which appeared the more tolerant of the two vector lines. The increase in biomass of the *ZmGSTF1*-expressors was then calculated relative to vector control plants following chlorotoluron and formulation-only treatments. Plants were also challenged with the herbicide alachlor to assess resistance to multiple herbicides with differing modes-of-action. Alachlor is a known substrate of *ZmGSTF1* and so it would be expected that *ZmGSTF1*-expressors would be more tolerant to this herbicide relative to vector control plants. Alachlor (1200 g active ingredient per hectare) was applied in an analogous manner to chlorotoluron by formulating with 0.1 % (v/v) Biopower, 1 % (v/v) acetone. To

calculate the relative changes in biomass between *ZmGSTF1*-expressors and vector control plants, treated pots were first counted for the number of individuals in each pot and then aerial tissue of each pot was harvested and weighed. For each pot, the mass per plant was calculated to normalise for small differences in germination and the differences in mass per plant were calculated between *ZmGSTF1*-expressors and vector control plants expressed as a percentage increase of the vector.

Whilst *ZmGSTF1*-expressors accumulated more biomass than vector control plants following all treatments, the increases in biomass were significantly greater following herbicide treatments compared with formulation alone (Figure 51).

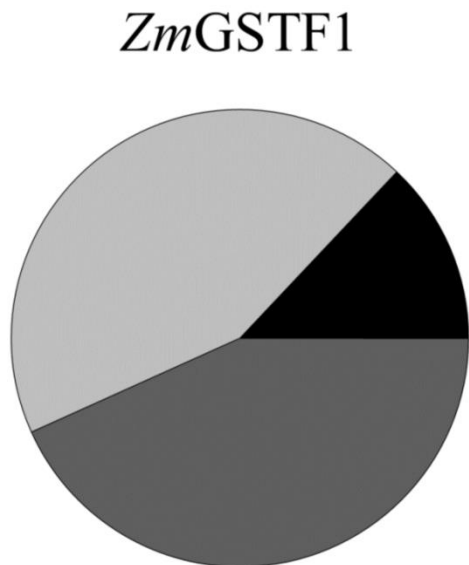


Figure 51: Increased biomass of transgenic *Arabidopsis* plants expressing *ZmGSTF1* relative to vector-only control plants following herbicide treatment. Plants of the following transgenic lines: *ZmGSTF1* 10-17 and vector 22-24, (20 seeds per pot) were grown in environmental growth chambers in duplicate for 14 days followed by an application of chlorotoluron (CHL; 60 g ai hectare⁻¹, 0.1 % biopower, 1 % acetone), alachlor (ALA; 1200 g ai hectare⁻¹, 0.1 % biopower, 1 % acetone) or an equivalent volume of formulation only (Form; 0.1 % biopower, 1 % acetone) and then maintained in growth chambers for a further 10 days. At this time aerial tissue of all lines was harvested and weighed. For each replicate the percentage increase in fresh weight per plant of the *ZmGSTF1*-expressors was calculated relative to the vector-only control plants and the mean percentage increase in fresh weight per plant for the *ZmGSTF1*-expressors relative to vector-only control plants is shown for the three chemical treatments; formulation only (black), chlorotoluron (light grey) and alachlor (dark grey).

Hence, *ZmGSTF1* induces MHR in *Arabidopsis* plants. *ZmGSTF1* has been shown to grant resistance to alachlor in transgenic tobacco plants with this presumed to be due to its ability to detoxify alachlor using GSH (Karavangeli *et al.*, 2005). However, by using chlorotoluron, this is the first demonstration that *ZmGSTF1* can grant resistance to herbicides independently of catalysis. Having observed that *AmGSTF1* expression in *Arabidopsis* induces increases in endogenous enzyme

activities and flavonoid accumulation that may contribute to the MHR phenotype (see section 4.3.6), *ZmGSTF1* was also screened for similar perturbations.

5.4.4 Biochemical characterisation of *ZmGSTF1*-expressors

For enzyme activity measurements, soluble protein extracts of *ZmGSTF1*-expressor line 10-17 and vector only (vector 22-24) plants were prepared by homogenising frozen tissue in aqueous buffer, discarding the solid cellular debris and precipitating protein using ammonium sulfate. Protein pellets were re-solubilised in aqueous buffer and reduced with dithiothreitol (DTT). DTT and other small molecular weight contaminants were removed using size-exclusion chromatography and the concentration of each sample was estimated using commercially available dye reagents. Samples were then assayed for specific activity towards four different substrates; CDNB, cumene hydroperoxide (CuOOH), 2-hydroxyethyl disulfide (HED) and crotonaldehyde.

With CDNB, a substrate that tests for GSH-conjugation and an excellent substrate for *ZmGSTF1*, an 18-fold increase in activity was detected in *ZmGSTF1*-expressors relative to vector control plants most likely due to expression of the transgene. Using crotonaldehyde, another substrate for GSH-conjugation by GSTs, a significant increase in the activity of endogenous GST activities was detected in *ZmGSTF1*-expressors relative to vector control plants, with no activity toward crotonaldehyde able to be detected in vector plants under these assay conditions (Table 22). The increase in activity toward crotonaldehyde must be due to endogenous GSTs as *ZmGSTF1* cannot use this compound as a substrate (Table 19).

With CuOOH, a substrate for glutathione peroxidases (GPOXs), specific activity toward the substrate was increased 2.4-fold in the *ZmGSTF1*-expressing lines relative to vector control plants (Table 22). *ZmGSTF1* has very little detectable activity toward CuOOH (Table 19) and hence the increase in GPOX activity in *ZmGSTF1*-expressors must be due to endogenous GPOX enzymes.

Similarly, with HED, a substrate for thiol transferases, a significant increase in activity was detected in the *ZmGSTF1*-expressing lines relative to vector control

plants (Table 22). HED cannot be used as a substrate by *ZmGSTF1* (Table 19) hence the increases in activity must be due to endogenous thiol transferase enzymes.

Table 22: Enzyme activities of transgenic *Arabidopsis* plants expressing *ZmGSTF1* or vector only. Soluble protein extracts of the following transgenic lines: *ZmGSTF1* 10-17 and vector 22-24, were tested for activity towards 1-chloro-2,4-dinitrobenzene (CDNB; GST substrate), cumene hydroperoxide (GPOX substrate), 2-hydroxyethyl disulfide (thiol transferase substrate) and crotonaldehyde (GST substrate). All measurements were performed in technical triplicate and are shown \pm SEM, n = 3. ND: not detected.

Substrate	Transgenic line	
	Vector	<i>ZmGSTF1</i>
CDNB	220 \pm 50	4020 \pm 20
Cumene hydroperoxide	19.3 \pm 5	46 \pm 8
2-hydroxyethyl disulfide	175 \pm 6	196 \pm 2
Crotonaldehyde	ND	22 \pm 3

For flavonoid analysis, frozen tissue of the transgenic lines was homogenised in acidified methanol containing the flavonol kaempferol as an internal standard with the solid cellular debris being discarded. Samples were then separated into component compounds using high-performance liquid chromatography (HPLC) based on a published method (Cummins *et al.*, 2006) using a chromatographic matrix designed to better retain and separate aromatic compounds. Eluting compounds were measured for absorbance at 287 nm. To allow for reliable quantification, samples were run in technical triplicate. Flavonoid profiles of all extracts were then normalised and quantified, relative to that of vector 22-24, using the peak areas of the respective internal kaempferol standards.

Like with *AmGSTF1*-expressors, flavonoid profiles were very similar between *ZmGSTF1*-expressors and vector control plants with no novel flavonoid compounds identified between samples. However, unlike *AmGSTF1*-expressors, *ZmGSTF1*-expressors did not accumulate more of the major flavonoid compound present in all samples. *ZmGSTF1*-expressors instead displayed a small decrease in the accumulation of the major flavonoid present (Figure 52 and Table 23).

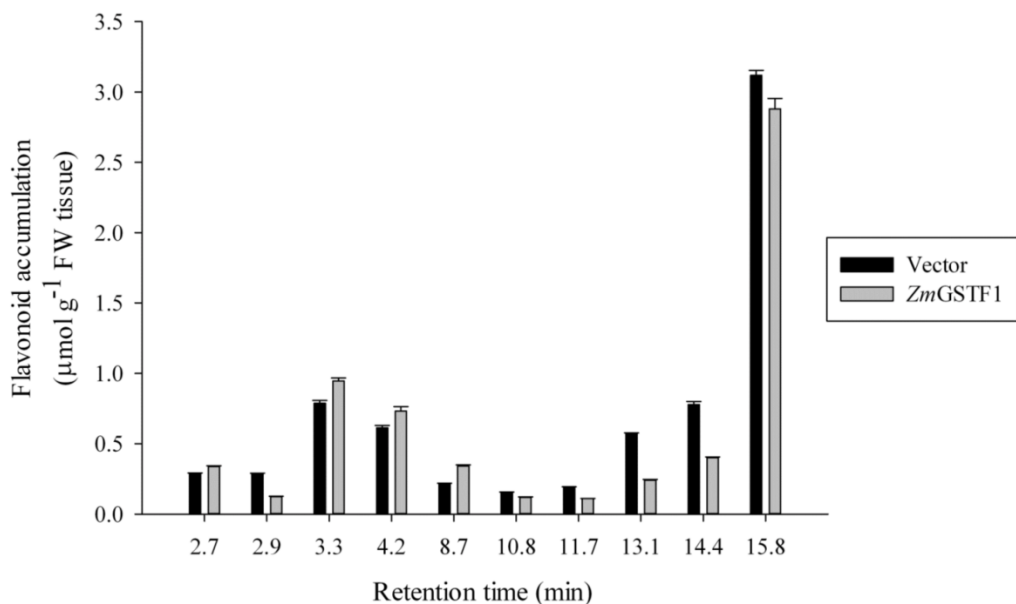


Figure 52: Flavonoid profile of transgenic *Arabidopsis* plants expressing *ZmGSTF1* or vector only. Acidified methanolic extracts of the following transgenic lines: *ZmGSTF1* 10-17 and vector 22-24, were separated using high performance liquid chromatography and visualised at 287 nm. Profiles were normalised to an internal kaempferol standard with the standard used to quantify flavonoid concentrations. Quantified peaks are shown as a function of chromatographic retention time (min). All measurements were performed in technical triplicate and are shown \pm SEM, n = 3. FW – fresh weight.

Table 23: Quantification of the major flavonoid that accumulated in transgenic *Arabidopsis* plants expressing *ZmGSTF1* or vector only. Flavonoid accumulation was calculated relative to an internal kaempferol standard. RT – chromatographic retention time. The quantified metabolite is shown \pm SEM, n = 3. FW – fresh weight.

Metabolite	RT (min)	Transgenic line	
		Vector	<i>ZmGSTF1</i>
Major flavonoid	15.8	3.12 ± 0.04	2.88 ± 0.08

5.4.5 Isolation of *ZmGSTF1* from transgenic *Arabidopsis* plants

ZmGSTF1 increased the activities of endogenous detoxification enzymes. It is not clear how *ZmGSTF1* performs this function. The observed increases are very similar to those observed in *AmGSTF1*-expressors, which do not induce increases in endogenous enzyme activities by perturbing gene expression. It remains to be determined if *ZmGSTF1* perturbs gene expression in transgenic *Arabidopsis* plants. However, at this preliminary stage, it is possible that these increases in endogenous enzyme activities could be due to a direct interaction with *ZmGSTF1* or by an

effector protein that interacts with *ZmGSTF1*. In an analogous manner to that used with *AmGSTF1*-, C120V- and S12A-expressors, *ZmGSTF1* was purified from transgenic *Arabidopsis* plants in an attempt to isolate potential protein binding-partners.

Soluble protein extracts of the highest *ZmGSTF1*-expressing line (*ZmGSTF1* 10-17) and vector only (vector 22-24) plants were prepared by homogenising approximately 1 g frozen tissue in aqueous buffer and discarding the solid cellular debris. Samples were then passed over *Strep*-tactin resin and the resin washed extensively with buffer. Retained proteins were eluted using desthiobiotin to competitively displace *Strep*-tagged components from the resin. Eluted samples were concentrated using size-exclusion chromatography and protein components separated using SDS-PAGE. Using this methodology, *ZmGSTF1* was barely detected using sensitive silver nitrate staining or Western blotting (Figure 53). Two additional proteins were also detected. However, these were also present in the vector sample and appear to be non-specific contaminants (Figure 53A).

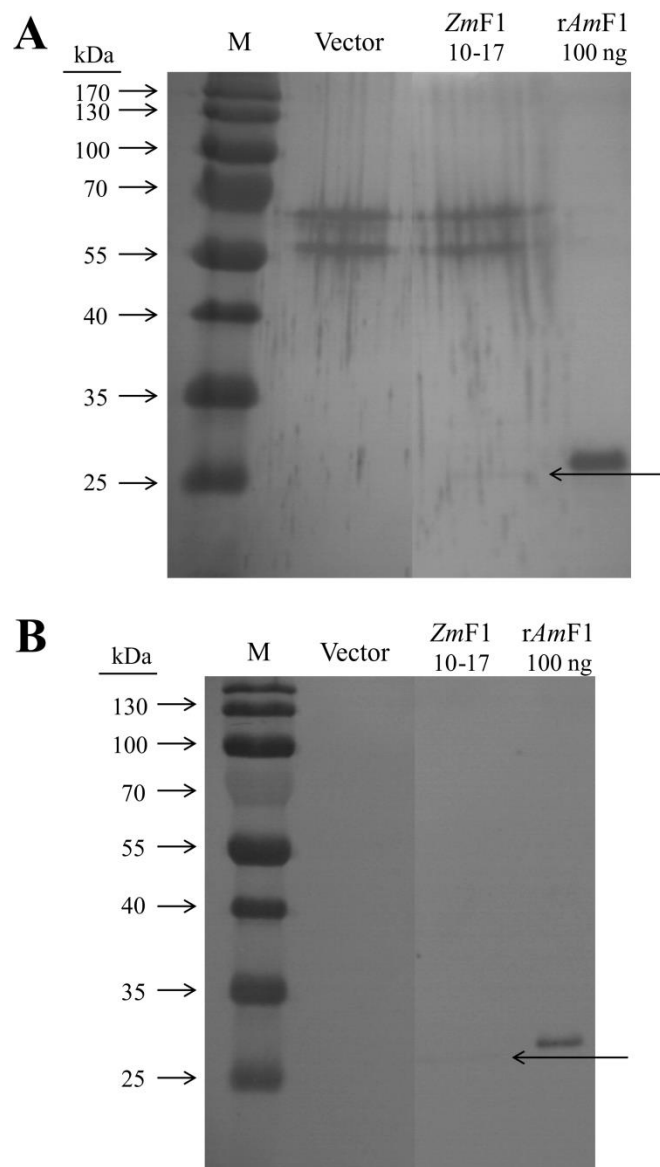


Figure 53: Isolation of Strep II tagged GSTs from transgenic Arabidopsis lines. Strep II tagged GSTs were isolated from soluble protein extracts of the following transgenic lines: ZmGSTF1 10-17 and vector 22-24, using Strep-tactin affinity chromatography. Proteins were detected by (A) staining with silver nitrate or (B) Western blotting with an antiserum raised against the maize ZmGSTF1-2 heterodimer. ZmGSTF1 is indicated (black arrow). Recombinant AmGSTF1 (rAmF1) was stained as a positive control. M – protein markers. Molecular weights (kDa) of protein markers are shown.

5.5 Discussion and future work

Studies with *ZmGSTF1*-expressing *Arabidopsis* plants demonstrate that *ZmGSTF1* can elicit MHR in a heterologous host plant (Figure 50 and Figure 51). By using a herbicide which cannot be detoxified directly by GSTs, it is now clear that *ZmGSTF1* catalytic activity is not absolutely essential to elicit resistance. The resistant phenotype correlated with increased activities of endogenous detoxification enzymes (Table 22), as seen with *AmGSTF1*-expressors. However, unlike *AmGSTF1*, *ZmGSTF1* can also directly detoxify a subset of herbicides, including alachlor, using GSH (Dixon *et al.*, 1997). Therefore, it is reasonable to assume that *ZmGSTF1* may elicit resistance to some herbicides, detoxified using GSH, using both catalytic and non-catalytic mechanisms. Herbicide metabolism studies were not performed during the present studies and are required to determine if the relative rates of chlorotoluron and alachlor detoxification are increased in *ZmGSTF1*-expressors relative to vector control plants. *AmGSTF1* is known to induce increases in the activities of endogenous GSTs capable of detoxifying alachlor using GSH (Dr. I. Cummins and Prof. R. Edwards, unpublished work at the start of this project). Subsequently, herbicide metabolism studies alone would not be unequivocal in establishing the requirement for *ZmGSTF1* to elicit resistance to alachlor by direct detoxification with GSH. To fully understand the requirement for *ZmGSTF1* catalysis to promote resistance to alachlor, a catalytically-retarded *ZmGSTF1* mutant should be transgenically expressed in *Arabidopsis* with the phenotype and relative rate of alachlor detoxification determined.

With that being said, these studies do show that, whilst being only 63 % identical in amino acid sequence, *AmGSTF1* and *ZmGSTF1* both elicit MHR in a heterologous host plant (Figure 41, Figure 42, Figure 50 and Figure 51) and elicit similar changes in endogenous detoxification enzymes (Table 16 and Table 22). Fundamentally, this means that multiple grass species have independently evolved to constitutively express GSTF1 orthologues that can enhance components of the xenome and increase resistance to xenobiotic toxins. This would strongly suggest that other close orthologues, for example *LrGSTF1*, would also possess the same functional properties to induce MHR. This is supported using *in vitro* studies with *LrGSTF1*. The *in vitro* studies show that *LrGSTF1* displays a very similar substrate profile

compared to *AmGSTF1* (Table 19) and displays very similar sensitivities to inhibitory compounds (Figure 48).

Unlike *AmGSTF1*, *ZmGSTF1* did not induce the accumulation of flavonoids. This would suggest that this is not essential for an MHR phenotype. Instead, this may be a function specific to *AmGSTF1*.

Also, *ZmGSTF1*-expressors had similar increases in endogenous detoxification enzyme activities as those detected with *AmGSTF1*-expressors but were clearly far more tolerant to herbicide treatment (Figure 50 and Figure 41). Whilst discussed separately, all transgenic *Arabidopsis* lines were grown, treated and maintained under identical conditions and so the results of spray trials with *AmGSTF1*-expressors and *ZmGSTF1*-expressors can be directly compared. Therefore, *ZmGSTF1* must induce additional changes in *Arabidopsis* that contribute to the MHR phenotype that were not detected in these studies. In relation to additional undetected changes, when *ZmGSTF1*-expressor lines were maintained in growth chambers for an extended period of time following treatment with formulation alone, these lines displayed an early bolting and flowering phenotype that was not seen with vector only plants or *AmGSTF1*-expressors (Figure 54).

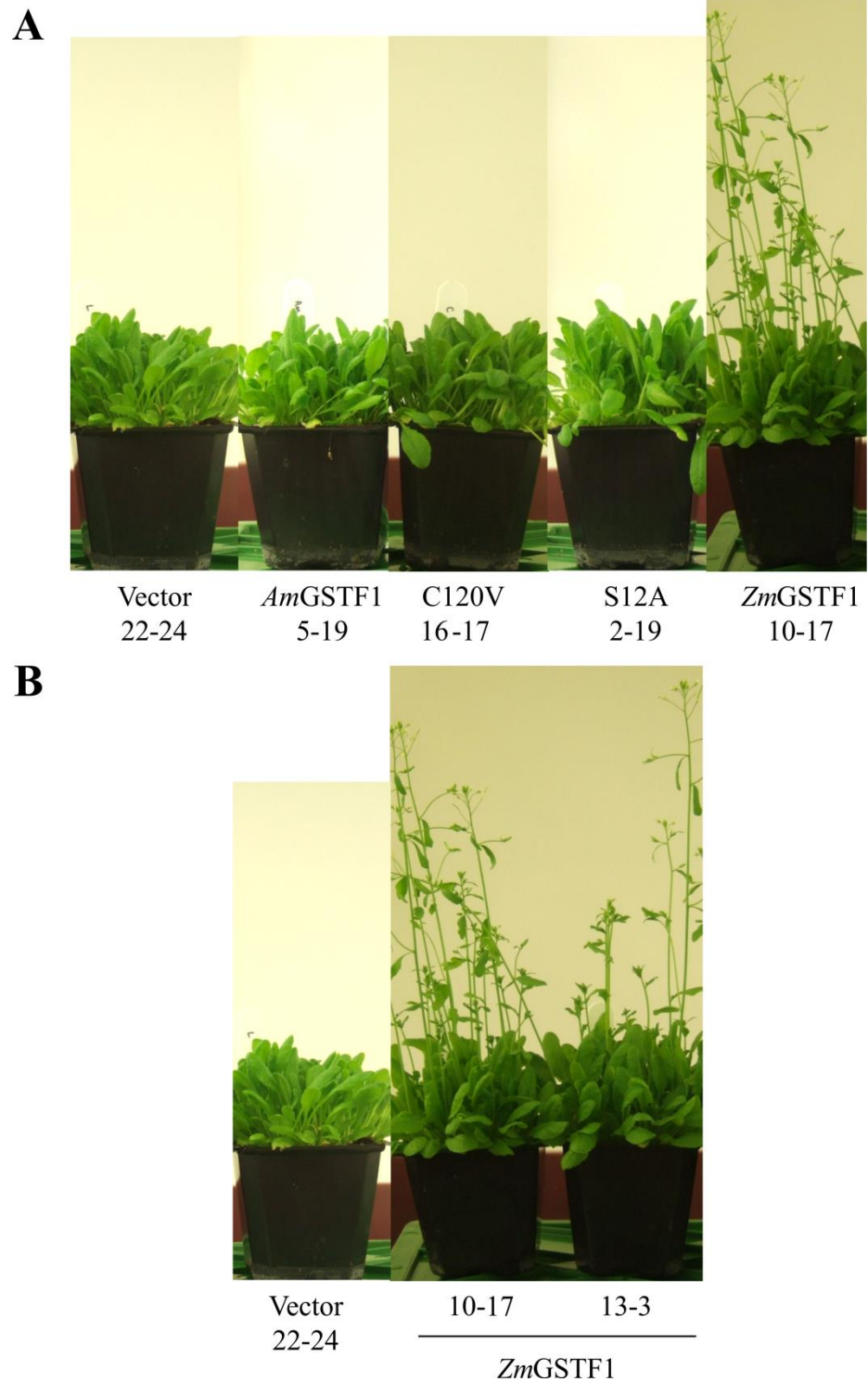


Figure 54: Early bolting phenotype of *ZmGSTF1*-expressors relative to other GST constructs and vector-only control plants. (A) *ZmGSTF1*-expressors displayed an early bolting phenotype that was not seen with other GST-expressing lines or vector-only control plants. (B) The phenotype was confirmed in two independent *ZmGSTF1*-expressing lines. Seeds of each independent line of each construct were sown on soil (30 per pot) and maintained in environmental growth chambers for 14 days followed by an application of formulation only (0.1 % biopower, 1 % acetone). Plants were maintained in environmental growth chambers for a further 14 days and then photographed. Numbers below vector and enzyme names (e.g. *AmGSTF1* 5-19) denote unique identification numbers of each independent T₂ line.

Clearly, *ZmGSTF1* expression elicits multiple biochemical changes in *Arabidopsis* plants, and based on the MHR phenotype induced, it would appear that not all were detected in these studies. Whilst specific GSTs are known to play a regulatory role regarding the accumulation and/or protection of reactive secondary metabolites *in planta* (Martinoia *et al.*, 1993; Dixon *et al.*, 2008; Dixon and Edwards, 2009; Dixon *et al.*, 2011), the effects of *ZmGSTF1* on bolting suggests this protein is directly affecting plant development. In maize plants, *ZmGSTF1* expression contributes approximately 1 % of the total soluble leaf protein (Mozer *et al.*, 1983) although it is unknown why the enzyme is so highly expressed. The studies presented here would now suggest that perhaps *ZmGSTF1* expression grants plants a competitive advantage by inducing faster growth and reproduction as well as enhanced resistance to exogenous toxins. One possibility for stimulation of plant growth would be interactions between *ZmGSTF1* and plant growth hormones. Studies with recombinant *ZmGSTF1* have suggested a direct interaction between the enzyme and the plant growth hormone gibberellic acid (Axarli *et al.*, 2004). Studies found that the rate of irreversible inhibition of the enzyme, due to covalent binding with an artificial dye, was significantly slower when in the presence of gibberellic acid and proposed this was due to competition for binding to the enzyme (Axarli *et al.*, 2004).

Fusion of the *ZmGSTF1* protein with an *N*-terminal Strep II tag was purposefully designed to facilitate the isolation of *ZmGSTF1* from transgenic plants in an attempt to identify any possible binding-partners. Preliminary studies to identify protein binding-partners were unsuccessful due to the low recovery of *ZmGSTF1* (Figure 53). These experiments are worth repeating with increased tissue mass and resin volumes. Additionally, two-dimensional gel electrophoresis of the total protein complements of *ZmGSTF1*-expressors, alongside *AmGSTF1*-expressors and vector control plants, would be a valuable tool to identify differential protein expression/modification. Analysis of the transcriptomes of *ZmGSTF1*-expressors should also be pursued. Whilst *AmGSTF1* does not elicit changes in gene expression, *ZmGSTF1* clearly perturbs additional pathways *in planta* that *AmGSTF1* does not interact with, as demonstrated by the changes in *ZmGSTF1*-expressor plant growth and life-cycle (Figure 54).

Chapter 6 – Final Discussion

Plant GSTs and herbicide resistance have intrinsically been associated, with GSTs first being discovered in plants over 40 years ago because of their ability to detoxify a subset of herbicides via conjugation with GSH (Frear and Swanson, 1970; Shimabukuro *et al.*, 1971). Since that time, a plethora of GSTs of the phi (F) and tau (U) classes from a variety of crop plants including maize, soybean and wheat, have been identified, characterised and shown to be able to detoxify a subset of herbicide chemistries via conjugation with GSH (Andrews *et al.*, 1997; Dixon *et al.*, 1997; Cummins *et al.*, 1997a; Sommer and Boger, 1999; Cummins *et al.*, 2003; Andrews *et al.*, 2005). Some of these GSTs can also function as GPOXs and use GSH as a co-factor to reduce toxic hydroperoxide species, that can accumulate following herbicide treatment (Kunert *et al.*, 1985), to the hydroxylated derivatives (Sommer and Boger, 1999; Cummins *et al.*, 2003; Andrews *et al.*, 2005). Hence, GSTs in crops can directly detoxify herbicides and also detoxify reactive oxygenated species formed as a downstream consequence of herbicide treatment.

It is therefore not surprising that populations of weed species, which compete with the aforementioned crops, have evolved herbicide resistance by enhancing the expression and/or activities of herbicide-detoxifying GSTs. Enhanced herbicide metabolism via GST-catalysed GSH-conjugation was first discovered in atrazine-resistant velvetleaf (Anderson and Gronwald, 1991) and has since been reported in another 4 weed species, including black-grass. (Hall *et al.*, 1997; Cummins *et al.*, 1997b; Fraga and Tasende, 2003; Bakkali *et al.*, 2007). Some GST isoforms, isolated from herbicide resistant black-grass, could also function as GPOX enzymes and detoxify toxic hydroperoxide species (Cummins *et al.*, 1999).

Unpublished work in the Edwards laboratory demonstrated that *AmGSTF1*, a GST constitutively-expressed in MHR black-grass, that cannot detoxify herbicides but is an active GPOX enzyme, elicited MHR in transgenic *Arabidopsis* plants. Unexpectedly, *AmGSTF1* also induced increases in the activities of endogenous detoxification enzymes, including enzymes that could detoxify herbicides using GSH, and caused flavonoids to be accumulated (Dr. I. Cummins and Prof. R. Edwards, unpublished work at the start of this project). These biochemical changes

closely mirrored those induced in MHR black-grass (Cummins *et al.*, 2009). Therefore, *AmGSTF1* appears to be a key component of MHR.

The studies presented in this thesis were driven by the question: ‘What is the molecular mechanism/s by which *AmGSTF1* elicits these changes in a transgenic host plant?’

By first analysing the transcriptome of *AmGSTF1*-expressing *Arabidopsis* plants, it was determined that the enzyme did not elicit these changes by perturbing gene expression (see section 3.3). Hence, *AmGSTF1* must elicit these changes post-transcriptionally. Furthermore, it was not clear if MHR was a product of *AmGSTF1* GPOX activity, or of increases in endogenous detoxification enzyme activities, or a product of both mechanisms.

To interrogate the requirement of *AmGSTF1*-catalysed GPOX activity for an MHR phenotype, a point mutant, S12A, was generated that was severely catalytically retarded (Table 8). Expression of this mutant in transgenic *Arabidopsis* plants still granted the host plants an MHR phenotype (Figure 41). S12A also induced increases in endogenous detoxification enzymes, including GPOX enzymes (Table 16). The enhancement of herbicide tolerance and increases in detoxification enzyme activities were highly similar to transgenic plants expressing *AmGSTF1* (Figure 41 and Table 16). Hence, catalytic activity of *AmGSTF1* is not required to elicit MHR. This is the first demonstration that a GST from any plant species can elicit herbicide resistance independently of catalysis. By increasing the activities of multiple endogenous detoxification enzymes, it seems unlikely that *AmGSTF1* would directly interact with each one independently. It is more plausible that *AmGSTF1* most likely binds effector proteins or small molecules. Preliminary attempts to isolate a protein binding-partner were unsuccessful (Figure 44) but do require further study. An alternative approach may be to employ yeast two-hybrid screening with *AmGSTF1* as bait protein and a library of *Arabidopsis* and black-grass prey proteins.

A second point mutant, C120V, for which the residue Cys120 was replaced with a valine residue, was used to interrogate the interaction of *AmGSTF1* with inhibitory compounds. Before the work described in this thesis, it was known that Cys120

could be alkylated by NBD-Cl, correlating with inhibition of *AmGSTF1*. Furthermore, NBD-Cl restored sensitivity to herbicides in MHR black-grass (Dr. I. Cummins and Prof. R. Edwards, unpublished work at the start of this project). IC₅₀ determinations demonstrated that NBD-Cl was a relatively strong inhibitor of *AmGSTF1* (Figure 28). Using C120V, alkylation of *AmGSTF1* was shown to be the principal mechanism of inhibition (Figure 28). Furthermore, *AmGSTF1* was selectively alkylated on Cys120 (Table 10). Alkylation of Cys120 with a different thiol alkylating agent did not inhibit the enzyme (Figure 32 and Table 13), indicating that NBD-Cl most likely induces a conformational change of *AmGSTF1* structure following binding. With Cys120 playing a key role in the interaction of *AmGSTF1* with NBD-Cl, this suggested Cys120 may play a key role in eliciting an MHR phenotype. However, expression of C120V in transgenic *Arabidopsis* plants demonstrated that Cys120 is not required to elicit MHR (Figure 41 and Figure 42). Rather, C120V-expressors demonstrated similar increases in resistance to multiple herbicides and in endogenous detoxification enzyme activities as those found in *AmGSTF1*- and S12A-expressors (Table 16).

Hence, *AmGSTF1* elicits MHR independently of catalysis and of Cys120. Cys120 does however play a key role in the interaction of the enzyme with reactive electrophiles. It may be possible that Cys120 is required to bind reactive electrophiles *in planta* and to transport these to compounds to subcellular compartments for further processing, although this remains to be determined. Importantly, from a commercial perspective, studies with C120V indicate that evolution of this single point mutation would abolish any significant interaction between *AmGSTF1* and NBD-Cl whilst preserving an MHR phenotype. Subsequently, if NBD-Cl derivatives were developed as synergists in the field they would require careful management practices.

Interestingly, these studies highlighted several functional parallels with GSTP1, an evolutionarily distinct GST that is overexpressed in multi-drug resistant (MDR) human cancers. GSTP1 can; (i) directly detoxify chemotherapeutic drugs, such as ethacrynic acid, using GSH (Ploemen *et al.*, 1994), (ii) interact with and be inhibited by xenobiotics, including NBD-Cl, via binding to Cys47 (Ricci *et al.*, 2003), (iii) regulate the activity of a glutathione peroxidase enzyme via direct physical

interactions (Zhou *et al.*, 2013). With regards to Cys47, this residue plays a key role in regulating GSTP1 activity by transmitting conformational signals across the GST dimer when inhibited by NBD-Cl (Ricci *et al.*, 2003). Results with *AmGSTF1* suggest that a similar mechanism may be in operation (Figure 29). Hence, where GSTs were once thought to be a downstream effector protein of an organised stress response, studies with *AmGSTF1* and GSTP1 implicate that specific GSTs play a far more central role in co-ordinating the response. Significantly, the evolutionary divergence of these two GSTs demonstrates that stress regulation co-ordinated by GSTs extends across multiple organism kingdoms. Due to the large functional overlap between *AmGSTF1* and GSTP1, it would be interesting to determine if GSTP1 could also induce herbicide resistance in a transgenic host plant and by what mechanism.

Having established the central role of *AmGSTF1* in co-ordinating MHR in a heterologous host plant, it was of interest to determine the role of orthologues in other grass species. Firstly, *LrGSTF1* (91 % amino acid identity), isolated from MHR annual rye-grass, was characterised *in vitro* and found to be near-identical to *AmGSTF1* in catalytic function and interactions with inhibitors (Table 19 and Figure 48). Whilst the ability of *LrGSTF1* to elicit MHR in a heterologous host plant was not determined in these studies, the *in vitro* results strongly suggest that *LrGSTF1* would play a very similar functional role to *AmGSTF1* in eliciting MHR. Hence, GSTF1-induced MHR appears to have evolved in multiple weed species from geographically discrete locations. Furthermore, studies with an *AmGSTF1* orthologue from maize, *ZmGSTF1* (63 % amino acid identity), demonstrated that a GSTF1 orthologue from a crop also induced MHR. To date, *ZmGSTF1*-mediated herbicide resistance has been believed to be due to its ability to detoxify a subset of herbicide chemistries using GSH. However, the current studies found that *ZmGSTF1* induced a highly resistant phenotype toward a herbicide that cannot be detoxified using GSH (Figure 50). Instead, *ZmGSTF1* induced increases in endogenous antioxidant activities (Table 22), as seen with *AmGSTF1*-expressors. *ZmGSTF1* had very little detectable GPOX activity and possessed a valine residue at position 120 (Table 19 and Figure 45). Hence, studies with *ZmGSTF1* support the findings with *AmGSTF1* that GPOX activity of the transgene and Cys120 are not essential for an MHR phenotype. As *ZmGSTF1* shares only 63 % amino acid identity with

AmGSTF1 and yet still induces an MHR phenotype, this lends further support to the hypothesis that *LrGSTF1* would also induce MHR in a heterologous host plant. Unlike *AmGSTF1*, *ZmGSTF1* induced additional changes in transgenic host plants including an early bolting and flowering phenotype. The mechanism by which *ZmGSTF1* elicited these changes still remains to be determined and the transcriptome of *ZmGSTF1*-expressing *Arabidopsis* plants should be analysed. The phenotype was not an artefact of transgene insertion and has very recently been described for *Arabidopsis* plants genetically modified to express a lambda-class GST from rice, *OsGSTL2* (Kumar *et al.*, 2013). *ZmGSTF1* is highly expressed in domesticated maize plants (1 % total soluble leaf protein) (Mozer *et al.*, 1983) and it is interesting to consider that expression of *ZmGSTF1* may have granted a selective advantage for individuals during domestication by enhancing tolerance to exogenous toxins and accelerating plant growth and reproduction. Other crop species, including barley, wheat and rice, also possess GSTF1 orthologues (Wu *et al.*, 1999; Scalla and Roulet, 2002; Theodoulou *et al.*, 2003) (Figure 55).

		Amino acid identity with AmGSTF1 (%)
AmGSTF1	MAPVKVFGPAMSTINVARVTLCLLEEVGAEEYVVNI DENTMEHKSPPEHLARNPFGQI PAFQD	60
LrGSTF1	MAPVKVFGPAMSTINVARVLVFLLEVGADYEVVDMDFKVMEHKSPPEHLARNPFGQI PAFQD	60
HvGST6	MAPVKVFGPAMSTINVARVLVCLLEEVGAEEYVVDI DFKAMEHKSPPEHLVRNPFGQI PAFQD	60
TaGST19E50	MAPVKVFGPAMSTINVARVLVCLLEEVGAEEYVVDI DFKAMEHKSPPEHLVRNPFGQI PAFQD	60
OsGSTF1	MTPVKVFGPQSTINVARVLLCLLEEVGAEEYVVNDFTVMEMHKSPPEHLKRNPFGQI PAFQD	60
ZmGSTF1	MAPMKLYGA[MSWNLRCATALEEAGSDYEIVPINPATAEHKSPEHLVRNPFGQVPAQD	60
	*: *: *: * . * *: * . * *: *: * . * *: * *: * *: * *: *	63
AmGSTF1	GDLLLWESRAISKYVLRKYKTDEV DLLRESNLLEAAMVDWVTEVDAHTYNPALSPIVYQC	120
LrGSTF1	GDLLLWESRAISKYVLRKYKTGEV DLLREGNLKEAAMVDWVTEVDAHTYNPALSPIVYQC	120
HvGST6	GDLLLWESRAISKYVLRKYKTGEV DLLREGNLKEAAMVDWVTEVDAHTYNPALSPIVYEC	120
TaGST19E50	GDLLLWESRAISKYVLRKYKTNGVDLLREGDLKEAAMVDWVTEVDAHTYNPAISPIVYEC	120
OsGSTF1	GDLYLFESRAIGKYILRKYKTREADLLREGNLREAAMVDWVTEVETHQYNSAISPIVYEC	120
ZmGSTF1	GDLYLFESRAICKYAAARKNK---PELLREGNLLEAAMVDWVIEVEANQYTAALNPILEQV	117
	*: *: *: * . * *: * . * *: *: * . * *: *: *: *	
AmGSTF1	LFNPFMGRGLPTDEKVVAESLEKLKKVLEVYEARLSKHSYLAGDFVSFADLNHF PYTFYFM	180
LrGSTF1	LFNPFMGRGLPTDEKVVAESLEKLKKVLEVYEARLSQHEYLAGDFVSFADLNHF PYTFYFM	180
HvGST6	LIINPLMRGLPTNQTVVDESLEKLKKVLEVYEARLSQHQYLAGDFVSFADLNHF PYTFYFM	180
TaGST19E50	LIINPLMRGLPTNQTVVDESLEKLKKVLEVYEARLSRHEYLAGDFVSFADLNHF PYTFYFM	180
OsGSTF1	IINPAMRGITPTNQKVVDESAEKLKKVLEVYEARLSQSTYLAGDFVSFADLNHF PYTFYFM	180
ZmGSTF1	LIISHLIGG-TTDQKVVDENLEKLKKVLEVYEARLTCKYLAGDFLSADLNHVSVTLCF	176
	: : * : * . * : * . * *: *: *: *: *: *: * . *: :	
AmGSTF1	ATPAHALFDSDYPHVKAwwDRIMARPAPVKKIAATMVPPKA	219
LrGSTF1	ATPAHALFGSYPHVKAwwERIMARPAPIKKISATMVPPKA	219
HvGST6	ATPAHALFDSDYPHVKAwwESLMARPAIKKLAQMVPKKP	219
TaGST19E50	ATPAHALFDSDYPHVKAwwERIMARPAPVKKLAQMVPKKP	219
OsGSTF1	GTPYASLFDSDYPHVKAwwERIMARPSVKKLAAMAPQGA	219
ZmGSTF1	ATPYASVLDAYPHVKAwwSGLMERPSVQKVAAIMKPSA-	214
	*: *: *: : *: *: *: *: *: *: *: *: *: *	

Figure 55: Multiple sequence alignment of AmGSTF1 and orthologues. AmGSTF1 orthologues were identified by BLAST searching (NCBI database) using AmGSTF1 protein sequence as a query. Orthologues were identified from annual rye-grass (*LrGSTF1*; accession M5BPX4), barley (*HvGST6*; accession AF430069), wheat (*TaGST19E50*; accession AY64481), rice (*OsGSTF1*; accession OsO1g0371200) and maize (*ZmGSTF1*; accession NP_001105412). Sequences were aligned using Clustal Omega (1.1.0) (EBI web servers). Amino acid identity with AmGSTF1 is shown for each orthologue. Active site residues based on the *ZmGSTF1* crystal structure are boxed. * indicate identical amino acid residues whilst : and . indicate residues with similar chemical properties.

The barley orthologue protein, *HvGST6*, has been functionally characterised *in vitro* and behaved as both a GST and a GPOX (Scalla and Roulet, 2002). The orthologous rice and wheat proteins have not been functionally characterised. All three orthologues are induced by herbicide safener treatment, chemicals that enhance herbicide resistance in cereal crops (Wu *et al.*, 1999; Scalla and Roulet, 2002; Theodoulou *et al.*, 2003). Hence, a link may exist between GSTF1 expression and crop domestication. Very recently, a further putative GSTF1 orthologue has been identified in the draft genome of the bread wheat progenitor species *Triticum urartu* (88 % amino acid sequence identity with AmGSTF1; accession EMS47979). It would be of interest to determine the relative expression levels of the respective GSTF1 enzymes in the progenitor species and the domesticated crop, along with relative levels of herbicide resistance.

AmGSTF1 also induced hyper-accumulation of flavonoids and anthocyanins when first expressed in transgenic Arabidopsis plants (Dr. I. Cummins and Prof. R.

Edwards, unpublished work at the start of this project). Due to their known antioxidant properties, it was proposed that this accumulation may play a role in eliciting MHR. However, the current studies detected the accumulation of only one flavonoid compound in *AmGSTF1*-, C120V- and S12A-expressors, whilst *ZmGSTF1*-expressors did not accumulate flavonoids but still displayed an MHR phenotype. Therefore, the current results cast doubt on the necessity of flavonoid accumulation for an MHR phenotype. Flavonoids do however promote resistance to stresses such as UV irradiation (Winkel-Shirley, 2002). It would be interesting to expose the transgenic constructs to UV irradiation and determine if the accumulated flavonoids in *AmGSTF1*-expressors provide any extra measure of protection.

To conclude, the exact mechanism/s by which *AmGSTF1* and orthologous proteins elicit MHR remains unknown. However, the studies in this thesis have established that the mechanism operates independently of catalysis. Instead, the MHR phenotype appears closely related to a co-ordinated increase in endogenous detoxification enzyme activities. The identification of GSTF1 orthologues in other weed and crop species demonstrates that GSTF1-mediated MHR may be a powerful adaptation that has independently evolved in multiple species. Furthermore, GST-mediated MHR has close functional parallels with GST-mediated MDR and highlights a far more integral role for GSTs in co-ordinating stress responses than has previously been considered. These studies have raised many more interesting questions regarding the role of GSTF proteins in MHR and offer exciting new avenues of study for plant GST biochemistry.

List of abbreviations and symbols

4-HPPD	4-hydroxyphenylpyruvate dioxygenase
6-BP	6-bromopurine
6-CP	6-chloropurine
6-MP	6-mercaptopurine
A	Absorbance
ABC	Adenosine triphosphate-binding cassette
ACCase	Acetyl-coA carboxylase
AHAS	Acetohydroxy acid synthase
ai	Active ingredient
ALS	Acetolactate synthase
<i>Am</i>	<i>Alopecurus myosuroides</i>
AOPP	Aryloxyphenoxypropionate
<i>At</i>	<i>Arabidopsis thaliana</i>
AT	Auxin transport
ATP	Adenosine triphosphate
BITC	Benzyl isothiocyanate

c	Concentration
C120V	<i>AmGSTF1</i> point mutant with a valine residue at position 120
CamV 35S	Cauliflower mosaic virus 35S promoter
CDF	Clodinafop-propargyl
cDNA	Complementary deoxyribonucleic acid
CDNB	1-chloro-2,4-dinitrobenzene
CDS	Cloned deoxyribonucleic acid sequence
CHL	Chlorotoluron
cm	Centimetre
CT	Carboxyltransferase
CuOOH	Cumene hydroperoxide
CYP	Cytochrome P450 mixed-function oxidase
Da	Dalton
DHPS	Dihydropteroate synthase
DMSO	Dimethyl sulfoxide
dNTP	Deoxyribonucleotide triphosphate
DTB	Desthiobiotin
DTT	Dithiothreitol

EDTA	Ethylenediaminetetraacetic acid
EPSPS	5-enolpyruvylshikimate-3-phosphate synthase
ESI-MS	Electrospray ionisation mass spectrometry
EST	Expressed sequence tag
EtOH	Ethanol
FLU	Fluorodifen
Form	Formulation
FW	Fresh weight
FXP	Fenoxaprop-p-ethyl
g	Gram or relative centrifugal force (context specific)
Gm	<i>Glycine max</i>
GPOX	Glutathione peroxidase
GR	Glutathione reductase
GS	Glutamine synthetase
GSH	Reduced glutathione
GSSG	Oxidised glutathione
GST	Glutathione transferase
GSTF	Phi-class glutathione transferase

GSTP	Pi-class glutathione transferase
GSTU	Tau-class glutathione transferase
GT	Glycosyl transferase
HABA	2-(4-hydroxyphenylazo)benzoic acid
HCl	Hydrochloric acid
HED	2-hydroxyethyl disulfide
hmGSH	Hydroxymethylglutathione
homoGSH	Homoglutathione
HPLC	High performance liquid chromatography
hr	Hour
HRAC	Herbicide resistance action committee
H ⁺	Proton
I	Iodoacetamide
IC ₅₀	Half maximal inhibitory concentration of a compound
IPTG	Isopropyl β-D-1-thiogalactopyranoside
kb	Kilobase
k _{cat}	Enzymatic reaction turnover constant
k _{cat} / K _M	Enzyme catalytic efficiency constant

kDa	Kilodalton
K_M	Michaelis constant
kV	Kilovolt
l	Path length of light
L	Litre
LB	Luria-Bertani broth
LC	Lycopene cyclase
LinOOH	Linoleic acid hydroperoxide
<i>Lr</i>	<i>Lolium rigidum</i>
LS	Lipid synthesis
m	Metre
M	Molar
MA	Microtubule assembly
MD	Membrane disruption
MeOH	Methanol
mg	Milligram
MHR	Multiple herbicide resistance
min	Minute

mL	Millilitre
mm	Millimetre
mM	Millimolar
MP	Microtubule polymerisation
mRNA	Messenger ribonucleic acid
ms	Millisecond
m / z	Mass to charge ratio
MΩ	Megohm
n	Number of replicates
NA	Not assayed
NADP ⁺	Oxidised nicotinamide adenine dinucleotide phosphate
NADPH	Reduced nicotinamide adenine dinucleotide phosphate
NBD-Cl	4-chloro-7-nitro-benzoxadiazole
NBDHEX	6-(7-nitro-1,2,3-benzoxadiazol-4-ylthio)hexanol
NBD-SG	Nitrobenzoxadiazole-glutathione conjugate
ND	Not detected
NDA-6-CP	3,3-deazonitro-6-chloropurine
NEM	<i>N</i> -ethylmaleimide

NGS	Next generation sequencing
nm	Nanometre
nM	Nanomolar
nmol	Nanomole
NPA	4-nitrophenyl acetate
nt	Nucleotide base-pair length
NTSR	Non-target-site resistance
PAGE	Polyacrylamide gel electrophoresis
PARA	Paraquat
PCR	Polymerase chain reaction
PDS	Phytoene desaturase
pK _a	Logarithmic acid dissociation constant
pmol	Picomole
PPO	Protoporphyrinogen oxidase
PS	Photosystem
psi	Pressure per square inch
PVDF	Polyvinylidene difluoride
PVPP	Polyvinylpolypyrollidone

RACE	Rapid amplification from complementary deoxyribonucleic acid ends
RNA	Ribonucleic acid
rpm	Revolutions per minute
s	Second
S12A	<i>AmGSTF1</i> point mutant with an alanine residue at position 12
SD	Standard deviation
SDS	Sodium dodecyl sulfate
SEM	Standard error of the mean
T-DNA	Transferred deoxyribonucleic acid
TEMED	Tetramethylethylenediamine
tRNA	Transfer ribonucleic acid
TSR	Target-site resistance
U	Unit of enzyme activity
UDP	Uridine diphosphate
UV-vis	Ultraviolet-visible
V	Volt
v / v	Volume to volume

VLCFAS	Very-long-chain fatty-acid synthesis
V_{\max}	Maximal velocity
w / v	Weight to volume
WTS	Wild-type sensitive
Zm	<i>Zea mays</i>
χ^2	Chi-squared
°C	Degrees celsius
μE	Microeinsteins
μF	Microfarad
μg	Microgram
μL	Microlitre
μmol	Micromole
μM	Micromolar
μm	Micron
ϵ	Molar extinction coefficient

References

- Adler, V., Yin, Z. M., Fuchs, S. Y., Benezra, M., Rosario, L., Tew, K. D., Pincus, M. R., Sardana, M., Henderson, C. J., Wolf, C. R., Davis, R. J. and Ronai, Z. (1999). Regulation of JNK signaling by GSTp. *EMBO Journal* **18**: 1321-1334.
- Ahmad-Hamdani, M. S., Yu, Q., Han, H. P., Cawthray, G. R., Wang, S. F. and Powles, S. B. (2013). Herbicide resistance endowed by enhanced rates of herbicide metabolism in wild oat (*Avena spp.*). *Weed Science* **61**: 55-62.
- Alfenito, M. R., Souer, E., Goodman, C. D., Buell, R., Mol, J., Koes, R. and Walbot, V. (1998). Functional complementation of anthocyanin sequestration in the vacuole by widely divergent glutathione S-transferases. *Plant Cell* **10**: 1135-1149.
- Anderson, M. P. and Gronwald, J. W. (1991). Atrazine resistance in a velvetleaf (*Abutilon theophrasti*) biotype due to enhanced glutathione S-transferase activity. *Plant Physiology* **96**: 104-109.
- Andrews, C. J., Cummins, I., Skipsey, M., Grundy, N. M., Jepson, I., Townson, J. and Edwards, R. (2005). Purification and characterisation of a family of glutathione transferases with roles in herbicide detoxification in soybean (*Glycine max* L.); selective enhancement by herbicides and herbicide safeners. *Pesticide Biochemistry and Physiology* **82**: 205-219.
- Andrews, C. J., Skipsey, M., Townson, J. K., Morris, C., Jepson, I. and Edwards, R. (1997). Glutathione transferase activities toward herbicides used selectively in soybean. *Pesticide Science* **51**: 213-222.
- Armstrong, R. N. (1997). Structure, catalytic mechanism, and evolution of the glutathione transferases. *Chemical Research in Toxicology* **10**: 2-18.
- Awasthi, S., Srivastava, S. K., Ahmad, F., Ahmad, H. and Ansari, G. A. S. (1993). Interactions of glutathione S-transferase pi with ethacrynic acid and its glutathione conjugate. *Biochimica Et Biophysica Acta* **1164**: 173-178.

Axarli, I., Dhavala, P., Papageorgiou, A. C. and Labrou, N. E. (2009a). Crystal structure of *Glycine max* glutathione transferase in complex with glutathione: investigation of the mechanism operating by the tau class glutathione transferases. *Biochemical Journal* **422**: 247-256.

Axarli, I., Dhavala, P., Papageorgiou, A. C. and Labrou, N. E. (2009b). Crystallographic and functional characterization of the fluorodifen-inducible glutathione transferase from *Glycine max* reveals an active site topography suited for diphenylether herbicides and a novel L-site. *Journal of Molecular Biology* **385**: 984-1002.

Axarli, I. A., Rigden, D. J. and Labrou, N. E. (2004). Characterization of the ligandin site of maize glutathione S-transferase I. *Biochemical Journal* **382**: 885-893.

Bailly, G. C., Dale, R. P., Archer, S. A., Wright, D. J. and Kaundun, S. S. (2012). Role of residual herbicides for the management of multiple herbicide resistance to ACCase and ALS inhibitors in a black-grass population. *Crop Protection* **34**: 96-103.

Bakkali, Y., Ruiz-Santaella, J. P., Osuna, M. D., Wagner, J., Fischer, A. J. and De Prado, R. (2007). Late watergrass (*Echinochloa phyllospadix*): Mechanisms involved in the resistance to fenoxaprop-p-ethyl. *Journal of Agricultural and Food Chemistry* **55**: 4052-4058.

Bartholomew, D. M., Van Dyk, D. E., Lau, S. M. C., O'Keefe, D. P., Rea, P. A. and Viitanen, P. V. (2002). Alternate energy-dependent pathways for the vacuolar uptake of glucose and glutathione conjugates. *Plant Physiology* **130**: 1562-1572.

Benekos, K., Kissoudis, C., Nianioti-Obeidat, I., Labrou, N., Madesis, P., Kalamaki, M., Makris, A. and Tsaftaris, A. (2010). Overexpression of a specific soybean *GmGSTU4* isoenzyme improves diphenyl ether and chloroacetanilide herbicide tolerance of transgenic tobacco plants. *Journal of Biotechnology* **150**: 195-201.

Berhane, K., Widersten, M., Engstrom, A., Kozarich, J. W. and Mannervik, B. (1994). Detoxication of base propenals and other α,β -unsaturated aldehyde products of radical reactions and lipid peroxidation by human glutathione transferases. *Proceedings of the National Academy of Sciences of the United States of America* **91**: 1480-1484.

Bernasconi, P., Woodworth, A. R., Rosen, B. A., Subramanian, M. V. and Siehl, D. L. (1995). A naturally-occurring point mutation confers broad range tolerance to herbicides that target acetolactate synthase. *Journal of Biological Chemistry* **270**: 17381-17385.

Bowles, D., Isayenkova, J., Lim, E. K. and Poppenberger, B. (2005). Glycosyltransferases: managers of small molecules. *Current Opinion in Plant Biology* **8**: 254-263.

Brazier, M., Cole, D. J. and Edwards, R. (2002). *O*-glucosyltransferase activities toward phenolic natural products and xenobiotics in wheat and herbicide-resistant and herbicide-susceptible black-grass (*Alopecurus myosuroides*). *Phytochemistry* **59**: 149-156.

Brenchley, R., Spannagl, M., Pfeifer, M., Barker, G. L. A., D'Amore, R., Allen, A. M., McKenzie, N., Kramer, M., Kerhornou, A., Bolser, D., Kay, S., Waite, D., Trick, M., Bancroft, I., Gu, Y., Huo, N., Luo, M. C., Sehgal, S., Gill, B., Kianian, S., Anderson, O., Kersey, P., Dvorak, J., McCombie, W. R., Hall, A., Mayer, K. F. X., Edwards, K. J., Bevan, M. W. and Hall, N. (2012). Analysis of the bread wheat genome using whole-genome shotgun sequencing. *Nature* **491**: 705-710.

Bridges, D. C. (1994). Impact of weeds on human endeavors. *Weed Technology* **8**: 392-395.

Caccuri, A. M., Ascenzi, P., Antonini, G., Parker, M. W., Oakley, A. J., Chiessi, E., Nuccetelli, M., Battistoni, A., Bellizia, A. and Ricci, G. (1996). Structural flexibility modulates the activity of human glutathione transferase P1-1 - Influence of a poor

co-substrate on dynamics and kinetics of human glutathione transferase. *Journal of Biological Chemistry* **271**: 16193-16198.

Cho, S. G., Lee, Y. H., Park, H. S., Ryoo, K., Kang, K. W., Park, J., Eom, S. J., Kim, M. J., Chang, T. S., Choi, S. Y., Shim, J., Kim, Y., Dong, M. S., Lee, M. J., Kim, S. G., Ichijo, H. and Choi, E. J. (2001). Glutathione S-transferase mu modulates the stress-activated signals by suppressing apoptosis signal-regulating kinase 1. *Journal of Biological Chemistry* **276**: 12749-12755.

Christopher, J. T., Powles, S. B., Liljegren, D. R. and Holtum, J. A. M. (1991). Cross-resistance to herbicides in annual rye-grass (*Lolium rigidum*). 2. Chlorsulfuron resistance involves a wheat-like detoxification system. *Plant Physiology* **95**: 1036-1043.

Christopher, J. T., Preston, C. and Powles, S. B. (1994). Malathion antagonizes metabolism-based chlorsulfuron resistance in *Lolium rigidum*. *Pesticide Biochemistry and Physiology* **49**: 172-182.

Clough, S. J. and Bent, A. F. (1998). Floral dip: a simplified method for Agrobacterium-mediated transformation of *Arabidopsis thaliana*. *Plant Journal* **16**: 735-743.

Cocker, K. M., Northcroft, D. S., Coleman, J. O. D. and Moss, S. R. (2001). Resistance to ACCase-inhibiting herbicides and isoproturon in UK populations of *Lolium multiflorum*: mechanisms of resistance and implications for control. *Pest Management Science* **57**: 587-597.

Cummins, I., Brazier-Hicks, M., Stobiecki, M., Franski, R. and Edwards, R. (2006). Selective disruption of wheat secondary metabolism by herbicide safeners. *Phytochemistry* **67**: 1722-1730.

Cummins, I., Bryant, D. N. and Edwards, R. (2009). Safener responsiveness and multiple herbicide resistance in the weed black-grass (*Alopecurus myosuroides*). *Plant Biotechnology Journal* **7**: 807-820.

Cummins, I., Cole, D. J. and Edwards, R. (1997a). Purification of multiple glutathione transferases involved in herbicide detoxification from wheat (*Triticum aestivum* L.) treated with the safener fenchlorazole-ethyl. *Pesticide Biochemistry and Physiology* **59**: 35-49.

Cummins, I., Cole, D. J. and Edwards, R. (1999). A role for glutathione transferases functioning as glutathione peroxidases in resistance to multiple herbicides in black-grass. *Plant Journal* **18**: 285-292.

Cummins, I., Dixon, D. P., Freitag-Pohl, S., Skipsey, M. and Edwards, R. (2011). Multiple roles for plant glutathione transferases in xenobiotic detoxification. *Drug Metabolism Reviews* **43**: 266-280.

Cummins, I. and Edwards, R. (2010). The biochemistry of herbicide resistance in weeds. *Outlooks on Pest Management* **21**: 73-77.

Cummins, I., Moss, S., Cole, D. J. and Edwards, R. (1997b). Glutathione transferases in herbicide-resistant and herbicide-susceptible black-grass (*Alopecurus myosuroides*). *Pesticide Science* **51**: 244-250.

Cummins, I., O'Hagan, D., Jablonkai, I., Cole, D. J., Hehn, A., Werck-Reichhart, D. and Edwards, R. (2003). Cloning, characterization and regulation of a family of phi class glutathione transferases from wheat. *Plant Molecular Biology* **52**: 591-603.

Dayan, F. E., Daga, P. R., Duke, S. O., Lee, R. M., Tranel, P. J. and Doerksen, R. J. (2010). Biochemical and structural consequences of a glycine deletion in the α -8 helix of protoporphyrinogen oxidase. *Biochimica Et Biophysica Acta - Proteins and Proteomics* **1804**: 1548-1556.

Del Buono, D. and Ioli, G. (2011). Glutathione S-transferases of italian rye-grass (*Lolium multiflorum*): Activity toward some chemicals, safener modulation and persistence of atrazine and fluorodifen in the shoots. *Journal of Agricultural and Food Chemistry* **59**: 1324-1329.

Delye, C. (2005). Weed resistance to acetyl-coenzyme A carboxylase inhibitors: an update. *Weed Science* **53**: 728-746.

Delye, C. and Boucansaud, K. (2008). A molecular assay for the proactive detection of target site-based resistance to herbicides inhibiting acetolactate synthase in *Alopecurus myosuroides*. *Weed Research* **48**: 97-101.

Delye, C., Gardin, J. A. C., Boucansaud, K., Chauvel, B. and Petit, C. (2011). Non-target-site-based resistance should be the centre of attention for herbicide resistance research: *Alopecurus myosuroides* as an illustration. *Weed Research* **51**: 433-437.

Delye, C., Zhang, X. Q., Michel, S., Matejicek, A. and Powles, S. B. (2005). Molecular bases for sensitivity to acetyl-coenzyme A carboxylase inhibitors in black-grass. *Plant Physiology* **137**: 794-806.

Didierjean, L., Gondet, L., Perkins, R., Lau, S. M. C., Schaller, H., O'Keefe, D. P. and Werck-Reichhart, D. (2002). Engineering herbicide metabolism in tobacco and *Arabidopsis* with CYP76B1, a cytochrome P450 enzyme from Jerusalem artichoke. *Plant Physiology* **130**: 179-189.

Dixon, D., Cole, D. J. and Edwards, R. (1997). Characterisation of multiple glutathione transferases containing the GST I subunit with activities toward herbicide substrates in maize (*Zea mays*). *Pesticide Science* **50**: 72-82.

Dixon, D. P., Cole, D. J. and Edwards, R. (1998). Purification, regulation and cloning of a glutathione transferase (GST) from maize resembling the auxin-inducible type-III GSTs. *Plant Molecular Biology* **36**: 75-87.

Dixon, D. P., Cole, D. J. and Edwards, R. (1999). Dimerisation of maize glutathione transferases in recombinant bacteria. *Plant Molecular Biology* **40**: 997-1008.

Dixon, D. P., Davis, B. G. and Edwards, R. (2002). Functional divergence in the glutathione transferase superfamily in plants - Identification of two classes with putative functions in redox homeostasis in *Arabidopsis thaliana*. *Journal of Biological Chemistry* **277**: 30859-30869.

Dixon, D. P. and Edwards, R. (2009). Selective binding of glutathione conjugates of fatty acid derivatives by plant glutathione transferases. *Journal of Biological Chemistry* **284**: 21249-21256.

Dixon, D. P. and Edwards, R. (2010). Glutathione Transferases. *The Arabidopsis Book* **8**: e0131.

Dixon, D. P., Hawkins, T., Hussey, P. J. and Edwards, R. (2009). Enzyme activities and subcellular localization of members of the Arabidopsis glutathione transferase superfamily. *Journal of Experimental Botany* **60**: 1207-1218.

Dixon, D. P., Lapthorn, A., Madesis, P., Mudd, E. A., Day, A. and Edwards, R. (2008). Binding and glutathione conjugation of porphyrinogens by plant glutathione transferases. *Journal of Biological Chemistry* **283**: 20268-20276.

Dixon, D. P., McEwen, A. G., Lapthorn, A. J. and Edwards, R. (2003). Forced evolution of a herbicide detoxifying glutathione transferase. *Journal of Biological Chemistry* **278**: 23930-23935.

Dixon, D. P., Sellars, J. D. and Edwards, R. (2011). The Arabidopsis phi class glutathione transferase AtGSTF2: binding and regulation by biologically active heterocyclic ligands. *Biochemical Journal* **438**: 63-70.

Duggleby, R. G., McCourt, J. A. and Guddat, L. W. (2008). Structure and mechanism of inhibition of plant acetohydroxyacid synthase. *Plant Physiology and Biochemistry* **46**: 309-324.

Duke, S. O. (2012). Why have no new herbicide modes of action appeared in recent years? *Pest Management Science* **68**: 505-512.

Duke, S. O., Lydon, J., Becerril, J. M., Sherman, T. D., Lehnert, L. P. and Matsumoto, H. (1991). Protoporphyrinogen oxidase-inhibiting herbicides. *Weed Science* **39**: 465-473.

Duke, S. O. and Powles, S. B. (2008). Glyphosate: a once-in-a-century herbicide. *Pest Management Science* **64**: 319-325.

Edwards, R., Brazier-Hicks, M., Dixon, D. P. and Cummins, I. (2005a). Chemical manipulation of antioxidant defences in plants. *Advances in Botanical Research* **42**: 1-32.

Edwards, R. and Dixon, D. P. (2005). Plant glutathione transferases. *Methods in Enzymology* **401**: 169-186.

Edwards, R., Dixon, D. P., Cummins, I., Brazier-Hicks, M. and Skipsey, M. (2011). New perspectives on the metabolism and detoxification of synthetic compounds in plants. *Organic xenobiotics and plants: from mode of action to ecophysiology*. P. Schröder and C. D. Collins (Eds.), Springer. **8**: 125-148.

Edwards, R., Dixon, D. P. and Walbot, V. (2000). Plant glutathione S-transferases: enzymes with multiple functions in sickness and in health. *Trends in Plant Science* **5**: 193-198.

Federici, L., Lo Sterzo, C., Pezzola, S., Di Matteo, A., Scaloni, F., Federici, G. and Caccuri, A. M. (2009). Structural basis for the binding of the anticancer compound 6-(7-nitro-2,1,3-benzoxadiazol-4-ylthio)hexanol to human glutathione S-transferases. *Cancer Research* **69**: 8025-8034.

Fischer, T. C., Klattig, J. T. and Gierl, A. (2001). A general cloning strategy for divergent plant cytochrome P450 genes and its application in *Lolium rigidum* and *Ocimum basilicum*. *Theoretical and Applied Genetics* **103**: 1014-1021.

Flohe, L. and Gunzler, W. A. (1984). Assays of glutathione peroxidase. *Methods in Enzymology* **105**: 114-121.

Fraga, M. I. and Tasende, M. G. (2003). Mechanisms of resistance to simazine in *Sonchus oleraceus*. *Weed Research* **43**: 333-340.

Frear, D. S. and Swanson, H. R. (1970). Biosynthesis of *S*-(4-ethylamino-6-isopropylamino-2-*S*-triazino)glutathione - partial purification and properties of a glutathione *S*-transferase from corn. *Phytochemistry* **9**: 2123-2132.

Frear, D. S., Swanson, H. R. and Mansager, E. R. (1989). Picloram metabolism in leafy spurge - isolation and identification of glucose and gentiobiose conjugates. *Journal of Agricultural and Food Chemistry* **37**: 1408-1412.

Gaines, T. A., Zhang, W. L., Wang, D. F., Bukun, B., Chisholm, S. T., Shaner, D. L., Nissen, S. J., Patzoldt, W. L., Tranel, P. J., Culpepper, A. S., Grey, T. L., Webster, T. M., Vencill, W. K., Sammons, R. D., Jiang, J. M., Preston, C., Leach, J. E. and Westra, P. (2010). Gene amplification confers glyphosate resistance in *Amaranthus palmeri*. *Proceedings of the National Academy of Sciences of the United States of America* **107**: 1029-1034.

Gelvin, S. B. (2003). Agrobacterium-mediated plant transformation: The biology behind the "gene-jockeying" tool. *Microbiology and Molecular Biology Reviews* **67**: 16-37.

Gimenez-Espinosa, R., Romera, E., Tena, M. and DePrado, R. (1996). Fate of atrazine in treated and pristine accessions of three *Setaria* species. *Pesticide Biochemistry and Physiology* **56**: 196-207.

Gomez, C., Conejero, G., Torregrosa, L., Cheynier, V., Terrier, N. and Ageorges, A. (2011). *In vivo* grapevine anthocyanin transport involves vesicle-mediated trafficking and the contribution of anthoMATE transporters and GST. *Plant Journal* **67**: 960-970.

Gressel, J. (2009). Evolving understanding of the evolution of herbicide resistance. *Pest Management Science* **65**: 1164-1173.

Gronwald, J. W., Andersen, R. N. and Yee, C. (1989). Atrazine resistance in velvetleaf (*Abutilon theophrasti*) due to enhanced atrazine detoxification. *Pesticide Biochemistry and Physiology* **34**: 149-163.

Habig, W. H., Pabst, M. J. and Jakoby, W. B. (1974). Glutathione S-transferases - first enzymatic step in mercapturic acid formation. *Journal of Biological Chemistry* **249**: 7130-7139.

Hall, L. M., Moss, S. R. and Powles, S. B. (1995). Mechanism of resistance to chlorotoluron in two biotypes of the grass weed *Alopecurus myosuroides*. *Pesticide Biochemistry and Physiology* **53**: 180-192.

Hall, L. M., Moss, S. R. and Powles, S. B. (1997). Mechanisms of resistance to aryloxyphenoxypropionate herbicides in two resistant biotypes of *Alopecurus myosuroides* (black-grass): Herbicide metabolism as a cross-resistance mechanism. *Pesticide Biochemistry and Physiology* **57**: 87-98.

Han, H. P., Yu, Q., Purba, E., Li, M., Walsh, M., Friesen, S. and Powles, S. B. (2012). A novel amino acid substitution Ala-122-Tyr in ALS confers high-level and broad resistance across ALS-inhibiting herbicides. *Pest Management Science* **68**: 1164-1170.

Hatton, P. J., Cummins, I., Cole, D. J. and Edwards, R. (1999). Glutathione transferases involved in herbicide detoxification in the leaves of *Setaria faberii* (giant foxtail). *Physiologia Plantarum* **105**: 9-16.

Hatzios, K. K. and Burgos, N. (2004). Metabolism-based herbicide resistance: regulation by safeners. *Weed Science* **52**: 454-467.

Hayes, J. D., Flanagan, J. U. and Jowsey, I. R. (2005). Glutathione transferases. *Annual Review of Pharmacology and Toxicology* **45**: 51-88.

Hayes, J. D. and Mantle, T. J. (1986). Anomalous electrophoretic behavior of the glutathione S-transferase Ya and Yk subunits isolated from man and rodents - a potential pitfall for nomenclature. *Biochemical Journal* **237**: 731-740.

Heap, I. (2013). The International Survey of Herbicide Resistant Weeds. *Online*. Available at www.weedscience.com: Accessed 1/4/13

Hernandez, I. and Van Breusegem, F. (2010). Opinion on the possible role of flavonoids as energy escape valves: Novel tools for nature's Swiss army knife? *Plant Science* **179**: 297-301.

Heukeshoven, J. and Dernick, R. (1985). Simplified method for silver staining of proteins in polyacrylamide gels and the mechanism of silver staining. *Electrophoresis* **6**: 103-112.

Hirose, S., Kawahigashi, H., Ozawa, K., Shiota, N., Inui, H., Ohkawa, H. and Ohkawa, Y. (2005). Transgenic rice containing human CYP2B6 detoxifies various classes of herbicides. *Journal of Agricultural and Food Chemistry* **53**: 3461-3467.

Hyde, R. J., Hallahan, D. L. and Bowyer, J. R. (1996). Chlorotoluron metabolism in leaves of resistant and susceptible biotypes of the grass weed *Alopecurus myosuroides*. *Pesticide Science* **47**: 185-190.

Inclondon, B. J. and Hall, J. C. (1997). Acetyl-coenzyme A carboxylase: Quaternary structure and inhibition by graminicidal herbicides. *Pesticide Biochemistry and Physiology* **57**: 255-271.

Irzyk, G. P. and Fuerst, E. P. (1993). Purification and characterization of a glutathione S-transferase from benoxacor-treated maize (*Zea mays*). *Plant Physiology* **102**: 803-810.

Jain, M., Ghanashyam, C. and Bhattacharjee, A. (2010). Comprehensive expression analysis suggests overlapping and specific roles of rice glutathione S-transferase genes during development and stress responses. *BMC Genomics* **11**: 73.

Jang, S. R., Marjanovic, J. and Gornicki, P. (2013). Resistance to herbicides caused by single amino acid mutations in acetyl-CoA carboxylase in resistant populations of grassy weeds. *New Phytologist* **197**: 1110-1116.

Jasieniuk, M., BruleBabel, A. L. and Morrison, I. N. (1996). The evolution and genetics of herbicide resistance in weeds. *Weed Science* **44**: 176-193.

Karavangeli, M., Labrou, N. E., Clonis, Y. D. and Tsafaris, A. (2005). Development of transgenic tobacco plants overexpressing maize glutathione S-transferase I for chloroacetanilide herbicides phytoremediation. *Biomolecular Engineering* **22**: 121-128.

Kaundun, S. S., Bailly, G. C., Dale, R. P., Hutchings, S. J. and McIndoe, E. (2013). A novel W1999S mutation and non-target-site resistance impact on acetyl-CoA carboxylase inhibiting herbicides to varying degrees in a UK *Lolium multiflorum* population. *PLoS ONE* **8**: e58012.

Kaundun, S. S., Hutchings, S. J., Dale, R. P. and McIndoe, E. (2012). Broad resistance to ACCase inhibiting herbicides in a rye-grass population is due only to a cysteine to arginine mutation in the target enzyme. *PLoS ONE* **7**: e39759.

Keen, J. H. and Jakoby, W. B. (1978). Glutathione transferases - catalysis of nucleophilic reactions of glutathione. *Journal of Biological Chemistry* **253**: 5654-5657.

Kitamura, S., Akita, Y., Ishizaka, H., Narumi, I. and Tanaka, A. (2012). Molecular characterization of an anthocyanin-related glutathione S-transferase gene in cyclamen. *Journal of Plant Physiology* **169**: 636-642.

Klein, M., Weissenbock, G., Dufaud, A., Gaillard, C., Kreuz, K. and Martinoia, E. (1996). Different energization mechanisms drive the vacuolar uptake of a flavonoid glucoside and a herbicide glucoside. *Journal of Biological Chemistry* **271**: 29666-29671.

Kolm, R. H., Danielson, U. H., Zhang, Y. S., Talalay, P. and Mannervik, B. (1995). Isothiocyanates as substrates for human glutathione transferases - structure-activity studies. *Biochemical Journal* **311**: 453-459.

Koncz, C. and Schell, J. (1986). The promoter of T_L-DNA gene 5 controls the tissue-specific expression of chimeric genes carried by a novel type of Agrobacterium binary vector. *Molecular & General Genetics* **204**: 383-396.

Konishi, T. and Sasaki, Y. (1994). Compartmentalization of two forms of acetyl-CoA carboxylase in plants and the origin of their tolerance toward herbicides. *Proceedings of the National Academy of Sciences of the United States of America* **91**: 3598-3601.

Kumar, S., Asif, M. H., Chakrabarty, D., Tripathi, R. D., Dubey, R. S. and Trivedi, P. K. (2013). Expression of a rice lambda-class of glutathione *S*-transferase, *OsGSTL2*, in *Arabidopsis* provides tolerance to heavy metal and other abiotic stresses. *Journal of Hazardous Materials* **248**: 228-237.

Kunert, K. J., Homrighausen, C., Bohme, H. and Boger, P. (1985). Oxyfluorfen and lipid peroxidation - protein damage as a phytotoxic consequence. *Weed Science* **33**: 766-770.

Labrou, N. E., Mello, L. V. and Clonis, Y. D. (2001). Functional and structural roles of the glutathione-binding residues in maize (*Zea mays*) glutathione *S*-transferase I. *Biochemical Journal* **358**: 101-110.

Laemmli, U. K. (1970). Cleavage of structural proteins during assembly of head of bacteriophage T4. *Nature* **227**: 680-685.

Lu, Y. P., Li, Z. S., Drozdowicz, Y. M., Hortensteiner, S., Martinoia, E. and Rea, P. A. (1998). *AtMRP2*, an *Arabidopsis* ATP binding cassette transporter able to transport glutathione *S*-conjugates and chlorophyll catabolites: Functional comparisons with *AtMRP1*. *Plant Cell* **10**: 267-282.

Lu, Y. P., Li, Z. S. and Rea, P. A. (1997). *AtMRP1* gene of *Arabidopsis* encodes a glutathione *S*-conjugate pump: Isolation and functional definition of a plant ATP-binding cassette transporter gene. *Proceedings of the National Academy of Sciences of the United States of America* **94**: 8243-8248.

Mannervik, B. and Danielson, U. H. (1988). Glutathione transferases - structure and catalytic activity. *Critical Reviews in Biochemistry* **23**: 283-337.

Marrs, K. A. (1996). The functions and regulation of glutathione S-transferases in plants. *Annual Review of Plant Physiology and Plant Molecular Biology* **47**: 127-158.

Marrs, K. A., Alfenito, M. R., Lloyd, A. M. and Walbot, V. (1995). A glutathione S-transferase involved in vacuolar transfer encoded by the maize gene bronze-2. *Nature* **375**: 397-400.

Martinoia, E., Grill, E., Tommasini, R., Kreuz, K. and Amrhein, N. (1993). ATP-dependent glutathione S-conjugate export pump in the vacuolar membrane of plants. *Nature* **364**: 247-249.

Mayer, K. F. X., Waugh, R., Langridge, P., Close, T. J., Wise, R. P., Graner, A., Matsumoto, T., Sato, K., Schulman, A., Muehlbauer, G. J., Stein, N., Ariyadasa, R., Schulte, D., Poursarebani, N., Zhou, R. N., Steuernagel, B., Mascher, M., Scholz, U., Shi, B. J., Langridge, P., Madishetty, K., Svensson, J. T., Bhat, P., Moscou, M., Resnik, J., Close, T. J., Muehlbauer, G. J., Hedley, P., Liu, H., Morris, J., Waugh, R., Frenkel, Z., Korol, A., Berges, H., Graner, A., Stein, N., Steuernagel, B., Taudien, S., Groth, M., Felder, M., Platzer, M., Brown, J. W. S., Schulman, A., Platzer, M., Fincher, G. B., Muehlbauer, G. J., Sato, K., Taudien, S., Sampath, D., Swarbreck, D., Scalabrin, S., Zuccolo, A., Vendramin, V., Morgante, M., Mayer, K. F. X., Schulman, A. and Conso, I. B. G. S. (2012). A physical, genetic and functional sequence assembly of the barley genome. *Nature* **491**: 711-716.

McCourt, J. A., Pang, S. S., King-Scott, J., Guddat, L. W. and Duggleby, R. G. (2006). Herbicide-binding sites revealed in the structure of plant acetohydroxyacid synthase. *Proceedings of the National Academy of Sciences of the United States of America* **103**: 569-573.

McGonigle, B., Keeler, S. J., Lan, S. M. C., Koeppe, M. K. and O'Keefe, D. P. (2000). A genomics approach to the comprehensive analysis of the glutathione S-transferase gene family in soybean and maize. *Plant Physiology* **124**: 1105-1120.

Menchari, Y., Chauvel, B., Darmency, H. and Delye, C. (2008). Fitness costs associated with three mutant acetyl-coenzyme A carboxylase alleles endowing herbicide resistance in black-grass (*Alopecurus myosuroides*). *Journal of Applied Ecology* **45**: 939-947.

Milligan, A. S., Daly, A., Parry, M. A. J., Lazzeri, P. A. and Jepson, I. (2001). The expression of a maize glutathione S-transferase gene in transgenic wheat confers herbicide tolerance, both *in planta* and *in vitro*. *Molecular Breeding* **7**: 301-315.

Moss, S. R. (1990). Herbicide cross-resistance in slender foxtail (*Alopecurus myosuroides*). *Weed Science* **38**: 492-496.

Moss, S. R., Marshall, R., Hull, R. and Alarcon-Reverte, R. (2011). Current status of herbicide resistant weeds in the United Kingdom. *Aspects of Applied Biology* **106**: 1-10.

Moss, S. R., Perryman, S. A. M. and Tatnell, L. V. (2007). Managing herbicide-resistant black-grass (*Alopecurus myosuroides*): Theory and practice. *Weed Technology* **21**: 300-309.

Mozer, T. J., Tiemeier, D. C. and Jaworski, E. G. (1983). Purification and characterization of corn glutathione S-transferase. *Biochemistry* **22**: 1068-1072.

Mueller, L. A., Goodman, C. D., Silady, R. A. and Walbot, V. (2000). AN9, a petunia glutathione S-transferase required for anthocyanin sequestration, is a flavonoid-binding protein. *Plant Physiology* **123**: 1561-1570.

Neuefeind, T., Huber, R., Dasenbrock, H., Prade, L. and Bieseler, B. (1997a). Crystal structure of herbicide-detoxifying maize glutathione S-transferase I in complex with lactoylglutathione: Evidence for an induced-fit mechanism. *Journal of Molecular Biology* **274**: 446-453.

Neuefeind, T., Huber, R., Reinemer, P., Knablein, J., Prade, L., Mann, K. and Bieseler, B. (1997b). Cloning, sequencing, crystallization and x-ray structure of

glutathione S-transferase III from *Zea mays* var. mutin: A leading enzyme in detoxification of maize herbicides. *Journal of Molecular Biology* **274**: 577-587.

Noctor, G., Queval, G., Mhamdi, A., Chaouch, S. and Foyer, C. H. (2011). Glutathione. *The Arabidopsis Book* **9**: e0142.

O'Connell, K. M., Breaux, E. J. and Fraley, R. T. (1988). Different rates of metabolism of two chloroacetanilide herbicides in Pioneer-3320 corn. *Plant Physiology* **86**: 359-363.

Patzoldt, W. L., Hager, A. G., McCormick, J. S. and Tranel, P. J. (2006). A codon deletion confers resistance to herbicides inhibiting protoporphyrinogen oxidase. *Proceedings of the National Academy of Sciences of the United States of America* **103**: 12329-12334.

Peng, Y. H., Abercrombie, L. L. G., Yuan, J. S., Riggins, C. W., Sammons, R. D., Tranel, P. J. and Stewart, C. N. (2010). Characterization of the horseweed (*Conyza canadensis*) transcriptome using GS-FLX 454 pyrosequencing and its application for expression analysis of candidate non-target herbicide resistance genes. *Pest Management Science* **66**: 1053-1062.

Petit, C., Bay, G., Pernin, F. and Delye, C. (2010). Prevalence of cross- or multiple resistance to the acetyl-coenzyme A carboxylase inhibitors fenoxaprop, clodinafop and pinoxaden in black-grass (*Alopecurus myosuroides* Huds.) in France. *Pest Management Science* **66**: 168-177.

Plaisance, K. L. and Gronwald, J. W. (1999). Enhanced catalytic constant for glutathione S-transferase (atrazine) activity in an atrazine-resistant *Abutilon theophrasti* biotype. *Pesticide Biochemistry and Physiology* **63**: 34-49.

Ploemen, J. H. T. M., Vanschanke, A., Vanommen, B. and Vanbladeren, P. J. (1994). Reversible conjugation of ethacrynic acid with glutathione and human glutathione S-transferase P1-1. *Cancer Research* **54**: 915-919.

Powles, S. B. and Yu, Q. (2010). Evolution in action: plants resistant to herbicides. *Annual Review of Plant Biology* **61**: 317-347.

Prade, L., Huber, R. and Bieseler, B. (1998). Structures of herbicides in complex with their detoxifying enzyme glutathione S-transferase - explanations for the selectivity of the enzyme in plants. *Structure with Folding & Design* **6**: 1445-1452.

Preston, C., Tardif, F. J., Christopher, J. T. and Powles, S. B. (1996). Multiple resistance to dissimilar herbicide chemistries in a biotype of *Lolium rigidum* due to enhanced activity of several herbicide degrading enzymes. *Pesticide Biochemistry and Physiology* **54**: 123-134.

Rea, P. A. (1999). MRP subfamily ABC transporters from plants and yeast. *Journal of Experimental Botany* **50**: 895-913.

Rea, P. A. (2007). Plant ATP-Binding cassette transporters. *Annual Review of Plant Biology* **58**: 347-375.

Ricci, G., Caccuri, A. M., Lo Bello, M., Parker, M. W., Nuccetelli, M., Turella, P., Stella, L., Di Iorio, E. E. and Federici, G. (2003). Glutathione transferase P1-1: self-preservation of an anti-cancer enzyme. *Biochemical Journal* **376**: 71-76.

Ricci, G., De Maria, F., Antonini, G., Turella, P., Bullo, A., Stella, L., Filomeni, G., Federici, G. and Caccuri, A. M. (2005). 7-nitro-2,1,3-benzoxadiazole derivatives, a new class of suicide inhibitors for glutathione S-transferases - Mechanism of action of potential anticancer drugs. *Journal of Biological Chemistry* **280**: 26397-26405.

Ricci, G., Lobello, M., Caccuri, A. M., Pastore, A., Nuccetelli, M., Parker, M. W. and Federici, G. (1995). Site-directed mutagenesis of human glutathione transferase P1-1 - mutation of Cys-47 induces a positive cooperativity in glutathione transferase P1-1. *Journal of Biological Chemistry* **270**: 1243-1248.

Riggins, C. W., Peng, Y. H., Stewart, C. N. and Tranel, P. J. (2010). Characterization of *de novo* transcriptome for waterhemp (*Amaranthus tuberculatus*) using GS-FLX

454 pyrosequencing and its application for studies of herbicide target-site genes. *Pest Management Science* **66**: 1042-1052.

Ryan, G. F. (1970). Resistance of common groundsel to simazine and atrazine. *Weed Science* **18**: 614-616.

Ryan, P. J., Gross, D., Owen, W. J. and Laanio, T. L. (1981). The metabolism of chlortoluron, diuron, and CGA43057 in tolerant and susceptible plants. *Pesticide Biochemistry and Physiology* **16**: 213-221.

Salas, R. A., Dayan, F. E., Pan, Z. Q., Watson, S. B., Dickson, J. W., Scott, R. C. and Burgos, N. R. (2012). EPSPS gene amplification in glyphosate-resistant Italian ryegrass (*Lolium perenne* ssp *multiflorum*) from Arkansas. *Pest Management Science* **68**: 1223-1230.

Sandermann, H. (2004). Bound and unextractable pesticidal plant residues: chemical characterization and consumer exposure. *Pest Management Science* **60**: 613-623.

Scalla, R. and Roulet, A. (2002). Cloning and characterization of a glutathione S-transferase induced by a herbicide safener in barley (*Hordeum vulgare*). *Physiologia Plantarum* **116**: 336-344.

Schloss, J. V. (1990). Acetolactate synthase, mechanism of action and its herbicide binding-site. *Pesticide Science* **29**: 283-292.

Schmidt, T. G. M. and Skerra, A. (2007). The Strep-tag system for one-step purification and high-affinity detection or capturing of proteins. *Nature Protocols* **2**: 1528-1535.

Shaner, D. L., Lindenmeyer, R. B. and Ostlie, M. H. (2012). What have the mechanisms of resistance to glyphosate taught us? *Pest Management Science* **68**: 3-9.

Shimabukuro, R. H., Frear, D. S., Swanson, H. R. and Walsh, W. C. (1971). Glutathione conjugation - enzymatic basis for atrazine resistance in corn. *Plant Physiology* **47**: 10-14.

Shimabukuro, R. H., Kadunce, R. E. and Frear, D. S. (1966). Dealkylation of atrazine in mature pea plants. *Journal of Agricultural and Food Chemistry* **14**: 392-395.

Shimabukuro, R. H., Walsh, W. C. and Hoerauf, R. A. (1979). Metabolism and selectivity of diclofop-methyl in wild oat and wheat. *Journal of Agricultural and Food Chemistry* **27**: 615-623.

Siminszky, B. (2006). Plant cytochrome P450-mediated herbicide metabolism. *Phytochemistry Reviews* **5**: 445-458.

Siminszky, B., Corbin, F. T., Ward, E. R., Fleischmann, T. J. and Dewey, R. E. (1999). Expression of a soybean cytochrome P450 monooxygenase cDNA in yeast and tobacco enhances the metabolism of phenylurea herbicides. *Proceedings of the National Academy of Sciences of the United States of America* **96**: 1750-1755.

Skipsey, M., Andrews, C. J., Townson, J. K., Jepson, I. and Edwards, R. (1997). Substrate and thiol specificity of a stress-inducible glutathione transferase from soybean. *FEBS Letters* **409**: 370-374.

Skipsey, M., Cummins, I., Andrews, C. J., Jepson, I. and Edwards, R. (2005). Manipulation of plant tolerance to herbicides through co-ordinated metabolic engineering of a detoxifying glutathione transferase and thiol cosubstrate. *Plant Biotechnology Journal* **3**: 409-420.

Sommer, A. and Boger, P. (1999). Characterization of recombinant corn glutathione S-transferase isoforms I, II, III, and IV. *Pesticide Biochemistry and Physiology* **63**: 127-138.

Steinrucken, H. C. and Amrhein, N. (1980). The herbicide glyphosate is a potent inhibitor of 5-enolpyruvylshikimic acid-3-phosphate synthase. *Biochemical and Biophysical Research Communications* **94**: 1207-1212.

Swanson, C. R., Kadunce, R. E., Hodgson, R. H. and Frear, D. S. (1966). Amiben metabolism in plants I. Isolation and identification of an *N*-glucosyl complex. *Weeds* **14**: 319-323.

Sweetser, P. B., Schow, G. S. and Hutchison, J. M. (1982). Metabolism of chlorsulfuron by plants - biological basis for selectivity of a new herbicide for cereals. *Pesticide Biochemistry and Physiology* **17**: 18-23.

Szewczyk, E., Nayak, T., Oakley, C. E., Edgerton, H., Xiong, Y., Taheri-Talesh, N., Osmani, S. A. and Oakley, B. R. (2006). Fusion PCR and gene targeting in *Aspergillus nidulans*. *Nature Protocols* **1**: 3111-3120.

Tal, A., Romano, M. L., Stephenson, G. R., Schwan, A. L. and Hall, J. C. (1993). Glutathione conjugation - a detoxification pathway for fenoxaprop-ethyl in barley, crabgrass, oat, and wheat. *Pesticide Biochemistry and Physiology* **46**: 190-199.

Tamai, K., Satoh, K., Tsuchida, S., Hatayama, I., Maki, T. and Sato, K. (1990). Specific inactivation of glutathione *S*-transferases in class pi by SH-modifiers. *Biochemical and Biophysical Research Communications* **167**: 331-338.

Theodoulou, F. L., Clark, I. M., He, X. L., Pallett, K. E., Cole, D. J. and Hallahan, D. L. (2003). Co-induction of glutathione *S*-transferases and multi-drug resistance associated protein by xenobiotics in wheat. *Pest Management Science* **59**: 202-214.

Thinglum, K. A., Riggins, C. W., Davis, A. S., Bradley, K. W., Al-Khatib, K. and Tranel, P. J. (2011). Wide distribution of the waterhemp (*Amaranthus tuberculatus*) delta G210 PPX2 mutation, which confers resistance to PPO-inhibiting herbicides. *Weed Science* **59**: 22-27.

Thom, R., Cummins, I., Dixon, D. P., Edwards, R., Cole, D. J. and Lapthorn, A. J. (2002). Structure of a tau class glutathione S-transferase from wheat active in herbicide detoxification. *Biochemistry* **41**: 7008-7020.

Tranel, P. J. and Wright, T. R. (2002). Resistance of weeds to ALS-inhibiting herbicides: what have we learned? *Weed Science* **50**: 700-712.

Tranel, P. J., Wright, T. R. and Heap, I. M. (2013). Mutations in herbicide-resistant weeds to ALS inhibitors. *Online*. Accessed at <http://www.weedscience.com>: Accessed 4/5/2013.

Turella, P., Cerella, C., Filomeni, G., Bullo, A., De Maria, F., Ghibelli, L., Ciriolo, M. R., Cianfriglia, M., Mattei, M., Federici, G., Ricci, G. and Caccuri, A. M. (2005). Proapoptotic activity of new glutathione S-transferase inhibitors. *Cancer Research* **65**: 3751-3761.

Van Eerd, L. L., Hoagland, R. E., Zablotowicz, R. M. and Hall, J. C. (2003). Pesticide metabolism in plants and microorganisms. *Weed Science* **51**: 472-495.

van Zanden, J. J., Ben Hamman, O., van Lersel, M. L. P. S., Boeren, S., Cnubben, N. H. P., Lo Bello, M., Vervoort, J., van Bladeren, P. J. and Rietjens, I. M. C. M. (2003). Inhibition of human glutathione S-transferase P1-1 by the flavonoid quercetin. *Chemico-Biological Interactions* **145**: 139-148.

Wagner, U., Edwards, R., Dixon, D. P. and Mauch, F. (2002). Probing the diversity of the *Arabidopsis* glutathione S-transferase gene family. *Plant Molecular Biology* **49**: 515-532.

Werck-Reichhart, D., Hehn, A. and Didierjean, L. (2000). Cytochromes P450 for engineering herbicide tolerance. *Trends in Plant Science* **5**: 116-123.

Windsor, B., Roux, S. J. and Lloyd, A. (2003). Multiherbicide tolerance conferred by *AtPgp1* and apyrase overexpression in *Arabidopsis thaliana*. *Nature Biotechnology* **21**: 428-433.

Winkel-Shirley, B. (2002). Biosynthesis of flavonoids and effects of stress. *Current Opinion in Plant Biology* **5**: 218-223.

Witte, C. P., Noel, L. D., Gielbert, J., Parker, J. E. and Romeis, T. (2004). Rapid one-step protein purification from plant material using the eight-amino acid *Strep* II epitope. *Plant Molecular Biology* **55**: 135-147.

Wu, J. R., Cramer, C. L. and Hatzios, K. K. (1999). Characterization of two cDNAs encoding glutathione *S*-transferases in rice and induction of their transcripts by the herbicide safener fenclorim. *Physiologia Plantarum* **105**: 102-108.

Wu, Z. X., Minhas, G. S., Wen, D. Y., Jiang, H. L., Chen, K. X., Zimniak, P. and Zheng, J. (2004). Design, synthesis, and structure-activity relationships of haloenol lactones: Site-directed and isozyme-selective glutathione *S*-transferase inhibitors. *Journal of Medicinal Chemistry* **47**: 3282-3294.

Xiang, S., Callaghan, M. M., Watson, K. G. and Tong, L. (2009). A different mechanism for the inhibition of the carboxyltransferase domain of acetyl-coenzyme A carboxylase by tepraloxydim. *Proceedings of the National Academy of Sciences of the United States of America* **106**: 20723-20727.

Yu, L. P. C., Kim, Y. S. and Tong, L. A. (2010). Mechanism for the inhibition of the carboxyltransferase domain of acetyl-coenzyme A carboxylase by pinoxaden. *Proceedings of the National Academy of Sciences of the United States of America* **107**: 22072-22077.

Yu, Q., Collavo, A., Zheng, M. Q., Owen, M., Sattin, M. and Powles, S. B. (2007a). Diversity of acetyl-coenzyme A carboxylase mutations in resistant *Lolium* populations: Evaluation using clethodim. *Plant Physiology* **145**: 547-558.

Yu, Q., Han, H. P. and Powles, S. B. (2008). Mutations of the ALS gene endowing resistance to ALS-inhibiting herbicides in *Lolium rigidum* populations. *Pest Management Science* **64**: 1229-1236.

Yuan, J. S., Tranel, P. J. and Stewart, C. N. (2007). Non-target-site herbicide resistance: a family business. *Trends in Plant Science* **12**: 6-13.

Yun, M. S., Yogo, Y., Miura, R., Yamasue, Y. and Fischer, A. J. (2005). Cytochrome P450 monooxygenase activity in herbicide-resistant and -susceptible late watergrass (*Echinochloa phyllopogon*). *Pesticide Biochemistry and Physiology* **83**: 107-114.

Zhang, H. L., Tweel, B. and Tong, L. (2004). Molecular basis for the inhibition of the carboxyltransferase domain of acetyl-coenzyme A carboxylase by haloxyfop and diclofop. *Proceedings of the National Academy of Sciences of the United States of America* **101**: 5910-5915.

Zhang, X. Q. and Powles, S. B. (2006a). The molecular bases for resistance to acetyl co-enzyme A carboxylase (ACCase) inhibiting herbicides in two target-based resistant biotypes of annual rye-grass (*Lolium rigidum*). *Planta* **223**: 550-557.

Zhang, X. Q. and Powles, S. B. (2006b). Six amino acid substitutions in the carboxyl-transferase domain of the plastidic acetyl-CoA carboxylase gene are linked with resistance to herbicides in a *Lolium rigidum* population. *New Phytologist* **172**: 636-645.

Zheng, J. A., Mitchell, A. E., Jones, A. D. and Hammock, B. D. (1996). Haloenol lactone is a new isozyme-selective and active site-directed inactivator of glutathione S-transferase. *Journal of Biological Chemistry* **271**: 20421-20425.

Zhou, S. P., Lien, Y. C., Shuvaeva, T., DeBolt, K., Feinstein, S. I. and Fisher, A. B. (2013). Functional interaction of glutathione S-transferase pi and peroxiredoxin 6 in intact cells. *International Journal of Biochemistry & Cell Biology* **45**: 401-407.